Nucleon Structure Functions, their Medium Modification and the Polarized EMC effect

Ian C. Cloët

Supervisors: Prof. A. W. Thomas and A/Prof. D. B. Leinweber

Special Research Centre for the Subatomic Structure of Matter
and
Department of Physics,
University of Adelaide,
Australia

December 2006

Abstract

The central theme of this thesis is an investigation of the in-medium modifications to nucleon structure. We focus on the medium modifications to the three twist-two quark lightcone momentum distributions and associated structure functions. To achieve this we utilize the Nambu–Jona-Lasinio model, with the proper-time regularization scheme, in which confinement is simulated by eliminating unphysical thresholds for nucleon decay into quarks. The nucleon bound state is obtained by solving the relativistic Faddeev equation in the quark-diquark approximation, where both scalar and axial-vector diquark channels are included.

In this framework we obtain excellent results for the free spin-independent and spin-dependent quark distributions. The transversity distributions satisfy the Soffer inequality and are similar to the spin-dependent distributions. With the introduction of mean scalar and vector fields that couple to the quarks in the nucleon, we obtain a good description of many nuclear matter properties, including saturation at the correct energy and density.

The medium modifications to the nucleon structure functions are investigated in both infinite nuclear matter and for the nuclei ^{7}Li, ^{11}B, ^{15}N, ^{27}Al and the closed shell neighbours ^{12}C, ^{16}O and ^{28}Si. In each case the in-medium quark degrees of freedom are accessed via the convolution formalism. For finite nuclei we use a relativistic shell model including mean scalar and vector fields. We derive, for the first time, relativistic expressions for the nucleon distributions in a nucleus, that retain the phenomenologically important lower components of the nucleon wavefunction. We find that we are readily able to reproduce the experimental F_{2A}/F_{2N} ratio, that is, the EMC effect. However, the main focus of this thesis is on a new ratio – the nuclear structure function, g_{1A}, divided by the naive free result – which we refer to as the polarized EMC effect. We find that the medium modifications of the spin structure functions are remarkably large, up to twice the usual EMC effect. This result has important experimental implications, and may provide the impetus for future polarized deep inelastic experiments on nuclei.

Statement of Originality

This work contains no material which has been accepted for the award of any other degree or diploma in any university or other tertiary institution and, to the best of my knowledge and belief, contains no material previously published or written by another person, except where due reference has been made in the text.

I give consent to this copy of my thesis, when deposited in the University Library, being available for loan and photocopying.

8th February 2007

Acknowledgements

The work presented in this thesis would not have been possible without the generous guidance, support and encouragement I received from my supervisor Tony Thomas and our collaborator Wolfgang Bentz. Tony's support as a supervisor has far exceeded my expectations. He has provided me with almost unlimited opportunities to grow as a physicist and greatly helped me to pursue a research topic that I found extremely interesting and rewarding. I thank Wolfgang for an immensely rewarding collaboration and for the large amount of work he did in helping guide the research in this thesis. To both Tony and Wolfgang, I have thoroughly enjoyed our friendship and collaboration, and look forward to it continuing into the future.

I must also thank my other thesis supervisor, Derek Leinweber, who while not directly involved with the research in this thesis, played a pivotal role in the early stages of my graduate studies. Derek has taught me a great deal, and without our early collaboration I am quite certain I would not have pursued a PhD. I look forward to possible collaborations in the future.

My years as a graduate student have been made far more enjoyable through friendships made at the CSSM and JLab. In particular I thank Ben, Mark, Sarah and Alex for our many discussions, Jorge and Ross for helping me through my time at Newport News, Wally for being Wally and Jo for his English humour. I also thank Susan for all her help, and Ross and Wally for many useful physics discussions.

Most importantly, I thank Heidi for her never ending support and much more.

Contents

1 Introduction

Developing a vigorous and complete understanding of Quantum Chromodynamics (QCD) is arguably the most exciting and potentially rewarding challenge confronting the nuclear and particle physics community. The solution of QCD strikes at the heart of our modern understanding of asymptotically free gauge theories. It could either solve or shed light many unresolved problems in nuclear physics, particle physics and even cosmology. For example a solution to QCD would provide a far greater understanding of the Big Bang and the first few seconds of the universe, the observed matter–anti-matter asymmetry and the formation of stars and atomic nuclei. It may even provide answers to philosophical questions, akin to those offered by Quantum Mechanics.

The solution to QCD appears at the moment to be extremely difficult, currently the only known approach is to solve the path integral directly on a Euclidean spacetime lattice. However this method has its own shortcomings, which will probably prevent it from ever providing a complete solution to QCD. The incredible complexity of QCD results from the simple fact that the gauge boson of the theory, the gluon, carries the colour charge. This is in contrast to the well understood theory of Quantum Electrodynamics (QED), where the photon does not carry the electromagnetic charge. The consequences of the gluons possessing the colour degree of freedom are immense, for example the perturbative techniques used so successfully in QED are now valid only at large momentum transfer or equivalently at small distances scales. However, even at the extremely high energies of modern particle accelerators the non-perturbative nature of QCD cannot be avoided. For example, in deep inelastic scattering experiments, the non-perturbative physics is encapsulated by the quark distribution functions.

From its beginnings at SLAC in the late 60s deep inelastic scattering (DIS) has played a fundamental role in developing our understanding of the quark-gluon structure of hadrons and consequently of QCD. A paradigm shift in our understanding came in 1982 when the European Muon Collaboration at CERN measured the $F_2(x)$ structure function of iron and compared it to that of the deuteron. Nuclear effects in DIS were thought to be largely negligible, except at large x where Fermi motion becomes important. The nucleus was viewed as a system of quasi-free nucleons where, because of the large differences in energy scales, the quark structure of the nucleons was thought to be insensitive to the nuclear environment. However, when the ratio of the iron F_2 structure function and the F_2 deuteron structure function was taken, a large deviation from one was observed in the valence quark region ($0.2 \lesssim x \lesssim 0.8$). This indicates that the quark structure of the nucleon has substantial nuclear environment sensitively.

This result, which became known as the EMC effect, brought to the fore the importance of quarks in traditional nuclear physics and has generated an enormous amount of experimental and theoretical activity. The initial interest in this result was propelled by the hope that it could help bridge the gap between our knowledge of QCD at short distances and its completely unknown implications at the distance scales of traditional nuclear physics. This has indeed happened, however the fundamental mechanism responsible for the EMC effect remains unknown.

Another paradigm shift occurred when the European Muon Collaboration made a precise measurement of the proton spin structure function $g_1(x)$. They found that the fraction of the proton's spin carried by the quarks is unexpectedly small. At the time the estimate was consistent with zero, but modern results find that about 20-40% of the nucleon's spin comes from the spin of the quarks. This result became known as the "proton spin crisis" and gave rise to many new experiments and a large amount of theoretical activity. In particular the important role played by the axial anomaly in the singlet sector of $g_1(x)$ was highlighted. This anomaly produces a gluonic correction to the spin structure function at all values at Q^2. This implies that the measured singlet contribution to the first moment of $g_{1p}(x)$, which we denote by $\Delta\Sigma$, has a gluonic correction given by

$$\Delta\Sigma = \Delta\Sigma_0 - 3\frac{\alpha_s(Q^2)}{2\pi}\,\Delta g(Q^2), \tag{1.1}$$

where $\Delta\Sigma_0$ is the object normally associated with spin, as it satisfies the usual $SU(2)$ commutation relations. Although this gluonic correction does reduce the spin sum, it is not large enough to resolve the spin crisis. Theoretical work from many directions has made substantial process in understanding the proton spin structure, however a full resolution of the proton spin crisis is still lacking.

In light of these two ground breaking experiments it is surprising that there has been no polarized deep inelastic scattering experiments on nuclear targets, where the potential for new and even fundamental discoveries appears quite possible. The alleviation of this shortcoming, from a theoretical perspective, is the main goal of this thesis. In each successive chapter of this thesis we build the formalism necessary to determine the spin structure functions of atomic nuclei. In Chapter 6 we define a new ratio – the nuclear spin structure function g_{1A} divided by the naive free result – which we call the polarized EMC ratio. The deviation from unity of this ratio measures the degree of medium modifications of the spin-dependent quark distributions in an analogous fashion to the usual EMC ratio for the spin-independent distributions. We find large medium modifications to the spin structure function, and a substantial decrease in the fraction of the spin carried by the quarks in a bound proton relative to that of a free proton. We hope that these potentially exciting results may provide the impetus needed to develop new experimental programs to perform polarized deep inelastic scattering on nuclei.

The outline of this thesis is as follows: In Chapter 2 we give a brief overview of the formalism of inclusive deep inelastic scattering (DIS), introducing the three twist-two quark distribution functions, first in the parton model and then more formally in the context of factorization theorems. Finally we touch on the Drell-Yan and semi-inclusive DIS processes that can be used to measure the transversity quark distribution functions.

As we have mentioned, a full solution to QCD is still some time away. Therefore to study the in-medium modifications to the nucleon and determine nuclear structure functions we must use a model of QCD. In Chapter 3 we introduce such a model, the Nambu–Jona-Lasinio (NJL) model, which is interpreted as a chiral effective quark theory of QCD. In this chapter we focus on the constraints imposed by chiral symmetry and on the solution of the three-quark bound state problem in the relativistic Faddeev framework. In Chapter 4 we present important results for the spin-independent, spin-dependent and transversity quark distribution functions obtained using the NJL model and the proper-time regularized scheme.

The results we present in Chapter 5 have produced a large amount of experimental interest, particularly for the 12 GeV upgrade at Jefferson Lab. Here we extend the NJL model to finite density and calculate the EMC, polarized EMC and transversity EMC effects in nuclear matter. We find excellent agreement with data for the EMC effect and large medium modification to the spin and transversity structure functions.

Finally, in Chapter 6 we utilize a relativistic shell model to extend our in-medium results to finite nuclei. Here we focus only on spin-independent and spin-dependent distribution functions, as the QCD evolution of transversity quark distributions for targets with $J \geqslant 1$ is still not fully resolved. Then, in Chapter 7 we summarize and discuss possible future research directions that could utilize the formalism developed in this thesis.

We also include a large amount of detail in the appendices that the reader may consult if further details are required. In particular we give the full derivation of the transversity quark distribution functions in the NJL model (Appendix D) and the derivation of the relativistic nucleon distributions in the nucleus (Appendix H).

2

Deep Inelastic Scattering

The archetypal process for probing hadronic structure is inclusive deep inelastic scattering (DIS). Many important insights into nucleon structure and Quantum Chromodynamics (QCD) have been obtained through DIS experiments. For example, the measurements of the spin averaged structure functions, $F_1(x, Q^2)$ and $F_2(x, Q^2)$, which exhibit the predicted Bjorken scaling [1], was one of the first confirmations of strong interaction physics. Later, small Q^2 scaling violations were observed and these were found to be described perfectly by perturbative QCD. This important result led to an almost universal acceptance of QCD as the correct theory of strong interactions. Further polarized DIS experiments measured the spin-dependent structure functions $g_1(x, Q^2)$ and $g_2(x, Q^2)$. A precise measurement of $g_1(x, Q^2)$ by the European Muon Collaboration [2] found that the fraction of the spin of the proton carried by the quarks seemed to be very small and even consistent with zero [3]. This become known as the "proton spin crisis". Modern analysis finds a spin fraction of $\Delta\Sigma = 0.213 \pm 0.138$ [4], however a resolution of this problem remains an open and intensely debated question [5–8]. DIS experiments have also provided precision determinations of the strong coupling constant α_s [9,10]. And importantly, as it is the focus of this thesis, DIS experiments on nuclear targets (e.g. carbon, aluminium and iron) have shown that the nuclear medium modifies the nucleon structure functions [11].

In this chapter we review the formalism of DIS with a focus on spin-$\frac{1}{2}$ targets, like the nucleon. Later, in Chapter 6, we will generalize this discussion to include DIS on an arbitrary spin target. We begin this chapter by introducing the kinematic variables of the DIS process. We then discuss the differential cross-section and the associated structure functions. A brief introduction and motivation for Feynman's parton model is also included. We examine the Factorization theorems with a focus on the link these provide between the parton model and QCD. Finally, we will finish with a brief discussion of the chiral-odd transversity quark distributions and describe deep inelastic scattering processes that are sensitive to these distribution functions.

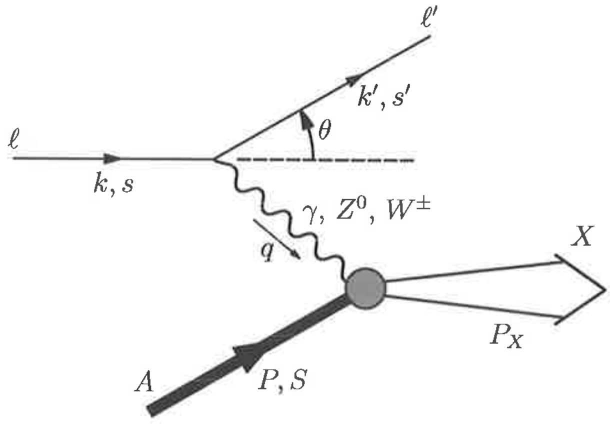

Figure 2.1: The lowest order graph for DIS. The quantities k, s and k', s' are the initial and final lepton momenta and spin, P, S is the target momentum and spin, while q is the momentum transfered to the target by the exchanged vector boson. The angle θ between the incoming and outgoing lepton is defined in the target rest frame.

2.1 Reactions and Kinematics

Deep inelastic scattering is the process where a lepton, in practice an electron, muon or neutrino is scattered from a target (usually a nucleus) transferring large amounts of energy and four-momentum squared. The DIS process is depicted diagrammatically in Fig. 2.1 in the one boson exchange approximation and can be written in the form

$$\ell(k, s) + A(P, S) \longrightarrow \ell'(k', s') + X(P_X), \tag{2.1}$$

where ℓ is the initial lepton, A is the target, ℓ' is the scattered lepton and X represents the undetected final hadronic state. In brackets we label the four-momentum and spin of each state. The only quantities measured experimentally in inclusive DIS are the energy, E', and the scattering angle, θ, of the final state lepton ℓ'.

Each of the three electroweak gauge bosons can play a role in DIS (see Fig. 2.1). These are usually referred to as the electromagnetic current (γ), neutral current (Z^0) or charged current ($W^\pm$) exchange. For charged current exchange the initial or final lepton must be either a neutrino or an anti-neutrino to conserve charge at the lepton-boson vertex. The four basic process are

$$\left.\begin{array}{rcl} \ell + A & \xrightarrow{\gamma, Z^0} & \ell + X \\ (\overline{\nu})\nu + A & \xrightarrow{Z^0} & (\overline{\nu})\nu + X \end{array}\right\} \quad \text{Electromagnetic and Neutral Current,} \tag{2.2}$$

$$\left.\begin{array}{rcl} \ell^{\pm} + A & \xrightarrow{W^{\pm}} & (\overline{\nu})\nu + X \\ (\overline{\nu})\nu + A & \xrightarrow{W^{\pm}} & \ell^{\pm} + X \end{array}\right\} \quad \text{Charged Current.} \tag{2.3}$$

Reactions where the final state lepton is a neutrino represent a significant experimental challenge because of the immense difficulty in detecting this neutrino. Experiments have been proposed to measure cross-sections for these processes, however they rely on determining the missing transverse momentum in the final state X or on "likelihood" estimates [12].

Neutrino DIS has two significant shortcomings, one is the difficulty in accurately determining the energy and momentum of the initial neutrino and the another is that the target must be very large (e.g. several tonnes of iron) because of the very small neutrino cross-sections. This makes polarized DIS extremely difficult. The experimental benefit of charged current neutrino DIS is its quark flavour sensitivity (a consequence of charge conservation) and this is the impetus behind neutrino facilities such as Fermilab.

There are three independent kinematical variables in inclusive DIS. Working in the target rest frame, where

$$P^{\mu} = (M_A, 0, 0, 0), \tag{2.4}$$

and neglecting lepton masses, these are often chosen to be

$$Q^2 \equiv -q^2 = (k' - k)^2 = 4\, E\, E' \sin^2\left(\frac{\theta}{2}\right), \tag{2.5}$$

$$s \equiv (k + P)^2 = 2\, M_A\, E + M_A^2, \tag{2.6}$$

$$W^2 \equiv P_X^2 = (P + q)^2, \tag{2.7}$$

where $E\,(E')$ is the energy of the initial (final) lepton and θ is the lepton scattering angle with respect to the incoming lepton beam. The interpretation of these quantities is: Q^2 is the negative of the time-like four-momentum squared transfered to the target, s is the centre-of-mass energy squared and W^2 is the squared mass of the final hadronic state. The physical region for the DIS process is

$$s \geqslant M_A^2, \qquad Q^2 \geqslant 0, \qquad W^2 \geqslant (M_A + m_\pi)^2, \tag{2.8}$$

where m_π is the pion mass. Other important invariants are

$$x = \frac{Q^2}{2\,P\cdot q} = \frac{Q^2}{2\,M_A\,\nu}, \tag{2.9}$$

$$y = \frac{P\cdot q}{P\cdot k} = \frac{\nu}{E}, \tag{2.10}$$

$$\nu = \frac{P\cdot q}{M_A} = E - E', \tag{2.11}$$

where y is the fractional energy loss of the lepton, ν the energy transfered to the target and x (Bjorken x) is interpreted as the fraction of the nucleon momentum carried by the struck quark. We will discuss the significance of this variable in Section 2.3.[1]

Noting that $W^2 \geqslant M_A^2$ it is easy to show using Eqs. (2.7) and (2.11) that the Bjorken scaling variable x lies in the range $0 < x \leqslant 1$ and that the fractional energy loss is bound by $0 \leqslant y \leqslant 1$. Further, using Eq. (2.7) we find

$$x = 1 - \frac{W^2 - M_A^2}{2P\cdot q}. \tag{2.12}$$

Therefore $x = 1$ implies $W^2 = M_A^2$ and hence the $x = 1$ limit corresponds to elastic scattering. Rearranging Eq. (2.12) gives

$$x = \frac{1}{1 + (W^2 - M_A^2)/Q^2}, \tag{2.13}$$

which implies that any state X with fixed mass, for example resonance production, can only contribute very near $x = 1$ in the deep inelastic limit.

2.2 Cross-Sections and Structure Functions

Experimentally what is measured is the differential cross section. Using the usual rules [13, 14], the scattering cross-section for inclusive DIS is [15]

$$d\sigma = \frac{1}{4J}\frac{d^3k'}{2E'(2\pi)^3}\sum_X\prod_{i=1}^{n_X}\int\frac{d^3p_i}{(2\pi)^3 2E_i}\,|\mathcal{M}|^2\,(2\pi)^4\delta^4\left(P + q - \sum_{i=1}^{n_X} p_i\right), \tag{2.14}$$

where $J = P\cdot k$ is the flux factor, which equals $J = 4\,M_A\,E$ in the target rest frame. The sum is over all final hadronic states X, each consisting of n_X particles

[1] In this chapter we shall denote the target scaling variable simply by x, to avoid cluttering the notation. However in Chapter 6 where we discuss nuclear targets, the target scaling variable will be x_A and the variable x is reserved for the nucleon.

which are not observed. Assuming that the Lorentz invariant squared-amplitude only has a contribution from one photon exchange we have

$$|\mathcal{M}|^2 = \sum_{s'} \left| \bar{u}(k',s')\gamma^\mu u(k,s) \, \frac{ie^2 g_{\mu\nu}}{q^2} \, \langle X|J^\nu(0)|P,s_N\rangle \right|^2 . \tag{2.15}$$

Therefore the DIS differential cross-section can be written as the product of two tensors

$$d\sigma = \frac{1}{4J} \frac{d^3k'}{2E'(2\pi)^3} \frac{e^4}{Q^4} 2\pi \, L_{\mu\nu} W^{\mu\nu}, \tag{2.16}$$

where $L_{\mu\nu}$ is the leptonic tensor defined by

$$\begin{aligned} L^{\mu\nu} &\equiv \sum_{s'} \left| \bar{u}(k',s')\gamma^\mu u(k,s) \right|^2, \\ &= 2\left(k^\mu \, k'^\nu + k^\nu \, k'^\mu - g^{\mu\nu} k \cdot k' + i\,\varepsilon^{\mu\nu\lambda\sigma} q_\lambda \, k_\sigma\right), \end{aligned} \tag{2.17}$$

and the hadronic tensor, $W^{\mu\nu}$, has the form

$$\begin{aligned} W_{\mu\nu} &\equiv \frac{1}{2\pi} \sum_{X_i} \prod_{i=1}^{n_X} \int \frac{d^3p_i}{(2\pi)^3 2E_i} \delta^4\left(p+q-p_X\right) \left| \langle X_i | J_\nu(0) | p, s_A \rangle \right|^2, \\ &= \frac{1}{2\pi} \int d\xi \, e^{i\,q\cdot\xi} \, \langle P,S | J_\mu(\xi) \, J_\nu(0) | P,S \rangle, \\ &= \frac{1}{2\pi} \int d\xi \, e^{i\,q\cdot\xi} \, \langle P,S | [J_\mu(\xi), J_\nu(0)] | P,S \rangle. \end{aligned} \tag{2.18}$$

The full derivation of the leptonic and hadronic tensors is given in Appendix B. Therefore in the target rest frame Eq. (2.14) reads

$$\frac{d\sigma}{d\Omega \, dE'} = \frac{\alpha_{\rm em}^2}{2\,M_A\,Q^4} \frac{E'}{E} \, L_{\mu\nu} W^{\mu\nu}, \tag{2.19}$$

where $\alpha_{\rm em} = e^2/4\pi$ and Ω is the solid angle into which the lepton scatters.[2]

In Fig. 2.2 we give a diagrammatic representation of the leptonic and hadronic tensors. We see that the lepton tensor is purely perturbative and can be determined fully using Quantum Electrodynamics (QED), however the hadronic tensor contains highly non-perturbative quark-gluon interactions and therefore cannot be calculated using perturbative QCD.

As illustrated in Fig. 2.1, the exchange of Z^0 gauge bosons can play a role in DIS processes. Therefore, if there exists both electromagnetic and neutral

[2]In deriving this expression the result $k'_\mu = E'(1, \sin\theta\cos\phi, \sin\theta\sin\phi, \cos\theta)$ is useful.

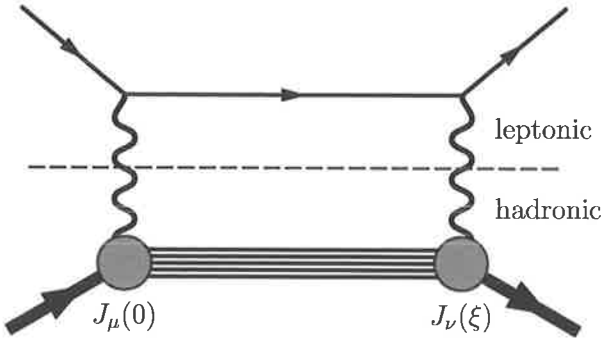

Figure 2.2: Diagrammatic representation of the perturbative leptonic tensor and the non-perturbative hadronic tensor in the one boson exchange approximation. The electroweak current, J_μ, is inserted at the origin and removed at position ξ.

current exchange, the squared amplitude has the form $|\mathcal{M}|^2 = |\mathcal{M}_\gamma + \mathcal{M}_Z|^2$. Hence there are three terms; a purely electromagnetic term, $|\mathcal{M}_\gamma|^2$, a purely weak term, $|\mathcal{M}_Z|^2$, and an interference term of the form $\mathcal{M}_\gamma \mathcal{M}_Z^* + \mathcal{M}_Z \mathcal{M}_\gamma^*$. It is easy to show, following similar steps that led to Eq. (2.19), that the full differential cross-section including both γ and Z^0 exchange, is given by

$$\frac{d\sigma_{nc}}{d\Omega\, dE'} = \frac{\alpha_{\rm em}^2}{2\, M_A\, Q^4}\frac{E'}{E} \sum_{i=\gamma,\gamma Z,Z} L^i_{\mu\nu} W_i^{\mu\nu}\, \eta^i, \tag{2.20}$$

where

$$\eta^\gamma = 1, \qquad \eta^{\gamma Z} = \left(\frac{G_F\, M_Z^2}{2\sqrt{2}\,\pi\alpha_{\rm em}}\right)\left(\frac{Q^2}{Q^2 + M_Z^2}\right), \qquad \eta^Z = \left(\eta^{\gamma Z}\right)^2, \tag{2.21}$$

and

$$L^{\gamma Z}_{\mu\nu} = (g_V - \lambda g_A) L^\gamma_{\mu\nu}, \qquad L^Z_{\mu\nu} = (g_V - \lambda g_A)^2 L^\gamma_{\mu\nu}. \tag{2.22}$$

The sign of the incoming lepton helicity is denoted by λ, therefore $\lambda = \pm 1$. The relations in Eq. (2.22) hold for negatively charged incoming leptons, for positively charged leptons one simply replaces g_A by $-g_A$, where [16] [3]

$$g_V = -\frac{1}{2} + 2\sin^2\theta_W, \qquad g_A = -\frac{1}{2}. \tag{2.23}$$

The charged current cross-section is given by an analogous expression to that in Eq. (2.20) except that the sum is over the appropriate W boson and

$$\eta^W = \frac{1}{2}\left(\frac{G_F\, M_W^2}{4\,\pi\alpha_{\rm em}}\right)\left(\frac{Q^2}{Q^2 + M_W^2}\right), \qquad L^{W^\pm}_{\mu\nu} = (1 \pm 2\lambda)^2\, L^\gamma_{\mu\nu}. \tag{2.24}$$

[3]The coupling constants g_V and g_A discussed here should not be confused with the vector and axial-vector coupling associated with the baryon number and Bjorken sum rules.

The interesting physics in DIS is contained in the hadronic tensor, which from a theoretical standpoint is extremely difficult to calculate. The most general form of the hadronic tensor that is both Lorentz and CP invariant can be expressed in terms of eight independent structure functions F_1^i, F_2^i, F_3^i, g_1^i, g_2^i, g_3^i, g_4^i, g_5^i and has the form

$$\begin{aligned} W_{\mu\nu}^i = & -2g_{\mu\nu}\, F_1^i + \frac{2P_\mu P_\nu}{P\cdot q}\, F_2^i + i\frac{\varepsilon_{\mu\nu\alpha\beta}}{P\cdot q} P^\alpha q^\beta\, F_3^i \\ & + i\frac{2M_A\varepsilon_{\mu\nu\alpha\beta}}{P\cdot q}\left[q^\alpha S^\beta\, g_1^i - 2xP^\alpha S^\beta\, g_2^i\right] - \frac{2M_A}{P\cdot q}\left[P_\mu S_\nu + S_\mu P_\nu\right] g_3^i \\ & + 2M_A\frac{S\cdot q}{(P\cdot q)^2} P_\mu P_\nu\, g_4^i + 2M_A\frac{S\cdot q}{P\cdot q} g_{\mu\nu}\, g_5^i, \end{aligned} \tag{2.25}$$

where $i \in \gamma,\ \gamma Z, Z, W^\pm$. In deriving Eq. (2.25) we can ignore terms proportional to q^μ and q^ν, as these terms do not contribute to the cross-section, since the lepton tensor is conserved, that is $q^\mu L_{\mu\nu} = q^\nu L_{\mu\nu} = 0$. The structure functions F_j^i, g_j^i are functions of x and Q^2 and are expected to scale in the Bjorken limit, that is $F_j^i(x, Q^2) \to F_j^i(x)$ and $g_j^i(x, Q^2) \to g_j^i(x)$ as $Q^2 \to \infty$. The weak interaction is parity violating hence Eq. (2.25) contains both second rank tensors and pseudo-tensors. However, in the case of purely electromagnetic interaction (i.e. one photon exchange), which is parity conserving, we have

$$F_3^\gamma = g_3^\gamma = g_4^\gamma = g_5^\gamma = 0. \tag{2.26}$$

Restricting ourselves to the purely electromagnetic case for simplicity we can now obtain the differential cross-section in terms of the structure functions. If we sum over the initial electron helicities in Eq. (2.19) we obtain the unpolarized cross-section, which has the form

$$\frac{d\bar{\sigma}}{dxdyd\phi} = \frac{e^4}{4\pi^2 Q^2}\left\{\frac{y}{2}F_1(x,Q^2) + \frac{1}{2xy}\left(1 - y - \frac{y^2}{4}(\kappa - 1)F_2(x,Q^2)\right)\right\}, \tag{2.27}$$

where $\kappa = 1 - \frac{4x^2M_A^2}{Q^2}$. Instead, if the difference between the positive and negative lepton helicity cross-sections is taken, access to the spin-dependent structure functions is possible. The spin-dependent cross-section is given by

$$\frac{d\Delta\sigma}{dxdyd\phi} = \frac{e^4}{4\pi^2 Q^2}\left\{\left[1 - \frac{y}{2} - \frac{y^2}{4}(\kappa - 1)\right] g_1(x,Q^2) - \frac{y}{2}(\kappa - 1) g_2(x,Q^2)\right\}, \tag{2.28}$$

where we have assumed that the target is polarized parallel to the lepton beam. In obtaining these expressions the following result is useful:

$$\frac{d\sigma}{dxdyd\phi} = \frac{M_A\,\nu}{E'}\frac{d\sigma}{dE'd\Omega}. \tag{2.29}$$

2.3 Quark-Parton Model and Bjorken Scaling

In 1968 (based on current algebra arguments) Bjorken predicted [1] that in the limit

$$Q^2,\ \nu \longrightarrow \infty \quad \text{with} \quad x = \text{fixed}, \tag{2.30}$$

the (spin-independent) structure functions would become independent of Q^2, that is

$$F_1(x, Q^2) \longrightarrow F_1(x), \qquad F_2(x, Q^2) \longrightarrow F_2(x). \tag{2.31}$$

This kinematical limit is now known as the Bjorken or scaling limit. Bjorken's prediction was almost immediately observed at SLAC [17–19] and was the impetus behind the famous parton model of Feynman [20, 21].

The parton model, which assumes that the nucleon is made of point-like constituents called partons (which were later identified as the quarks and gluons) still plays a fundamental role in our understanding of high energy scattering within QCD. In particular, the parton picture provides a connection between perturbative QCD and hadrons, a connection that has thus far not been derived from QCD itself.

The principal assumption of the quark-parton model is that the quarks inside the target can be treated as free massless particles. For historical reasons it has therefore been conventional to formulate the parton model in the *infinite momentum frame*[4]. Time dilation effects were then used to argue that the interactions between the partons can be ignored, on the time scale relevant to the parton probe interaction. However this is slightly erroneous, the true reason partons can be treated as free is because of asymptotic freedom, not a particular choice of reference frame.

The hadron tensor in the parton model is given by the *handbag diagram* which is illustrated in Fig. 2.3. It is easy to show within the parton model that all other diagrams are suppressed by at least $1/Q^2$ and hence approach zero in the Bjorken limit [22].[5] When deriving the parton model it is assumed the target is made of collinear moving partons each with a fraction ξ_i of the total target momentum (where $0 < \xi_i \leqslant 1$ and $\sum_i \xi_i = 1$). The contribution to the hadronic

[4] In the infinite momentum frame the target is assumed to have momentum $P^\mu = (P + M_A^2/(2P), 0, 0, -P)$ where $P \longrightarrow \infty$.

[5] This is also true in full QCD, as a careful use of the operator product expansion (OPE) can demonstrate.

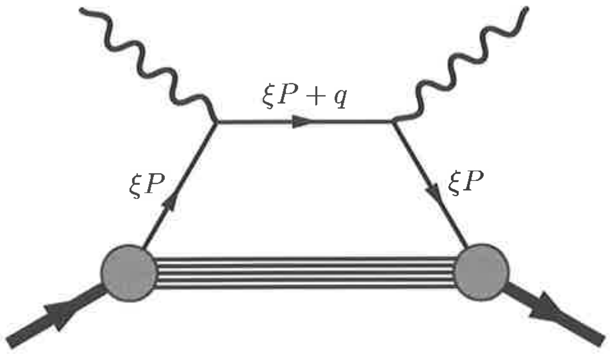

Figure 2.3: This diagram represents the hadronic tensor in the parton model and is known as the handbag diagram (c.f. Fig. 2.2). It can be rigorously shown in QCD, using the OPE, that in the Bjorken limit this is the only diagram that contributes to the hadronic tensor, as all other diagrams are suppressed by at least $1/Q^2$.

tensor from a single parton is therefore given by

$$\begin{aligned} w_{\mu\nu} &= \frac{1}{2\pi}\frac{1}{\xi}\int \frac{d^3p'}{(2\pi)^3 2E_{p'}}(2\pi)^4\delta^4\left(\xi P + q - p'\right)\left|\langle \xi P, s|J_\mu(0)|p', s'\rangle\right|^2, \\ &= \frac{1}{2\pi}\frac{1}{\xi}e_q^2\int \frac{d^3p'}{(2\pi)^3 2E_{p'}}(2\pi)^4\delta^4\left(\xi P + q - p'\right)\left|\overline{u}(\xi P, s)\,\gamma_\mu u(p', s')\right|^2, \end{aligned} \tag{2.32}$$

where e_q^2 is the charge of the parton and the factor $1/\xi$ comes from converting the parton flux factor in the cross-section to that of the nucleon, since $E \simeq \xi E_N$. Using the identity

$$\int \frac{d^3p'}{(2\pi)^3 2E_{p'}} = \int \frac{d^4p'}{(2\pi)^4}\delta\left[(\xi P + q - p')^2\right] = \int \frac{d^4p'}{(2\pi)^4}\frac{2\pi}{2P\cdot q}\delta\left(\xi + \frac{q^2}{2P\cdot q}\right), \tag{2.33}$$

and performing an analogous calculation to that of the lepton tensor given in Appendix B we obtain

$$w_{\mu\nu} = \frac{e_q^2}{2\xi P\cdot q}\left(2\xi^2 P_\nu P_\nu - g_{\mu\nu}\xi P\cdot q + i\lambda\,\xi\varepsilon_{\mu\nu\alpha\beta}q^\alpha P^\beta\right)\delta(\xi - x), \tag{2.34}$$

where we have used $p' = \xi P + q$ and $s_\beta = \lambda\xi P_\beta$ (here λ is the parton helicity). Therefore the parton model implies $x = \xi$ and hence the Bjorken scaling variable, x, is interpreted as the fraction of the target momentum carried by the struck parton. The final step in obtaining the full hadronic tensor in the parton model is to integrate over ξ weighted by the probability to find a parton with momentum fraction ξ and helicity λ. To achieve this we define the quark distribution functions $q_+(\xi)$ and $q_-(\xi)$ to be the probability to strike a quark with momentum fraction ξ and helicity parallel (+) or anti-parallel (−) to the target helicity. Therefore the full hadronic tensor is

$$\begin{aligned}W_{\mu\nu} &= \sum_q \int_0^1 d\xi\ [q_+(\xi) w_{\mu\nu} + q_-(\xi) w_{\mu\nu}]\,, \\ &= -2g_{\mu\nu} \sum_q \frac{e_q^2}{2} [q_+(x) + q_-(x)] + \frac{2P_\mu P_\nu}{P\cdot q} \sum_q e_q^2\, x\, [q_+(x) + q_-(x)] \\ &\quad + i\frac{2\varepsilon_{\mu\nu\alpha\beta}}{P\cdot q} q^\alpha P^\beta \sum_q \frac{e_q^2}{2} [q_+(x) - q_-(x)]\,. \end{aligned} \tag{2.35}$$

Comparing Eq. (2.35) with the electromagnetic part of the hadronic tensor given in Eq. (2.25), we obtain the familiar parton model formulas for the structure functions, namely

$$F_1(x) = \frac{1}{2}\sum_q e_q^2\ [q(x) + \bar{q}(x)]\,, \tag{2.36}$$

$$F_2(x) = x\sum_q e_q^2\ [q(x) + \bar{q}(x)]\,, \tag{2.37}$$

$$g_1(x) = \frac{1}{2}\sum_q e_q^2\ [\Delta q(x) + \Delta\bar{q}(x)]\,, \tag{2.38}$$

$$g_2(x) = 0. \tag{2.39}$$

In Eqs. (2.36)–(2.39) we have defined the spin-independent quark distribution as $q(x) \equiv q_+(x) + q_-(x)$ and the spin-dependent quark distribution as $\Delta q(x) \equiv q_+(x) - q_-(x)$. We have also included the contributions from the anti-quarks in Eqs. (2.36)–(2.39), which can be derived in an analogous manner to the quarks. Analogous parton model expressions can also be derived for the neutral and charged current structure functions, these results can be found in, for example, Ref. [23].

An important feature of this result is that the structure functions have no Q^2 dependence and hence the parton model provides a very clear physical interpretation of Bjorken scaling. Another feature of this result is the relation

$$F_2(x) = 2x\, F_1(x), \tag{2.40}$$

which is known as the Callen-Gross relation [24].[6] This identity is only approx-

[6]The experimental confirmation of the Callan-Gross relation indicates that the quarks have spin-$\frac{1}{2}$, because for example, if the quarks had zero spin we would have

$$\langle \xi P\,|J_\mu|\,\xi P + q\rangle \propto 2\xi P_\mu + q_\mu,$$

which would imply $F_1(x) = 0$.

imately true in QCD, as it is broken by the perturbative gluon field.

The continuing importance of the parton model lies in the fact that it remains valid in QCD, where it is viewed as a zeroth order result. The α_s corrections can be determined using perturbative QCD, which we will discuss further in Section 2.5 when we examine structure function factorization.

2.4 Lightcone dominance

Recall that the hadronic tensor is given by

$$W_{\mu\nu} = \frac{1}{2\pi} \int d\xi \, e^{i q \cdot \xi} \, \langle P, S | [J_\mu(\xi), J_\nu(0)] | P, S \rangle, \tag{2.41}$$

where ξ is the distance between the two current insertions. To determine the important distance scales in DIS we must examine the integral in Eq. (2.41). The Riemann-Lebesgue lemma states

$$\lim_{|q| \to \infty} \int_a^b d\xi \, e^{i\xi q} \, f(\xi) = 0, \tag{2.42}$$

for any Riemann-integrable function in the domain $a \leqslant \xi \leqslant b$. Therefore $W_{\mu\nu}$ will be dominated by the region where $|q \cdot \xi|$ is finite. The dot-product $q \cdot \xi$ is Lorentz invariant, so we choose to work in the target rest frame with the incident photon moving in the z-direction, therefore

$$q = \left(\nu, 0, 0, -\sqrt{\nu^2 + Q^2}\right). \tag{2.43}$$

In the Bjorken limit this becomes

$$q \to (\nu, 0, 0, -\nu - M_A \, x) \, . \tag{2.44}$$

Introducing lightcone coordinates where

$$q^\pm \equiv \frac{1}{\sqrt{2}} \left(q^0 \pm q^3\right), \tag{2.45}$$

we see that in the Bjorken limit $q^- \to \infty$ and $q^+ \to -M_A \, x/\sqrt{2}$. Therefore a finite $|q \cdot \xi|$ requires $\xi^+ \sim 0$ and $|\xi^-| \sim \sqrt{2}/(M_A \, x)$.[7]

To maintain causality the commutator in Eq. (2.41) must vanish for $\xi^2 < 0$ [14] and hence, since $\xi^2 = 2\xi^+\xi^- - \vec{\xi}_\perp^{\,2}$, this implies $\vec{\xi}_\perp \to 0$. Therefore all

[7]The dot-product in lightcone coordinates is given by $a \cdot b = a^+b^- + a^-b^+ - \vec{a}_\perp \vec{b}_\perp$.

components of ξ^μ vanish in the Bjorken limit except ξ^-, and thus DIS is not a short distance phenomenon ($\xi^\mu \to 0$), but is instead a lightcone dominated ($\xi^2 \to 0$) process. In fact the two constraints $\xi^+ \to 0$ and $\xi^- \sim \sqrt{2}/(M_A\, x)$ imply $|\xi^0| \sim |\xi^3| \sim 1/(M_A\, x)$. From this relation we can get a feel for how far the struck quark propagates, for example with $x = 0.5$ we have $\xi^3 \sim 0.4\,\text{fm}$, similarly $x \sim 0.05$ implies $\xi^3 \sim 4\,\text{fm}$. Therefore as x becomes small the quark-quark correlation length probed by DIS gets rather large, and when compared to the size of the nucleon can definitely not be considered short distance.

2.5 Factorization and Quark Distributions

In general a hadronic cross-section includes contributions from both short and long distance physics, contains mass singularities and is infrared divergent. Therefore hadronic cross-sections cannot be computed using perturbative QCD. Factorization theorems state that for certain processes, in particular kinematical regimes, the hadronic cross-section can be *factorized* as a convolution of a renormalized soft non-perturbative piece and a hard scattering piece that is free of long distance singularities. The idea of factorization is nicely illustrated by the following identity

$$1 + \alpha \ln\left(\frac{q^2}{p^2}\right) + \ldots = \left[1 + \alpha \ln\left(\frac{\mu_f^2}{p^2}\right) + \ldots\right]\left[1 + \alpha \ln\left(\frac{q^2}{\mu_f^2}\right) + \ldots\right], \tag{2.46}$$

where the factorization scale, μ_f, is an appropriate scale at which this separation is valid.

For inclusive DIS cross-sections this implies that the structure functions can be written as [25, 26]

$$F_1(x, Q^2) = \sum_q \int_x^1 \frac{d\xi}{\xi}\, q_A(\xi, \mu_f, \mu)\, H_{1q}\left(\frac{x}{\xi}, \frac{Q}{\mu}, \frac{\mu_f}{\mu}, \alpha_s(\mu)\right) + \ldots, \tag{2.47}$$

$$F_2(x, Q^2) = \sum_q \int_x^1 d\xi\, q_A(\xi, \mu_f, \mu)\, H_{2q}\left(\frac{x}{\xi}, \frac{Q}{\mu}, \frac{\mu_f}{\mu}, \alpha_s(\mu)\right) + \ldots, \tag{2.48}$$

$$g_1(x, Q^2) = \sum_q \int_x^1 \frac{d\xi}{\xi}\, \Delta q_A(\xi, \mu_f, \mu)\, G_{1q}\left(\frac{x}{\xi}, \frac{Q}{\mu}, \frac{\mu_f}{\mu}, \alpha_s(\mu)\right) + \ldots. \tag{2.49}$$

The ellipsis $(\ldots)$ represent higher twist contributions and terms of order $\mathcal{O}\left(p^2/\mu_f^2\right)$. This factorization of the DIS cross-section has been proven to all orders in perturbation theory [27] and is the basis of all other cross-section factorizations, for example the Drell-Yan reactions and semi-inclusive DIS.

The hard scattering functions, H_{iq}, are infrared finite and calculable in perturbation theory. In general they depend on the type of exchanged electroweak vector boson and the type of parton, but are completely independent of long distance interactions. The functions q_A, Δq_A are the parton distributions discussed in Section 2.3 and contain all the long distance non-perturbative effects of the original cross-section. These functions depend on the type of target, A, but have no dependence on the probe which is used to measure them. This important result gives rise to the notion of the universality of the parton distribution functions [28]. This means, for example, that each structure function in Eq. (2.25), with $i \in \gamma,\ Z^0,\ \gamma Z^0,\ W^{\pm}$, can be expressed in terms of the same quark distributions, with only the hard coefficient functions differing.

The universal nature of the quark distributions greatly increases the predictive power and utility of QCD, since, for example, these functions can be measured in DIS experiments at Jefferson lab or Hermes and then used as inputs in analysing the pp collisions at the Large Hadron Collider (LHC) at CERN.

At twist-two for a spin-$\frac{1}{2}$ target like the nucleon, there are three independent quark distribution functions for each quark flavour. These are the spin-independent distribution, $q(x)$, the helicity or spin-dependent distribution $\Delta q(x)$ and the transversity or traverse polarization distribution $\Delta_T q(x)$ [29]. This can be seen by inspecting the Dirac structure of the nucleon wavefunction in the Bjorken limit [29] or by analysing the number of independent helicity amplitudes [30].

All three distributions yield a probabilistic interpretation: $q(x)$ is the probability of striking a quark with longitudinal momentum fraction x of the parent hadron, $\Delta q(x)$ measures the number density of quarks with spin parallel to the target minus those with spin anti-parallel, each with momentum fraction x of a longitudinally polarized target. If we define the quantities $q_{\pm}(x)$ as the number densities of quarks with helicity $\pm\frac{1}{2}$, as in Sections 2.3, then we have

$$q(x) = q_+(x) + q_-(x), \tag{2.50}$$

$$\Delta q(x) = q_+(x) - q_-(x). \tag{2.51}$$

The transversity distribution has an analogous interpretation to $\Delta q(x)$ except that the hadron is transversely polarized. In a transverse basis we have

$$\Delta_T q(x) = q_{\uparrow}(x) - q_{\downarrow}(x), \tag{2.52}$$

where, $\uparrow$, denotes transverse polarization parallel to the target and, $\downarrow$, transverse polarization anti-parallel to the target. In this basis we must also have

$$q(x) = q_{\uparrow}(x) + q_{\downarrow}(x). \tag{2.53}$$

Nucleon quark distributions are defined field theoretically as lightcone Fourier transforms of forward nucleon matrix elements and are given by [29, 31]

$$q(x) = \int \frac{d\xi^-}{4\pi}\, e^{i\,x\,P^+\,\xi^-} \langle p, s\,|\overline{\psi}(0)\,\gamma^+\,\mathcal{G}\,\psi(\xi^-)|\,p, s\rangle, \tag{2.54}$$

$$\Delta q(x) = \int \frac{d\xi^-}{4\pi}\, e^{i\,x\,P^+\,\xi^-} \langle p, s\,|\overline{\psi}(0)\,\gamma^+\gamma_5\,\mathcal{G}\,\psi(\xi^-)|\,p, s\rangle, \tag{2.55}$$

$$\Delta_T q(x) = \int \frac{d\xi^-}{4\pi}\, e^{i\,x\,P^+\,\xi^-} \langle p, s\,|\overline{\psi}(0)\,\gamma^+\gamma^1\gamma_5\,\mathcal{G}\,\psi(\xi^-)|\,p, s\rangle, \tag{2.56}$$

where for the transversity distribution we have assumed that the target hadron is polarized along the x-axis. If the y-axis is chosen for the transverse polarization then one simply replaces γ^1 with γ^2 in Eq. (2.56). The factor $\mathcal{G}$ is the path dependent link operator which joins the two quark fields, rendering the definitions gauge invariant, and is given by

$$\mathcal{G} = \mathcal{P}\, e^{-ig\int_0^{\xi^-} ds_\mu\, A^\mu(s)}, \tag{2.57}$$

where $\mathcal{P}$ is the path-ordering operator and A^μ the gluon field. By working in the axial gauge, $A^+ = 0$, and by choosing an appropriate path along the lightcone we have $\mathcal{G} = 1$ [26]. Therefore, from here on we simply assume $\mathcal{G}$ is unity. The derivation of Eqs. (2.54)–(2.56) is rather tedious and the interested reader should consult Refs. [26, 29]. The basic idea is that the operator $\overline{\psi}\,\gamma^+\,\psi$ is the number operator for the "good components" of the quark wavefunctions, relevant to physics near the lightcone. The other operators with a γ_5 or $\gamma^1\gamma_5$ simply project out the desired spin components of the quark wavefunctions.

The anti-quark distributions are easily obtained from the following relations [29]

$$\overline{q}(x) = -q(-x), \tag{2.58}$$

$$\Delta\overline{q}(x) = \Delta q(-x), \tag{2.59}$$

$$\Delta_T\overline{q}(x) = -\Delta_T q(-x). \tag{2.60}$$

It is important to note that $\Delta_T q(x)$ is a chirally odd distribution, which is easily seen from the operator structure in Eq. (2.56), and therefore cannot be measured in inclusive DIS. This point will be discussed further in Section 2.7.

2.6 QCD Evolution of Quark Distributions

In the quark-parton model the quark distributions are independent of Q^2, however in QCD the quark distributions have a weak logarithmic Q^2 dependence.

In a triumph for perturbative QCD these scaling violations can be described by the DGLAP (Dokshitzer-Gribov-Lipatov, Altarelli-Parisi) evolution equations [32, 33].

The DGLAP equations can be obtained from the renormalization group equations, however this derivation is rather complicated and involves a careful use of the operator product expansion [26]. A more intuitive approach [34, 35] is simply to realize that as Q^2 increases, so does the resolving power of the probe, and therefore there is a finite probability that a single parton will be resolved as two or more partons.

With this in mind there are three classes of parton distributions: the gluon distributions, quark distributions that mix with the gluons and quark distributions that do not. The later are called non-singlet quark distributions[8] and are of the form

$$q^{\mathrm{NS}}(x) = q(x) - \bar{q}(x), \tag{2.61}$$

with the valence quark distributions, $q_v(x) \equiv q(x) - \bar{q}(x)$, being the prime example. The non-singlet evolution equation has the form

$$\frac{\partial\, q^{\mathrm{NS}}(x, Q^2)}{\partial \ln(Q^2)} = P_{qq}\big(x, \alpha_s(Q^2)\big) \otimes q^{\mathrm{NS}}(x, Q^2), \tag{2.62}$$

where the convolution product is defined as

$$P(x) \otimes q(x) \equiv \int_x^1 \frac{dz}{z}\, P\left(\frac{x}{z}\right) q(z), \tag{2.63}$$

and P_{qq} is the q-q splitting function. Physically a splitting function $P_{p'p}(x/z)$ represents the probability for a parton of type p with momentum fraction z to emit a quark or gluon, and become a parton of type p' with momentum fraction x.

Because the number of valence quarks must remain independent of the resolution of the probe we must have

$$\frac{\partial}{\partial\, \ln(Q^2)} \int_0^1 dx\, q^{\mathrm{NS}}(x, Q^2) = 0, \tag{2.64}$$

therefore using Eq. (2.62) the q-q splitting function must satisfy

$$\int_0^1 dz\, P_{qq}(z) = 0. \tag{2.65}$$

[8]The formal reason for the name is that differences of the type $q - \bar{q}$ transform as the adjoint representation of the $SU(3)$ flavour group.

Quark distributions that mix with the gluons are called singlet distributions and are of the form

$$q^{S}(x) = q(x) + \bar{q}(x). \tag{2.66}$$

These distributions appear, for example, in the structure functions F_1, F_2 and g_1. Because we have mixing between the singlet and gluon distributions the DGLAP equations are coupled and have the form

$$\frac{\partial}{\partial \ln(Q^2)} \begin{pmatrix} q^S(x,Q^2) \\ g(x,Q^2) \end{pmatrix} = \begin{pmatrix} P_{qq}\,(x,\alpha_s(Q^2)) & P_{qg}\,(x,\alpha_s(Q^2)) \\ P_{gq}\,(x,\alpha_s(Q^2)) & P_{gg}\,(x,\alpha_s(Q^2)) \end{pmatrix} \otimes \begin{pmatrix} q^S(x,Q^2) \\ g(x,Q^2) \end{pmatrix}. \tag{2.67}$$

The QCD evolution equations for the helicity distributions are analogous to Eqs. (2.62) and (2.67), with just a change of notation. For the traverse case however, there is no coupling between the quarks and gluons because of the chiral-odd nature of this distribution. Hence the transversity evolution is simply described by evolution equations of the non-singlet form, namely

$$\frac{\partial}{\partial \ln(Q^2)} \Delta_T q^-(x,Q^2) = \Delta_T P_{qq,-} \otimes \Delta_T q^-(x,Q^2), \tag{2.68}$$

$$\frac{\partial}{\partial \ln(Q^2)} \Delta_T q^+(x,Q^2) = \Delta_T P_{qq,+} \otimes \Delta_T q^+(x,Q^2), \tag{2.69}$$

where $\Delta_T q^+ = q_\uparrow + q_\downarrow$ and $\Delta_T q^- = q_\uparrow - q_\downarrow$. The splitting functions $\Delta_T P_{qq,-}$ and $\Delta_T P_{qq,+}$ are given in Ref. [36].

The reason there is no twist-2 transversity distribution for the gluon in the nucleon, is easily seen if we consider the helicity amplitude. Transverse polarization distributions are related to helicity flip amplitudes. Gluons have helicity ± 1 and hence to conserve angular momentum the nucleon must undergo a helicity change of ± 2, which is clearly not possible. However, for higher spin targets like the deuteron or ρ, helicity conservation can be satisfied. Therefore, gluon transversity distributions do exist for targets with $J \geqslant 1$ and hence transversity singlet quark distributions will couple to the gluons.

The splitting functions are calculated in perturbative QCD, with an expansion of the form

$$P(z,Q^2) = \left(\frac{\alpha_s}{2\pi}\right) P^{(0)}(z) + \left(\frac{\alpha_s}{2\pi}\right)^2 P^{(1)}(z) + \ldots \tag{2.70}$$

where $P^{(0)}$ is the leading order (LO) and $P^{(1)}$ is the next-to-leading order (NLO) result. Expressions up to NNLO for all three distributions can be found in Ref. [37] and in Fig. (2.4) we give the diagrams that contribute at LO. For a

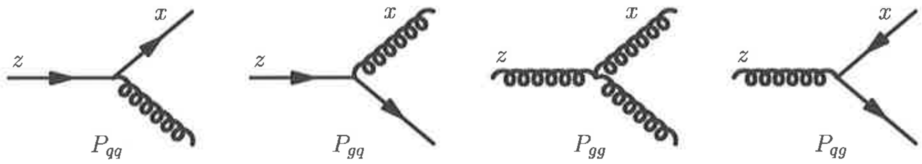

Figure 2.4: These diagrams are the LO splitting functions that form the kernel of the evolution equations. The function $P_{p'p}$ is the probability for a parton of type p with momentum fraction z to emit a particle (a quark or gluon) and become a parton of type p' with momentum fraction x.

consistent solution of the DGLAP equations we also require α_s up to the order we are working. The NLO result is

$$\alpha_s(Q^2) = \frac{4\pi}{\beta_0} \frac{1}{\ln(Q_\Lambda)} \left[1 - \frac{\beta_1}{\beta_0} \frac{\ln\ln(Q_\Lambda)}{\ln(Q_\Lambda)} + \mathcal{O}\left(\frac{1}{\ln^2(Q_\Lambda)} \right) \right], \tag{2.71}$$

where

$$Q_\Lambda = \frac{Q^2}{\Lambda^2_{QCD}}, \quad \beta_0 = \frac{11}{3} N_C - \frac{4}{3} T_f, \quad \beta_1 = \frac{34}{3} N_C^2 - \frac{10}{3} N_C n_f - 2 C_F n_f, \tag{2.72}$$

and N_C is the number of colours, n_f the number of active flavors and $C_F = 4/3$. The value of Λ_{QCD} depends on the number of active flavours and the renormalization scheme, in the $\overline{MS}$ scheme typical values are [36]

$$\Lambda_{QCD}^{(n_f=3,4,5,6)} = (0.248, 0.200, 0.131, 0.050) \text{ GeV}. \tag{2.73}$$

From a theoretical viewpoint determining the number of active flavours is non-trivial. In the $\overline{MS}$ scheme the renormalization scale for a heavy quark is usually chosen as $\mu_q = m_q$, therefore as a rule of thumb n_f is the number of quarks with $m_q \leqslant Q$. For a discussion on the role of the charm quark and in particular charm quark thresholds in the nucleon, see, for example Ref. [38].

Solving the DGLAP equations is non-trivial and must be done numerically, except in the special case of LO non-singlet equation. There are several computer codes available which solve these equations, with algorithms based on Mellin moments [39], Laguerre expansions [40–42], recursion relations [36,37] or "brute force" techniques [43–45]. In this work we utilize the latter approach.

2.7 Transversity Cross-sections

Despite its fundamental importance there is currently no experimental information on $\Delta_T q(x)$. The reason that the transversity distribution is not observable in inclusive DIS is that it is chirally odd and the electroweak and strong interactions conserve chirality. Therefore $\Delta_T q(x)$ must couple to another chiral-odd function which is not possible in inclusive DIS. However $\Delta_T q(x)$ appears in certain semi-inclusive DIS reactions and also in hadronic reactions like Drell-Yan [46].

The Drell-Yan process is the reaction

$$A + B \longrightarrow \ell^- + \ell^+ + X, \tag{2.74}$$

where A and B are initial hadrons which collide producing a virtual photon which decays into a lepton–anti-lepton pair and X is the unobserved hadronic final states as in DIS. The Drell-Yan double spin asymmetry

$$A_{TT} \equiv \frac{d\sigma^{\uparrow\uparrow} - d\sigma^{\uparrow\downarrow}}{d\sigma^{\uparrow\uparrow} + d\sigma^{\uparrow\downarrow}}, \tag{2.75}$$

for two transversely polarized protons, $p^\uparrow p^\uparrow \longrightarrow \ell^- \ell^+ + X$, at leading order in the parton model is given by [29]

$$A_{TT}^{pp} \propto \frac{\sum_q e_q^2 \left[\Delta_T q(x_1, Q^2)\, \Delta_T \bar{q}(x_2, Q^2) + \Delta_T q(x_2, Q^2)\, \Delta_T \bar{q}(x_1, Q^2)\right]}{\sum_q e_q^2 \left[q(x_1, Q^2)\, \bar{q}(x_2, Q^2) + q(x_2, Q^2)\, \bar{q}(x_1, Q^2)\right]}. \tag{2.76}$$

We see that $\Delta_T q(x)$ appears with $\Delta_T \bar{q}(x)$ and hence the product is chirally even. However $\Delta_T \bar{q}(x)$ is expected to be small for $x \gtrsim 0.2$ and the size of this asymmetry is expected to be only a few percent.

A more promising reaction is Drell-Yan with protons and anti-protons. In this case the double spin asymmetry is given by

$$A_{TT}^{p\bar{p}} \propto \frac{\sum_q e_q^2 \left[\Delta_T q(x_1, Q^2)\, \Delta_T q(x_2, Q^2) + \Delta_T \bar{q}(x_2, Q^2)\, \Delta_T \bar{q}(x_1, Q^2)\right]}{\sum_q e_q^2 \left[q(x_1, Q^2)\, \bar{q}(x_2, Q^2) + \bar{q}(x_2, Q^2)\, \bar{q}(x_1, Q^2)\right]}. \tag{2.77}$$

This reaction provides one of the few processes that give direct access to the transversity distributions. Predictions for this asymmetry were calculated in Refs. [47, 48] where saturation of the Soffer inequality [49]

$$2\,|\Delta_T q(x)| \leqslant q(x) + \Delta q(x), \tag{2.78}$$

was assumed. An effect of the order 20-40% was found.

For semi-inclusive DIS there are broadly three different processes that give access to the transversity distributions [29]. These are semi-inclusive DIS on a transversely polarized target with lepton-production of

- a transversely polarized hadron,
- an unpolarized hadron,
- two hadrons.

For semi-inclusive DIS the measured asymmetries involve the product of the transversity distribution with a chiral-odd fragmentation function, which describes the probability for a quark with momentum fraction x to "fragment" in a particular hadron. To do this topic justice would take us too far afield, so we refer the interested reader to Ref. [29].

The major drawback of semi-inclusive DIS transversity experiments is that they do not give direct access to the transversity distributions, only to their product with the poorly known fragmentation functions. Hence the most promising experimental process is Drell-Yan with transversely polarized protons and anti-protons which gives a direct measurement of $\Delta_T q$ (see Eq. 2.77), however these experiments are still in the proposal stage [50].

2.8 Summary

In this chapter we have tried to give an brief overview of deep inelastic scattering on a spin-$\frac{1}{2}$ target, in particular the nucleon. We have seen that the structure functions which parametrize the DIS cross-section can be factorized into a hard part calculable in perturbative QCD (the coefficient functions) and a soft non-perturbative piece – the quark distributions – that currently remains incalculable in QCD. We have tried to emphasize the important role the parton model plays in our modern QCD based understanding of the strong interaction. In particular, how the model provides a physical connection between perturbative QCD, based on the QCD Lagrangian, and the inherently non-perturbative bound states – the mesons and baryons – which are detected in experiments.

Notable omissions from this chapter include a discussion of the operator product expansion (OPE) (which gives rise to the twist expansion) and also the renormalization group equations. Thorough treatments of these topics can be found in many standard texts, for example Refs. [46, 51–53].

3

Nambu–Jona-Lasinio Model

Quantum Chromodynamics (QCD) is almost universally accepted as the theory that correctly describes the strong interaction. The utility of QCD has been convincingly demonstrated for hard processes in the large momentum transfer regime, where asymptotic freedom permits a meaningful perturbative expansion. However, at low energies or large distances where the QCD coupling is large, the theory remains poorly understood. In fact, there is currently no *ab initio* calculation of a hadronic observable in the non-perturbative sector of QCD.

At the moment the most direct method with which to gain access to the long distance behaviour of QCD is to evaluate the path integral on a 4-dimensional space-time lattice, that is, lattice QCD. This method has its own problems however, the most pressing of which is its computational intensity. Nobody knows exactly how much computing power is needed to perform a realistic calculation at physical quark masses, as the behaviour of QCD as a function of m_q is unknown. However, the minimum requirement is probably several hundred tetraflops [54]. In addition, finite density lattice QCD calculations appear to be formidable, if not an impossibility, even for the modest densities of nuclear matter. This is because the introduction of a chemical potential into the QCD Lagrangian results in a complex path integral measure, which renders standard importance sampling techniques unusable.

With this in mind, the importance of models that have strong overlap with the underlying theory and wide ranging applicability cannot be overstated. These models should posses many of the same symmetries as the full theory, exhibit relevant symmetry breaking mechanisms and also include important phenomenological constraints. The candidate model that we consider here, which meets all these requirements, is the Nambu–Jona-Lasinio (NJL) model [55, 56], regularized using the Schwinger proper-time scheme [57, 58].

The NJL model was first proposed by Y. Nambu and G. Jona-Lasinio in the early sixties as an effective theory of strongly interacting particles, which at the time were primarily the nucleon and pion. Motivation for the NJL model was derived from the BCS theory of superconductivity [59, 60], which today is interpreted as a low energy effective of QED, although this link has not be proven.

With the advent of QCD the NJL model was initially criticized because of its non-fundamental nature, but was soon re-expressed as an effective theory of QCD in terms of quark degrees of freedom. Since then, the NJL model has achieved considerable success in the study of a vast array of strong interaction phenomena. For example, the vacuum structure of QCD [61], the meson and baryon spectrum [62] and nuclear physics applications such as neutron and quark stars [63, 64].

In this chapter we will give a brief review of the NJL model with a focus on the constraints imposed by chiral symmetry and the Faddeev description of baryons.

3.1 NJL Lagrangian and Regularization

The non-renormalized QCD Lagrangian has the form [46]

$$\mathcal{L}_{QCD} = \overline{\psi}\left(i\not{D} - m_q\right)\psi - \frac{1}{4}\mathcal{F}^a_{\mu\nu}\mathcal{F}^{\mu\nu}_a, \tag{3.1}$$

where $\not{D}$ is the covariant derivative, m_q is the quark mass matrix and $\mathcal{F}^a_{\mu\nu}$ the gluon field strength tensor [46]. The known symmetries of QCD are

$$\mathcal{S} = SU(N_f)_L \otimes SU(N_f)_R \otimes SU(N_c) \otimes U(1)_V \otimes C \otimes P \otimes T, \tag{3.2}$$

where N_f is the number of flavors, N_c the number of colours, $SU(N_f)_L \otimes SU(N_f)_R$ is the chiral symmetry (realized as $m_q \to 0$), $SU(N_c)$ the colour gauge symmetry, $U(1)_V$ is the baryon number symmetry and CPT are the usual discrete symmetries. Note, the QCD Lagrangian has an axial $U(1)$ symmetry, but this is broken by the QCD vacuum and hence is not a symmetry of the theory [46].

The NJL model is the minimal chiral effective theory of QCD involving only quark degrees of freedom (the gluon degrees of freedom have been absorbed into the effective coupling). The general form of the NJL Lagrangian is

$$\mathcal{L}_{NJL} = \overline{\psi}\left(i\not{\partial} - m_q\right)\psi + \mathcal{L}_{4q} + \mathcal{L}_{6q} + \ldots \tag{3.3}$$

where $\mathcal{L}_{4q}$, $\mathcal{L}_{6q}$, etc are the 4-, 6-quark interaction terms. The 6-quark term is introduced to explicitly break the axial $U(1)$ symmetry in the $SU(3)_F$ NJL model. It is usually taken to have the 't Hooft determinant form [65]

$$\mathcal{L}_{6q} = K\left\{\det\left[\overline{\psi}\left(1+\gamma_5\right)\psi\right] + \det\left[\overline{\psi}\left(1-\gamma_5\right)\psi\right]\right\}, \tag{3.4}$$

where K is the effective coupling. This term has been used extensively in NJL model studies [62, 66, 67], especially in the meson sector where it provides a mechanism to induce the η–η' mass splitting [62]. However its use should be treated with caution, as it has been argued in Ref. [68–70] that the consequences of the dynamical breaking of the $U(1)_A$ symmetry in QCD, cannot be modelled by adding an explicit symmetry breaking term to any effective Lagrangian.

Further, and potentially more troublesome, is the fact that the inclusion of the 't Hooft term gives rise to an effective potential that is unbounded from below [71, 72]. An immediate consequence of which is an unstable pion with respect to the strong interactions. The authors in Refs. [71, 72] propose the introduction of an 8-quark interaction term, $\mathcal{L}_{8q}$, along with the usual 't Hooft term. They find a stable vacuum, provided certain inequalities between the effective couplings are satisfied. However the problem of explicitly breaking the $U(1)$ axial symmetry remains.

In this work we restrict ourselves to the 4-quark interaction only, and view the dynamical breaking of the $U(1)$ axial symmetry as a very interesting open question within the NJL model. Moreover, the focus here is on baryons, in the quark–diquark approximation, and the 't Hooft term does not directly influence diquark structure, since there cannot be any flavour singlet diquarks. Consequently, in the quark–diquark approximation to the baryon sector, the effects of the 't Hooft term can simply be incorporated via a renormalization of the 4-Fermi coupling constants.

There have been many 4-Fermi interaction Lagrangians utilized in the literature, in the original paper the form was

$$\mathcal{L}_{4q} = G\left[\left(\overline{\psi}\psi\right)^2 - \left(\overline{\psi}\gamma_5\vec{\tau}\psi\right)^2\right]. \tag{3.5}$$

Another popular choice is the so-called colour-current interaction Lagrangian used in Refs. [62, 73, 74], which has the form

$$\mathcal{L}_{4q} = -G\sum_{c=1}^{8}\left(\overline{\psi}\gamma_\mu\tfrac{1}{2}\lambda_c\psi\right)^2, \tag{3.6}$$

where λ_c are the SU(3) Gell-Mann matrices. In this work we do not choose a particular form for the 4-quark interaction. Instead we use a Fierz symmetrized

Lagrangian	G_π/G	G_s/G	G_a/G
$G\left[(1,1)-(\gamma_5\tau_i,\gamma_5\tau_i)\right]$	$\frac{13}{12}$	$\frac{1}{6}$	$\frac{1}{12}$
$G\left[(\frac{1}{2}\lambda_c,\frac{1}{2}\lambda_c)-(\frac{1}{2}\lambda_c\gamma_5\tau_i,\frac{1}{2}\lambda_c\gamma_5\tau_i)\right]$	$\frac{1}{9}$	$-\frac{1}{9}$	$-\frac{1}{18}$
$G(\gamma_\mu,\gamma^\mu)$	$-\frac{1}{6}$	$\frac{1}{6}$	$\frac{1}{12}$
$G(\frac{1}{2}\lambda_c\gamma_\mu,\frac{1}{2}\lambda_c\gamma^\mu)$	$-\frac{2}{9}$	$-\frac{1}{9}$	$-\frac{1}{18}$
$G(\gamma_\mu\gamma_5,\gamma^\mu\gamma_5)$	$\frac{1}{6}$	$\frac{1}{6}$	$-\frac{1}{12}$
$G(\frac{1}{2}\lambda_c\gamma_\mu\gamma_5,\frac{1}{2}\lambda_c\gamma^\mu\gamma_5)$	$\frac{2}{9}$	$-\frac{1}{9}$	$\frac{1}{18}$

Table 3.1: This table is reproduced from Ref. [75]. The left column refers to the different interaction Lagrangians where, $(\Gamma_1,\Gamma_2)\equiv(\overline{\psi}\Gamma_1\psi)(\overline{\psi}\Gamma_2\psi)$ and the remaining columns indicate the interaction strength in the pionic, scalar diquark and axial-vector diquark channels.

form of the Lagrangian, where the interaction strength in a particular channel can be read off directly (see Ref. [75] for further details) and exchange terms are automatically included. Then different choices for the initial interaction Lagrangian simply result in differing coupling strengths in each particular channel. In Table 3.1 we illustrate this by giving examples for the pionic $\overline{q}q$ and diquark qq channel, where we include both scalar and axial-vector terms.

In this work we relax the constraints on the coupling G_π, G_s, G_a, etc implied by the Fierz transformation and simply treat these couplings as free parameters, to be fixed phenomenologically. In this way we use the physics to determine $\mathcal{L}_I$. It should always be possible work backward to find an interaction Lagrangian that gives the desired coupling under Fierz transformation, if one is sufficiently keen.

The NJL model is non-renormalizable, which is easily seen, for example, by the fact that the effective coupling constants are dimensionful. Therefore to fully define the model one must specify the regularization scheme. The most important feature of the regularization scheme is that it must preserve as many of the symmetries as possible. For the NJL model this means in particular that it should be covariant and not break chiral symmetry.

There are in principle an infinite number of regularization schemes. Here we quickly review some popular examples that have been utilized in NJL model studies. In all cases discussed below the regularization is in momentum space, we denote the integration variable by p and the regularization scale by Λ:

- **Three-momentum cutoff**: In this scheme one integrates over p_0, then imposes the constraint $\vec{p}^2 < \Lambda^2$. The main drawback of this approach is that it is non-covariant.

- **Euclidean four-momentum cutoff**: Here one Wick rotates and imposes the constraint $p_E^2 < \Lambda^2$.

- **Pauli-Villars**: This method is implemented via the following modification to a product of quark propagators [76]

$$\prod_{j=1}^{N} \frac{1}{k_j^2 - M^2} \longrightarrow \sum_{i=0}^{n} c_i \left\{ \prod_{j=1}^{N} \frac{1}{k_j^2 - M^2 - \Lambda_i^2} \right\}, \tag{3.7}$$

  where $c_0 = 1$, $\Lambda_0 = 0$ and an arbitrary number (n) of regulating masses Λ_i and constants c_i have been introduced. To guarantee convergence of the loop integrals the following conditions must be satisfied

$$\sum_i c_i = 0, \qquad \sum_i c_i \Lambda_i^2 = 0. \tag{3.8}$$

  Therefore $n \geqslant 2$ is required. Pauli-Villars is attractive because it preserves gauge invariance, but in the NJL context it explicitly breaks chiral symmetry through the introduction of the regulating masses, which cannot be taken to infinity.

- **Proper-time**: In the NJL context this method is implemented on a product of propagators by first introducing Feynman parametrization, then Wick rotating and finally using the result [57, 58]

$$\frac{1}{X^n} = \frac{1}{(n-1)!} \int_0^\infty d\tau \tau^{n-1} e^{-\tau X} \longrightarrow \frac{1}{(n-1)!} \int_{1/\Lambda_{UV}^2}^{1/\Lambda_{IR}^2} d\tau \tau^{n-1} e^{-\tau X}. \tag{3.9}$$

  Here X is the result after introducing the Feynman parametrization and performing Wick rotation. To render divergent loop integrals finite it is only necessary to introduce the UV cutoff, however we will also include the infrared cutoff, Λ_{IR}. The infrared cutoff removes the imaginary piece of the loop integrals and hence eliminates the unphysical thresholds for hadron decay into quarks, thereby simulating an important aspect of confinement.

Throughout this thesis we will utilize the Schwinger proper-time regularization scheme. An important caveat in the regularization of the NJL model is that it is usual to assume that the regularization scheme respects all symmetries. That is, one can freely shift integration variables, etc, and only at the end is the regularization introduced.

Figure 3.1: Diagrammatic representation of the gap equation. The bold line represents the propagator of the dynamically generated massive (constituent) quark, while the thin line is the current quark propagator.

3.2 Gap Equation and Dynamical Mass Generation

The gap equation is a one-body equation that describes the interaction of a particle with the vacuum. This equation is represented diagrammatically in Fig. 3.1, for the NJL model. For a parity conserving and Lorentz invariant vacuum, in the mean-field approximation, the only non-zero contribution to the fermion loop in Fig. 3.1 is from the scalar 4-Fermi interaction, that is $(\overline{\psi}\psi)^2$ [62][1]. Therefore, in the NJL model the gap equation has the form

$$M = m_q + 2iG_\pi \lim_{y \to x^+} \mathrm{Tr}\left[S_F(x-y)\right], \tag{3.10}$$

where M is the dynamically generated quark mass, m_q the current quark mass in the NJL Lagrangian and G_π is the coupling in the scalar $\overline{q}q$ channel. In the mean-field approximation the $\overline{q}q$ condensate is given by [62]

$$\langle\overline{\psi}\psi\rangle = -i \lim_{y \to x^+} \mathrm{Tr}\left[S_F(x-y)\right]. \tag{3.11}$$

Hence the gap equation can be expressed as

$$M = m_q - 2G_\pi\langle\overline{\psi}\psi\rangle. \tag{3.12}$$

Evaluating Eq. (3.10) using proper-time regularization gives

$$M = m_q + \frac{3}{\pi^2}\, M\, G_\pi \int d\tau \frac{1}{\tau^2}\, e^{-\tau M^2}, \tag{3.13}$$

where the integral is appropriately regularized (Section A.12 presents a derivation of this result).[2]

[1]For additional arguments that also consider the $1/N$ expansion, see for example Ref. [77]

[2]Throughout this thesis we will regularly leave absent the integration limits on the proper-time integration over τ. However, in each case the integration limits are implied in the sense of Eq. (3.9).

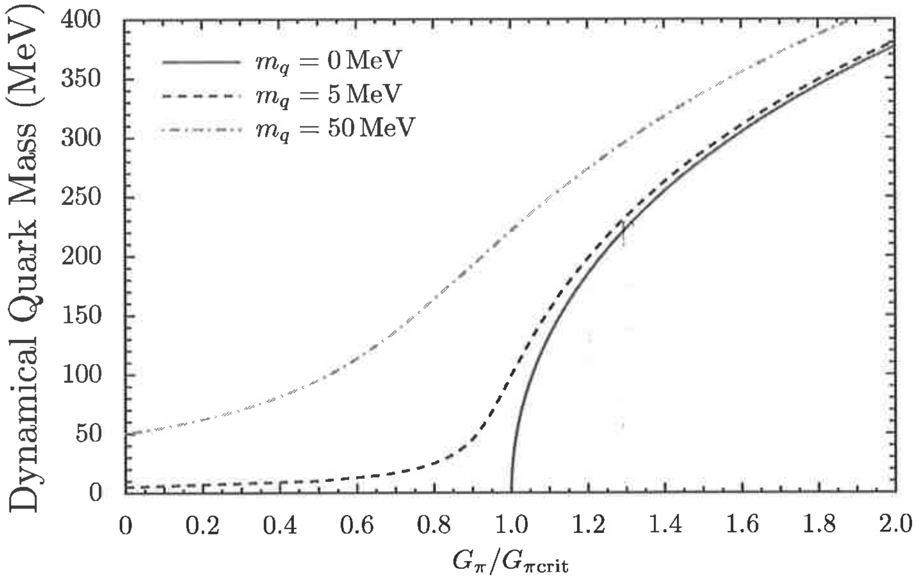

Figure 3.2: Dynamical quark mass generation as a function of $G_\pi/G_{\pi\mathrm{crit}}$.

It is clear that Eq. (3.13) permits a trivial solution when $G_\pi = 0$, however if G_π is large there also exists a non-perturbative solution. If $m_q = 0$ this critical coupling is given by

$$G_{\pi\mathrm{crit}} = \frac{\pi^2}{3}\left(\Lambda_{UV}^2 - \Lambda_{IR}^2\right)^{-1}. \tag{3.14}$$

From Eq. (3.12) we see that if $M \neq m_q$ then $\langle\overline{\psi}\psi\rangle \neq 0$, hence dynamical mass generation is also associated with the generation of a non-zero chiral condensate. In Fig. 3.2 we plot solutions of Eq. (3.13) as a function of $G_\pi/G_{\pi\mathrm{crit}}$. In the chiral limit with $G_\pi < G_{\pi\mathrm{crit}}$ we see that both the quark mass and hence also the chiral condensate are zero, this is the Wigner-Weyl phase. For $G_\pi > G_{\pi\mathrm{crit}}$ the chiral condensate becomes non-zero and we are in the Nambu-Goldstone phase where chiral symmetry has been dynamically broken.

Chiral symmetry and its breaking play a pivotal role in low energy QCD. In this section we have tried to demonstrate that the NJL model provides a transparent mechanism for the breaking of chiral symmetry and is an excellent tool with which to study this phenomenon.

3.3 The Pion and Chiral Symmetry

The usual method with which to study the pion and other mesons in the NJL model, is to solve the relativistic two-body bound state equation, that is, the

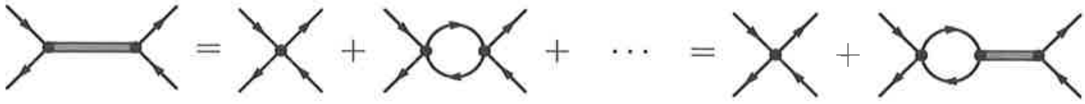

Figure 3.3: Beth-Salpeter equation for a quark and an anti-quark. The shaded line represents the meson t-matrix and the solid lines represent a dressed quark propagator.

Bethe-Salpeter equation (BSE) [78]. The Bethe-Salpeter equation for mesons in the NJL model is represented diagrammatically in Fig. (3.3) and is given analytically by [75]

$$\mathcal{T}_{\alpha\beta,\gamma\delta}(k) = \mathcal{K}_{\alpha\beta,\gamma\delta} + \int \frac{d^4q}{(2\pi)^4} K_{\alpha\beta,\lambda\varepsilon}\, S_{\varepsilon\varepsilon'}(k+q)\, S_{\lambda\lambda'}(q)\, \mathcal{T}_{\varepsilon'\lambda',\gamma\delta}(k). \tag{3.15}$$

In Eq. (3.15) the two-body t-matrix is denoted by $\mathcal{T}$, S is the fermion propagtor, K is the appropriate interaction kernel and the indices label Dirac, isospin and colour degrees of freedom.

For the pion the interaction kernel has the form

$$K_{\alpha\beta,\gamma\delta} = -2i\, G_\pi\, (\gamma_5\tau_i)_{\alpha\beta}(\gamma_5\tau_i)_{\gamma\delta}. \tag{3.16}$$

The solution to the Bethe-Salpeter equation is given by

$$\mathcal{T}_{\alpha\beta,\gamma\delta}(k) = (\gamma_5\tau_i)_{\alpha\beta}\, \tau_\pi(k)\, (\gamma_5\tau_i)_{\gamma\delta}, \tag{3.17}$$

where

$$\tau_\pi(k) = \frac{-2G_\pi}{1+2G_\pi\, \Pi_\pi(k^2)}, \tag{3.18}$$

and the quark–anti-quark bubble graph has the form

$$\Pi_\pi(k^2) = 6i \int \frac{d^4q}{(2\pi)^4} \mathrm{Tr}\left[\gamma_5\, S(q)\gamma_5 S_F(k+q)\right]. \tag{3.19}$$

The mass of the pion is then given by the pole in the t-matrix, that is

$$1 + 2G_\pi\, \Pi_\pi(k^2 = m_\pi^2) = 0. \tag{3.20}$$

It is easy to show that

$$\Pi_\pi(m_\pi^2) = -\frac{3}{2\pi^2}\int d\tau \frac{1}{\tau^2}\, e^{-\tau M^2} - \frac{3}{4\pi^2} m_\pi^2\, I(m_\pi^2), \tag{3.21}$$

where

$$I(m_\pi^2) = \int_0^1 d\alpha \int d\tau \frac{1}{\tau^2}\, e^{-\tau\left[m_\pi^2(\alpha^2-\alpha)+M^2\right]}. \tag{3.22}$$

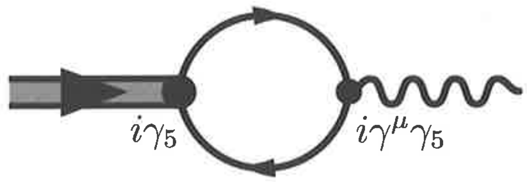

Figure 3.4: Diagram representing pion decay in the NJL model.

Therefore, using the gap equation result given in Eq. (3.13), we obtain the following expression

$$m_\pi^2 = -\frac{m_q}{M}\frac{1}{\frac{3}{2\pi^2}\,G_\pi\,I(m_\pi^2)}. \tag{3.23}$$

We have therefore derived the important result that the pion mass vanishes in the correct chiral limit, that is $m_q \longrightarrow 0$, not $M \longrightarrow 0$.

Another important pionic observable is the pion decay constant, f_π, which is defined via the matrix element

$$\langle 0\left|\overline{\psi}\gamma_\mu\gamma_5\tfrac{1}{2}\tau_a\right|\pi_b(q)\rangle = i\,f_\pi\,q_\mu\delta_{ab}, \tag{3.24}$$

where π_b is a pion with isospin b. For the NJL model, the diagrammatic representation of this matrix element is given in Fig. 3.4. Analytically, Eq. (3.24) can be expressed as

$$i\,f_\pi\,q_\mu = 3\sqrt{g_\pi}\int\frac{d^4k}{(2\pi)^2}\,\mathrm{Tr}\left[\gamma_5\,S(k)\,\gamma\!\!/\mu\gamma_5\,S(k-q)\right], \tag{3.25}$$

where g_π is the effective pion–quark-quark coupling, defined by

$$\begin{aligned} g_\pi^{-1} &= -\partial\,\Pi_\pi(q^2)/\partial q^2\big|_{q^2=m_\pi^2} \\ &= \frac{3}{4\pi^2}\int_0^1 d\alpha\int d\tau\left[\frac{1}{\tau^2}-m_\pi^2(\alpha^2-\alpha)\right]\,e^{-\tau\left[m_\pi^2(\alpha^2-\alpha)+M^2\right]}. \end{aligned} \tag{3.26}$$

With this result, the gap equation (Eq. (3.12)) and the pion mass condition (Eq. (3.23)), it is easy to obtain the following expression

$$f_\pi^2 m_\pi^2 \simeq -m_q\langle\overline{\psi}\psi\rangle. \tag{3.27}$$

This result is the first-order approximation to the Gell-Mann–Oakes–Renner current algebra relation [79], given by

$$f_\pi^2 m_\pi^2 = -\frac{1}{2}\,(m_u+m_d)\,\langle\overline{u}u+\overline{d}d\rangle. \tag{3.28}$$

In this section we have explicitly demonstrated that the key consequences of chiral symmetry are not destroyed by the introduction of the proper-time regularization scheme to the NJL model.

3.4 Baryons

Any model framework for hadrons must include a description of baryons, however because of their minimal 3-quark nature they are notoriously difficult to model. There have been many different approaches in the literature, ranging from the MIT and cloudy bag models, to solitons and lattice QCD. Within the NJL model, two approaches are popular, the soliton approach motivated by the large N_c expansion of QCD and the Faddeev framework, that is, solving the relativistic 3-body bound state equation.

The solitonic approach originates from work by 't Hooft that showed in the limit of a large number of colours, N_c, QCD can be regarded as an effective theory of mesons and glueballs [80]. Subsequently, it was argued by Witten [81,82], but not proven, that baryons emerge as solitonic solutions of this underlining mesonic theory. For a review of this approach see for example Refs. [77,83].

The 3-body Faddeev approach for baryons, which is the focus of this section, can be seen as the natural extension of the 2-body Bethe-Salpeter formalism used successfully in the meson sector. In this section we will outline a derivation of the relativistic three-body Faddeev equations [74,84,85], for a general introduction to the 3-body problem see Refs. [86–89].

The complete solution to the relativistic 3-body problem is encapsulated by the Dyson equation for the 3-body propagator. In operator form the Dyson equation is given by

$$G = G_0 + G_0\, K\, G, \tag{3.29}$$

where G_0 is the product of three quark-propagators and K is the interaction kernel, which contains all 2- and 3-quark irreducible diagrams. The formal solution of Eq. (3.29) is

$$G = \frac{G_0}{1 - G_0\, K}, \tag{3.30}$$

which makes sense mathematically, but it is difficult to interpret physically. If we introduce the "Faddeev approximation", which is to neglect all 3-quark irreducible diagrams, the interaction kernel can be written as

$$K = K_1 + K_2 + K_3. \tag{3.31}$$

Here K_i represents the kernel for the interaction of quarks j and k, where quark i is a spectator. It is convenient to introduce the 2-body propagtor in the 3-body Hilbert space, g_i, which satisfies the equation

$$g_i = G_0 + G_0\, K_i\, g_i. \tag{3.32}$$

The general solution of this equation is

$$g_i = \frac{G_0}{1 - G_0\, K_i}. \tag{3.33}$$

Using the identity

$$\frac{1}{1 - G_0\, K} = \frac{1}{1 - G_0\, K_i} + \frac{G_0}{1 - G_0\, K_i}\,(K_j + K_k)\,\frac{1}{1 - G_0\, K}, \tag{3.34}$$

we can express Eq. (3.29) in the form

$$G = g_i + g_i(K_j + K_k)G. \tag{3.35}$$

The 2-body t-matrix in the 3-body Hilbert space, $\tilde{t}_i$, is obtained by amputating all external quark legs from the connected part of g_i, and satisfies

$$g_i = \left(1 + G_0\, \tilde{t}_i\right) G_0. \tag{3.36}$$

It is easy to show using the above result and Eq. (3.35) that the 2-body t-matrix, $\tilde{t}_i$, also satisfies

$$\tilde{t}_i = K_i + K_i\, G_0\, \tilde{t}_i. \tag{3.37}$$

Using the Faddeev decomposition of G, which is

$$G = G_0 + G_1 + G_2 + G_3, \qquad G_i = G_0\, K_i\, G, \quad i = 1,\ 2,\ 3, \tag{3.38}$$

and Eq. (3.36) we obtain

$$G_i = G_0\, \tilde{t}_i\, G_0 + G_0\, \tilde{t}_i\, (G_j + G_k)\,. \tag{3.39}$$

The three-body t-matrix is given by $T = \sum_i T_i$, where $G_i = G_0\, T_i\, G_0$ and each component satisfies

$$T_i = \tilde{t}_i + \tilde{t}_i\, G_0\, (G_j + G_k)\,. \tag{3.40}$$

These coupled 4-dimensional equations are the familiar Faddeev equations, which relate the Faddeev three-body components, T_i, to the full 2-quark t-matrix in the three-body Hilbert space, $\tilde{t}_i$. Where $\tilde{t}_i$ are obtained as solutions of Eq. (3.37).

We can simplify this result slightly by noting that the Faddeev components T_i contain reducible three-body processes, and that these can be separated via the introduction of quantities Y_{ij} which satisfy

$$T_i = \tilde{t}_i + \sum_m \tilde{t}_i\, Y_{im}\, \tilde{t}_m. \tag{3.41}$$

Physically the term $\tilde{t}_i\, Y_{im}\, \tilde{t}_m$ describes three-body irreducible processes where the pair j interacts first and the pair i second. If we now introduce the quantities $X_{ji} = S_{Fj}^{-1}\, Y_{ij}\, S_{Fi}^{-1}$, the Faddeev equation can be expressed as [75]

$$X_{ji} = \bar{\delta}_{ijk} S_{Fk} + \sum_{\ell\ell'} S_{F\ell}\, S_{F\ell'}\, t_\ell\, X_{ji}, \tag{3.42}$$

$$T_i = t_i\, S_{Fi}^{-1} + \sum_m t_i\, X_{im}\, t_m, \tag{3.43}$$

$$T = \sum_i T_i, \tag{3.44}$$

where $\bar{\delta}_{ijk} = 1$ if $i \neq j \neq k$ or zero otherwise. The usual two-body t-matrix in Eqs (3.42) and (3.43) is related to $\tilde{t}_i$ by, $\tilde{t}_i = t_i\, S_{Fi}^{-1}$.

The Faddeev equations, expressed in Eqs. (3.42)–(3.44), are in principle far simpler to solve than the original 8-dimensional Dyson equation, given in Eq. (3.29). However, solving these equations is still a formidable task and it is necessary to make further approximations, in particular assumptions regarding the form of the 2-quark t-matrix, $\tilde{t}_i$, are usually made.

In the derivation so far we have not assumed a particular form for the interaction kernel, K. However, the 4-Fermi interaction of the NJL model is separable, and this facilitates a significant simplification of Eq. (3.42). For the general case of a separable interaction the Faddeev equation has been reduced to an effective two-body equation, describing the scattering of a quark on a pair of quarks (quasi-particle). The resulting simplification to Eq. (3.42) is a Fredholm integral equation of the second kind, which in operator form is given by

$$X = Z + K\, X, \tag{3.45}$$

or explicitly

$$X^{\beta\alpha}(p',p) = Z^{\beta\alpha}(p',p) + \int \frac{d^4p''}{(2\pi)^4}\, Z^{\beta\gamma}(p',p'')\, S_F^{\gamma\delta}\left(\tfrac{1}{2}P + p''\right)\, \tau\left(\tfrac{1}{2}P - p''\right) X^{\delta\alpha}(p,p''). \tag{3.46}$$

The full derivation of this result can be found in Ref. [75]. In Eq. (3.46), τ, is the two-body t-matrix for the two-quark quasi-particle, and we associate this particle with a diquark in the nucleon. In Fig. 3.5 we illustrate Eq. (3.46) diagrammatically. All that remains is to specify the form of the interaction kernel, from which we can determine the form of $Z^{\beta\alpha}$ and the two-body t-matrix τ.

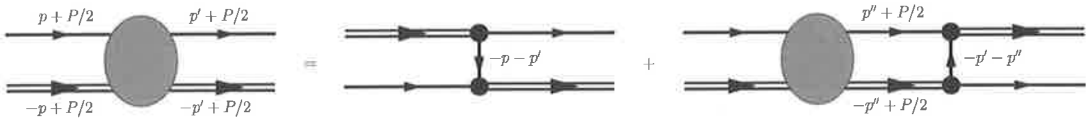

Figure 3.5: Diagrammatic representation of the Faddeev equation expressed in Eq. (3.46). The single line is a quark and the double line represents a diquark.

In this work the baryon two-body components are restricted to the scalar and axial-vector diquarks. The NJL interaction Lagrangians in these channels are respectively

$$\mathcal{L}_s = G_s\left(\overline{\psi}\,\gamma_5 C\tau_2\beta^A\,\overline{\psi}^T\right)\left(\psi\, C^{-1}\gamma_5\tau_2\beta^A\overline{\psi}^T\right), \tag{3.47}$$

$$\mathcal{L}_a = G_a\left(\overline{\psi}\,\gamma_\mu C\tau_i\tau_2\beta^A\,\overline{\psi}^T\right)\left(\psi\, C^{-1}\gamma^\mu\tau_i\tau_2\beta^A\,\overline{\psi}^T\right). \tag{3.48}$$

Performing the colour and isospin projections the $T=\frac{1}{2}$ quark exchange kernel becomes [75]

$$Z(p',p) = -3\begin{pmatrix} \gamma_5\, S_F(p'+p)\,\gamma_5 & \sqrt{3}\gamma^\mu\, S_F(p'+p)\,\gamma_5 \\ \sqrt{3}\gamma_5\, S_F(p'+p)\,\gamma^\mu & -\gamma^\mu\, S_F(p'+p)\,\gamma^{\mu'} \end{pmatrix}, \tag{3.49}$$

and the $T=\frac{3}{2}$ quark exchange kernel is [75]

$$Z(p',p) = -6\left(\gamma^\mu\, S_F(p'+p)\,\gamma^{\mu'}\right). \tag{3.50}$$

The kernel in Eq. (3.50) only contains the axial-vector two-body channel and after spin projection it will correspond to the Delta baryon. The kernel given in Eq. (3.49), which after spin-projection will correspond to the nucleon, contains both scalar and axial-vector diquarks, where the off-diagonal terms represent coupling between these two channels. For details of the spin-projection see Ref. [75]. The full Faddeev kernel is therefore

$$K = Z(p',p)\, S_F\left(\tfrac{1}{2}P+p\right)\tau\left(\tfrac{1}{2}P-p\right). \tag{3.51}$$

Throughout this work we will employ the "static-approximation" [74] to the quark exchange kernel. That is, we neglect the momentum dependence of the exchanged quark, therefore $S_F(p'+p) \to -\frac{1}{M}$ in Eqs. (3.49) and (3.50). The quark exchange kernel for the nucleon therefore becomes

$$Z = \frac{3}{M}\begin{pmatrix} 1 & \sqrt{3}\gamma^\mu\gamma_5 \\ \sqrt{3}\gamma_5\,\gamma^\mu & -\gamma^\mu\,\gamma^{\mu'} \end{pmatrix}, \tag{3.52}$$

while for the Delta we simply have

$$Z = \frac{6}{M}\left(\gamma^{\mu}\,\gamma^{\mu'}\right). \tag{3.53}$$

We make this approximation because we wish to study the nucleon at finite density. Therefore we require a good description of nuclear matter, in particular we need nuclear matter saturation. It was demonstrated in Ref. [58], that in the NJL model this seems to be achievable only by using proper-time regularization. This scheme has the added advantage that it simulates some important aspects of confinement. However it obscures the pole structure of the Faddeev equation, making a full numerical solution very difficult.

In the static approximation to the NJL model, the nucleon T-matrix satisfies the equation

$$T = Z + K\,T = Z + Z\,\Pi_N\,T, \tag{3.54}$$

or equivalently

$$T = Z + T\,\overline{K} = Z + T\,\Pi_N\,Z, \tag{3.55}$$

where Z is given in Eq. (3.52) and Π_N represents the nucleon quark-diquark bubble graph. Including both scalar and axial-vector diquarks the nucleon bubble graph is given by

$$\Pi_N^{cd}(p) = \int \frac{d^4q}{(2\pi)^4}\,\tau^{cd}(q)\,S(p-k), \tag{3.56}$$

where

$$\tau^{cd}(q) = \begin{pmatrix} \tau_s(q) & 0 \\ 0 & \tau_a^{\mu\nu}(q) \end{pmatrix}. \tag{3.57}$$

The quantities $\tau_s(q)$ and $\tau_a^{\mu\nu}(q)$ in Eq. (3.57) are solutions of the Bethe-Salpeter equation in the scalar and axial-vector diquark channels, respectively. These diquark t-matrices have the form [75]

$$\tau_\pi(q) = \frac{-2iG_\pi}{1 + 2\,G_\pi\,\Pi_s(q^2)}, \tag{3.58}$$

$$\tau_a^{\mu\nu}(q) = 4\,i\,G_a\left[g^{\mu\nu} - \frac{2G_a\Pi_a(q^2)}{1+2G_a\Pi_a(q^2)}\left(g^{\mu\nu} - \frac{q^\mu\,q^\nu}{q^2}\right)\right], \tag{3.59}$$

where the quark-quark bubble graphs are given by

$$\Pi_s(q^2) = 6i\int \frac{d^4k}{(2\pi)^4}\,\mathrm{Tr}\Big[\gamma_5\,S(k)\,\gamma_5\,S(k-q)\Big], \tag{3.60}$$

$$\Pi_a(q^2)\left(g^{\mu\nu} - \frac{q^\mu\,q^\nu}{M_a^2}\right) = 6i\int \frac{d^4k}{(2\pi)^4}\,\mathrm{Tr}\Big[\gamma^\mu\,S(k)\,\gamma^\nu\,S(k-q)\Big]. \tag{3.61}$$

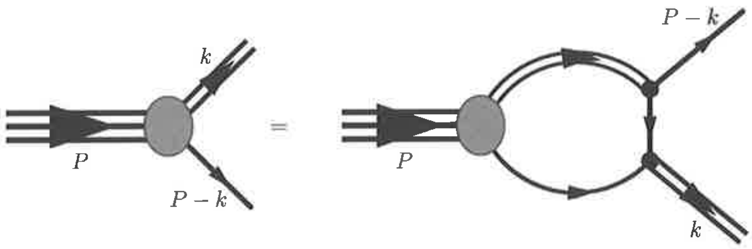

Figure 3.6: The diagrammatic representation of the homogeneous Faddeev equation expressed in Eq. (3.65). The shaded area represents the nucleon vertex, the single line represents a quark and the double line a diquark.

Explicit expressions for these bubble graphs are given in Section A.8.

In the lightcone normalization, the three-body T-matrix near a three-body bound state of mass M_N, behaves as

$$T \longrightarrow \frac{\Gamma_N \overline{\Gamma}_N}{p_+ - \varepsilon_p}, \tag{3.62}$$

where $\varepsilon_p = \frac{M_N^2}{2p_-}$. This defines the three-body vertex function Γ_N. Therefore near this T-matrix pole Eqs. (3.54) and (3.55) become

$$\Gamma_N \overline{\Gamma}_N = (p_+ - \varepsilon_p)\, Z + Z\, \Pi_N\, \Gamma_N\, \overline{\Gamma}_N, \tag{3.63}$$
$$\Gamma_N \overline{\Gamma}_N = (p_+ - \varepsilon_p)\, Z + \Gamma_N\, \overline{\Gamma}_N\, \Pi_N\, Z. \tag{3.64}$$

Taking the limit $p_+ \longrightarrow \varepsilon_p$, we obtain the homogeneous Faddeev equations for the nucleon vertex and conjugate vertex functions (in the static approximation), that is

$$\Gamma_N = Z\, \Pi_N\, \Gamma_N = K\, \Gamma_N, \tag{3.65}$$
$$\overline{\Gamma}_N = \overline{\Gamma}_N\, \Pi_N\, Z = \overline{\Gamma}_N\, \overline{K}. \tag{3.66}$$

A diagrammatic representation of the homogeneous Faddeev equation for the nucleon vertex function, Γ_N, is given in Fig. 3.6.

In Ref. [90] the form of the nucleon vertex function in the static approximation was obtained. In the lightcone normalization this result becomes

$$\begin{aligned}\Gamma_N(p,s) &= \sqrt{-Z_N \tfrac{M_N}{p_-}} \begin{bmatrix} \Gamma \\ \Gamma^\mu \end{bmatrix}, \\ &= \sqrt{-Z_N \tfrac{M_N}{p_-}} \begin{bmatrix} \alpha_1 \\ \alpha_2\, \frac{p^\mu}{M_N}\, \gamma_5 \;+ \alpha_3\, \gamma^\mu \gamma_5 \end{bmatrix} u_N(p,s),\end{aligned} \tag{3.67}$$

where Z_N is the nucleon vertex normalization (see Section C.3 for its definition and its explicit form). To solve for the conjugate spinor we note

$$\overline{K} = U\left(\gamma_0\, K^\dagger\, \gamma_0\right) U, \tag{3.68}$$

where

$$U = \begin{pmatrix} 1 & 0 \\ 0 & -1 \end{pmatrix}. \tag{3.69}$$

Taking the hermitian conjugate of the Faddeev equation for the nucleon spinor we obtain

$$\Gamma_N^\dagger = \Gamma_N^\dagger\, K^\dagger. \tag{3.70}$$

Multiplying from the right by $\gamma_o\, U$ and inserting $\gamma_o\, U\, U\, \gamma_0 = \mathbb{1}$, we obtain

$$\Gamma_N^\dagger\, \gamma_o\, U = \Gamma_N^\dagger\, \gamma_o\, U\left(U\, \gamma_0\, K^\dagger\, \gamma_o\, U\right) = \left(\Gamma_N^\dagger\, \gamma_o\, U\right) \overline{K}. \tag{3.71}$$

Therefore the conjugate vertex function must have the form

$$\overline{\Gamma}_N(p,s) = \left(\Gamma_N^\dagger\, \gamma_0\right) U. \tag{3.72}$$

We obtain

$$\begin{aligned} \overline{\Gamma}_N(p,s) &= \sqrt{-Z_N \tfrac{M_N}{p_-}}\left[\overline{\Gamma} \quad \overline{\Gamma}^\mu\right], \\ &= \overline{u}_N(p,s)\sqrt{-Z_N \tfrac{M_N}{p_-}}\left[\alpha_1 \quad \left(\alpha_2\, \tfrac{p^\mu}{M_N}\, \gamma_5 \, + \alpha_3\, \gamma_5 \gamma^\mu\right)\right]. \end{aligned} \tag{3.73}$$

3.5 Summary

In this chapter we have given a brief introduction to the NJL model, its initial motivation and its utility in the description of both mesons and baryons. In particular we have demonstrated that the NJL model encapsulates much of the phenomenology demanded by chiral symmetry. For example, quark masses are dynamically generated in the NJL model, with this mass generation explicitly linked to the formation of a non-zero chiral condensate. We have also shown that the Gell-Mann–Oakes–Renner relation is satisfied and that in the limit of vanishing current quark mass we have $m_\pi^2 \to 0$.

A large section of the chapter was focused on baryons, where we utilized the Faddeev framework to solve the three-body bound state problem. This method is superior to the mean-field methods of Refs. [91, 92] and complements the bosonization approach of Ref. [83]. The advantage of solving the Faddeev equation is that the nucleon bound state is obtained in terms of the quark degrees of freedom. This maintains a strong connection to the Bethe-Salpeter framework, which has proven to be very successful in NJL model studies of the meson sector.

4

Quark Distributions from the Nambu–Jona-Lasinio model

The discovery in the late 1980's by the European Muon Collaboration (EMC) that the fraction of the spin of the proton carried by the quarks is unexpectedly small [2], caused much excitement in the nuclear and particle physics communities. The "proton spin crisis" prompted many new experiments, leading to major new insights into the spin structure of the proton. Recent experiments at Hermes [93], using semi-inclusive DIS, have also made some headway in determining the transverse spin structure of the nucleon. Future experiments, possibly at Jefferson Lab [94], promise further exciting results, enabling for the first time a thorough experimental determination of the entire triplet of the twist-two quark distributions. However, a thorough theoretical understanding of these non-perturbative parton distributions is lacking, and remains a very important and exciting challenge.

In this chapter we aim to alleviate this shortcoming by calculating the spin-independent, spin-dependent (helicity) and transverse (transversity) quark distributions in the Nambu–Jona-Lasinio (NJL) model [56] framework. While not QCD, the NJL model possesses many important attributes of QCD, such as covariance and a transparent description of spontaneous chiral symmetry breaking, as detailed in Chapter 3. In particular, the proper-time regularization is applied to the NJL model in order to simulate the effects of confinement [95]. We will utilize the formalism presented in Section 3.4 and construct the nucleon as a bound state solution of the relativistic Faddeev equation [75, 85, 96, 97] in the quark-diquark approximation [58], where both scalar and axial-vector diquark channels are included. This quark-diquark description of the single nucleon has the further advantage that it can be extended to finite baryon density [98], which is the focus of the next chapter. We will pay special attention to the helicity and transversity structure of the nucleon, the related axial and tensor charges and also their QCD evolution. Where available we will compare our results for the quark distributions and charges with the empirical data.

4.1 Quark distributions

The triplet of leading twist nucleon quark lightcone momentum distributions are defined via lightcone Fourier transforms of particular nucleon-nucleon matrix elements. Explicitly, the definitions are

$$q(x) = p_- \int \frac{d\xi^-}{2\pi} e^{i x p^+ \xi^-} \langle p, s|\overline{\psi}_q(0)\, \gamma^+ \psi_q(\xi^-)|p, s\rangle_c, \tag{4.1}$$

$$\Delta q(x) = p_- \int \frac{d\xi^-}{2\pi} e^{i x p^+ \xi^-} \langle p, s|\overline{\psi}_q(0)\, \gamma^+ \gamma_5 \psi_q(\xi^-)|p, s\rangle_c, \tag{4.2}$$

$$\Delta_T q(x) = p_- \int \frac{d\xi^-}{2\pi} e^{i x p^+ \xi^-} \langle p, s|\overline{\psi}_q(0)\, \gamma^+ \gamma^1 \gamma_5 \psi_q(\xi^-)|p, s\rangle_c, \tag{4.3}$$

where ψ_q is the quark field of flavour q and x is the Bjorken scaling variable.[1] The subscript c reminds us that only connected matrix elements are included, that is, vacuum transitions of the form $\langle 0\,|J_\mu J_\nu|\,0\rangle\langle p|p\rangle$ do not contribute to the quark distributions. The γ^1 in Eq. (4.3) implies that the transverse axis is chosen in the x-direction, similarly a γ^2 in Eq. (4.3) would imply that the transverse axis is in the y-direction. Clearly, the choice of the transverse axis cannot change the final result, but does influence how the Dirac spinors are constructed, as we will illustrate in Sections A.13 and A.14. We normalize the nucleon state vector according to non-covariant lightcone normalization: $\langle p, s|\overline{\psi}_q\, \gamma^+ \psi_q|p, s\rangle_c = 3$.

To determine the quark distributions in this model, it is convenient to express Eqs. (4.1)–(4.3) in the form [22, 29]

$$q(x) = -i \int \frac{d^4k}{(2\pi)^4}\, \delta\!\left(x - \tfrac{k_-}{p_-}\right) \mathrm{Tr}\left[\gamma^+ M_q\,(p, k)\right], \tag{4.4}$$

$$\Delta q(x) = -i \int \frac{d^4k}{(2\pi)^4}\, \delta\!\left(x - \tfrac{k_-}{p_-}\right) \mathrm{Tr}\left[\gamma^+ \gamma_5\, M_q\,(p, k)\right], \tag{4.5}$$

$$\Delta_T q(x) = -i \int \frac{d^4k}{(2\pi)^4}\, \delta\!\left(x - \tfrac{k_-}{p_-}\right) \mathrm{Tr}\left[\gamma^+ \gamma^1 \gamma_5\, M_q\,(p, k)\right], \tag{4.6}$$

[1] Throughout this thesis we will denote the spin-independent distributions by $q(x)$, or when a particular flavour is discussed by $u(x)$, for example. Similarly we label the helicity distribution by $\Delta q(x)$ and the transversity by $\Delta_T q(x)$. For the moments of these distributions, we will drop the function variable x, for example the moment of the transverse up quark distribution will be denoted by $\Delta_T u$. We mention this explicitly as there is potential confusion in the literature, because for example, in the Jaffe-Ji convention the helicity quark distributions are labeled as $g_1(x)$, which should not be confused with the universally accepted name for the spin-dependent structure function $g_1(x)$. For further discussion see Ref. [29].

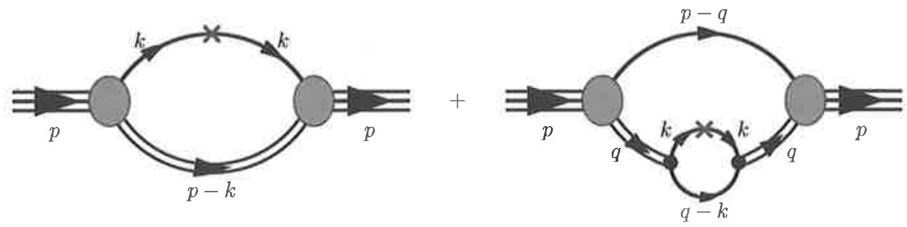

Figure 4.1: Feynman diagrams representing the quark distributions in the nucleon, needed in the evaluation of Eqs. (4.1)–(4.3). The single line represents the quark propagator and the double line the diquark t-matrix. The shaded oval denotes the quark-diquark vertex function. The operator insertion has the form $\gamma^+ \delta\!\left(x - \frac{k_-}{p_-}\right) \frac{1}{2}(1 \pm \tau_z)$ for the spin-independent distribution, for the spin-dependent case we have $\gamma^+ \to \gamma^+\gamma_5$ and similarly for transversity the operator is $\gamma^+ \to \gamma^+\gamma^1\gamma_5$.

where $M_q\,(p,k)$ is the quark two-point function in the nucleon, defined by

$$M_q(p,k) = i \int d^4\omega\, e^{i\,k\cdot\omega} \langle N,p|T\left[\overline{\psi}_q(0)\psi_q(\omega)\right]|N,p\rangle. \tag{4.7}$$

Hence, within any model that describes the nucleon as a bound state of quarks, the distribution functions can be associated with a straightforward Feynman diagram calculation.

The Feynman diagrams considered here are given in Fig. 4.1, where in our model the resulting distributions have no support for negative x. Therefore this is essentially a valence quark picture. The diagram on the left in Fig. 4.1 we call a "quark diagram" because the operator insertion is on a quark, similarly the diagram on the right is a "diquark diagram" as the operator insertion is on a quark in the diquark. By separating the isospin factors, the spin-dependent u- and d-quark distributions in the proton can be expressed as

$$\Delta u_v(x) = \Delta f^s_{q/N}(x) + \frac{1}{2}\,\Delta f^s_{q(D)/N}(x) + \frac{1}{3}\,\Delta f^a_{q/N}(x) \\ + \frac{5}{6}\,\Delta f^a_{q(D)/N}(x) + \frac{1}{2\sqrt{3}}\Delta f^m_{q(D)/N}(x), \tag{4.8}$$

$$\Delta d_v(x) = \frac{1}{2}\,\Delta f^s_{q(D)/N}(x) + \frac{2}{3}\,\Delta f^a_{q/N}(x) \\ + \frac{1}{6}\,\Delta f^a_{q(D)/N}(x) - \frac{1}{2\sqrt{3}}\Delta f^m_{q(D)/N}(x). \tag{4.9}$$

The superscripts s, a and m refer to the scalar, axial-vector or mixing terms, respectively, the subscript q/N implies a quark diagram and similarly $q(D)/N$ a diquark diagram. Similar expressions hold for the spin-independent and transversity distributions, however for the spin-independent case there is no mixing contribution $\left(\text{i.e.} f^{m}_{q(D)/N}(x) = 0\right)$ [90]. Further, since the scalar diquark has spin zero, we have $\Delta f^{s}_{q(D)/N}(x) = 0$ and $\Delta_T f^{s}_{q(D)/N}(x) = 0$, hence the polarization of the d-quark arises exclusively from the axial-vector and the mixing terms.

Importantly, in this covariant framework, the Ward identities corresponding to number and momentum conservation are satisfied from the outset, guaranteeing the validity of the baryon number and momentum sum rules [95, 99]. That is

$$\int_0^1 dx\, u_v(x) = 2\int_0^1 dx\, d_v(x) = 2, \tag{4.10}$$

$$\int_0^1 dx\, x\, [u_v(x) + d_v(x)] = 1. \tag{4.11}$$

4.2 The nucleon in the NJL model

The NJL model is a chiral effective quark theory that is characterized by a 4-Fermi contact interaction of the form, $\mathcal{L}_I = \sum_i G_i \left(\overline{\psi}\,\Gamma_i\,\psi\right)^2$, where the Γ_i represent matrices in Dirac, colour and flavour space and G_i are coupling constants [56]. Applying Fierz transformations, the interaction Lagrangian can be decomposed into various interacting $q\overline{q}$ and qq channels. Writing only those terms relevant to this discussion, we have

$$\mathcal{L} = \overline{\psi}\left(i\partial\!\!\!/ - m_q\right)\psi + \mathcal{L}_{I,\pi} + \mathcal{L}_{I,s} + \mathcal{L}_{I,a}, \tag{4.12}$$

where m_q is the current quark mass. The interaction terms are given by

$$\mathcal{L}_{I,\pi} = \frac{1}{2}G_\pi\left(\left(\overline{\psi}\psi\right)^2 - \left(\overline{\psi}\,\gamma_5\vec{\tau}\,\psi\right)^2\right), \tag{4.13}$$

$$\mathcal{L}_{I,s} = G_s\Big(\overline{\psi}\,\gamma_5 C\tau_2\beta^A\,\overline{\psi}^T\Big)\Big(\psi^T\,C^{-1}\gamma_5\tau_2\beta^A\,\psi\Big), \tag{4.14}$$

$$\mathcal{L}_{I,a} = G_a\Big(\overline{\psi}\,\gamma_\mu C\tau_i\tau_2\beta^A\,\overline{\psi}^T\Big)\Big(\psi^T\,C^{-1}\gamma^\mu\tau_2\tau_i\beta^A\,\psi\Big), \tag{4.15}$$

where $\beta^A = \sqrt{\frac{3}{2}}\lambda^A$ $(A = 2,5,7)$ are the colour $\overline{3}$ matrices and $C = i\gamma_2\gamma_0$. The familiar term $\mathcal{L}_{I,\pi}$ generates the constituent quark mass, M, via the gap equation and the pion as a $q\overline{q}$ bound state. The terms $\mathcal{L}_{I,s}$ and $\mathcal{L}_{I,a}$ represent the interactions in the scalar $(J^\pi = 0^+, T = 0, \text{colour}\,\overline{3})$ and axial-vector $(J^\pi = 1^+, T = 1, \text{colour}\,\overline{3})$ diquark channels and are used to construct the nucleon as a quark-diquark bound state. The couplings G_π, G_s and G_a are related to the original couplings, G_i, via the Fierz transformation, but we use them here as free parameters which will be fixed by the properties of the pion and the nucleon.

Solving the appropriate Bethe-Salpeter equations, the standard NJL results for the diquark t-matrices are obtained [75,90]. As explained in Ref. [58], these can be accurately approximated by the forms

$$\tau_s(q) = 4i\,G_s - \frac{ig_s}{q^2 - M_s^2}, \tag{4.16}$$

$$\tau_a^{\mu\nu}(q) = 4iG_a\,g^{\mu\nu} - \frac{ig_a}{q^2 - M_a^2}\left(g^{\mu\nu} - \frac{q^\mu q^\nu}{M_a^2}\right), \tag{4.17}$$

which we also use here. The masses of the diquarks M_s, M_a and their couplings to the quarks g_s, g_a are defined as the poles and residues of the appropriate full diquark t-matrices (see Section A.9).

The nucleon (quark-diquark) t-matrix satisfies the Faddeev equation

$$T = Z + Z\,\Pi_N\,T = Z + T\,\Pi_N\,Z, \tag{4.18}$$

where Z is the quark exchange kernel and Π_N the product of a quark propagator and a diquark t-matrix. In the non-covariant lightcone normalization used already in Eqs. (4.1)–(4.3), the quark-diquark vertex function, Γ_N, is defined by the behaviour of T near the pole

$$T \overset{p_+\to\varepsilon_p}{\longrightarrow} \frac{\Gamma_N\,\overline{\Gamma}_N}{p_+ - \varepsilon_p}, \tag{4.19}$$

where $\varepsilon_p = \frac{M_N^2}{2p_-}$ is the lightcone energy. Substituting this result into Eq. (4.18) gives the homogeneous Faddeev equations for the vertex functions

$$\Gamma_N = Z\,\Pi_N\,\Gamma_N, \quad \text{and} \quad \overline{\Gamma}_N = \overline{\Gamma}_N\,\Pi_N\,Z. \tag{4.20}$$

For this investigation we restrict ourselves to the static approximation, where we neglect the momentum dependence of the quark exchange kernel, Z. Including both scalar and axial-vector diquark channels, Z takes the following form in the colour singlet and isospin-$\frac{1}{2}$ channel

$$Z = \frac{3}{M}\begin{pmatrix} 1 & \sqrt{3}\gamma_{\mu'}\gamma_5 \\ \sqrt{3}\gamma_5\gamma^\mu & -\gamma_{\mu'}\gamma^\mu \end{pmatrix}. \tag{4.21}$$

The quantity Π_N effectively becomes the quark-diquark bubble graph

$$\Pi_N(p) = \int \frac{d^4k}{(2\pi)^4}\,\tau(p-k)\,S(k), \tag{4.22}$$

where

$$\tau(q) = \begin{pmatrix} \tau_s(q) & 0 \\ 0 & \tau_a^{\mu\nu}(q) \end{pmatrix}. \tag{4.23}$$

The eigenfunction of the kernel $K \equiv Z\,\Pi_N$, in Eq. (4.20), has the following form, up to normalization:

$$\Gamma(p,s) = \begin{bmatrix} \alpha_1 \\ \alpha_2\,\frac{p^\mu}{M_N}\,\gamma_5 \;+\alpha_3\,\gamma^\mu\gamma_5 \end{bmatrix} u_N(p,s), \tag{4.24}$$

where the upper and lower component refer to the scalar and axial-vector diquark channels, respectively and u_N is a free Dirac spinor with mass M_N. We choose the normalization $\overline{u}_N u_N = 1 = \overline{\Gamma}\Gamma$.[2] Inserting this form into Eq. (4.20) gives three homogeneous equations for the α's and the nucleon mass M_N is determined by the requirement that the eigenvalue of K, in Eq. (4.20), equal 1.

The normalization of the vertex function follows from the definition given in Eq. (4.19), we obtain

$$\Gamma_N(p,s) = \sqrt{-Z_N\frac{M_N}{p_-}}\,\Gamma(p,s), \tag{4.25}$$

where

$$Z_N = \frac{p_-}{M_N}\,\frac{-1}{\overline{\Gamma}(p)\,\frac{\partial\Pi_N(p)}{\partial p_+}\,\Gamma(p)}. \tag{4.26}$$

In Appendix C we explicitly solve the Faddeev Equation, Eq.(4.20), and show our result for the normalization Z_N.

As with any non-renormalizable theory a regularization prescription must be specified to fully define the model. We choose the proper-time regularization scheme [57, 58, 100, 101], where loop integrals of products of propagators are evaluated by introducing Feynman parameters, Wick rotating and making the denominator replacement

$$\frac{1}{X^n} \longrightarrow \frac{1}{(n-1)!}\int_{1/(\Lambda_{UV})^2}^{1/(\Lambda_{IR})^2} d\tau\,\tau^{n-1}\,e^{-\tau X}, \tag{4.27}$$

where Λ_{IR} and Λ_{UV} are, respectively, ultraviolet and infrared cutoffs. The former has the effect of eliminating unphysical thresholds for hadron decay into quarks, hence simulating an important aspect of confinement [101].

[2] The conjugate vertex function, $\overline{\Gamma}$, which is a left eigenfunction of $\overline{K} \equiv \Pi_N\,Z$, is obtained by taking the ordinary hermitian conjugate of Γ and introducing a minus sign for the axial-vector components.

4.3 Results

The parameters of the model are Λ_{IR}, Λ_{UV}, m, G_π, G_s and G_a. The infrared scale is expected to be of order Λ_{QCD} and we set it to $\Lambda_{IR} = 240\,\text{MeV}$. This is slightly larger than our previous work [95], because our studies of the saturation properties of nuclear matter favour this [98]. The parameters m_q, Λ_{UV} and G_π are determined by requiring $M = 400\,\text{MeV}$ via the gap equation, $f_\pi = 93\,\text{MeV}$ from the familiar one loop pion decay diagram and $m_\pi = 140\,\text{MeV}$ from the pole of the $q\bar{q}$ t-matrix in the pion channel. This gives $m_q = 16.4\,\text{MeV}$, $\Lambda_{UV} = 645\,\text{MeV}$ and $G_\pi = 19.04\,\text{GeV}^{-2}$. The couplings G_s and G_a are determined by reproducing the nucleon mass $M_N = 940\,\text{MeV}$ as the solution of Eq. (4.20) and satisfying the Bjorken sum rule within our model, where $g_A = 1.267$. We obtain $G_s = 7.49\,\text{GeV}^{-2}$ and $G_a = 2.80\,\text{GeV}^{-2}$. With these model parameters the diquark masses are $M_s = 687\,\text{MeV}$ and $M_a = 1027\,\text{MeV}$ and the coefficients in the nucleon vertex function, Eq.(4.24), are $(\alpha_1, \alpha_2, \alpha_3) = (0.43,\ 0.02,\ -0.45)$.

To compare the predictions of the model with experimental data as well as the empirical parameterizations, it is necessary to determine the model scale, Q_0^2. We do this by optimizing Q_0^2 such that the spin-independent distribution, $u_v(x)$, best reproduces the empirical parameterization after Q^2 evolution. We find a model scale of $Q_0^2 = 0.16\ \text{GeV}^2$, which is typical of valence dominated models [90, 99, 102].

Results for all three valence u- and d-quark distributions are presented in Figs. 4.2 and 4.3, respectively. We see that the helicity and transversity distributions are quite similar in magnitude, although $\Delta_T d(x)$ is rather suppressed at small x relative to $\Delta d(x)$. Note, that the difference between $\Delta q(x)$ and $\Delta_T q(x)$ is a purely relativistic effect, and therefore in any non-relativistic model, like the constituent quark model, these distributions are identical.

There are a few positivity constraints that should be satisfied by any model calculation of the quark distributions. The simplest follows directly from the probability interpretation of the quark distributions, expressed in Eqs. (2.50)–(2.53), which states

$$\left|\Delta q(x)\right| \leqslant q(x), \quad \text{and} \quad \left|\Delta_T q(x)\right| \leqslant q(x). \tag{4.28}$$

The other inequality, which relates all three twist-two quark distributions, was derived relatively recently by Soffer [49], and has the form

$$q(x) + \Delta q(x) \geqslant 2\left|\Delta_T q(x)\right|. \tag{4.29}$$

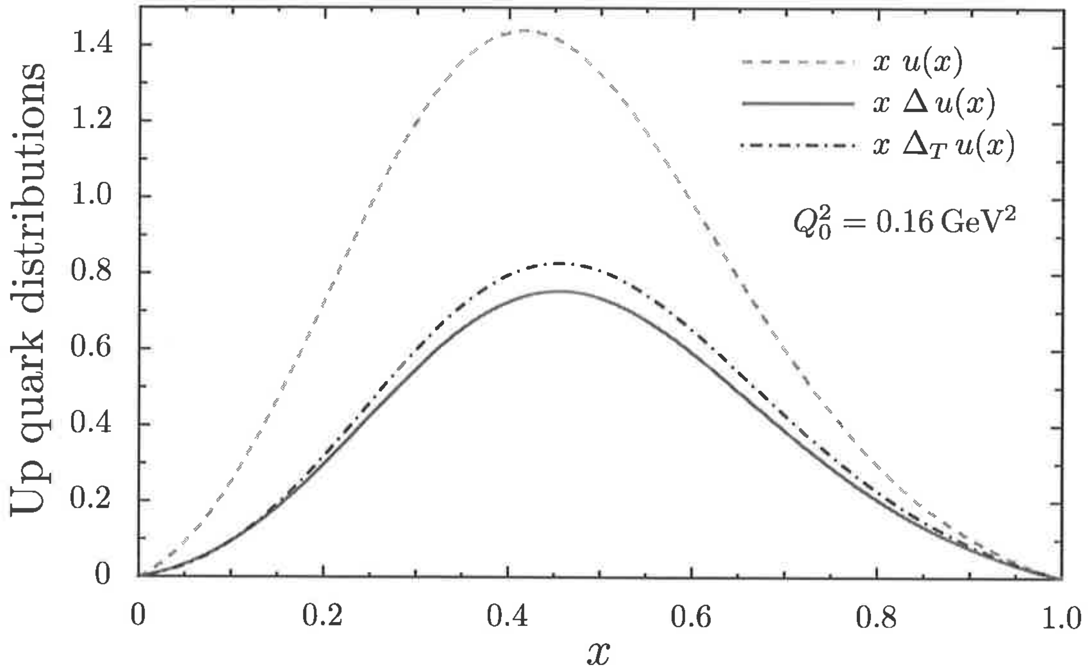

Figure 4.2: NJL results for the twist-two valence u-quark distributions multiplied by Bjorken x, at the NJL model scale of $Q_0^2 = 0.16$ GeV^2

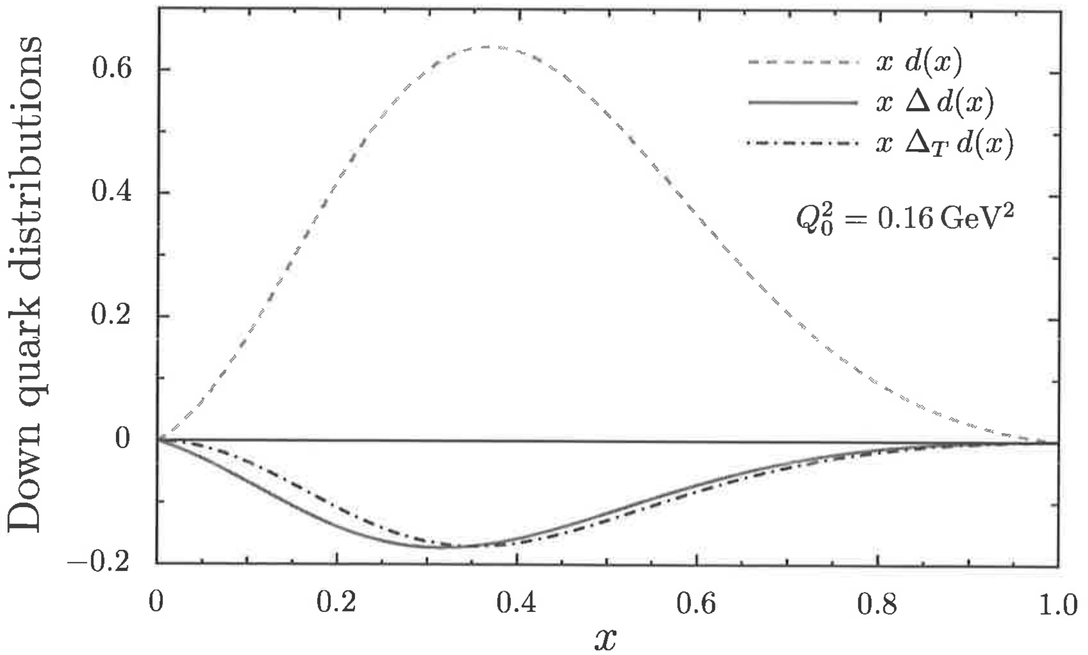

Figure 4.3: NJL results for the twist-two valence d-quark distributions multiplied by Bjorken x, at the NJL model scale of $Q_0^2 = 0.16$ GeV^2

	u	d	Δu	Δd	$\Delta_T u$	$\Delta_T d$	g_A	g_T
NJL	2	1	0.967	-0.300	1.044	-0.236	1.267	1.280
Experiment	2	1	0.926(14)	-0.343(18)	?	?	1.267(8)	?

Table 4.1: Moments of the quark distributions and the nucleon axial and tensor charges. The experimental values for Δu, Δd and g_A are take from Ref. [103], however the experimental results given in Refs. [104, 105] agree to within two significant figures. Note we have used g_A as a constraint.

It is clear from Figs. 4.2 and 4.3 that the calculated quark distributions satisfy these three inequalities. These quark distribution inequalities clearly constrain the moments as well, in particular the Soffer inequality implies

$$|\Delta_T u_v| \leqslant 1 + \tfrac{1}{2}\,\Delta u_v, \tag{4.30}$$

$$|\Delta_T d_v| \leqslant \tfrac{1}{2} + \tfrac{1}{2}\,\Delta d_v. \tag{4.31}$$

Empirically the u-quark moment, Δu_v, is of order one which implies $|\Delta_T u_v| \lesssim \frac{3}{2}$. However since $\Delta d_v < 0$ a stronger constraint on $\Delta_T d_v$ is possible. If $|\Delta d_v| \geqslant \frac{1}{3}$, which current empirical results imply [103], we must have $|\Delta_T d_v| \leqslant \frac{1}{3}$ and hence the d-quark contribution to the axial charge must be greater than its contribution to the tensor charge.

The nucleon vector, axial and tensor charges are related to the moments of the twist-two quark distributions. In the absence of anti-quark distributions these relations are

$$\int_0^1 dx\,[u(x) - d(x)] = g_V, \tag{4.32}$$

$$\int_0^1 dx\,[\Delta u(x) - \Delta d(x)] = g_A, \tag{4.33}$$

$$\int_0^1 [\Delta_T u(x) - \Delta_T d(x)] = g_T, \tag{4.34}$$

where the vector charge, g_V, is simply the baryon number. In Table 4.1 we give our results for the moments of the quark distributions and the related nucleon charges. We find $\Delta_T u > \Delta u$ and $\Delta_T d < \Delta d$ with $g_A \sim g_T$, which is potentially an interesting result. Relativistic effects cause significant differences between the helicity and transversity quark distributions, however these largely cancel for the nucleon axial and tensor charges. It is widely believed that it should be possible to derive a relation between $\Delta q(x)$ and $\Delta_T q(x)$, since

$$q_+(x) + q_-(x) = q_\uparrow(x) + q_\downarrow(x), \tag{4.35}$$

however such a relation is yet to be obtained. Further investigation of our results is necessary to see if there is an underlying reason for the similarity between g_A and g_T, or if it is mere coincidence.

Our model results for the first polarized moments are $\Delta u_v = 0.967$ and $\Delta d_v = -0.300$ which agree quite well with the values $\Delta u_v = 0.926 \pm 0.014$ and $\Delta d_v = -0.341 \pm 0.018$ determined from the axial coupling constants of octet baryons discussed in Ref. [103]. This emphasizes the importance of including axial-vector diquark correlations, since the pure scalar model would give a vanishing Δd_v and a somewhat smaller Δu_v. The spin sum in our model is $\Delta\Sigma = 0.667$, which is smaller than the result of the pure scalar model, but still somewhat larger than the accepted value of $\Delta\Sigma = 0.213 \pm 0.138$ [4]. Although a re-evaluation of the data may result in a somewhat larger value [106]. The discrepancy between our result and experiment may primarily reflect the absence of the $U(1)$ axial anomaly [5, 107] in our calculation. For the transversity moments there are no experimental numbers, however there have been a number of theoretical calculations, for example the MIT bag model [108], Chiral quark soliton model [109, 110], chiral constituent quark model [111] and some exploratory lattice studies [112, 113]. Between them they find $0.80 \leqslant \Delta_T u \leqslant 1.12$ and $-0.15 \leqslant \Delta_T d \leqslant -0.42$, therefore our values of $\Delta_T u = 1.04$ and $\Delta_T d = -0.24$ are consistent with previous work.

In Figs. 4.4 and 4.5 we show the results for all three u- and d-quark distributions after QCD evolution[3] to $Q^2 = 5.00\,\text{GeV}^2$. Empirical parameterizations exist for the spin-independent and helicity distributions and we illustrate these in Figs. 4.4 and 4.5, however it will be sometime before empirical parameterizations for the transversity distributions are available. We find excellent agreement between the model results and the parameterizations. Although the helicity d-quark distribution presented in Fig. 4.5 is a little small. This could be a result of the static approximation, because the quark exchange diagram, absent in this calculation, would contribute to this distribution. For the scalar diquark case in particular, this contribution may be rather large. This result illustrates the importance of going beyond the static approximation in future work. However, we should note that in comparison with the pure scalar model [95, 115], the agreement has improved substantially, especially for the spin-dependent case, illustrating the important role axial-vector diquarks play in nucleon spin structure.

[3] We utilize the computer program of Ref. [43] for the spin-independent case, of Ref. [44] for the spin-dependent case and of Ref. [45] for the transversity case. We choose DGLAP evolution with $N_f = 3$, $\Lambda_{\text{QCD}} = 250\,\text{MeV}$ in the $\overline{\text{MS}}$ renormalization scheme up to NLO.

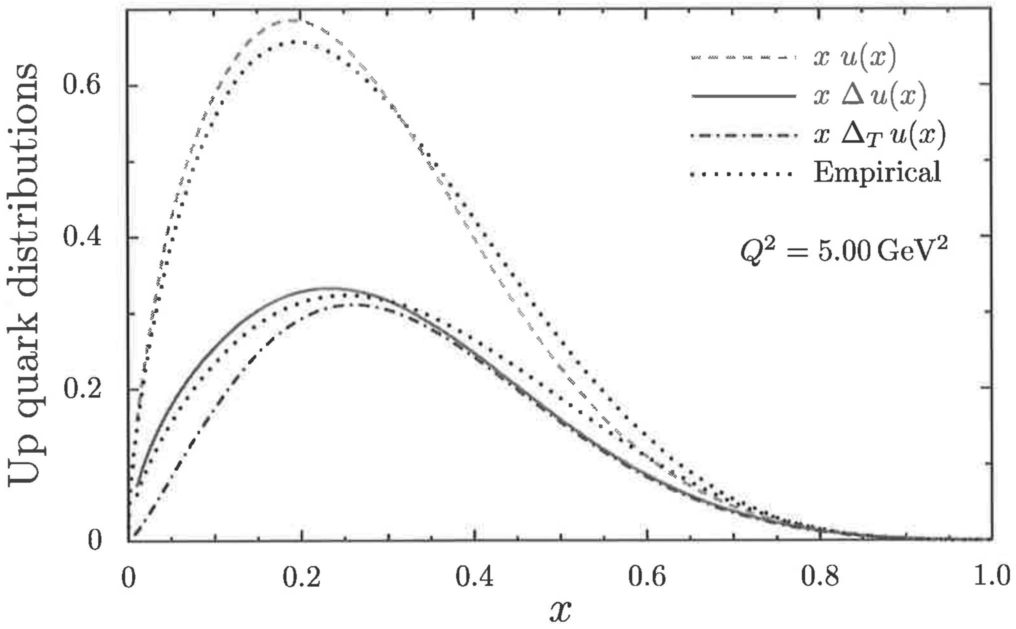

Figure 4.4: NJL results for the twist-two valence u-quark distributions multiplied by Bjorken x, evolved to the scale of $Q_0^2 = 5.00$ GeV^2. The empirical parameterizations are denoted by the dotted lines, where the spin-independent parameterization taken from Ref. [114] and helicity parameterization of Ref. [4].

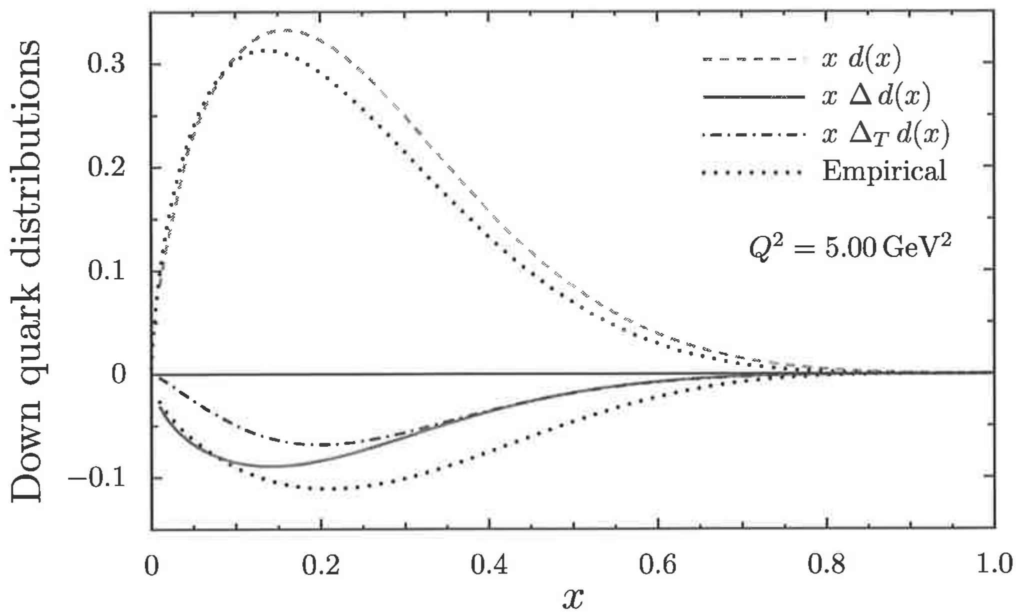

Figure 4.5: Caption as in Fig. 4.4 except here we show the valence d-quark distributions.

The behaviour of structure function and hence quark distribution ratios at large x has been an area of considerable debate [116,117] and is one of the regions where perturbative QCD (pQCD) offers firm predictions [118]. Experimentally, the ratio $d(x)/u(x)$ is surprisingly poorly known [119]. In the limit $x \to 1$ it is thought to lie somewhere between 0, the prediction based on scalar diquark dominance [120] and $\frac{1}{5}$, the pQCD result [118]. Analysis in Ref. [116] favours the pQCD prediction. The same predictions also hold for the spin-dependent ratio, $\Delta d(x)/\Delta u(x)$, as x approaches 1, however to our knowledge there remains no pQCD prediction for the transverse ratio.

In Fig. 4.6 we plot our results for the ratios $d_v(x)/u_v(x)$, $\Delta d_v(x)/\Delta u_v(x)$ and $\Delta_T d_v(x)/\Delta_T u_v(x)$, together with the ratios of the empirical distributions. The $x \to 1$ limit of the spin-independent ratio of $\sim \frac{1}{4}$ is slightly larger than the pQCD prediction. The spin-dependent ratio is less than or equal to zero and therefore has the opposite sign to the pQCD result. Although the empirical parameterizations are constrained to give 0 for these ratios as $x \to 1$, we note that the systematic errors in both empirical ratios are very large in the region $x \gtrsim 0.5$ [4,10,104,114].

It is important to note that the pQCD predictions for the mixed flavour ratios are somewhat model dependent, as assumptions have to be made about the relative strengths of the u- and d-quark contributions to the nucleon wavefunction. A more rigorous pQCD prediction, relying only on helicity conservation, is possible for the single flavour ratios $\Delta u(x)/u(x)$ and $\Delta d(x)/d(x)$. Perturbative QCD predicts that both these ratios should approach 1 for large x, which would require a change of sign in the Δd distribution. In Fig. 4.7 we plot our results of the single flavour ratios, we find in the larger x limit that the $\Delta q(x)/q(x)$ and $\Delta_T q(x)/q(x)$ ratios approach zero, while the $\Delta_T q(x)/\Delta q(x)$ ratio at large x remains finite.

In Fig. 4.8 we plot our results for the ratios $(\Delta q + \Delta\bar{q})\,/\,(q + \bar{q})$ where $q \in (u, d)$. Since we wish to compare these ratios directly to recent experimental data, we include sea quark distributions generated through the Q^2 evolution. In the $x \to 1$ limit our model ratios approach ≈ 0.8 for the u-quark and ≈ -0.25 for the d-quark. This seeming contradiction to pQCD has also been suggested by recent experiments by the Jefferson Lab Hall A collaboration [117,124], with our predictions consistent with their experimental results. This data is also shown in Fig. 4.8.

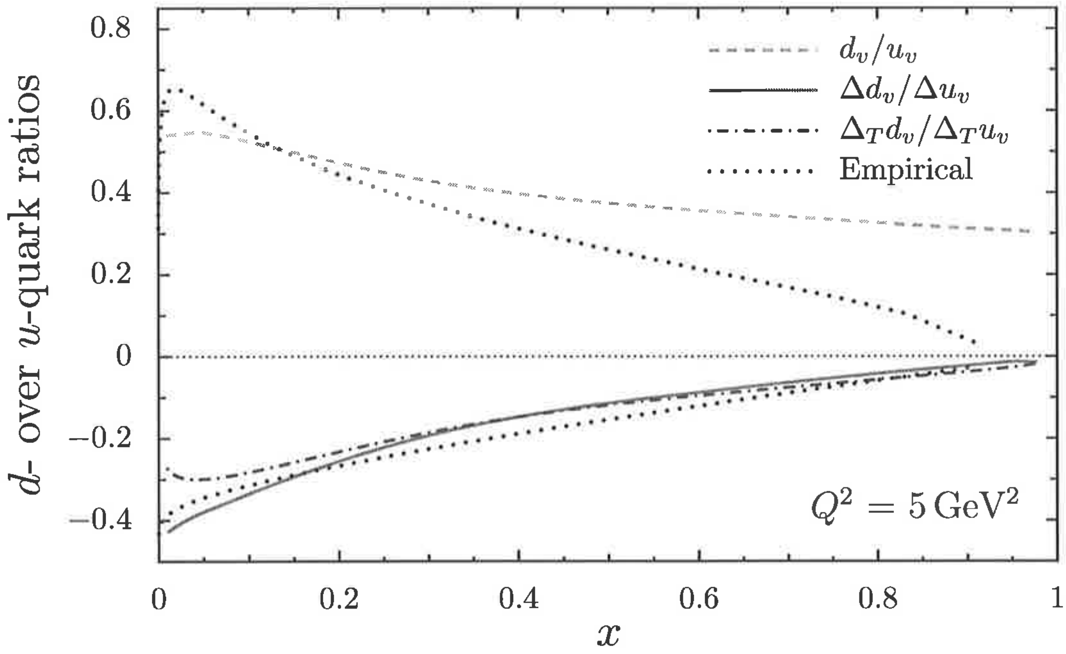

Figure 4.6: Mixed flavour ratios for the three twist-two quark distributions. Empirical results are shown as the dotted line for the spin-independent (upper line) [121] and helicity distributions (lower line) [4], respectively

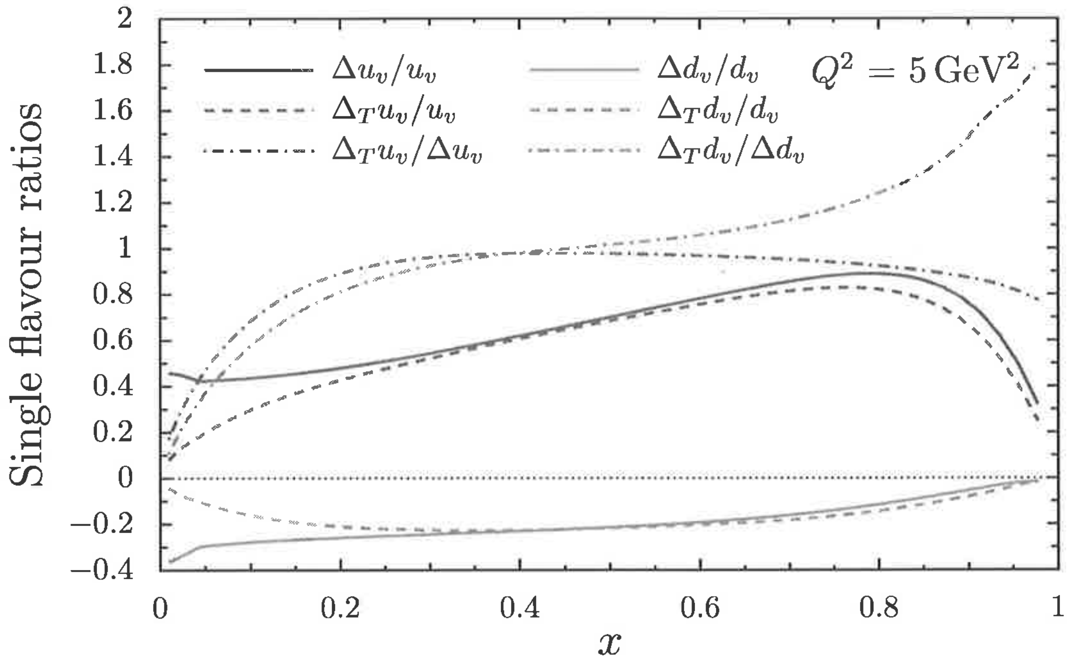

Figure 4.7: Single flavour ratios for the three twist-two quark distributions.

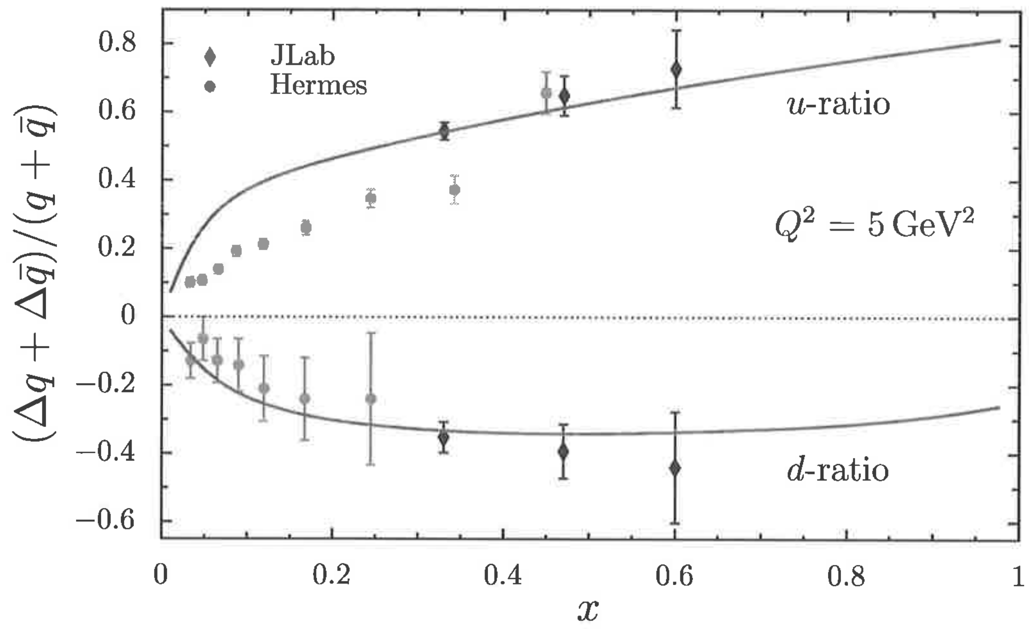

Figure 4.8: Single flavour ratios $(\Delta q + \Delta\bar{q}) \,/\, (q+\bar{q})$ where $q \in (u,d)$, at the scale $Q^2 = 5.0\,\mathrm{GeV}^2$. The experimental results are from Hall A at Jefferson Lab [117] (solid squares) and Hermes [122] (solid stars).

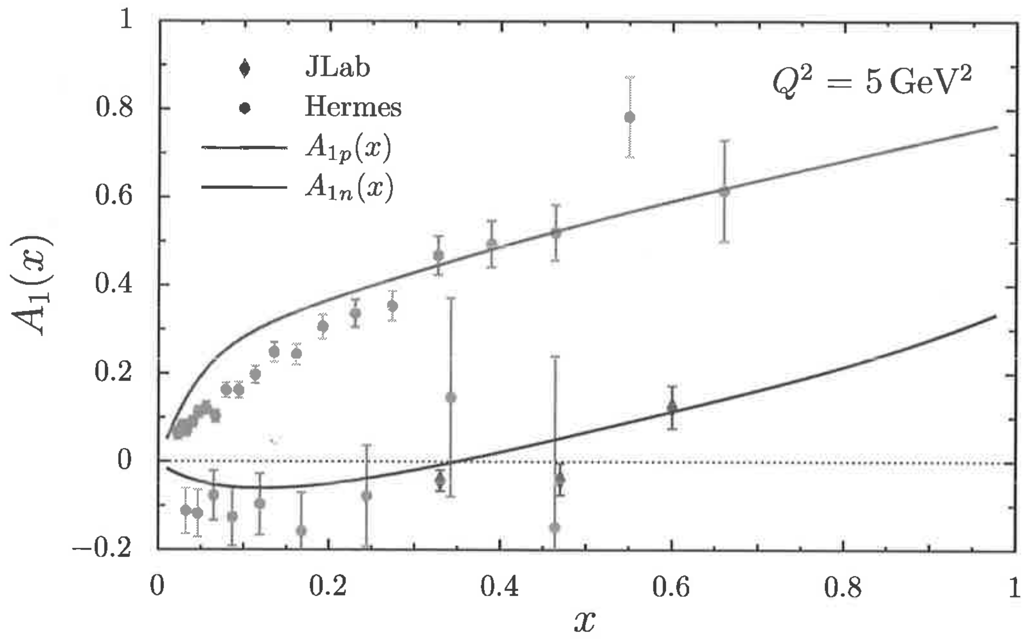

Figure 4.9: Structure function ratios A_{1p} and A_{1n}, at $Q^2 = 5\,\mathrm{GeV}^2$. The Jefferson Lab data is from Ref. [117] and the Hermes data is taken from Ref. [123].

The nucleon asymmetry A_1 is defined as

$$A_1 \equiv \frac{\sigma_{1/2} - \sigma_{3/2}}{\sigma_{1/2} + \sigma_{3/2}}, \tag{4.36}$$

where $\sigma_{3/2}$ is the photon cross-section where the photon and nucleon spin-components along the direction of photon momentum are aligned and $\sigma_{1/2}$ is the case where the nucleon spin is anti-aligned. Expressed in terms of structure functions the asymmetry becomes [117]

$$A_1 = \frac{g_1(x) - \gamma^2\, g_2(x)}{F_1(x)} \simeq \frac{g_1(x)}{F_1(x)}. \tag{4.37}$$

In Fig. 4.9 we show results for the asymmetries $A_{1p}(x)$ and $A_{1n}(x)$. We find excellent agreement with the Jefferson Lab data [117] in the valence quark region. However, for small x, $A_{1p}(x)$ is slightly too large, which reflects an enhancement of $g_{1p}(x)$ in the same region. This is most likely associated with the omission of the effects of the axial anomaly in the present work. It is also clear from the experimental data that the uncertainties in these ratios at large x, are still significant.

In Fig. 4.10 we give our results for the spin-dependent structure functions $g_{1p}(x)$ and $g_{1n}(x)$. The parameterizations of Ref. [104] are also included as the shaded areas, which indicate the empirical uncertainties. Our results compare well with the empirical parameterizations, lying within uncertainties for the region $x \gtrsim 0.3$. Comparison with experiment is also favorable, although the experimental determination for $g_{1n}(x)$ is less certain.

4.4 Conclusion

Using a covariant quark-diquark model for the nucleon, including both scalar and axial-vector diquark channels, we calculated the complete triplet of twist-two quark distributions, that is, the spin-independent, spin-dependent and transversity distribution functions. A key feature of the framework is that it produces quark distributions that have the correct support and obey the number and momentum sum rules. The model also incorporates important aspects of confinement by eliminating unphysical thresholds for nucleon decay into quarks.

Highlights of our results are obtaining values for the polarized first moments of the quark distributions $\Delta u_v = 0.967$ and $\Delta d_v = -0.300$, in good agreement with those obtained from axial couplings of octet baryons. We also obtain excellent agreement with empirical parameterizations of the valence quark distributions. We paid special attention to the single flavour ratios $(\Delta q + \Delta\bar{q})\,/\,(q + \bar{q})$

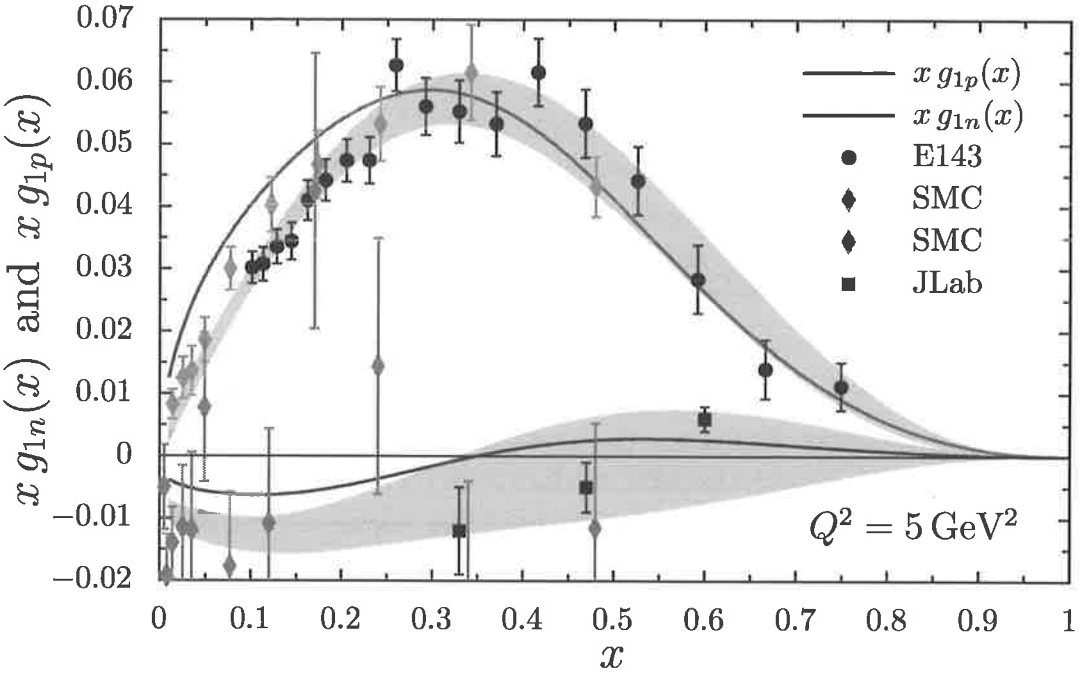

Figure 4.10: Polarized structure functions g_{1p} and g_{1n} at $Q^2 = 5\,\mathrm{GeV}^2$. The solid line is the model prediction, with the lower curve corresponding to g_{1n}. The shaded areas represent the empirical parameterizations with uncertainties of Ref. [104], at the same scale. The experimental data, with $1 \leq Q^2 \leq 10\,\mathrm{GeV}^2$, is from SMC [125] (open stars), SLAC E143 [126] (open circles) and JLab [117] (solid squares).

and the asymmetries A_{1p} and A_{1n}, finding good agreement with recent experimental results from JLab.

These results indicate that diquark correlations are an essential feature of the non-perturbative structure of the nucleon. In particular, the admixture of axial-vector diquarks, though small, is essential to obtain the observed agreement with empirical data.

Finally, we would like to mention that a very important advantage of this covariant quark-diquark model is that it can be readily extended to the case of finite nucleon density. The results presented in this chapter strongly suggest that this model should provide a reliable basis from which to begin investigation of the medium modifications of both spin-independent and spin-dependent structure functions. We investigate this in the following chapter.

5

Quark Distributions in Nuclear Matter

The discovery in the early 1980s by the European Muon Collaboration (EMC) that nuclear structure functions differ substantially from those of free nucleons [11, 127, 128] caused a shock in the nuclear physics community. Despite many attempts to understand this effect in terms of binding corrections it has become clear that one cannot understand it without a change in the structure of the nucleon-like quark clusters in matter [129–131]. Mean-field models of nuclear structure built at the quark level, which have been developed over the past 15 years, are yielding a quantitative description of the EMC effect. Most recently it has been demonstrated that at least one of these models leads naturally to a Skyrme-type force, with parameters in agreement with those found phenomenologically to describe a vast amount of nuclear data [132].

A second major discovery by the EMC concerned the so-called "spin crisis" [2], which corresponds to the discovery that the fraction of the spin of the proton carried by its quarks is unexpectedly small. This has led to major new insights into the famous $U(1)$ axial anomaly, prompting many new experiments. With this background, it is astonishing that, in the 19 years since the discovery of the spin crisis, there has been no experimental investigation of the spin-dependent structure functions of atomic nuclei. Of course, such experiments are more difficult because the nuclear spin is usually carried by just a single nucleon and hence the spin dependence is an $\mathcal{O}(1/A)$ effect. Nevertheless, as we shall see, such measurements promise another major surprise, with at least one model – which reproduces the EMC effect in nuclear matter – suggesting a modification of the spin structure function of a bound proton in nuclear matter roughly twice as large as the change in the spin-independent structure function.

Models of nuclear structure like the quark meson coupling (QMC) model, achieve saturation through the self-consistent change in the quark structure of the colorless, nucleon-like constituents – in particular, through its scalar polarizability [132, 133]. Physically the idea is extremely simple, light quarks respond rapidly to oppose an applied scalar field. Specifically, the lower components of the valence quark wave functions are enhanced and this in turn reduces the effective σN coupling. The fact that changes in the structure of bound nucleons are so difficult to find appears to be a result of this mechanism being extremely efficient and hence yielding only a small change in the dominant upper components of the valence quark wave functions.

On the other hand, the spin structure functions are particularly sensitive to the lower components and this is why measurement of the spin-dependent EMC effect is so promising. In this chapter we extend the NJL model discussed so far to enable finite density calculations, by introducing mean scalar and vector fields to the NJL Lagrangian. We find that with this finite density NJL model, coupled with the proper-time regularization [57,100,101], and the inclusion of both scalar and axial-vector diquarks, we readily obtain nuclear matter saturation at the correct energy and density. This model exhibits similar properties to the QMC model, with the advantage that it is covariant. We extend the work of the previous chapter by determining the medium modifications to the entire triplet of the twist-two quark distributions. We determine the medium modifications to the nucleon axial and tensor charges and calculate the EMC, polarized EMC and transversity EMC effects.

5.1 Finite Density Quark Distributions

The spin-dependent lightcone quark distribution per nucleon in a nucleus of mass number A, momentum P^μ and helicity H is defined as

$$\Delta q_A^{(H)}(x_A) = \frac{P_-}{A}\int \frac{d\omega^-}{2\pi} e^{iP_- x_A \omega^-/A}\, \langle A, P, H|\overline{\psi}_q(0)\,\gamma^+\gamma_5\,\psi_q(\omega^-)|A, P, H\rangle, \tag{5.1}$$

where ψ_q is the quark field and x_A is the Bjorken scaling variable for the nucleus multiplied by A, with support $0 < x_A \leqslant A$. We utilize the non-covariant lightcone normalization where

$$\langle A, P|\overline{\psi}_q\,\gamma^+\,\psi_q|A, P\rangle = 3A. \tag{5.2}$$

The definitions for the finite density spin-independent and transversity quark distributions are obtained in the usual way via the respective operator substitutions, $\gamma^+\gamma_5 \to \gamma^+$ and $\gamma^+\gamma_5 \to \gamma^+\gamma^1\gamma_5$, in Eq. (5.1).

The matrix element in Eq. (5.1) is extremely difficult to evaluate directly. Therefore we utilize the convolution formalism [22] and express Eq. (5.1) in the form

$$\Delta q_A^{(H)}(x_A) = \int_0^A dy_A \int_0^1 dx\ \delta(x_A - y_A\, x)\, \Delta q(x)\ \Delta f_{N/A}^{(H)}(y_A)\,, \tag{5.3}$$

where $\Delta q(x)$ is the medium modified spin-dependent quark lightcone momentum distribution in the nucleon and $\Delta f_{N/A}^{(H)}(y_A)$ is the spin-dependent lightcone momentum distribution of a nucleon in the nucleus. These distributions are defined by

$$\Delta q\,(x) = p_- \int \frac{d\omega^-}{2\pi} e^{iP_-\, x\, \omega^-}\ \langle N, p|\overline{\psi}_q(0)\,\gamma^+\gamma_5\,\psi_q(\omega^-)|N, p\rangle, \tag{5.4}$$

$$\Delta f_{N/A}\,(y_A) = \frac{P_-}{A} \int \frac{d\omega^-}{2\pi} e^{iP_-\, y_A\, \omega^-/A}\ \langle A, P|\overline{\psi}_N(0)\,\gamma^+\gamma_5\,\psi_N(\omega^-)|A, P\rangle, \tag{5.5}$$

with the normalizations

$$\langle N, p|\overline{\psi}_q\,\gamma^+\,\psi_q|N, p\rangle = 3, \tag{5.6}$$

$$\langle A, P|\overline{\psi}_N\,\gamma^+\,\psi_N|A, P\rangle = A. \tag{5.7}$$

Analogous expressions to those in Eqs. (5.3)–(5.5) hold for the spin-independent and transversity finite density quark distributions.

The convolution formalism is depicted diagrammatically in Fig. 5.1a, where all final state interactions between the nucleon and the remaining fragment of the nucleus are ignored. Examples of diagrams not included in the convolution formalism are illustrated in Figs. 5.1b and 5.1c. Unlike the discussion for the nucleon, the operator product expansion cannot be used to show that these non-handbag diagrams for the quark distributions in a nucleus are $\mathcal{O}\,(1/Q^2)$, and hence vanish in the Bjorken limit. Nevertheless we shall proceed and look for any deviations from the convolution model.[1]

To calculate the in-medium quark distributions within our model we once again express them in the form [22, 29]

$$q(x) = -i \int \frac{d^4k}{(2\pi)^4} \delta\!\left(x - \frac{k_-}{p_-}\right) \mathrm{Tr}\left[\gamma^+\, M(p, k)\right], \tag{5.8}$$

$$\Delta q(x) = -i \int \frac{d^4k}{(2\pi)^4} \delta\!\left(x - \frac{k_-}{p_-}\right) \mathrm{Tr}\left[\gamma^+\gamma_5\, M(p, k)\right], \tag{5.9}$$

$$\Delta_T q(x) = -i \int \frac{d^4k}{(2\pi)^4} \delta\!\left(x - \frac{k_-}{p_-}\right) \mathrm{Tr}\left[\gamma^+\gamma^1\gamma_5\, M(p, k)\right], \tag{5.10}$$

[1]Some experimental results that would indicate a breakdown of the convolution approach are discussed in the next chapter.

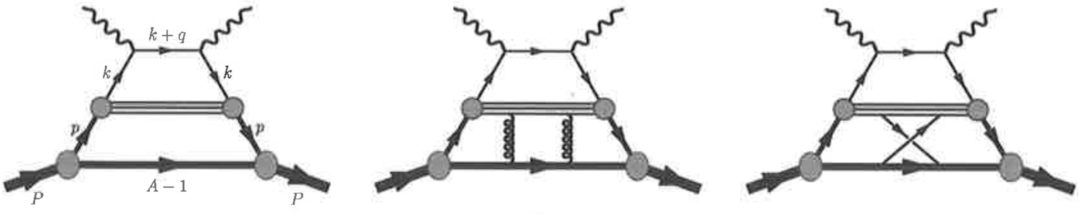

Figure 5.1: Figure (a) is a diagrammatic representation of the convolution formalism. Figures (b) and (c) are diagrams that are ignored in this approach.

where $M(p,k)$ is now the quark two-point function for a quark in a bound nucleon. Therefore, as in the previous chapter the quark distributions can be related to a straightforward Feynman diagram calculation (see Fig. 4.1), except here the propagators include the self consistent scalar and vector mean-fields in the nucleus. The quark propagator therefore becomes

$$S(k) = \frac{1}{\not{k} - M - \Phi - \not{V}} = \frac{1}{\not{k} - M^* - \not{V}}, \tag{5.11}$$

where Φ and $V^\mu = (V_0, \vec{0}\,)$ are the constant scalar and vector fields respectively.[2]

It is clear from Eq. (5.11) that the effect of the scalar field can simply be incorporated by replacing the free masses with the effective masses in the nuclear medium. In Ref. [95] it is demonstrated that the vector field dependence of the quark distributions in the nucleon can be expressed via a simple scale transformation on Bjorken x of the nucleon. That is

$$\Delta q(x) = \frac{p^+}{p^+ - 3V^+}\,\Delta q_0(x)\left(\frac{p^+}{p^+ - 3V^+}x - \frac{V^+}{p^+ - 3V^+}\right), \tag{5.12}$$

where the subscript 0 denotes a nucleon quark distribution uninfluenced by the vector potential, but includes the effects of the scalar field. Identical shifts to that of Eq. (5.12) also hold for the spin-independent and transversity distributions.

To derive Eq. (5.12) we note that the quark Hamiltonian for nuclear matter at rest has the form

$$\hat{H}_q = \hat{h}_q + V_0\hat{Q}, \tag{5.13}$$

where $\hat{h}_q$ is the quark Hamiltonian in the absence of the vector field and $\hat{Q}$ is the quark number operator, defined by

$$\hat{Q} = \int d^3x\, \psi^\dagger(x)\psi(x). \tag{5.14}$$

[2]Note, in infinite nuclear matter at rest there is no preferred direction, therefore the 3-vector part of V^μ must vanish.

Translational invariance of the quark field implies

$$\psi(\xi) = e^{i\hat{P}_q\cdot\xi}\,\psi(0)\,e^{-i\hat{P}_q\cdot\xi}, \tag{5.15}$$

which leads to [95]

$$\frac{\partial\psi(\xi)}{\partial V_0} = i\xi_0\left[\hat{Q},\psi(\xi)\right] = -i\xi_0\,\psi(\xi). \tag{5.16}$$

The solution of this equation is

$$\psi(\xi) = e^{-iV\cdot\xi}\,\psi_0(\xi), \tag{5.17}$$

where $\psi_0(\xi)$ is the quark field uninfluenced by the vector field. Therefore the dependence of the quark field on the vector potential is simply given by a local gauge transformation.

The second observation concerns the vector field dependence of the nucleon states. We denote the bound nucleon momentum, influenced only by the scalar field as p_N^μ, which is related to the nucleon momentum, p^μ, where both scalar and vector fields are present by

$$p_N^\mu = p^\mu - 3V^\mu. \tag{5.18}$$

If the nucleon state vector $|N,p\rangle$ is an eigenstate of $\hat{H}_q$ and $\hat{Q}$ with eigenvalues p_0 and 3 respectively, then

$$\hat{h}_q|N,p\rangle = (p_0 - 3V_0)\,|N,p\rangle = p_N^0|N,p\rangle. \tag{5.19}$$

The nucleon state in the absence of the vector potential is denoted by $|N,p_N\rangle_0$ and we have

$$\hat{H}_q|N,p_N\rangle_0 = \hat{H}_q|N,p\rangle, \quad \hat{Q}_q|N,p_N\rangle_0 = \hat{Q}_q|N,p\rangle, \quad \hat{h}_q|N,p_N\rangle_0 = \hat{h}_q|N,p\rangle, \tag{5.20}$$

therefore

$$|N,p\rangle = |N,p_N\rangle_0. \tag{5.21}$$

Substituting the results of Eqs. (5.21) and (5.17) into the definition of the quark distributions (Eq. (5.4) for example), it is easy to derive the scale transformation of Eq. (5.12).

As discussed earlier, the effects of Fermi motion are included via convolution (see Eq. (5.3)), where we defined the spin-dependent smearing function in Eq. (5.5). The primary focus of this chapter is the change in $q(x)$, $\Delta q(x)$ and

$\Delta_T q(x)$ in-medium. We therefore incorporate the Fermi motion effects on the bound proton quark distributions by replacing $\Delta f_{N/A}^{(H)}(y_A)$ and $\Delta_T f_{N/A}^{(H)}(y_A)$, in Eq. (5.3) (or the transversity equivalent), with the spin-independent distribution $f_{N/A}(y_A)$, calculated in infinite nuclear matter [95]. This is an excellent approximation for a nucleus with maximal spin projection, as we demonstrate in the following chapter.

It is convenient to express the spin-independent version of Eq. (5.5) as [29, 95, 130]

$$f_{N/A}(y_A) = -\frac{i}{A}\int \frac{d^4p}{(2\pi)^4}\delta\left(y_A - \frac{\sqrt{2}p_-}{M_N}\right)\mathrm{Tr}\left[\gamma^+ G_N(p)\right], \tag{5.22}$$

where $G_N(p)$ is the nucleon two-point function in medium, defined by

$$G_N(p) = i\int d^4\omega\, e^{ip\cdot\omega}\langle A, P|T\left[\overline{\psi}_N(0)\psi_N(\omega)\right]|A, P\rangle. \tag{5.23}$$

This two-point function is related to the in-medium Feynman propagtor by [134]

$$G_N(p) = \sqrt{2}\, V\, S_N(p), \tag{5.24}$$

where V is the volume of the system and the Feynman propagtor is given by [95]

$$\begin{aligned} S_N(p) &= S_{NF}(p) + S_{ND}(p), \\ &= \frac{1}{\not{p}_N - M_N + i\varepsilon} + i\pi\frac{\not{p}_N + M_N}{E_p}\,\delta\left(p_0 - E_P\right)\Theta\left(p_F - |\vec{p}\,|\right). \end{aligned} \tag{5.25}$$

The second term, $S_{ND}(p)$, accounts for the fact that the maximum nucleon momentum is p_F, the Fermi momentum. In the mean-field approximation one replaces $S_N(p)$ with $S_{ND}(p)$ in all loop integrals [95] and therefore Eq. (5.22) becomes

$$f_{N/A}(y_A) = -i\frac{\sqrt{2}}{\rho}\int \frac{d^4p}{(2\pi)^4}\delta\left(y_A - \frac{\sqrt{2}p_-}{M_N}\right)\mathrm{Tr}\left[\gamma^+ S_{ND}(p)\right], \tag{5.26}$$

This equation is represented diagrammatically in Fig. 5.2 and evaluates to the simple expression

$$f_{N/A}(y_A) = \frac{3}{4}\left(\frac{\varepsilon_F}{p_F}\right)^3\left[\left(\frac{\varepsilon_F}{p_F}\right)^2 - (1 - y_A)^2\right], \tag{5.27}$$

with support

$$1 - \frac{p_F}{\varepsilon_F} < y_A < 1 + \frac{p_F}{\varepsilon_F}. \tag{5.28}$$

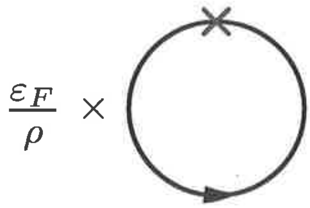

Figure 5.2: Feynman diagram representing the Fermi smearing function $f_{N/A}(y_A)$, given in Eq. (5.26). The solid line denotes the nucleon propagator, $S_{ND}(p)$, and the operator insertion has the form $\gamma^+ \delta\left(p_- - \frac{\varepsilon_F y_A}{\sqrt{2}}\right)$.

The Fermi energy, ε_F, and the vector potential are related via[3]

$$\varepsilon_F = \sqrt{p_F^2 + M_N^2} + 3V_0 \equiv E_F + 3V_0. \tag{5.29}$$

It is easily demonstrated that the vector field dependence of $f_{N/A}(y_A)$ is given by

$$f_{N/A}(y_A) = \frac{\varepsilon_F}{E_F} f_{N/A0}\left(\frac{\varepsilon_F}{E_F} y_A - \frac{3\,V_0}{E_F}\right), \tag{5.30}$$

where

$$f_{N/A0}(\tilde{y}_A) = \frac{3}{4}\left(\frac{E_F}{p_F}\right)^3 \left[\left(\frac{E_F}{p_F}\right)^2 - (1 - \tilde{y}_A)^2\right], \tag{5.31}$$

with support $1 - \frac{p_F}{E_F} < \tilde{y}_A < 1 + \frac{p_F}{E_F}$.

Substituting Eqs. (5.12) and (5.30) into Eq. (5.3), we obtain the full vector field dependence of the in-medium quark distribution as [95]

$$\Delta q_A(x_A) = \frac{\varepsilon_F}{E_F} \Delta q_{A0}\left(\frac{\varepsilon_F}{E_F} x_A - \frac{V_0}{E_F}\right), \tag{5.32}$$

where $\Delta q_0(\tilde{x}_A)$ is the quark distribution including both Fermi motion and the scalar field and is defined by

$$\Delta q_{A0}(\tilde{x}_A) = \int_0^A d\tilde{y}_A \int_0^1 dx\, \delta\left(\tilde{x}_A - \tilde{y}_A\, x\right)\, \Delta q_0(x)\, f_{N/A0}(\tilde{y}_A), \tag{5.33}$$

where $\Delta q_0(x)$ is the quark distribution where the free masses have been replaced by the effective masses in the nuclear medium. In obtaining Eq. (5.32) we have used $p^+ = \frac{1}{\sqrt{2}}\varepsilon_F$, which is valid for nuclear matter at saturation density.

[3] In deriving Eq. (5.27) we have used the fact that at the saturation density of nuclear matter, $\overline{M}_N = \varepsilon_F$.

The various distributions have support

$$q(x): \qquad 0 < x < 1, \tag{5.34}$$

$$q_0(x): \qquad 0 < x < 1, \tag{5.35}$$

$$f_{N/A0}(\tilde{y}_A): \qquad 1 - \frac{p_F}{E_F} < \tilde{x}_A < 1 + \frac{p_F}{E_F}, \tag{5.36}$$

$$q_{A0}(\tilde{x}_A): \qquad 0 < \tilde{x}_A < 1 + \frac{p_F}{E_F}, \tag{5.37}$$

$$q_A(x_A): \qquad \frac{V_0}{\varepsilon_F} < x_A < \frac{E_F + p_F + V_0}{\varepsilon_F}, \tag{5.38}$$

and Fermi smearing functions satisfy the sum rules

$$\int dy_A\ f_{N/A}(y_A) = \int dy_A\ y_A\, f_{N/A}(y_A) = 1, \tag{5.39}$$

$$\int d\tilde{y}_A\ f_{N/A0}(\tilde{y}_A) = \int d\tilde{y}_A\ \tilde{y}_A\, f_{N/A0}(\tilde{y}_A) = 1. \tag{5.40}$$

With this machinery it is now a relatively simple task to obtain results for the in-medium quark distributions. One simply takes the results of the previous chapter (see Section D.2 for explicit expressions), replace the free masses with the effective ones, perform the convolution with the Fermi smearing function and then shift the Bjorken scaling variable via Eq. 5.32. The remaining task is to determine the effective masses, E_F, p_F and V_0 in our NJL model for nuclear matter. This in the subject of the next section.

5.2 Finite Density NJL Model

The NJL model is a chiral effective quark theory that is characterized by a 4-Fermi contact interaction. Using Fierz transformations any 4-Fermi interaction can be expressed in the form $\sum_i G_i \left(\overline{\psi}\Gamma_i\psi\right)^2$, where the Γ_i are matrices in Dirac, colour and flavour space. The coupling constants G_i are functions of the original coupling appearing in the initial interaction Lagrangian.

We consider $\text{SU}(2)_f$ NJL Lagrangians; writing explicitly those terms relevant to this discussion

$$\mathcal{L} = \overline{\psi}\left(i\partial\!\!\!/ - m_q\right)\psi + G_\pi\left(\left(\overline{\psi}\psi\right)^2 - \left(\overline{\psi}\gamma_5\,\vec{\tau}\psi\right)^2\right) - G_\omega\left(\overline{\psi}\gamma^\mu\psi\right)^2 + \ldots, \tag{5.41}$$

where we include the scalar, pseudoscalar and vector terms and m_q is the current quark mass. Separating the nuclear matter ground state expectation values of

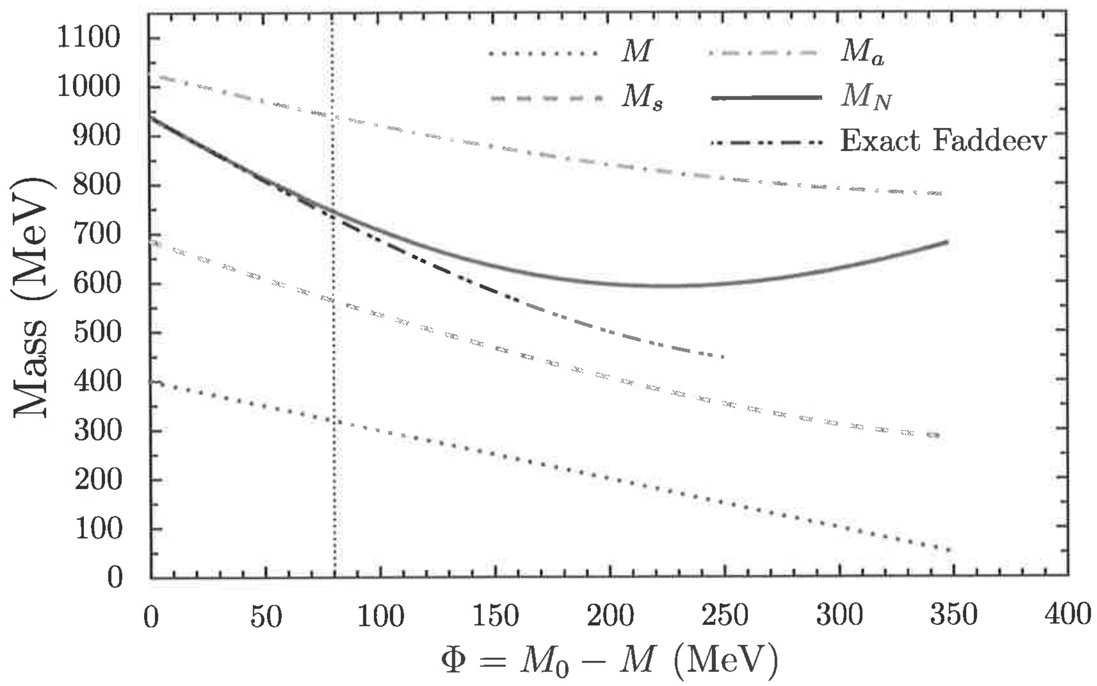

Figure 5.3: This figure shows the scalar diquark, axial-vector diquark and nucleon masses as a function of the scalar field, where the nucleon mass is obtained by solving the Faddeev equation using a modified static approximation. We show the exact Faddeev result of Ref. [75] and the vertical dotted line represents the strength of the scalar field at nuclear matter saturation.

the quark bilinears as, $\overline{\psi}\Upsilon\psi = \langle\rho|\overline{\psi}\Upsilon\psi|\rho\rangle +\ :\overline{\psi}\Upsilon\psi:$, where $\Upsilon = \mathbb{1}, \gamma^\mu$, the Lagrangian can be expressed as

$$\mathcal{L} = \overline{\psi}\left(i\partial\!\!\!/ - M - V\!\!\!/\right)\psi - \frac{(M-m)^2}{4\,G_\pi} + \frac{V_\mu V^\mu}{4G_\omega} + \mathcal{L}_I, \tag{5.42}$$

where we have defined $M = m - 2\,G_\pi\langle\rho|\overline{\psi}\psi|\rho\rangle$, $V^\mu = 2\,G_\omega\langle\rho|\overline{\psi}\gamma^\mu\psi|\rho\rangle$ and $\mathcal{L}_I$ is the normal ordered interaction Lagrangian.

In Fig. 5.3 we illustrate the dependence of the scalar diquark, axial-vector diquark and nucleon masses as a function of the scalar potential, $\Phi = M_0 - M$, where M_0 is the quark mass at zero density and M is the effective mass. In Ref. [58] it was found that in the static approximation the nucleon mass decreases far too rapidly, forcing a modification to the usual static approximation.[4] We introduce a parameter c which modifies the mass of the exchange quark, such

[4]Ref. [58] is a scalar diquark only model, however the inclusion of axial-vector diquarks does little to alleviate this problem.

that

$$\frac{1}{M} \longrightarrow \frac{1}{M_0}\frac{M_0+c}{M+c}, \tag{5.43}$$

in the Faddeev kernel. This variation effectively interpolates between the usual static approximation ($c = 0$) and the case where the mass of the exchange quark is fixed at the free mass ($c = \infty$). Our calculations tend to favour a value of $c \sim 1\,\text{GeV}$, where in Fig. 5.3 we have $c = 1.2\,\text{GeV}$. From Fig. 5.3 we see that the difference between our modified static results and the full Faddeev calculation of Ref. [75], is very small up to the saturation density of nuclear matter. The regularization used in Ref. [75] is the euclidean sharp cutoff and therefore caution should be taken when making a comparison with our results, which utilize the proper-time regularization scheme. We also find the potentially interesting result that our nucleon mass starts to increase for large values of the scalar field, however this effect has little impact on our results at saturation density.

To calculate the mean scalar and vector fields as a function of density, we need the equation of state for nuclear matter. The effective potential for nuclear matter can be rigorously derived for any NJL Lagrangian using hadronization techniques. This results in a complicated nonlocal effective Lagrangian, that in principle can be applied to nuclear matter. Using the mean-field approximation and ignoring diquark and baryon "trace log terms" in the effective Lagrangian we obtain the following effective potential from Eq. (5.42)

$$\mathcal{E} = \mathcal{E}_V - \frac{V_0^2}{4G_\omega} + \int \frac{d^3p}{(2\pi)^3}\,\Theta\left(p_F - |\vec{p}|\right)\varepsilon_p, \tag{5.44}$$

where $\varepsilon_p = \sqrt{\vec{p}^{\,2} + M_N^2} + 3\,V_0$. The vacuum contribution has the familiar "Mexican hat" shape, and is given by

$$\mathcal{E}_V = 12i\int \frac{d^4k}{(2\pi)^4}\ln\left(\frac{k^2 - M^2 + i\varepsilon}{k^2 - M_0^2 + i\varepsilon}\right) + \frac{(M-m)^2}{4G_\pi} - \frac{(M_0-m)^2}{4G_\pi}. \tag{5.45}$$

In this work we only consider nuclear matter at rest.

The zeroth component of the vector field can be eliminated in favour of the baryon density, ρ, via the condition

$$\frac{\partial\mathcal{E}}{\partial V_0} = 0, \tag{5.46}$$

which implies

$$V_0 = 6\,G_\omega\,\rho. \tag{5.47}$$

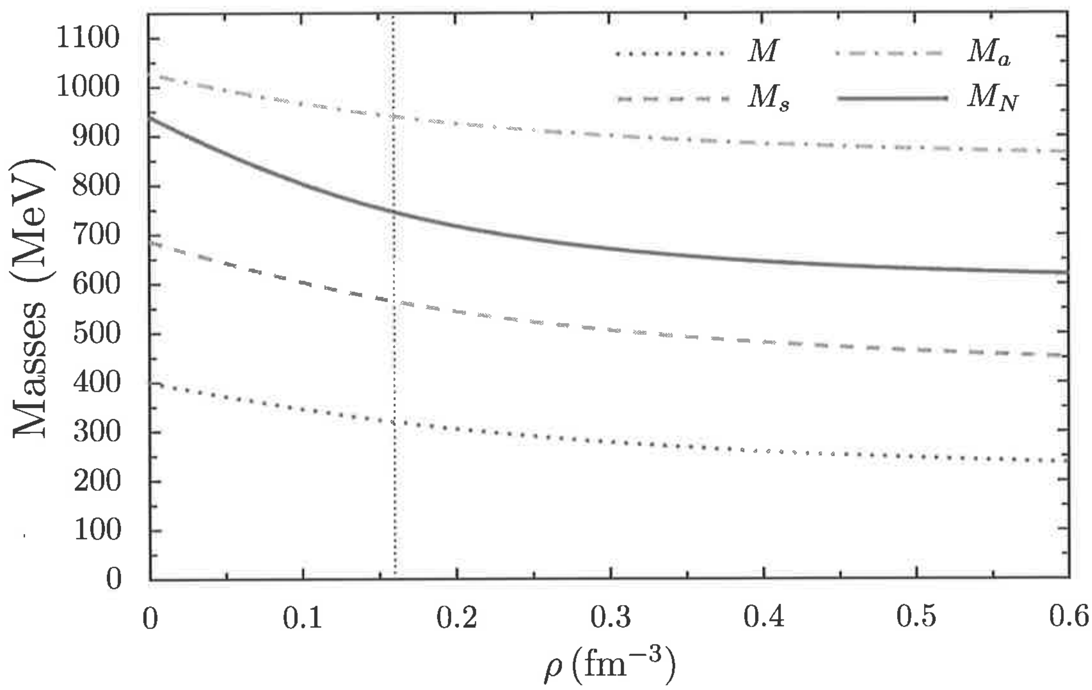

Figure 5.4: Effective quark, diquark and nucleon masses as a function of the density. The vertical dotted line is the density at nuclear matter saturation.

The constituent quark mass M, for a fixed density, then follows from the condition

$$\frac{\partial \mathcal{E}}{\partial M} = 0. \tag{5.48}$$

For a fully self-consistent calculation the constituent quark mass must satisfy the in-medium gap equation

$$M = m - 2G_\pi \langle \rho|\overline{\psi}\psi|\rho\rangle, \tag{5.49}$$

which is the case here, since

$$\frac{\partial \mathcal{E}}{\partial M} = \frac{M - m}{2\,G_\pi} + \langle \rho|\overline{\psi}\psi|\rho\rangle = 0. \tag{5.50}$$

In Fig. 5.4 we illustrate the density dependence of the quark, scalar diquark, axial-vector diquark and nucleon masses. Note, we discuss the values of the parameters of the model in the following section. We see in Fig. 5.4 that the nucleon mass does not approach zero with increasing density, consistent with expectations based on confinement. However, if the infrared cutoff, Λ_{IR}, is set to zero, thereby retaining the unphysical thresholds for nucleon decay into quarks, the nucleon mass is found to approach zero far more rapidly [58]. This provides

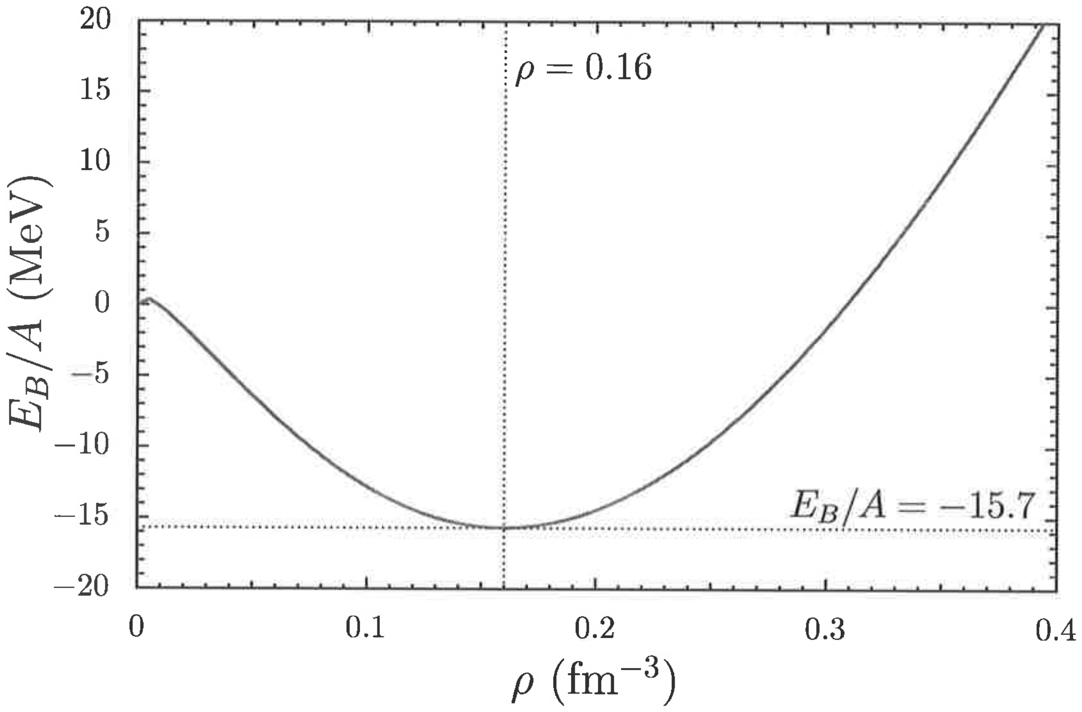

Figure 5.5: Binding energy per nucleon as a function of the density.

further evidence that the introduction of the infrared cutoff encapsulates many of the important aspects of confinement.

An important feature of any model of nuclear matter is that it obtain the correct values for nuclear matter saturation. This is not the case for the NJL model with scalar diquarks only [58], where saturation occurs at too large a density. However, with the inclusion of the axial-vector diquark channel in the nucleon wavefunction, we are able to obtain saturation of nuclear matter at the correct density and binding energy. We illustrate this in Fig. (5.5), where

$$\frac{E_B}{A} = \frac{\mathcal{E}}{\rho} - M_{N0}, \tag{5.51}$$

and M_{N0} is the physical nucleon mass at zero density.

5.3 Results for in-medium Quark Distributions

The parameters of the model are Λ_{IR}, Λ_{UV}, M_0, c, G_π, G_s, G_a and G_ω, where Λ_{IR} and Λ_{UV} are the infrared and ultraviolet cutoffs used in the proper-time regularization. The infrared scale is expected to be of the order Λ_{QCD} and we set it to $\Lambda_{IR} = 240\,\text{MeV}$. We also choose the free constituent quark mass to be $M_0 = 400\,\text{MeV}$ [5] and use this constraint to fix the static parameter, c. The remaining six parameters are fixed by requiring $f_\pi = 93$ MeV, $m_\pi = 140$ MeV, $M_N = 940\,\text{MeV}$, the saturation point of nuclear matter $(\rho_B, E_B) = \left(0.16\,\text{fm}^{-3}, 15.7\,\text{MeV}\right)$ and lastly the Bjorken sum rule at zero density to be satisfied, with $g_A = 1.267$. We obtain $\Lambda_{UV} = 645\,\text{MeV}$, $c = 1027\,\text{MeV}$, $G_\pi = 19.04\,\text{GeV}^{-2}$, $G_s = 7.49\,\text{GeV}^{-2}$, $G_a = 2.80\,\text{GeV}^{-2}$ and $G_\omega = 6.03\,\text{GeV}^{-2}$.

With these model parameters the diquark masses at zero density are $M_s = 687\,\text{MeV}$ and $M_a = 1027\,\text{MeV}$. At saturation density the effective masses become $M^* = 320\,\text{MeV}$, $M_s^* = 565\,\text{MeV}$, $M_a^* = 940\,\text{MeV}$ and $M_N^* = 746\,\text{MeV}$ and vector field strength is $V_0 = 44.5\,\text{MeV}$. The free effective diquark–quark-quark couplings are $g_s = 3.82$ and $g_a = 14.5$, in medium these become $g_s^* = 3.52$ and $g_a^* = 13.4$. Finally the free and in-medium nucleon vertex normalizations are $Z_N = 29.9$ and $Z_N^* = 36.0$, respectively.

The Fermi momentum can be determined from the nuclear matter formula

$$p_F^3 = \frac{3\pi^2}{2}\,\rho, \tag{5.52}$$

which gives $p_F = 263\,\text{MeV}$ and therefore we have a Fermi energy of $E_F = 790\,\text{MeV}$. A good test of our NJL model for nuclear matter is to determine the compressibility at saturation density, which is given by

$$K = 9\rho^2 \frac{\partial^2}{\partial \rho^2}\frac{E_B}{A}. \tag{5.53}$$

Physically plausible values for K are generally thought to lie in the range 200-400 MeV [135], with $K = 270 - 300\,\text{MeV}$ being the preferred experimental range. Our value of $K = 368\,\text{MeV}$ is therefore approximately 20% too large, but not unreasonable, and represents a significant improvement on Quantum Hadrodynamics, where values of $K > 450\,\text{MeV}$ are routinely obtained [136]. The introduction of a pion cloud to the nucleon and the inclusion of the ρ-meson in the nuclear medium may help reduce our value for K.

Using the parameters given at the beginning of this section in Eqs. (5.32) and (5.33) (and spin-independent and transversity equivalents) we obtain results for the in-medium u and d spin-independent, spin-dependent and transversity quark distributions. These results are presented in Figs. 5.6–5.8, at the model scale of

[5] Our results do not depend strongly on this choice, remaining almost unchanged with M_0 is between 350 and 450 MeV. This is also true for Λ_{IR}, where a change of $\pm 50\,\text{MeV}$ results in not qualitative differences.

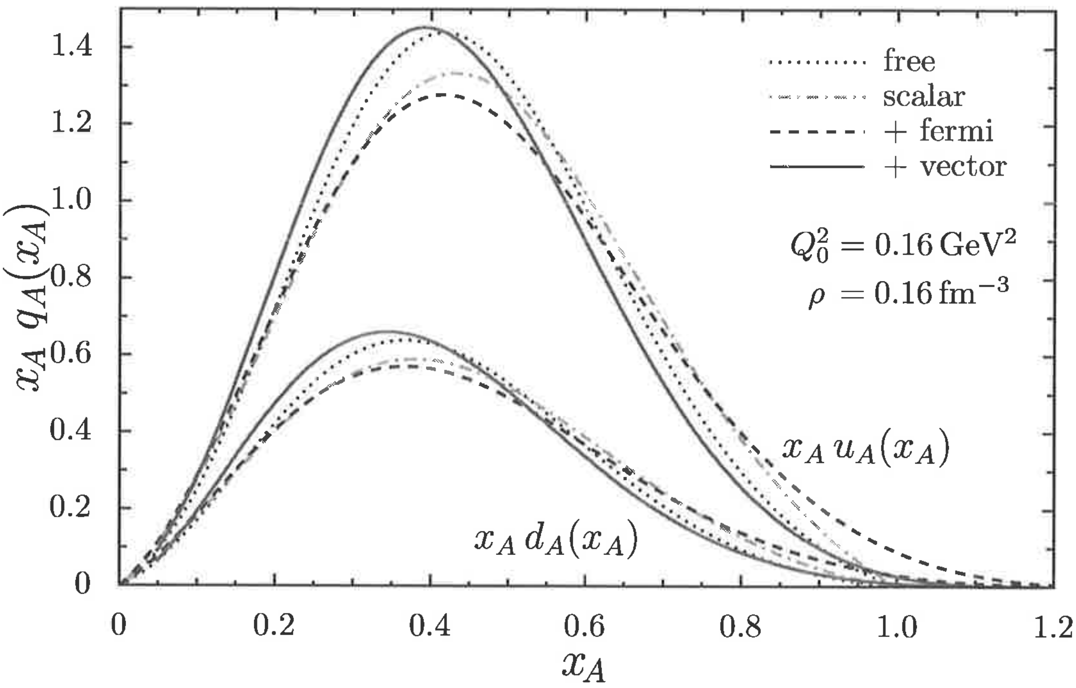

Figure 5.6: Spin-independent quark distributions, u_v and d_v, at the model scale, $Q_0^2 = 0.16$ GeV^2. There are four curves for each quark flavour, with the upper curves representing the u-quark distributions. The dotted line is the free nucleon distribution, the dot-dashed line illustrates the effect of replacing the free masses with the effective ones. This distribution convoluted with the Fermi smearing function, Eq. (5.33), is presented as the dashed line, and the final result where the vector field is also included via the scale transformation, Eq. (5.32), is represented by the solid line.

$Q_0^2 = 0.16\,\text{GeV}^2$. For each quark flavour and distribution there are four curves, representing the different stages leading to the full nuclear matter result. The dotted curve in each figure are the free results of Chapter 4, the dot-dashed line illustrates the effect of the scalar field only, that is, the free masses have been replaced by the effective masses at saturation density. The dashed line includes Fermi motion effects on the bound nucleon and is obtained by convoluting the dot-dashed line with the Fermi smearing function of Eq. (5.31), as expressed in Eq. (5.33). Finally the solid line also incorporates the effects of the vector potential, and is obtained by shifting the dashed curve using Eq. (5.32).

From Figs. 5.6–5.8 we see that the scalar field tends to suppress the distributions for $x_A \lesssim 0.6$ and enhance them for larger x_A. For the spin-independent distributions the baryon and momentum sum rules must remain satisfied in-

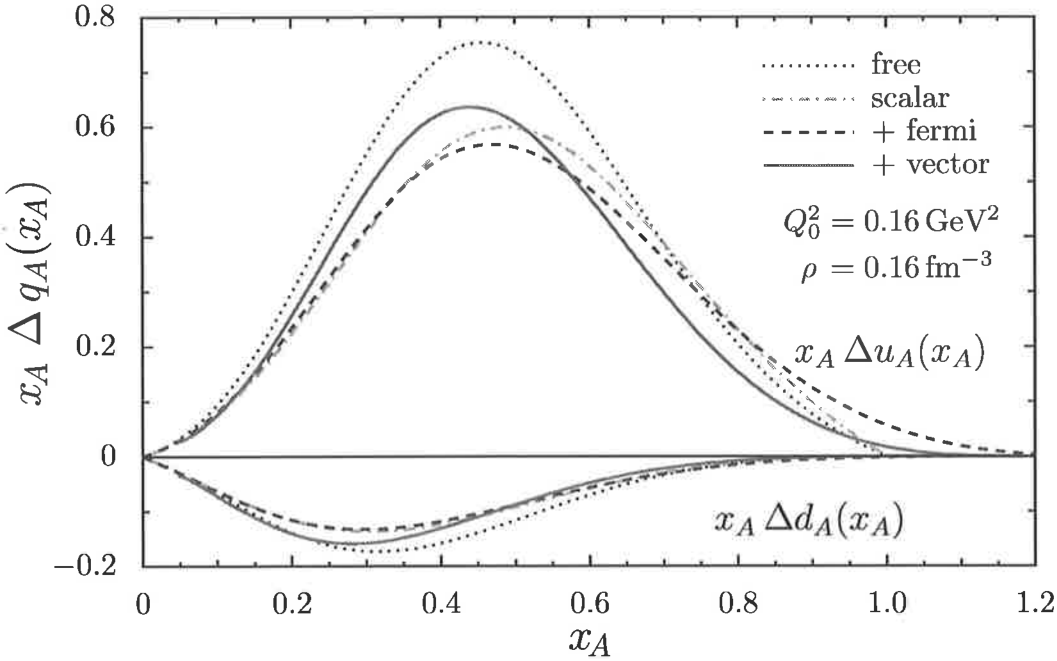

Figure 5.7: As in Fig. 5.6 except here we show the spin-dependent quark distributions Δu_v and Δd_v.

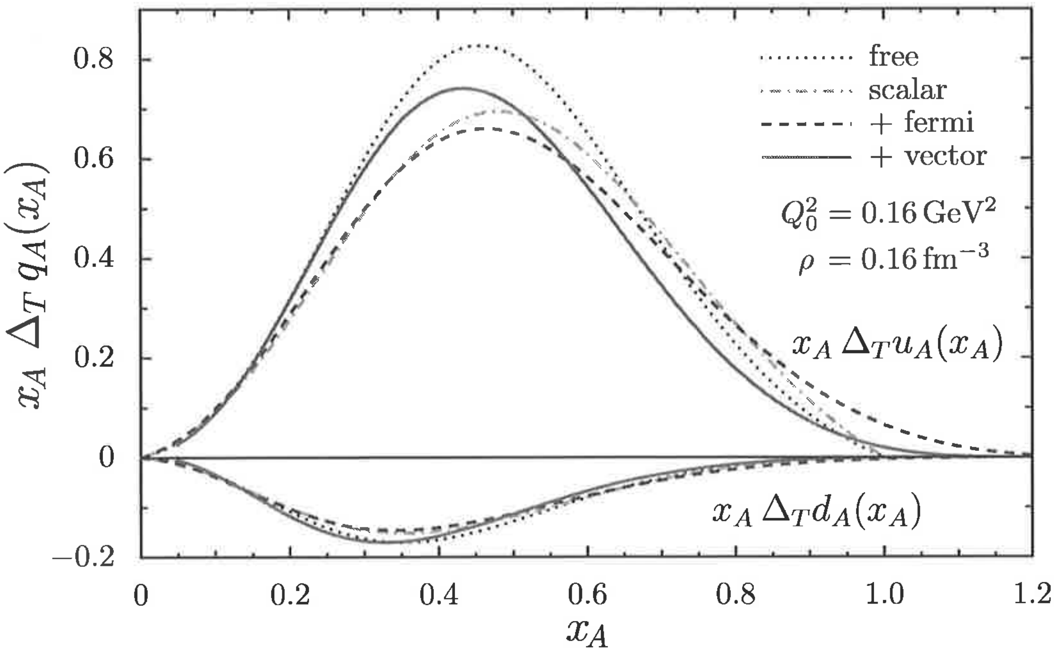

Figure 5.8: As in Fig. 5.6 except here we show the transversity quark distributions $\Delta_T u_v$ and $\Delta_T d_v$.

	u	d	Δu	Δd	$\Delta_T u$	$\Delta_T d$	g_A	g_T
Free	2	1	0.967	-0.300	1.044	-0.236	1.267	1.280
In-medium	2	1	0.790	-0.259	0.934	-0.227	1.049	1.161

Table 5.1: Moments of the free and in-medium quark distributions and the nucleon axial and tensor charges.

medium. For the helicity and transversity distributions there exists no such constraint and the introduction of the scalar field results in a quenching of the first moments of these distributions, thereby yielding a reduction of the nucleon axial and tensor charges in-medium. We will discuss this point further shortly. The effect of Fermi motion results in a broadening of the distributions toward larger x_A, where the distributions now extend beyond x_A equals one. The first moment of $f_{N/A0}$ is one, hence normalizations are maintained after Fermi smearing. However, if the correct smearing functions were used for the helicity and transversity distributions, their normalizations would differ slightly from one – this will be discussed in the following chapter.

The effect of the vector field on the distributions is a little more subtle, but basically the vector field results in a squeezing of the distributions either side of $x_A = \frac{1}{3}$. To illustrate this we note from Eq. (5.32) that

$$\tilde{x}_A = \frac{\varepsilon_F}{E_F}\, x_A - \frac{V_0}{E_F} = x_A \left(1 + \frac{3V_0}{E_F}\right) - \frac{V_0}{E_F}. \tag{5.54}$$

Therefore if $\tilde{x}_A < \frac{1}{3}$ this implies $x_A > \tilde{x}_A$, similarly if $\tilde{x}_A > \frac{1}{3}$ we have $x_A < \tilde{x}_A$ and clearly $\tilde{x}_A = \frac{1}{3} = x_A$. The overall factor $\frac{\varepsilon_F}{E_F}$ in Eq. (5.32) guarantees the vector field preserves the quark distribution normalizations.

The moments of the in-medium quark distributions enable us, via Eq. (4.34), to determine the in-medium values of the nucleon axial and tensor charges. We summarize our results in Table 5.1. We find that all in-medium moments are quenched, except those of the spin-independent distributions. In particular, the in-medium axial charge is reduced by approximately 17% and the in-medium tensor charge by 10%, relative to their free values. This quenching of g_A is consistent with nuclear beta decay studies which require a similar reduction of g_A to achieve agreement with empirical data. Currently there is no experimental information for either the free or in-medium values of the nucleon tensor charge.

Using the quark distributions of Figs. 5.6–5.8 we are able to construct the structure functions, $F_{2N}(x) = \frac{1}{2}\left[F_{2p} + F_{2n}\right]$, $g_{1p}(x)$, $h_{1p}(x)$ and the in-medium

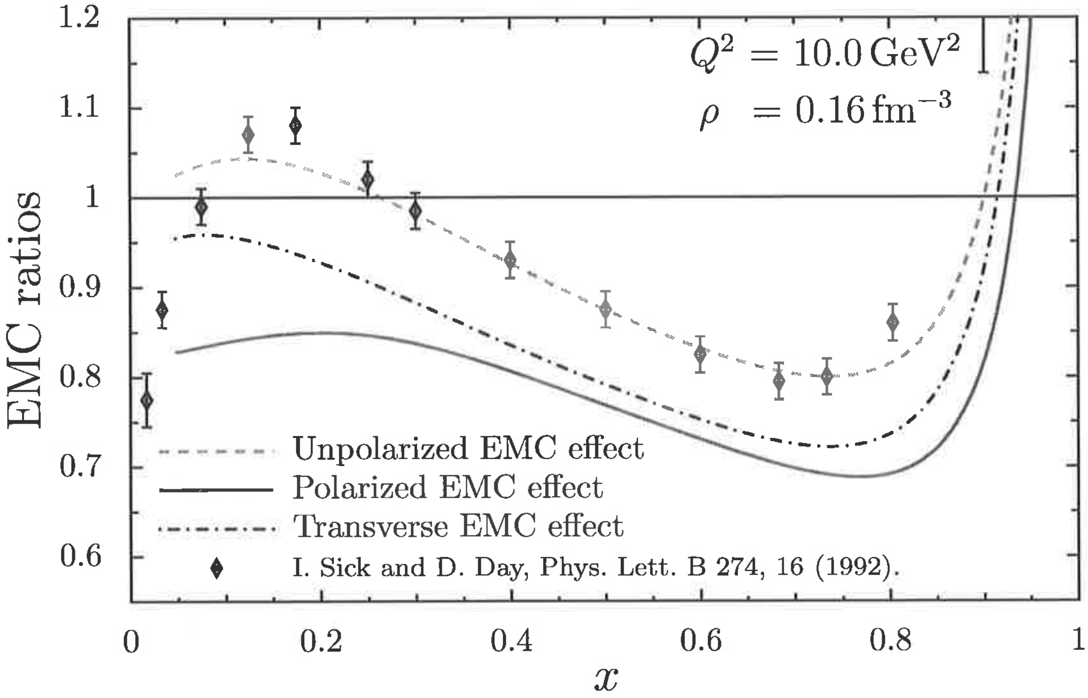

Figure 5.9: Ratios of in-medium over free structure functions at nuclear matter saturation density. The EMC data for nuclear matter are taken from Ref. [137].

equivalents $F_{2A}(x_A)$, $g_{A1p}(x_A)$, $h_{A1p}(x_A)$.[6] Evolving these distributions to a scale of $10\,\mathrm{GeV}^2$ using the NLO DGLAP evolution equations [43–45], we give in Fig. 5.9 our results for the ratios F_{2A}/F_{2N}, g_{A1p}/g_{1p} and h_{A1p}/h_{1p}, that is, the EMC, the polarized EMC and the transverse EMC effects in infinite nuclear matter. In the valence quark region, the model is able to reproduce the spin-independent EMC data [137] extremely well. For the polarized and transverse ratios we find a significant effect, where the polarized effect is approximately twice that of the unpolarized EMC result. To plot the structure function ratios in Fig. 5.9 we have used the relation

$$x_A = \frac{M_{N0}}{\varepsilon_F}\,x, \tag{5.55}$$

to express the in-medium quark distributions as a function of the Bjorken scaling variable for the nucleon.

The nuclear quenching effects on the individual quark flavours are presented in Fig. 5.10. We find that the effect on both the u- and d- quark distributions is

[6]Obviously infinite nuclear matter does not have a $g_{A1p}(x_A)$ or $h_{A1p}(x_A)$ structure function. Our results are therefore to be interpreted physically as the change in internal structure of a proton immersed in a background of constant scalar and vector fields.

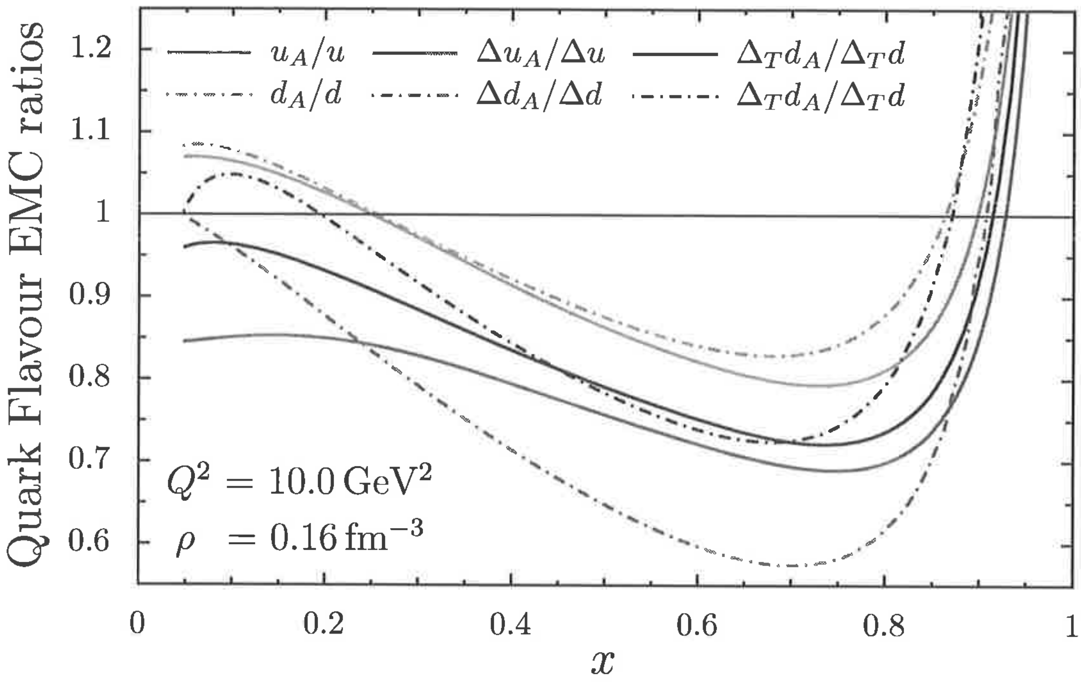

Figure 5.10: Ratio of the quark distributions in nuclear matter to the corresponding free distributions, at a scale of $Q^2 = 10\,\mathrm{GeV}^2$. Note, these distributions are the full quark distributions and hence include anti-quarks generated through Q^2 evolution.

large over the valence quark region. For the spin-independent and transversity ratios the modifications to the u and d distributions are approximately equal, however for the helicity ratio we find that the d-quark is modified much more than the u-quark distribution. The resemblance of the u-quark ratios in Fig. 5.10 to the corresponding EMC ratios arises from the up quark distribution being enhanced by a factor four relative to the down and strange quark distributions in proton structure functions. Absent from our model is the $U(1)$ axial anomaly and sea quarks (at the model scale), this prevents a reliable description of structure functions at small x. For this reason in Figs. 5.9 and 5.10 we do not plot our results in this region.

5.4 Conclusion

In this chapter we have studied the nuclear medium modifications to all three twist-two nucleon quark distributions, and their associated structure functions. We also investigated the properties of infinite nuclear matter using the proper-time regularized NJL model with both scalar and axial-vector diquarks in the nucleon wavefunction. We find that we are readily able to reproduce nuclear matter saturation at the correct energy and density, a feature of the model that is only possible with the inclusion of axial-vector diquarks.

It as been well reported that models using scalar and vector fields coupling to point nucleons, including Fermi motion, are unable to reproduce the EMC effect [138]. However, if these mean scalar and vector fields couple to the quarks in the nucleon – an idea first introduced by Guichon in Ref. [139] – thereby inducing a change in the internal structure of the nucleon, we find an EMC effect in almost perfect agreement with empirical data.

We made predictions for the polarized and transverse EMC effects and found remarkably large signatures. This suggests, at least for the polarized case, that an experimental measurement is feasible. Such a measurement would help provide an understanding of how nuclear medium effects arise from the fundamental degrees of freedom – the quarks and gluons – and represents an important challenge for the nuclear physics community.

6

Finite Nuclei Quark Distributions and the Polarized EMC effect

One of the greatest challenges confronting nuclear physics is to understand how the fundamental degrees of freedom – the quarks and gluons – give rise to the nucleons and to inter-nucleon forces that bind nuclei. Quark models such as the quark-meson coupling model (QMC) [139–141] in which the structure of the nucleon is self-consistently modified by the nuclear medium, can be re-expressed in terms of local effective forces which closely resemble the widely used and successful Skyrme forces [132, 142]. While this opens the possibility to describe the low energy nuclear structure in terms of quark degrees of freedom, it is also important to identify phenomena which provide explicit windows into quark-gluon effects in nuclei. Probably the most famous candidate is the EMC effect [11, 129, 143], which refers to the substantial depletion of the in-medium spin-independent nucleon structure functions in the valence quark region, relative to the free structure functions.

Considerable experimental and theoretical effort has been invested to try to understand the dynamical mechanisms responsible for the EMC effect. It is now widely accepted that binding corrections at the nucleon level cannot account for the observed depletion and a change in the internal structure of the nucleon-like quark clusters in nuclei is required [98, 138, 144]. Although the EMC effect has received the most attention, there are a number of other phenomena which may require a resolution at the quark level, such as the quenching of spin matrix elements in nuclei [145] and the quenching of the Coulomb sum-rule [146, 147]. Important hints for medium modification also come from recent electromagnetic form factor measurements on ^{4}He [148, 149], which suggest a reduction of the proton's electric to magnetic form factor ratio in-medium. Sophisticated nuclear structure calculations fail to fully account for the observed effect [150] and agreement with the data is only achieved by also including a small change in the internal structure of the nucleon [149], predicted a number of years before the experiment [151].

The focus of this chapter is on the medium modifications to the nucleon structure functions in nuclei. We calculate the nuclear quark distributions explicitly from the quark level using the convolution formalism [22]. The quark distributions in the bound nucleon are obtained using a confining Nambu–Jona-Lasinio (NJL) model, where the nucleon is described as a quark-diquark bound state in the relativistic Faddeev formalism. The nucleon distributions in the nucleus are determined using a relativistic single particle shell model, including scalar and vector mean-fields that couple to the quarks in the nucleon. This model, which is very similar in spirit to the QMC model, has the advantage that it is completely covariant, so that one can apply standard field theoretic methods to the calculation of the structure functions. Using this approach we are readily able to reproduce the EMC effect in nuclei. It will be some time before the transverse quark distributions of nuclei are measured experimentally. Therefore, the main focus of this chapter is on the nuclear spin structure function, g_{1A}, and in particular a new EMC ratio – g_{1A} divided by the naive free result – which we refer to as the "polarized EMC effect".

6.1 Deep inelastic scattering from nuclear targets

The formalism to describe deep inelastic scattering (DIS) from a target of arbitrary spin was developed in Refs. [152, 153]. We focus on results specific to the Bjorken limit, expanding on those points necessary for the following discussion.

When parameterized in terms of structure functions, the hadronic tensor in the Bjorken limit has the form

$$W_{\mu\nu}^{JH} = \left(g_{\mu\nu}\frac{P\cdot q}{q^2} + \frac{P_\mu P_\nu}{P\cdot q}\right) F_{2A}^{JH}(x_A) + i\,\frac{\varepsilon_{\mu\nu\lambda\sigma}q^\lambda P^\sigma}{P\cdot q}\, g_{1A}^{JH}(x_A), \tag{6.1}$$

for a target of 4-momentum P^μ, total angular momentum J and helicity H along the direction of the incoming electron momentum. In obtaining Eq. (6.1) we have used a generalization of the Callen-Gross relation, $F_{2A}^{JH} = 2\,\hat{x}_A\, F_{1A}^{JH}$, and ignore terms proportional to q_μ or q_ν as the lepton tensor is conserved, that is

$$q_\mu\, L^{\mu\nu} = q_\nu\, L^{\mu\nu} = 0. \tag{6.2}$$

We define the Bjorken scaling variable as

$$x_A = A\,\hat{x}_A = A\,\frac{Q^2}{2\,P\cdot q}, \tag{6.3}$$

so that the structure functions have support in the domain $0 < x_A \leqslant A$.

In the Bjorken limit the nuclear structure functions can be expressed as

$$F_{2A}^{JH}(x_A) = \sum_q e_q^2 x_A \left[q_A^{JH}(x_A) + \overline{q}_A^{JH}(x_A)\right], \tag{6.4}$$

$$g_{1A}^{JH}(x_A) = \frac{1}{2}\sum_q e_q^2 \left[\Delta q_A^{JH}(x_A) + \Delta\overline{q}_A^{JH}(x_A)\right], \tag{6.5}$$

where q represents the flavour and

$$q_A^{JH}(x_A) = q_{A\uparrow}^{JH}(x_A) + q_{A\downarrow}^{JH}(x_A), \tag{6.6}$$

$$\Delta q_A^{JH}(x_A) = q_{A\uparrow}^{JH}(x_A) - q_{A\downarrow}^{JH}(x_A), \tag{6.7}$$

are generalizations of the usual spin-$\frac{1}{2}$ quark distributions. The quark distributions, $q_{As}^{JH}(x_A)$, are interpreted as: *the probability to find a quark (of flavour q) with lightcone momentum fraction x_A/A and spin-component s in a target with helicity H*. Parity invariance of the strong interaction requires $q_{As}^{JH} = q_{A\,-s}^{J\,-H}$, so that $F_{2A}^{JH} = F_{2A}^{J\,-H}$ and $g_{1A}^{JH} = -g_{1A}^{J\,-H}$ and hence in the Bjorken limit there are $2J+1$ independent structure functions for a spin-J target.

For DIS on targets with $J \geqslant 1$ it is more convenient to work with multipole structure functions or quark distributions [153] rather than the helicity dependent quantities discussed above. The helicity and multipole representations are related by the following transformations

$$F_{2A}^{(JK)} = \sum_{H=-J,\ldots,J} A_H^{JK}\, F_{2A}^{JH}, \qquad K = 0, 2, \ldots, 2J, \tag{6.8}$$

$$g_{1A}^{(JK)} = \sum_{H=-J,\ldots,J} A_H^{JK}\, g_{1A}^{JH}, \qquad K = 1, 3, \ldots, 2J, \tag{6.9}$$

where

$$A_H^{JK} = (-1)^{J-H}\sqrt{2K+1}\begin{pmatrix} J & J & K \\ H & -H & 0 \end{pmatrix}, \tag{6.10}$$

and $(\cdots)$ is a Wigner $3j$-symbol. The inverse relations are

$$F_{2A}^{JH} = \sum_{k=0,2,\ldots,2j} A_H^{JK}\, F_{2A}^{(JK)}, \tag{6.11}$$

$$g_{1A}^{JH} = \sum_{k=1,3,\ldots,2j} A_H^{JK}\, g_{1A}^{(JK)}. \tag{6.12}$$

Identical multipole expansions can also be defined for the spin-independent and spin-dependent quark distributions. Comparing Eqs. (6.11) and (6.12) with the familiar Wigner-Eckart theorem, it is clear that $q_A^{(JK)}$ and $\Delta q_A^{(JK)}$ are reduced matrix elements of multipole operators of rank K. Some examples of the multipole transformations are given in Appendix G.

For nuclear targets the multipole formalism has several advantages, these include

- $F_{2A}^{(J0)} = \sqrt{2J+1}\,F_{2A}$, where F_{2A} is the familiar spin-averaged structure function.
- The number and spin sum-rules are completely saturated by the lowest multipoles, $K=0$ and $K=1$ respectively.
- In a single particle (shell) model for the nucleus, the spin saturated core contributes only to the $K=0$ multipole and all $K>0$ contributions come from the valence nucleons.
- In all cases investigated in this paper, we find that the lowest multipoles, $K=0$ for spin-independent and $K=1$ for spin-dependent, are by far the dominant distributions.
- The multipole quark distributions satisfy the sum rules [153]

$$\int_0^1 dx\, x^{n-1}\, q^{(JK)}(x) = 0, \qquad K, \quad n \text{ even}, \quad 2 \leqslant n < 2K, \tag{6.13}$$

$$\int_0^1 dx\, x^{n-1}\, \Delta q^{(JK)}(x) = 0, \qquad K, \quad n \text{ odd}, \quad 1 \leqslant n < 2K. \tag{6.14}$$

6.2 Nuclear distribution functions

The twist-2, spin-dependent quark distribution in a nucleus of mass number A, momentum P^μ and helicity H is defined as

$$\Delta q_A^{JH}(x_A) = \frac{P_-}{A}\int \frac{d\omega^-}{2\pi} e^{iP_- x_A \omega^-/A} \langle A, P, H|\overline{\psi}_q(0)\,\gamma^+\gamma_5\,\psi_q(\omega^-)|A, P, H\rangle, \tag{6.15}$$

where ψ_q is the quark field. To evaluate Eq. (6.15) we express it as the convolution of a quark distribution in a bound nucleon, with the nucleon distribution in the nucleus [22]. If a shell model is used to determine the nucleon distribution,

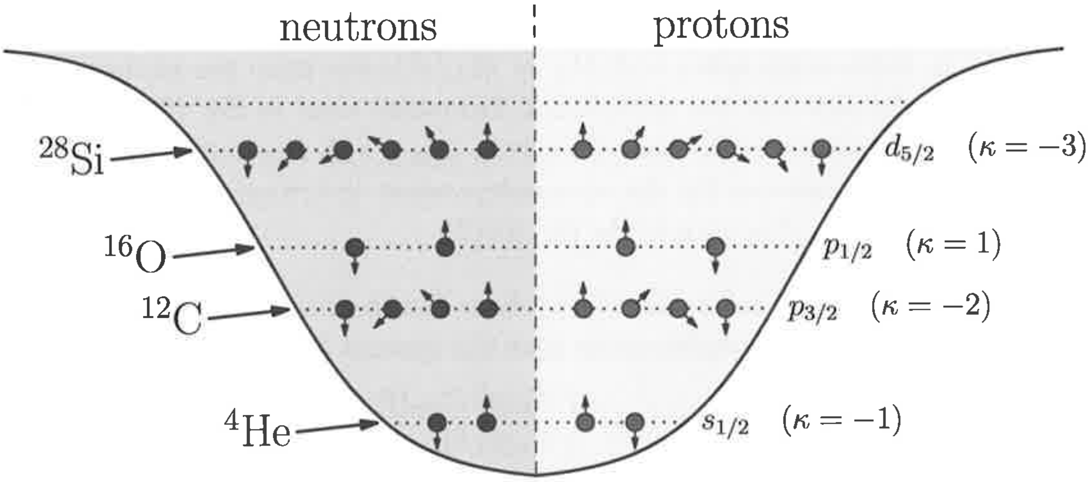

Figure 6.1: In this figure we illustrate the shell model structure of various nuclei. For example, the ground state of Silicon-28 has all single particle states filled up to and including the $d_{5/2}$ shell. The focus of this chapter is on spin-structure and in particular we are interested in ^{7}Li, ^{11}B, ^{15}N and ^{27}Al, where the last three nuclei each have a proton hole in their outer shell level for ground state configurations. The left hand side of the figure gives the correspondence between the shell energy level and its κ value.

then in the convolution formalism Eq. (6.15) has the form

$$\begin{aligned}\Delta q_A^{JH}(x_A) &= \sum_{\alpha,\kappa m} C_{\alpha,\kappa m}^{JH} \int_0^A dy_A \int_0^1 dx \delta(x_A - y_A x)\, \Delta q_{\alpha,\kappa}(x)\ \Delta f_{\kappa m}(y_A)\,, \\ &\equiv \sum_{\alpha,\kappa m} C_{\alpha,\kappa m}^{JH}\, \Delta q_{\alpha,\kappa}^m(x_A)\,, \end{aligned} \tag{6.16}$$

where $\alpha \in (p, n)$ label the nucleons and the sum over the Dirac quantum number κ and $j_z = m$ (that is, the occupied single particle states) is such that the coefficients $C_{\alpha,\kappa m}^{JH}$ guarantee the correct quantum numbers J, H, T and T_z for the nucleus. Note, in Eq. (6.16) a sum over the principle quantum number n is implicit. The correspondence between κ and the familiar shell model energy levels is illustrated in Fig. 6.1.[1]

The function, $\Delta f_{\kappa m}(y_A)$, in Eq. (6.16) is the spin-dependent nucleon distribution (in the state κm) in the nucleus and is defined by

$$\Delta f_{\kappa m}(y_A) = \sqrt{2} \int \frac{d^3p}{(2\pi)^3}\, \delta\!\left(y_A - \frac{p^3 + \varepsilon_\kappa}{\overline{M}_N}\right) \overline{\Psi}_{\kappa m}(\vec{p})\ \gamma^+ \gamma_5\, \Psi_{\kappa m}(\vec{p})\,, \tag{6.17}$$

[1]The conventions we use for κ are summarized in Eqs. (F.11) and (F.12).

where ε_κ is the single particle energy, $\Psi_{\kappa m}(\vec{p})$ are the single particle Dirac wavefunctions in momentum space and $\overline{M}_N = M_A/A$ is the mass per nucleon. Implicit in our definition of the convolution formalism used in Eq. (6.16) is that the quark distributions in the bound nucleon, $\Delta q_{\alpha,\kappa}(x_A)$, respond to the nuclear environment. Expressions for the spin-independent distributions are obtained by simply replacing $\gamma^+\gamma_5$ with γ^+ in Eq. (6.17).

First we obtain expressions for the nucleon distributions in the nucleus. The central potential Dirac eigenfunctions have the general form

$$\Psi_{\kappa m}(\vec{p}) = (-i)^\ell \begin{bmatrix} F_\kappa(p)\ \Omega_{\kappa m}(\theta,\phi) \\ G_\kappa(p)\ \Omega_{-\kappa m}(\theta,\phi) \end{bmatrix}, \tag{6.18}$$

where F_κ and G_κ are the radial wavefunctions in momentum space and $\Omega_{\kappa m}$ are the spherical two-spinors, given by

$$\Omega_{\kappa m}(\theta,\phi) = \sum_{m_\ell, m_s} \langle \ell\, m_\ell\, s\, m_s | j\, m\rangle\, Y_{\ell m_\ell}(\theta,\phi)\ \chi_{s m_s}, \tag{6.19}$$

where χ_{sm_s} are the usual Pauli spin vectors. The radial wavefunctions are normalized such that

$$\int_0^\infty \frac{d^3p}{(2\pi)^3}\, p^2 \left[F_\kappa(p)^2 + G_\kappa(p)^2\right] = 1. \tag{6.20}$$

Substituting Eq. (6.18) into Eq. (6.17) and also the spin-independent equivalent we obtain the following expressions for the single nucleon k-multipole distributions in the nucleus

$$\begin{aligned} f_{\kappa k}(y_A) = {} & (-1)^{j+\frac{1}{2}}\,(2j+1)\,(2\ell+1)\,\sqrt{2k+1} \\ & \begin{pmatrix} \ell & k & \ell \\ 0 & 0 & 0 \end{pmatrix} \begin{Bmatrix} \ell & k & \ell \\ j & s & j \end{Bmatrix} \frac{\overline{M}_N}{16\pi^3} \int_\Lambda^\infty dp\, p\, P_k\!\left(\frac{\overline{M}_N\, y_A - \varepsilon_\kappa}{p}\right) \\ & \left[F_\kappa(p)^2 + G_\kappa(p)^2 + \frac{2}{p}\left(\varepsilon_k - \overline{M}_N\, y_A\right) F_\kappa(p) G_\kappa(p)\right], \end{aligned} \tag{6.21}$$

$$\begin{aligned} \Delta f_{\kappa k}(y_A) = {} & (2j+1)\,\sqrt{2k+1}\,\frac{\overline{M}_N}{16\pi^3}\int_\Lambda^\infty dp\, p \\ & \Bigg\{ 2\, P_k\!\left(\frac{\overline{M}_N\, y_A - \varepsilon_\kappa}{p}\right) F_\kappa(p) G_\kappa(p) (-1)^{j-\frac{1}{2}} \\ & \sqrt{(2\ell+1)(2\tilde{\ell}+1)} \begin{pmatrix} \ell & k & \tilde{\ell} \\ 0 & 0 & 0 \end{pmatrix} \begin{Bmatrix} \ell & k & \tilde{\ell} \\ j & s & j \end{Bmatrix} \\ & - \sqrt{6}\,(-1)^\ell \sum_{L=k-1,k+1} (2L+1)\, P_L\!\left(\frac{\overline{M}_N\, y_A - \varepsilon_\kappa}{p}\right) \begin{pmatrix} L & 1 & k \\ 0 & 0 & 0 \end{pmatrix} \end{aligned}$$

$$\left[F_\kappa(p)^2(2\ell+1)\begin{pmatrix}\ell & L & \ell\\ 0 & 0 & 0\end{pmatrix}\begin{Bmatrix}\ell & s & j\\ L & 1 & k\\ \ell & s & j\end{Bmatrix}\right.$$

$$\left.\left.-G_\kappa(p)^2(2\tilde{\ell}+1)\begin{pmatrix}\tilde{\ell} & L & \tilde{\ell}\\ 0 & 0 & 0\end{pmatrix}\begin{Bmatrix}\tilde{\ell} & s & j\\ L & 1 & k\\ \tilde{\ell} & s & j\end{Bmatrix}\right]\right\}, \quad (6.22)$$

where P_k are Legendre polynomials of degree k and $\Lambda = \left|\overline{M}_N\, y_A - \varepsilon_\kappa\right|$. In deriving Eq. (6.21) it is convenient to use the identity $\Omega_{-\kappa m} = -\left(\vec{\sigma}\cdot\hat{p}\right)\Omega_{\kappa m}$.

The single nucleon wavefunctions (Eq. (6.18)) are solutions of the Dirac equation

$$\left[-i\,\vec{\alpha}\cdot\vec{\nabla} + \beta\, M_N(r) + V_N(r)\right]\psi_\kappa(r) = \varepsilon_\kappa\,\psi_\kappa(r), \quad (6.23)$$

with scalar, $S_N(r)$, and vector, $V_N(r)$, mean-fields. In principle these fields should be calculated self-consistently in our (NJL) model framework by minimizing the total energy of the system, as was done in the Chapter 5 and in Refs. [95, 98] for nuclear matter. Instead we choose Woods-Saxon potentials for $S_N(r)$ and $V_N(r)$, which have the form

$$S_N(r) = \frac{S_0}{1+\exp\left(\frac{r-R_s}{a_s}\right)}, \qquad V_N(r) = \frac{V_0}{1+\exp\left(\frac{r-R_v}{a_v}\right)}, \quad (6.24)$$

where: S_0, V_0 are the depth; a_s, a_v are the thickness or diffuseness; and R_s, R_v the range of each potential. The depth parameters are set to the strength of the scalar or vector field obtained from our self-consistent nuclear matter calculation in Chapter 5, that is $S_0 = -194$ MeV and $V_0 = 133$ MeV [98]. We choose standard values for the range $R_s = R_v = R = 1.2\ A^{1/3}$ fm and diffuseness $a_s = a_v = a = 0.65$ fm. The mass per nucleon $\overline{M}_N$, which would automatically be determined by a self-consistent calculation, is chosen such that the momentum sum rule for each nucleus is satisfied (see Appendix H.2.2).

Given the radial wavefunctions, we can determine the mean values of the scalar and vector fields experienced by the nucleon in the state κ, that is

$$M_{N\kappa} = \int d^3r\ \psi_\kappa^\dagger(r)\, M_N(r)\, \psi_\kappa(r), \quad (6.25)$$

$$V_{N\kappa} = \int d^3r\ \psi_\kappa^\dagger(r)\, V_N(r)\, \psi_\kappa(r), \quad (6.26)$$

where $M_N(r) = M_N + S_N(r)$. Using a local density approximation in our effective quark theory, the scalar field felt by the quarks in the nucleon can be evaluated by determining the quark mass, M_κ, that gives the appropriate nucleon mass, $M_{N\kappa}$, as the solution of the quark-diquark equation. The vector field felt by the quarks is simply one-third of that felt by the nucleon (i.e. $V_\kappa = V_{N\kappa}/3$). These fields are used in the calculation of the quark distributions in the bound nucleon.

In Table 6.1 we list some results for $\overline{M}_N$, $M_{N\kappa}$, $V_{N\kappa}$ and ε_κ for various nuclei. Using these results in Eqs. (6.21) and (6.22), and the appropriate radial wavefunctions, we plot in Figs. 6.2 and 6.3 examples of the nucleon distributions in ^{27}Al. Here we have chosen to present the results in the familiar J, H representation of the quark distributions, that is $f_{\kappa m}(y_A)$ and $\Delta f_{\kappa m}(y_A)$, rather than $f_{\kappa k}(y_A)$ and $\Delta f_{\kappa k}(y_A)$ of Eqs. (6.21) and (6.22). This way a more direct comparison can be made with the infinite nucleon matter smearing function used in Chapter 5.

Fig. 6.2 illustrates all spin-independent, $f_{\kappa m}(y_A)$, distributions and Fig. 6.3 presents all relevant ($\kappa = -3$) spin-dependent, $\Delta f_{\kappa m}(y_A)$, distributions. The full nucleon distribution in the nucleus can be obtained by simply summing over the appropriate single nucleon results presented in Figs. 6.2–6.3. For the spin-independent quark distributions all nucleons in the nucleus contribute, however for spin-dependent quark distributions only the valence nucleons play a role. This is easily seen because $\Delta f_{\kappa m}(y_A) = -\Delta f_{\kappa\, -m}(y_A)$, and hence the spin zero closed core cannot contribute to the spin-dependent quark distributions. If we ignore configuration mixing, the spin of Aluminium-27 is carried solely by the five valence protons, see Fig. 6.1, or equivalently by a single proton hole in the $d_{5/2}$ shell. Therefore in this approximation the curves in Fig. 6.3 represent the full spin-dependent nucleon distributions, for each spin state of ^{27}Al.

We find that these nucleon distributions have considerably more structure than the usual infinite nuclear matter result, this increased structure is clearly illustrated in Fig. 6.2. The reason the distributions are no longer symmetric about $y_A = 1$ is because there remains some angular dependence in the results, which is easily seen by the presence of the Legendre polynomials in Eqs. (6.21) and (6.22). Finally we point out that Eqs. (6.21) and (6.22) obey the sum rules given in Eqs. (6.13) and (6.14). In fact they satisfy a more tightly constrained set of sum rules where the restriction of $n =$ even and $n =$ odd in Eq. (6.13) and Eq. (6.14), respectively, no longer applies. This increased restriction results from using spherically symmetric potentials in the Dirac equation.

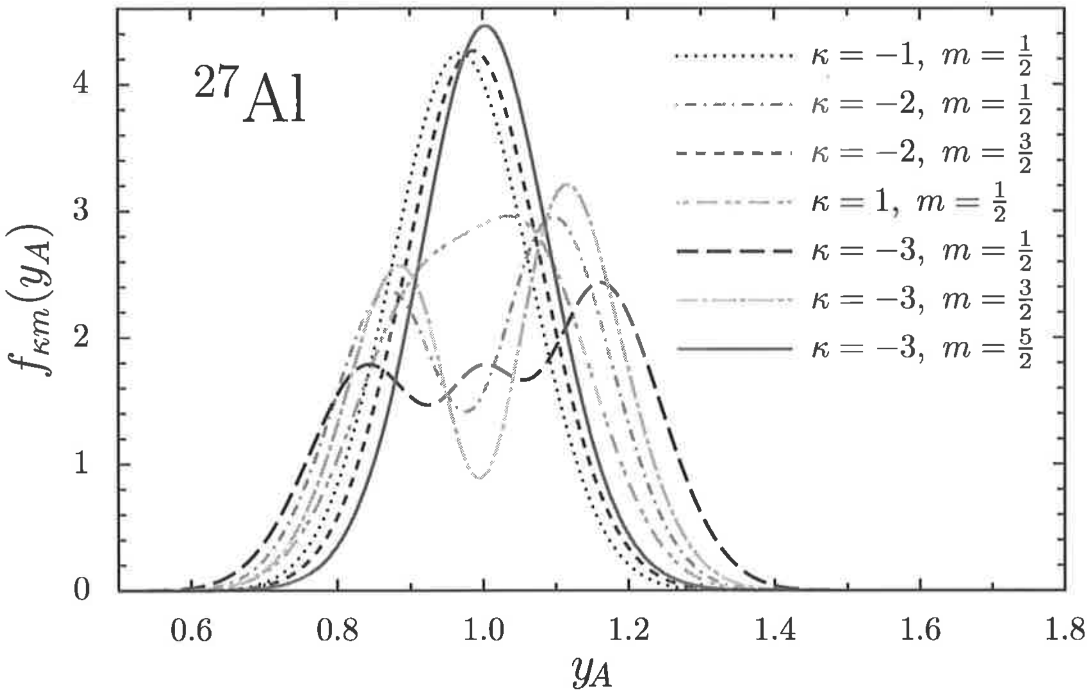

Figure 6.2: All spin-independent nucleon multipole distributions, $f_{\kappa m}(y_A)$, in ^{27}Al.

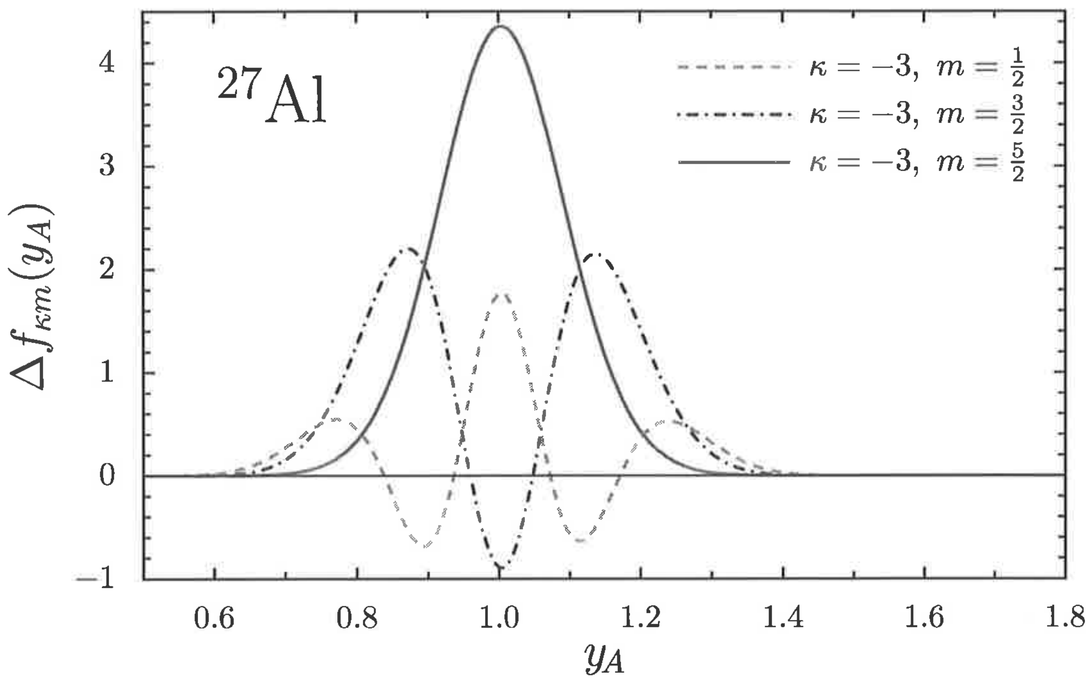

Figure 6.3: All relevant spin-dependent nucleon multipole distributions, $\Delta f_{\kappa m}(y_A)$, in ^{27}Al.

6.3 Medium modified quark distributions in the nucleon

To complete our description of quark distributions in nuclei we require the medium modified quark distributions in the bound nucleon. The infinite nuclear matter example was discussed in Chapter 5 and Refs. [95, 98, 154]. For finite nuclei the formalism is much the same, except the strength of the scalar and vector fields now depends on the energy level κ that the nucleon in the nucleus occupies. Also instead of solving for the in-medium constituent quark mass self-consistently, we determine M^*_κ by requiring that the Faddeev equation yield a nucleon of mass $M_{N\kappa}$.

For the sake of clarity we give a short summary of our formalism: The nucleon is described by solving the relativistic Faddeev equation including both scalar and axial-vector diquark correlations in a confining Nambu–Jona-Lasinio model framework. For this calculation we utilize the static approximation for the quark exchange kernel [74]. The quark distributions in the nucleon are obtained from a Feynman diagram calculation, where we give the relevant diagrams in Fig. 6.4. Medium effects are included by introducing the scalar and vector mean-fields, obtained from Eqs. (6.25) and (6.26), into the quark propagators. Inclusion of the vector field leads to a density dependent shift in the Bjorken scaling variable. Fermi motion effects are included via convolution with the smearing functions (Eq. (6.21) or (6.22)) after introducing the scalar field, but before the shift required by the vector field.

We now derive the shift induced by the vector field for the case of finite nuclei. Recall from Chapter 5 that the dependence of the in-medium quark distribution on the vector field can be expressed as (see Eq. (5.12))

$$\Delta q_{\alpha,\kappa}(x) = \frac{p^+}{p^+ - 3V_\kappa^+}\,\Delta q_{\alpha,\kappa 0}(x)\left(\frac{p^+}{p^+ - 3V_\kappa^+}x - \frac{V_\kappa^+}{p^+ - 3V_\kappa^+}\right), \tag{6.27}$$

where we have included a label κ on $\Delta q_{\alpha,\kappa 0}(x)$ and V_κ^+ to illustrate that the scalar and vector field strengths depend on the energy level. The subscript α indicates either a proton or neutron and is used in Eq. (6.16). Recall that p^μ is the in-medium nucleon momentum, V_κ^+ is the plus component of the vector field, $V_\kappa^\mu \equiv (V_{0\kappa}, \vec{0})$, acting on a quark[2] and $\Delta q_{\alpha 0,\kappa}$ is the quark distribution in the absence of the vector field [95, 155].

[2]For the lightcone coordinates we use $a_\pm = \frac{1}{\sqrt{2}}(a_0 \pm a_3)$.

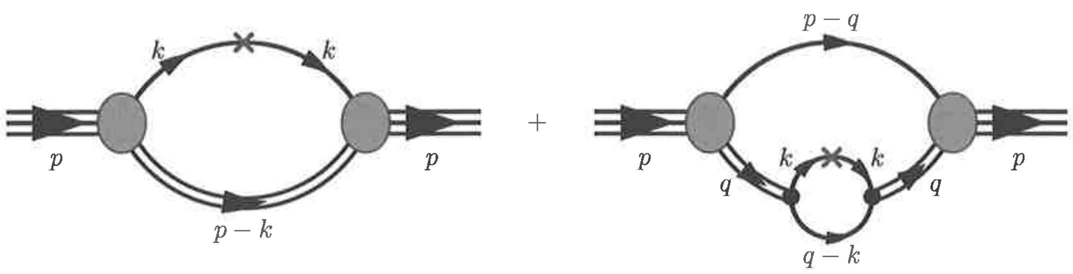

Figure 6.4: Feynman diagrams representing the quark distributions in the nucleon. The single line represents the quark propagator and the double line the diquark t-matrix. The shaded oval denotes the quark-diquark vertex function and the operator insertion has the form $\gamma^+\gamma_5\,\delta\Big(x-\frac{k_-}{p_-}\Big)\,\frac{1}{2}\,(1\pm\tau_z)$ for the spin-dependent distribution, while $\gamma^+\gamma_5 \to \gamma^+$ for the spin-independent case.

If we now define the auxiliary quantities

$$E_\kappa \equiv \varepsilon_\kappa - V_{N\kappa}, \qquad \hat{M}_{N\kappa} \equiv \overline{M}_N - V_{N\kappa}, \tag{6.28}$$

it is easy to rewrite the δ-function in Eq. (6.17) to show

$$\Delta f_{\kappa m}(y_A) = \frac{\overline{M}_N}{\hat{M}_{N\kappa}}\Delta f_{0,\kappa m}\left(\frac{\overline{M}_N}{\hat{M}_{N\kappa}}\,y_A - \frac{V_{N\kappa}}{\hat{M}_{N\kappa}}\right), \tag{6.29}$$

where the function $\Delta f_{0,\kappa m}$ has the same form as Eq. (6.17), except for the replacements $\varepsilon_\kappa \to E_\kappa$ and $\overline{M}_N \to \hat{M}_{N\kappa}$. Substituting Eqs. (6.27) and (6.29) into Eq. (6.16) and performing an analogous calculation to that found in Appendix C of Ref. [95] we obtain

$$\Delta q^m_{\alpha,\kappa}(x_A) = \frac{\overline{M}_N}{\hat{M}_{N\kappa}}\Delta q^m_{\alpha 0,\kappa}\left(\frac{\overline{M}_N}{\hat{M}_{N\kappa}}\,x_A - \frac{V_\kappa}{\hat{M}_{N\kappa}}\right), \tag{6.30}$$

where the distribution, $\Delta q^m_{\alpha 0,\kappa}$, is given by the convolution of $\Delta q_{\alpha 0,\kappa}$ and $\Delta f_{0,\kappa m}$. The full nuclear quark distribution can then be obtained from Eq. (6.16). An identical shift to that expressed in Eq. (6.30) is valid for the spin-independent distribution also.

An important feature of this approach is that the number and momentum sum rules are satisfied from the outset. For a nucleus of atomic number Z and mass number $A = N + Z$ this means

$$\int_0^A dx_A\, u_A(x_A) = 2Z + N, \tag{6.31}$$

$$\int_0^A dx_A\, d_A(x_A) = Z + 2N, \tag{6.32}$$

$$\int_0^A dx_A\, x_A\, [u_A(x_A) + d_A(x_A)] = A. \tag{6.33}$$

6.4 Results

The parameters for the quark-diquark model for the bound nucleon were discussed in Chapter 5 and Refs. [98, 154], so we will not repeat them. The new features presented in this chapter are those associated with finite nuclei. In Table 6.1 we give values for $\overline{M}_N$, $M_{N\kappa}$, $V_{N\kappa}$ and ε_κ obtained from the single particle shell model. These values are then used in Eq. (6.16) to calculate the nuclear quark distributions.

The unpolarized EMC effect is defined as the ratio of the spin-averaged structure function, F_{2A}, of a particular nucleus A divided by the naive expectation. That is

$$R_A = \frac{F_{2A}}{F_{2A}^{\text{naive}}} = \frac{F_{2A}}{Z\, F_{2p} + (A - Z)\, F_{2n}}, \tag{6.34}$$

where F_{2p} is the free proton structure function and F_{2n} the free neutron structure function[3]. In the limit of no Fermi motion and no medium effects of any kind, this ratio is unity. An equivalent EMC ratio can also be defined for the $K = 0$ multipole.

The polarized EMC effect is defined by an analogous ratio, which is the spin-dependent structure function for a particular nucleus with helicity H, divided by the naive expectation, that is

$$R_{As}^{JH} = \frac{g_{1A}^{JH}}{g_{1A,\text{naive}}^{JH}} = \frac{g_{1A}^{JH}}{P_p^{JH}\, g_{1p} + P_n^{JH}\, g_{1n}}. \tag{6.35}$$

Here g_{1p} and g_{1n} are the free nucleon structure functions and $P_{p(n)}^{JH}$ is the polarization of the protons (neutrons) in the nucleus with helicity H, defined by

$$P_\alpha^{JH} = \langle J, H | 2\, \hat{S}_z^\alpha | J, H \rangle, \qquad \alpha \in (p, n)\,, \tag{6.36}$$

[3]Experimental EMC ratios for $N \simeq Z$ nuclei are usually determined with the deuteron structure function F_{2D} in the denominator. In our mean field model we assume $F_{2D} \simeq F_{2p} + F_{2n}$. We therefore anticipate deuteron binding corrections of a few percent to our EMC ratios for $x \gtrsim 0.5$, when comparing with experimental data.

	$\overline{M}_N$	$M_{N\kappa}$				$V_{N\kappa}$				ε_κ			
		-1	-2	1	-3	-1	-2	1	-3	-1	-2	1	-3
^{7}Li	933	811	856	–	–	89	58	–	–	914	932	–	–
^{11}B	931	793	829	–	–	101	76	–	–	908	925	–	–
^{15}N	929	785	815	815	–	106	86	86	–	904	921	923	–
^{27}Al	930	771	794	793	820	115	101	101	82	898	913	914	927

Table 6.1: All quantities are in MeV. The labels -1, -2, 1, -3 refer to the Dirac quantum number κ, where $|\kappa| = j + \frac{1}{2}$.

where $\hat{S}_z^\alpha$ is the total spin operator for protons or neutrons. From an experimental standpoint one should simply use the best estimates of the polarization factors available in the literature. In this work we use the polarization factors obtained from the non-relativistic limit of Eq. (6.36), which differ from the relativistic values calculated within our model by less than 2%. If only a single valence nucleon or nucleon-hole contributes to the nuclear polarization, then in the non-relativistic limit the polarization factor is simply given by

$$P_\alpha^{JH} = \pm\frac{2\,H}{2\ell+1}, \tag{6.37}$$

where ℓ is the orbital angular momentum and the $\pm$ refers to the cases $J = \ell \pm \frac{1}{2}$.

The polarized EMC ratio can also be defined for the $K = 1$ multipole structure function and has the form

$$R_{As}^{(J1)} = \frac{g_{1A}^{(J1)}}{P_p^{(J1)}\,g_{1p} + P_n^{(J1)}\,g_{1n}}, \tag{6.38}$$

where $P_\alpha^{(J1)}$ is the reduced matrix element

$$P_\alpha^{(J1)} = \langle J||\,2\,\hat{S}^\alpha\,||J\rangle = \sqrt{\frac{(2J+1)(2J+2)}{6J}}\,P_\alpha^{JJ}. \tag{6.39}$$

Because the spin structure function g_{1n} is smaller than g_{1p} and remains poorly known, especially at large x, it is clear from Eqs. (6.35) and (6.38) that to determine the polarized EMC effect it is necessary to choose nuclei where $|P_n| \ll |P_p|$. There is also an upper limit on the mass number of nuclei that can be readily used to measure the polarized EMC effect, because for spin cross-sections the valence nucleons dominate and hence g_{1A} is suppressed by approximately $1/A$ relative to F_{2A}, where all nucleons contribute.

The best candidates are nuclei with a single valence proton or proton-hole, for example the stable nuclei ^{11}B, ^{15}N and ^{27}Al. Another good choice is ^{7}Li, where the nuclear polarization is largely dominated by the valence proton. Extensive studies of ^{7}Li, beginning in the 60s with the shell model [156], to modern state of the art Quantum Monte Carlo calculations [157], consistently find $P_p \simeq 0.86 - 0.88$. The Quantum Monte Carlo result for the neutron polarization is $P_n \simeq -0.04$.

First we discuss the nuclear quark distributions, focusing on ^{7}Li as its treatment is a little more involved compared with the other nuclei, because there are three valence nucleons coupled to $J = 3/2$ and $T = 1/2$. We utilize the shell model wavefunction found in Refs. [158,159] for the valence nucleons of ^{7}Li carrying z-component of angular momentum $J_z = \frac{3}{2}$, which is

$$\Psi^{3/2} = \frac{3}{\sqrt{15}}\left[p^{3/2}n^{3/2}n^{-3/2}\right] - \frac{2}{\sqrt{15}}\left[p^{3/2}n^{1/2}n^{-1/2}\right] - \frac{1}{\sqrt{15}}\left[p^{1/2}n^{3/2}n^{-1/2}\right] + \frac{1}{\sqrt{15}}\left[p^{-1/2}n^{3/2}n^{1/2}\right]. \quad (6.40)$$

Using the angular momentum lowering operator $\hat{J}_-$ and the results

$$\hat{J}_-\,\psi^{3/2} = \sqrt{3}\,\psi^{1/2}, \qquad \hat{J}_-\,\psi^{1/2} = 2\,\psi^{-1/2}, \qquad \hat{J}_-\,\psi^{-1/2} = \sqrt{3}\,\psi^{-3/2}, \qquad \hat{J}_-\,\psi^{-3/2} = 0, \quad (6.41)$$

it is easy to obtain the ^{7}Li wavefunction with $J_z = \frac{1}{2}$. Using Eq. (6.40) when evaluating the spin-independent analogue of Eq. (6.16) for the u-quark distribution in ^{7}Li we obtain

$$u_A^{3/2\,3/2}(x_A) = 2\left[u_{p,-1}^{1/2}(x_A) + d_{p,-1}^{1/2}(x_A)\right] + \frac{1}{15}\left[13\,u_{p,-2}^{3/2}(x_A) + 20\,d_{p,-2}^{3/2}(x_A) + 2u_{p,-2}^{1/2}(x_A) + 10\,d_{p,-2}^{1/2}(x_A)\right], \quad (6.42)$$

where we have used charge symmetry to relate $u_n \leftrightarrow d_p$. For clarification on the notation see Eq. (6.16). The spin-dependent distribution has the form

$$\Delta u_A^{3/2\,3/2}(x_A) = \frac{1}{15}\left[13\,\Delta u_{p,-2}^{3/2}(x_A) + 2\,\Delta d_{p,-2}^{3/2}(x_A)\right]. \quad (6.43)$$

Similar expressions hold for the $H = 1/2$ and d-quark distributions. With this wavefunction the ^{7}Li polarization factors are $P_p^{JH} = \frac{2H}{3}\frac{13}{15}$ and $P_n^{JH} = \frac{2H}{3}\frac{2}{15}$. For the other nuclei the situation is simpler as we make the approximation that the nuclear spin is carried solely by the valence proton-hole.

In Figs. 6.5–6.8 we show the leading multipole quark distributions for ^{11}B, together with the next-to-leading $K = 3$ multipole for the spin-dependent case, at the model scale of $Q_0^2 = 0.16$ GeV^2 [154]. The other nuclear quark distributions are similar, so we will not show them here, but these results can be found in Appendix I. The dotted line is the result without Fermi motion and medium effects, and is obtained from expressions like Eq. (6.16) by replacing each smearing function with a delta function (multiplied by the polarization factor for the spin-dependent case) and using the free results for the u- and d-quark distributions in the nucleon. The dot-dashed line includes the effect of the scalar field, and the dashed curve also incorporates Fermi motion, which is the result after convolution with the appropriate nucleon distribution (Eqs. (6.21) and (6.22)). The complete in-medium distribution is given by the solid line and is the result obtained after also shifting the scaling variable using Eq. (6.30).

For the spin-independent distributions all nucleons contribute. Therefore, in Figs. 6.5 and 6.6 we see that the u- and d-quark distributions are very similar. For the spin-dependent case (see Fig. 6.7) only the valence proton-hole contributes. Hence the distributions resemble those of the proton. We find that higher multipole distributions are greatly suppressed relative to the leading results, see for example the $K = 3$ distribution in Fig. 6.8 and results contained in Appendix I. The spin-independent $K = 2$ multipole is an order of magnitude smaller again and reflects the very weak helicity dependence of the F_{2A}^{JH} structure functions. This weak helicity dependence arises because the spin-zero core is the dominant contribution to F_{2A}^{JH}, and changes in H simply reflect different spin orientations of the valence nucleon(s). In Appendix I we give results for all multipole quark distributions for the nuclei ^{7}Li, ^{11}B, ^{12}C, ^{15}N, ^{16}O, ^{27}Al and ^{28}Si.

The main features of the medium effects displayed in Figs. 6.5 − 6.7 are similar to those found in the nuclear matter calculation of Chapter 5. The spin-independent distributions are quenched at large x and enhanced for small x, whereas the spin-dependent distributions are quenched for all x. The discussion on the effect of the vector potential presented in section 5.3 remains valid here.

The nuclear spin sum, $\Sigma^{(A)}$, and axial coupling, $g_A^{(A)}$, contain information on both nuclear and quark effects and are simply given by

$$\Sigma^{(A)} = \Delta u_A + \Delta d_A \equiv \Sigma\ (P_p + P_n)\,, \tag{6.44}$$

$$g_A^{(A)} = \Delta u_A - \Delta d_A \equiv g_A\ (P_p - P_n)\,, \tag{6.45}$$

where Δq_A represents the first moment of Δq_A^{JJ} and Σ, g_A are the medium

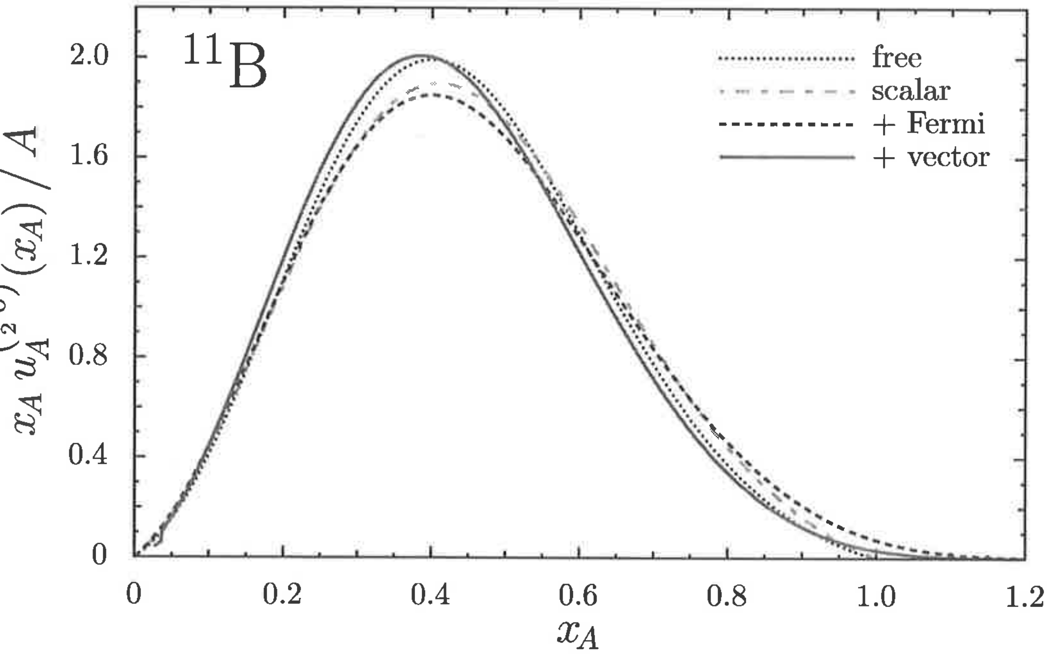

Figure 6.5: The first spin-independent multipole (K=0) u-quark distribution in ^{11}B (at $Q^2 = Q_0^2$).

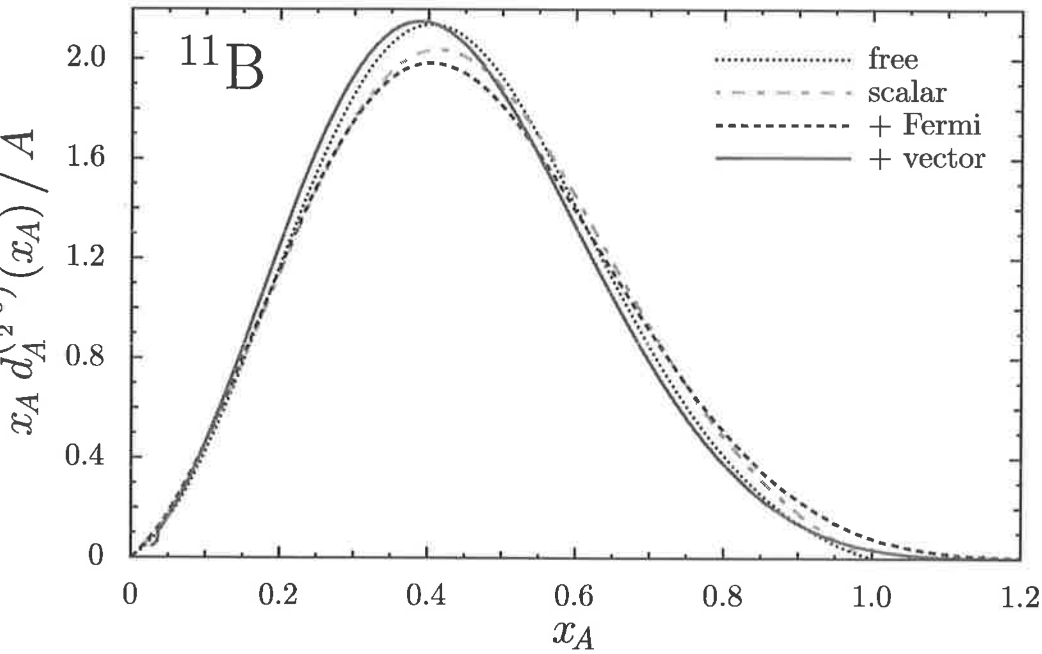

Figure 6.6: The first spin-independent multipole (K=0) d-quark distribution in ^{11}B (at $Q^2 = Q_0^2$).

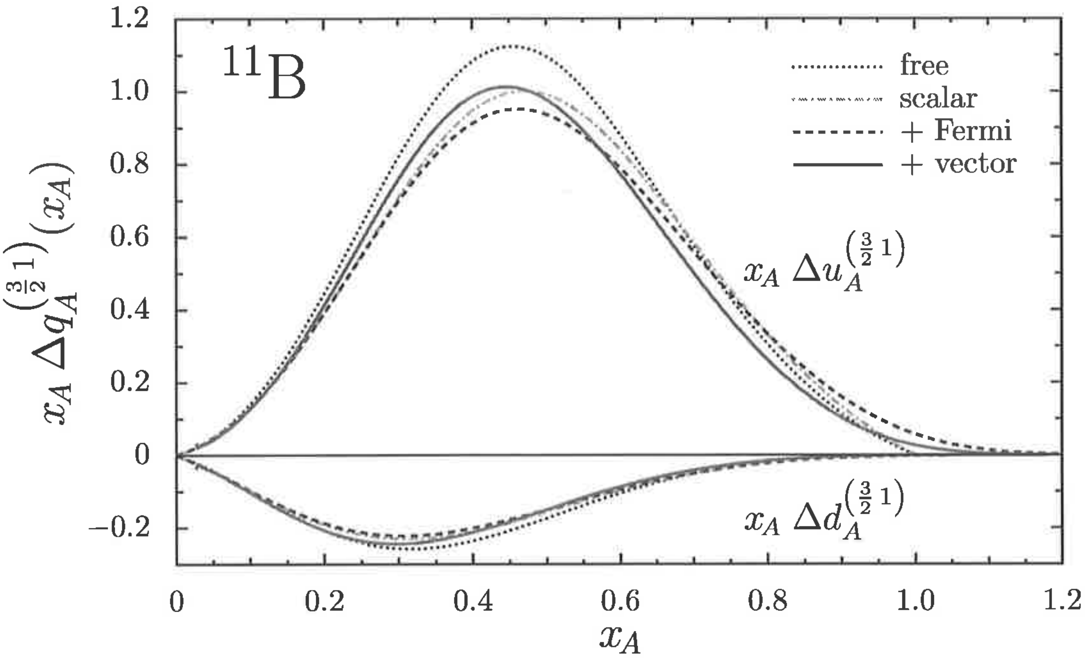

Figure 6.7: The first spin-dependent multipole (K=1) u- and d-quark distributions in ^{11}B (at $Q^2 = Q_0^2$).

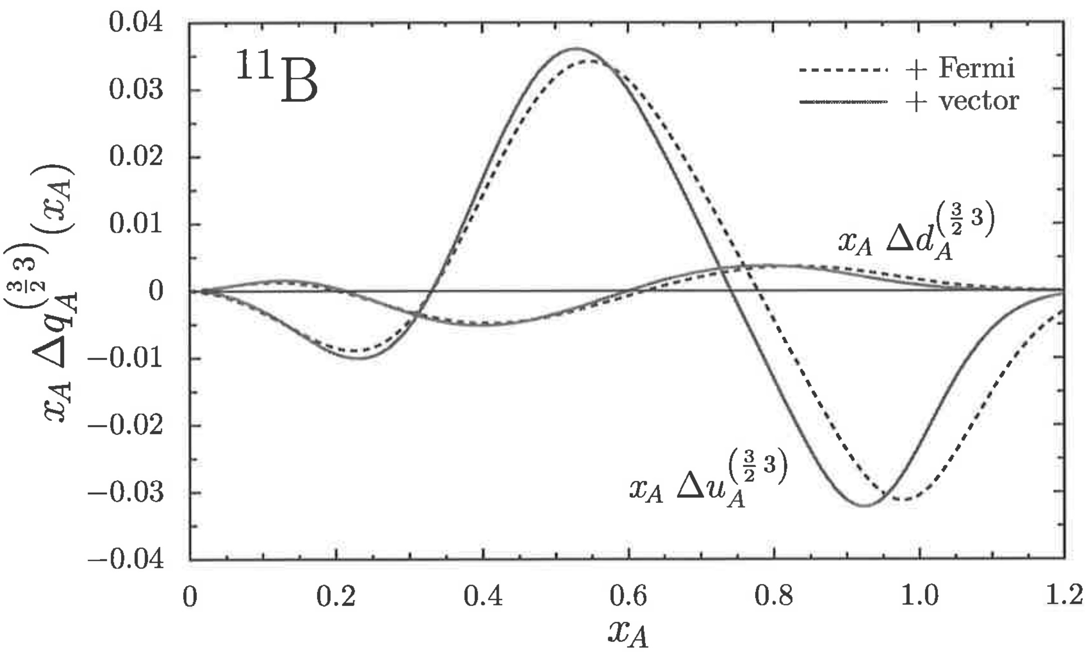

Figure 6.8: The second spin-dependent multipole (K=3) u- and d-quark distributions in ^{11}B (at $Q^2 = Q_0^2$).

	Δu	Δd	Σ	g_A
p	0.97	-0.30	0.67	1.267
^{7}Li	0.91	-0.29	0.62	1.19
^{11}B	0.88	-0.28	0.60	1.16
^{15}N	0.87	-0.28	0.59	1.15
^{27}Al	0.87	-0.28	0.59	1.15
Nuclear Matter	0.79	-0.26	0.53	1.05

Table 6.2: Results for the first moment of the in-medium quark distributions in the bound proton and the resulting spin sum and nucleon axial charge. It is clear that the moments tend to decrease with increasing A.

modified nucleon quantities, defined by dividing out the non-relativistic isoscalar and isovector polarization factors for $H = J$. We find that Σ and g_A are both suppressed in-medium relative to the free values, as summarized Table 6.2. This decrease of g_A in-medium is in agreement with the well known nuclear β-decay studies which, after taking into account the nuclear structure effects, require a quenching of g_A to achieve agreement with empirical data.[4]

In Figs. 6.9–6.12 we give results for the EMC and polarized EMC effect in ^{7}Li, ^{11}B, ^{15}N and ^{27}Al at $Q^2 = 5\,\text{GeV}^2$. The dashed line is the unpolarized EMC effect, the solid line is the $K = 1$ polarized EMC effect and the dotted line is the $M = J$ polarized EMC result (c.f. Eqs. (6.38) and (6.35), respectively). For the unpolarized EMC effect the results agree very well with the experimental data taken from Ref. [160], where importantly we obtain the correct A-dependence.

Consistent with previous nuclear matter studies, we find that the polarized EMC effect is larger than the unpolarized case, with the exception of the multipole result for ^{7}Li at $x \gtrsim 0.6$. Based on the wavefunction given in Eq. (6.40) the neutrons give a small contribution to the polarization. To test the dependence on the neutron polarization we also coupled the two neutrons to spin-zero, so that $P_n^{3/2\,3/2} = 0$, which is closer to the Quantum Monte Carlo result of -0.04 [157]. We find that these results are very similar to those in Fig. 6.9.

The unusual shape for the ^{15}N polarized EMC result is because our full result for $g_{1A}^{1/2\,1/2}$ changes sign at $x \simeq 0.8$ (see Fig. I.21), and hence the ratio

[4]The required quenching factors can be seen, for example, by comparing the experimental and calculated Gamow-Teller matrix elements given in Refs. [161, 162].

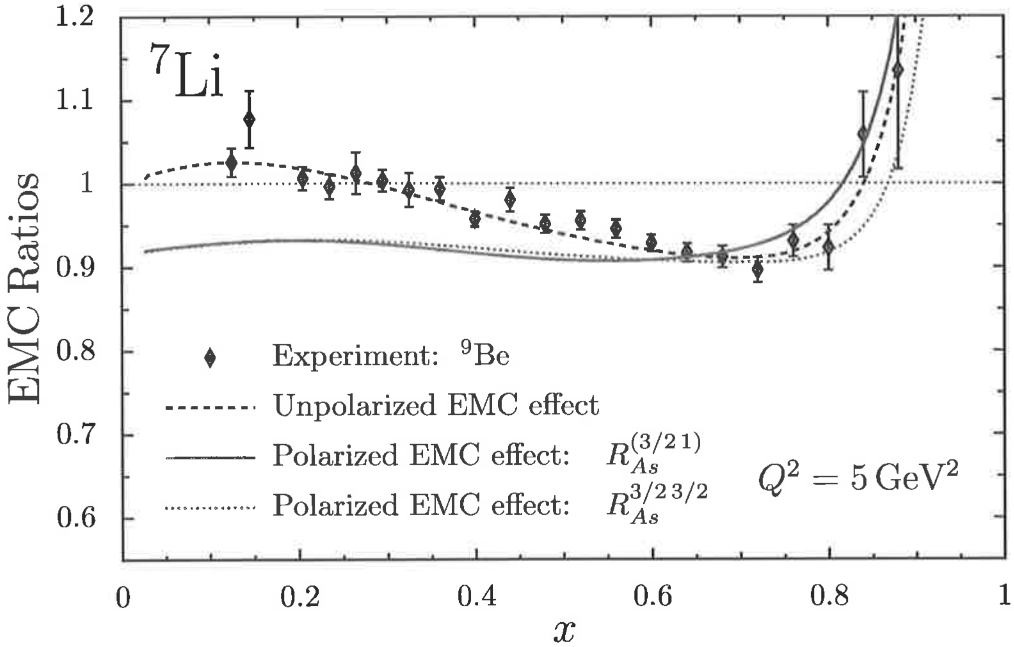

Figure 6.9: The EMC and polarized EMC effect in ^{7}Li. The empirical data is from Ref. [160].

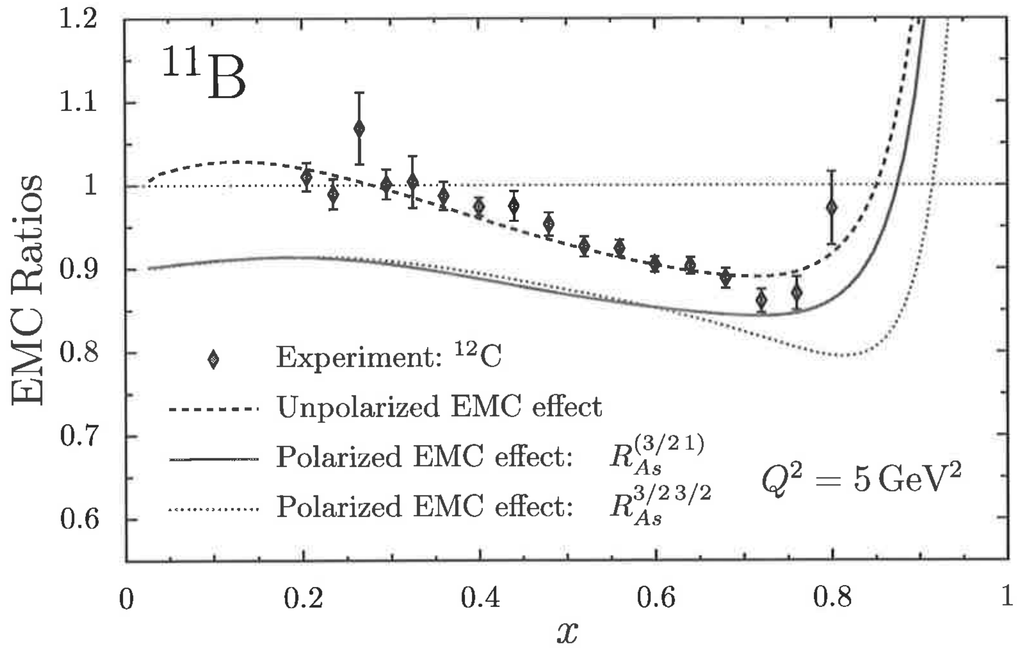

Figure 6.10: The EMC and polarized EMC effect in ^{11}B. The empirical data is from Ref. [160].

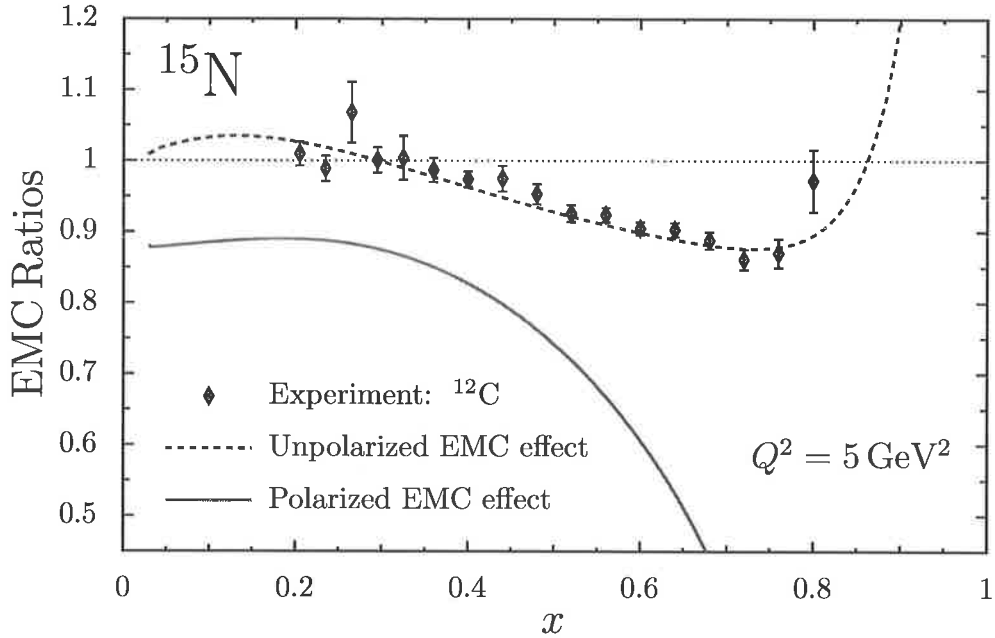

Figure 6.11: The EMC and polarized EMC effect in ^{15}N. The empirical data is from Ref. [160].

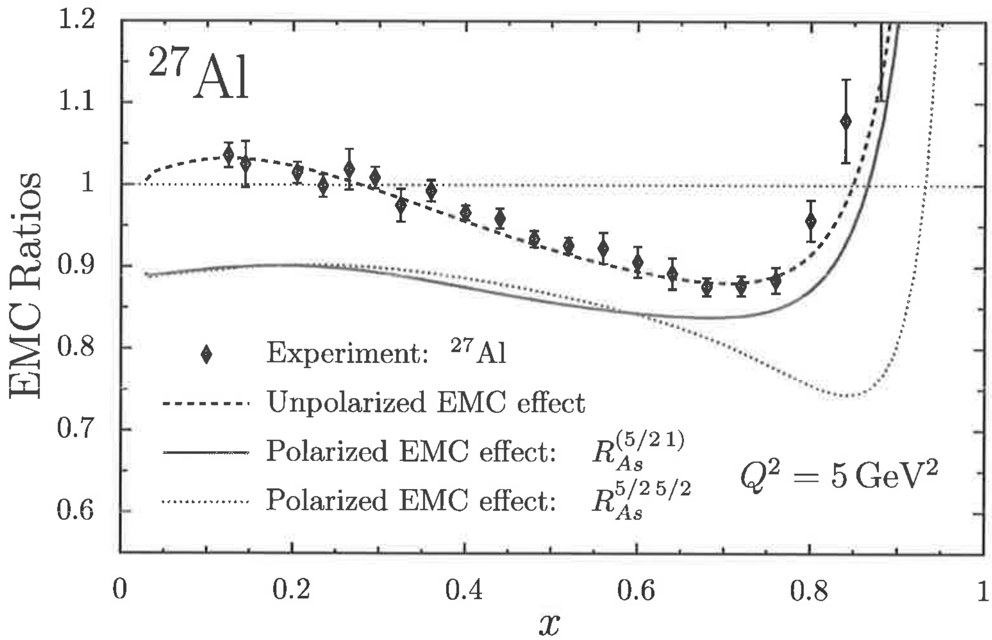

Figure 6.12: The EMC and polarized EMC effect in ^{27}Al. The empirical data is from Ref. [160].

must go to zero at this point. The origin of this sign change is the nucleon $p_{1/2}$ smearing function, which becomes positive for large y_A (see Fig. I.23). This result suggests ^{15}N may not be a good candidate with which to study nucleon medium modifications. The ^{11}B and ^{27}Al results resemble those obtained for nuclear matter in Chapter 5 and Ref. [98], where we find a polarized EMC effect roughly twice that of the unpolarized case. In Appendix I we give results for the EMC effect in ^{12}C, ^{16}O and ^{28}Si.

6.5 Conclusion

Using a relativistic formalism, where the quarks in the bound nucleons respond to the nuclear environment, we calculated the quark distributions and structure functions of ^{7}Li, ^{11}B, ^{15}N and ^{27}Al. For a spin-J target there are $2J+1$ independent quark distributions or structure functions in the Bjorken limit. For example, ^{27}Al therefore has six structure functions, however we find that the higher multipoles are suppressed relative to the leading result by at least an order of magnitude (see Appendix I).

We were readily able to describe the EMC effect in these nuclei, and importantly obtained the correct A-dependence. We also determined the EMC ratio for ^{12}C, ^{16}O and ^{28}Si and found ratios very similar to their $A-1$ neighbours, these results can be found in Appendix I. In Eq. (6.35) we define the polarized EMC ratio in nuclei. This ratio is such that in the extreme non-relativistic limit, with no medium modifications, it is unity. The results for the polarized EMC effect in nuclei corroborate our results in Chapter 5 and those in references [98, 163] for nuclear matter, the results for light nuclei of Ref. [164] and small x studies in Ref. [159] that find large medium modifications to the spin structure function relative to the unpolarized case. In particular, we find that the fraction of the spin of the nucleon carried by the quarks is decreased in nuclei (see Table 6.2). Experimental confirmation of this result would help test some quantitative differences with recent soliton model predictions for nuclear matter. Thereby giving important insights into in-medium quark dynamics, helping to quantify the role of quark degrees of freedom in the nuclear environment.

7

Summary and Outlook

QCD presents an immense, but incredibly rewarding challenge to the experimental and theoretical nuclear and particle physics communities. There are many different avenues one can pursue to gain insight into the quark-gluon structure of matter and the nature of QCD. It has been the goal of this thesis to bring to the fore the potential of nuclei as ideal laboratories with which to investigate quark-gluon dynamics and thereby extend our knowledge of QCD.

To achieve this we began with a chiral effective quark theory of QCD, the Nambu–Jona-Lasinio model, regularized using the proper-time scheme. This regularization method has many important attributes, most relevant to this discussion being that it simulates some important aspects of confinement and enables the saturation of nuclear matter. The nucleon as a bound state of three quarks was modelled using the relativistic Faddeev formalism. The use of proper-time regularization forced us to make a "modified static approximation" to the quark exchange kernel. Using this machinery we calculated the entire triplet of twist-two quark distribution functions. We obtained excellent results, which satisfied all known positivity constraints and agreed very well with available empirical parameterizations and experimental first moment data. A highlight of this study was the prediction that the nucleon tensor charge is very similar in magnitude to the nucleon axial charge.

Our successful description of the free quark distributions and our ability to model nuclear matter within the same framework, provided the motivation to study the in-medium modifications to the quark distributions. We determined the EMC, polarized EMC and transversity EMC effects in nuclear matter. Excellent agreement with nuclear matter data was achieved for the EMC effect and we predicted large deviations from unity for the other two EMC ratios. An immediate consequence of this result is that the spin structure of the nucleon undergoes significant modification in the nuclear medium. We find that the helicity spin sum is reduced by 20% and the transversity spin sum by 13%. Similar reductions in the nucleon axial and tensor charges were also found.

Infinite nuclear matter results are mainly of theoretical interest as all experiments are performed on finite nuclei. The lower components of quark wavefunctions play a pivotal role in nucleon spin structure. Therefore in any study of the spin structure of nuclei it is imperative to retain the lower components of the nucleon wavefunctions. To achieve this we used a relativistic shell model and derived expressions for the nucleon distributions in the nucleus, which are valid in any model using spherically symmetric potentials. The convolution formalism then provides access to the quark degrees of freedom in nuclei.

We calculated the EMC and polarized EMC ratios in the following nuclei: ^{7}Li, ^{11}B, ^{12}C, ^{15}N, ^{16}O, ^{27}Al and ^{28}SI. For the EMC effect we found excellent agreement with experimental data. The medium modifications for the polarized EMC effect were up to twice that of the familiar EMC ratio, in agreement with our nuclear matter studies. In-medium, we again found a quenching of the spin sum and the nucleon axial charge. The amount of quenching increased with A and appeared to converge to our nuclear matter result in each case.

The large signature for the polarized EMC effect has caught the attention of a number of experimentalist at Jefferson Lab. Experimentally the polarized EMC effect is suppressed by $1/A$ relative to that EMC ratio, because only the valence nucleons carry the spin of the nucleus. This almost definitely rules out a measurement of the g_{1A} structure function for nuclei with atomic mass larger than that of Aluminium. The best candidates for such a measurement are likely to be ^{7}Li and ^{11}B, with ^{7}Li receiving the most attention because of Jefferson Lab's proven ability to achieve target polarizations of at least 60%. The measurement of the polarized EMC effect has been earmarked as a potentially important experiment at Jefferson Lab after the 12 GeV upgrade. This interest has been spurred by the potential for such a measurement to shed new light on the role of quark-gluon dynamics in nuclei and the long range phenomenology of QCD.

The formalism developed in this thesis can be applied to a large array of interesting and important areas of nuclear physics. Possible future directions include the calculation of the generalized parton distributions of the nucleon and their modification in nuclei. The strange quark can easily be incorporated into the model, giving access to the hyperon spectrum. The hyperons could then be included in nuclear matter, having potentially important implications for neutron and quark stars. The inclusion of the ρ-meson would result in a quark flavour dependence to the scale transformation that incorporates the effect of the vector potential on the in-medium quark distributions. This would facilitate a very interesting investigation of charge symmetry violation in nuclei.

Incorporating the pion into the model is probably the most pressing improvement, as for example its introduction would enable the calculation of anti-quark distributions in the nucleon and in nuclei. Nuclear anti-quark distributions are largely unexplored, both experimentally and theoretically. From a theoretical perspective there are many interesting questions that remain unresolved. For example, to obtain the correct support for nuclear anti-quark distributions it appears that the anti-nucleons must play an important role. To my knowledge, this particularly interesting area of physics remains almost completely unexplored.

In this thesis we have presented some potentially important results for our understanding of the spin structure of nuclei. We have endeavored to highlight the incredible opportunities the nucleus provides as a laboratory for the study of QCD. There are many interesting and important theoretical and experimental investigations possible with nuclei, that may give new insights into QCD and in particular its long range structure. This would help us answer one of the most important questions confronting nuclear physics, which is: how do the fundamental degrees of freedom – the quarks and gluons – give rise to nucleons and the inter-nucleon forces that bind nuclei?

A

Notations, Conventions and Useful Results

A.1 Regularization and 4-D Polar Coordinates

$$\frac{1}{X^n} = \frac{1}{(n-1)!} \int_0^\infty d\tau\, \tau^{n-1}\, e^{-\tau X}, \tag{A.1}$$

$$\int \frac{d^4 k_E}{(2\pi)^4} \rangle \frac{1}{16\,\pi^2} \int_0^\infty dk_E^2\, k_E^2. \tag{A.2}$$

A.2 Useful Integrals

$$\int_0^\infty dq^2\, q^2\, e^{-\tau\left(q^2+A\right)} = \frac{e^{-\tau A}}{\tau^2}, \tag{A.3}$$

$$\int_0^\infty dq^2\, q^4\, e^{-\tau\left(q^2+A\right)} = \frac{2e^{-\tau A}}{\tau^3}, \tag{A.4}$$

$$\int_0^\infty dq^2\, q^6\, e^{-\tau\left(q^2+A\right)} = \frac{6e^{-\tau A}}{\tau^4}. \tag{A.5}$$

A.3 Lightcone Vectors

The lightcone contravariant four-vector is given by

$$a^\mu = \left(a^+,\ a^1,\ a^2,\ a^-\right) = \left(a^+,\ \vec{a}_\perp,\ a^-\right), \tag{A.6}$$

where, in the Kogut-Soper representation

$$a^+ = \frac{1}{\sqrt{2}}\left(a^0 + a^3\right), \qquad a^0 = \frac{1}{\sqrt{2}}\left(a^+ + a^-\right),$$

$$a^- = \frac{1}{\sqrt{2}}\left(a^0 - a^3\right), \qquad a^3 = \frac{1}{\sqrt{2}}\left(a^+ - a^-\right). \tag{A.7}$$

The Kogut-Soper γ-matrix structure is defined similarly, and the Dirac algebra $\{\gamma^\mu, \gamma^\nu\} = 2g^{\mu\nu}$ is of course satisfied. The covariant four-vectors are obtained via $x_\mu = g_{\mu\nu}x^\nu$ and the metric is given by

$$\{g^{\mu\nu}\} = \{g_{\mu\nu}\} = \begin{pmatrix} 0 & 0 & 0 & 1 \\ 0 & -1 & 0 & 0 \\ 0 & 0 & -1 & 0 \\ 1 & 0 & 0 & 0 \end{pmatrix} . \tag{A.8}$$

With this convention the Lorentz scalar product is

$$a \cdot b = a_\mu b^\mu = a_+ b^+ + a_- b^- - \vec{a}_\perp \vec{b}_\perp = a_+ b_- + a_- b_+ - \vec{a}_\perp \vec{b}_\perp . \tag{A.9}$$

Some useful relations are

$$\begin{aligned} \{\gamma^\mu, \gamma^5\} &= 0 \qquad & \{\gamma^+, \gamma^-\} &= 2 \qquad & \{\not{k}, \gamma^\pm\} &= 2\, k_\mp \mathbb{1}, \\ \gamma^+ \gamma^+ = \gamma^- \gamma^- &= 0 \qquad & \gamma^+ \gamma^- \gamma^+ &= 2\gamma^+ \qquad & \gamma^- \gamma^+ \gamma^- &= 2\gamma^- . \end{aligned} \tag{A.10}$$

A.4 Useful Relations

$$\begin{aligned} \left(\frac{k_- + \alpha q_-}{q_-}\right)^{n-1} &= \alpha^{n-1} + (n-1)\alpha^{n-2}\frac{k_-}{q_-} + \frac{1}{2}(n-1)(n-2)\alpha^{n-3}\frac{k_-^2}{q_-^2} + \ldots, \\ &= \alpha^{n-1} + \frac{k_-}{q_-}\frac{d}{d\alpha}\alpha^{n-1} + \frac{1}{2}\frac{k_-^2}{q_-^2}\frac{d^2}{d\alpha^2}\alpha^{n-1} + \ldots \end{aligned} \tag{A.11}$$

A.5 Feynman Parametrization

Using

$$\begin{aligned} \frac{1}{AB} &= \int_0^1 d\alpha \frac{1}{[\alpha A + (1-\alpha) B]^2}, \\ &\Longrightarrow \quad \frac{1}{AB^n} = \int_0^1 d\alpha \frac{n\,(1-\alpha)^{n-1}}{[\alpha A + (1-\alpha) B]^{n+1}}. \end{aligned} \tag{A.12}$$

Therefore

$$\begin{aligned} &\frac{1}{(k^2 - M_A^2 + i\varepsilon)(k^2 + p^2 - 2k \cdot p - M_B^2 + i\varepsilon)} \\ &\overset{k \to k + \alpha p}{=} \int_0^1 d\alpha \frac{1}{[k^2 - (\alpha^2 - \alpha)\, p^2 - \alpha M_B^2 - (1-\alpha)\, M_A^2 + i\varepsilon]^2}, \end{aligned} \tag{A.13}$$

$$\frac{1}{\left(k^2 - M_A^2 + i\,\varepsilon\right)^2 \left(k^2 + p^2 - 2k\cdot p - M_B^2 + i\varepsilon\right)}$$
$$\overset{k\to k+\alpha p}{=} \int_0^1 d\alpha \, \frac{2(1-\alpha)}{\left[k^2 - (\alpha^2-\alpha)\,p^2 - \alpha M_B^2 - (1-\alpha)\,M_A^2 + i\varepsilon\right]^3}. \quad (A.14)$$

A.6 Integral Relations

$$\int \frac{d^4k}{(2\pi)^4} \frac{k^\mu}{\left(k^2 - \Sigma + i\varepsilon\right)^n} = 0, \quad (A.15)$$

$$\int \frac{d^4k}{(2\pi)^4} \frac{k^\mu k^\nu}{\left(k^2 - \Sigma + i\varepsilon\right)^n} = \frac{1}{4} g^{\mu\nu} \int \frac{d^4k}{(2\pi)^4} \frac{k^2}{\left(k^2 - \Sigma + i\varepsilon\right)^n}, \quad (A.16)$$

$$\int \frac{d^4k}{(2\pi)^4} \frac{k^\mu k^\nu k^\rho k^\sigma}{\left(k^2 - \Sigma + i\varepsilon\right)^n}$$
$$= \frac{1}{24}\left(g^{\mu\nu}g^{\rho\sigma} + g^{\mu\rho}g^{\nu\sigma} + g^{\mu\sigma}g^{\nu\rho}\right) \int \frac{d^4k}{(2\pi)^4} \frac{k^4}{\left(k^2 - \Sigma + i\varepsilon\right)^n}, \quad (A.17)$$

$$\int \frac{d^4k}{(2\pi)^4} \frac{k^2}{\left(k^2 - \Sigma + i\varepsilon\right)^{n+1}} = \frac{2}{n} \int \frac{d^4k}{(2\pi)^4} \frac{1}{\left(k^2 - \Sigma + i\varepsilon\right)^n}, \quad (A.18)$$

where $n \geq 1$ and the function Σ has no k dependence. These relations are easily proved using integration by parts.

A.7 Wick Rotation

$$\int \frac{d^4k}{(2\pi)^4} \longrightarrow i \int \frac{d^4k_E}{(2\pi)^4}, \qquad (q^0, \vec{q}) \longrightarrow \left(iq_E^0, \vec{q}_E\right), \qquad q^2 \longrightarrow -q_E^2. \quad (A.19)$$

In an $O(4)$ invariant regularization we have

$$q_- q_+ \longrightarrow -\frac{1}{4} q_E^2, \quad (A.20)$$

$$q_- q_+ q_- q_+ \longrightarrow -\frac{1}{24} q_E^2. \quad (A.21)$$

A.8 Simple Bubble Graphs :- $\Pi_\pi(q^2)$, $\Pi_s(q^2)$ and $\Pi_a(q^2)$

$$\Pi_\pi(q^2) = \Pi_s(q^2) = 6i \int \frac{d^4k}{(2\pi)^4} \,\mathrm{Tr}\Big[\gamma_5\, S(k)\, \gamma_5\, S(k-q)\Big],$$

$$= -\frac{3}{2\,\pi^2} \int d\tau \left\{ \frac{1}{\tau^2}\, e^{-\tau M^2} + \frac{q^2}{2} \int_0^1 d\alpha\, \frac{1}{\tau} e^{-\tau\left[q^2(\alpha^2-\alpha)+M^2\right]} \right\}. \tag{A.22}$$

$$\Pi_a(q^2)\left(g^{\mu\nu} - \frac{q^\mu\, q^\nu}{M_a^2}\right) = 6i \int \frac{d^4k}{(2\pi)^4} \,\mathrm{Tr}\Big[\gamma^\mu\, S(k)\, \gamma^\nu\, S(k-q)\Big]. \tag{A.23}$$

$$\Pi_a(q^2) = -\frac{3}{\pi^2}\, q^2 \int_0^1 d\alpha \int d\tau\, \frac{1}{\tau}\, \alpha(1-\alpha)\, e^{-\tau\left[q^2(\alpha^2-\alpha)+M^2\right]}. \tag{A.24}$$

A.9 Effective Couplings :- g_π, g_s and g_a

$$g_\pi = \left.\frac{-1}{\partial\, \Pi_\pi(q^2)/\partial q^2}\right|_{q^2=m_\pi^2}, \tag{A.25}$$

$$g_\pi^{-1} = \frac{3}{4\pi^2} \int_0^1 d\alpha \int d\tau \left[\frac{1}{\tau} - m_\pi^2\, (\alpha^2-\alpha)\right] e^{-\tau\left[m_\pi^2(\alpha^2-\alpha)+M^2\right]}. \tag{A.26}$$

$$g_s = \left.\frac{-2}{\partial\, \Pi_s(q^2)/\partial q^2}\right|_{q^2=M_s^2}, \tag{A.27}$$

$$g_s^{-1} = \frac{3}{8\pi^2} \int_0^1 d\alpha \int d\tau \left[\frac{1}{\tau} - M_s^2\, (\alpha^2-\alpha)\right] e^{-\tau\left[M_s^2(\alpha^2-\alpha)+M^2\right]}. \tag{A.28}$$

$$g_a = \left.\frac{-2}{\partial\, \Pi_a(q^2)/\partial q^2}\right|_{q^2=M_a^2}, \tag{A.29}$$

$$g_a^{-1} = \frac{3}{2\pi^2} \int_0^1 d\alpha \int d\tau\, \alpha(1-\alpha) \left[\frac{1}{\tau} - M_a^2\, (\alpha^2-\alpha)\right] e^{-\tau\left[M_a^2(\alpha^2-\alpha)+M^2\right]}. \tag{A.30}$$

A.10 Propagators

$$S(k) = \frac{1}{\not{k} - M + i\,\varepsilon} = \frac{\not{k} + M}{k^2 - M^2 + i\,\varepsilon}, \tag{A.31}$$

$$\tau_\pi(q) = \frac{-2iG_\pi}{1 + 2\,G_\pi\,\Pi_s(q^2)} \longrightarrow -2\,i\,G_\pi + \frac{i\,g_\pi}{q^2 - m_\pi^2 + i\,\varepsilon}, \tag{A.32}$$

$$\tau_s(q) = \frac{4iG_s}{1 + 2\,G_s\,\Pi_s(q^2)} \longrightarrow 4\,i\,G_s - \frac{i\,g_s}{q^2 - M_s^2 + i\,\varepsilon}, \tag{A.33}$$

$$\tau_a^{\mu\nu}(q) = 4\,i\,G_a\left[g^{\mu\nu} - \frac{2G_a\Pi_a(q^2)}{1 + 2G_a\Pi_a(q^2)}\left(g^{\mu\nu} - \frac{q^\mu\,q^\nu}{q^2}\right)\right],$$

$$= 4\,i\,G_a\left[\frac{g^{\mu\nu} + 2G_a\Pi_a(q^2)\,\frac{q^\mu q^\nu}{q^2}}{1 + 2G_a\Pi_a(q^2)}\right], \tag{A.34}$$

$$\longrightarrow \left[4iG_a\,g^{\mu\nu} - \frac{i\,g_a}{q^2 - M_a^2 + i\,\varepsilon}\left(g^{\mu\nu} - \frac{q^\mu\,q^\nu}{M_a^2}\right)\right], \tag{A.35}$$

$$\longrightarrow \left(4\,i\,G_a - \frac{i\,g_a}{q^2 - M_a^2 + i\,\varepsilon}\right)g^{\mu\nu}. \tag{A.36}$$

In this analysis we use Eq. (A.36) as the axial-vector diquark propagator, since the term $\frac{q^\mu q^\nu}{M_a^2}$ only changes our results by less than 1%.

A.11 Pion Decay Constant f_π

The pion decay constant is defined by the matrix element

$$\langle 0|\overline{\psi}(0)\gamma_\mu\gamma_5\frac{\tau^a}{2}\psi(0)|\pi_b(q)\rangle = i\,f_\pi\,q_\mu\,\delta_{ab}. \tag{A.37}$$

Therefore

$$i\,f_\pi\,q_\mu\,\delta_{ab} = 3\sqrt{g_\pi}\,\delta_{ab}\int\frac{d^4k}{(2\pi)^4}\mathrm{Tr}\left[\gamma_5\,S(k)\gamma_\mu\gamma_5\,S(k-q)\right]. \tag{A.38}$$

This implies

$$f_\pi = -12\sqrt{g_\pi}i\int\frac{d^4k}{(2\pi)^4}\frac{M}{(k^2 - M^2 + i\varepsilon)\left[(k-q)^2 - M^2 + i\varepsilon\right]},$$

$$f_\pi = \frac{3}{4\pi^2}\,M\,\sqrt{g_\pi}\int_0^1 d\alpha\int d\tau\,\frac{1}{\tau}\,e^{-\tau\left[m_\pi^2(\alpha^2-\alpha)+M^2\right]}. \tag{A.39}$$

By defining $m_\pi = 140\,\mathrm{MeV}$, $M = 400\,\mathrm{MeV}$ $\Lambda_{IR} = 240$ MeV and $f_\pi = 93$ MeV, Eq. (A.39) enables us to determine $\Lambda_{UV} = 645\,\mathrm{MeV}$.

A.12 The Gap Equation

The gap equation has the form

$$M = m_q + 2i\, G_\pi \int \frac{d^4k}{(2\pi)^4}\, \mathrm{Tr}\,[S(k)]\,, \tag{A.40}$$

where M is the constituent quark mass, m_q the current quark mass, and the trace is over Dirac, colour and isospin indices. Therefore

$$\begin{aligned} M &= m_q + 2i\, G_\pi\, N_c\, N_f \int \frac{d^4k}{(2\pi)^4} \mathrm{Tr}\left[\frac{\not{k} + M}{k^2 - M^2 + i\varepsilon}\right], \\ &= m_q + 2i\, G_\pi\, N_c\, N_f \int \frac{d^4k}{(2\pi)^4} \frac{4M}{k^2 - M^2 + i\varepsilon}, \\ &= m_q + \frac{2\, G_\pi\, N_c\, N_f}{16\pi^2} \int_0^\infty dk_E^2\, k_E^2 \frac{4M}{k_E^2 + M^2}, \\ &= m_q + \frac{M\, G_\pi\, N_c\, N_f}{2\pi^2} \int d\tau \int_0^\infty dk_E^2\, k_E^2 e^{-\tau(k_E^2 + M^2)}, \\ &= m_q + \frac{M\, G_\pi\, N_c\, N_f}{2\pi^2} \int d\tau\, \frac{e^{-\tau M^2}}{\tau^2}. \end{aligned} \tag{A.41}$$

Therefore

$$m_q = M\left(1 - \frac{G_\pi\, N_c\, N_f}{2\pi^2} \int d\tau\, \frac{e^{-\tau M^2}}{\tau^2}\right). \tag{A.42}$$

For $M = 400\,\mathrm{MeV}$ and $G_\pi = 19.04\,\mathrm{GeV}^{-2}$ we find $m_q = 16.4\,\mathrm{MeV}$.

A.13 Dirac Spinors

Throughout this work we us the Dirac spinors of Kogut and Soper given in Ref. [165], which have the form

$$u_+(p) = \frac{1}{2^{\frac{1}{4}}\sqrt{p^+}} \begin{pmatrix} \sqrt{2}\, p^+ \\ p^1 + ip^2 \\ m \\ 0 \end{pmatrix}, \qquad u_-(p) = \frac{1}{2^{\frac{1}{4}}\sqrt{p^+}} \begin{pmatrix} 0 \\ m \\ -p^1 + ip^2 \\ \sqrt{2}\, p^+ \end{pmatrix}, \tag{A.43}$$

$$\overline{u}_+(p) = \frac{1}{2^{\frac{1}{4}}\sqrt{p^+}} \begin{pmatrix} m & 0 & \sqrt{2}\, p^+ & p_1 - ip_2 \end{pmatrix},$$

$$\overline{u}_-(p) = \frac{1}{2^{\frac{1}{4}}\sqrt{p^+}} \begin{pmatrix} -p_1 - ip_2 & \sqrt{2}\, p^+ & 0 & m \end{pmatrix}. \tag{A.44}$$

It is important to note that these spinors are defined with respect to the Kogut and Soper chiral representation of the Dirac matrices, which has the form

$$\gamma^0 = \begin{pmatrix} 0 & 1 \\ 1 & 0 \end{pmatrix}, \quad \gamma^i = \begin{pmatrix} 0 & -\sigma^i \\ \sigma^i & 0 \end{pmatrix}, \quad \gamma_5 \equiv i\gamma^0\gamma^1\gamma^2\gamma^3 = \begin{pmatrix} 1 & 0 \\ 0 & -1 \end{pmatrix}. \tag{A.45}$$

It is easy to demonstrate that these spinors are solutions to the Dirac equation using the result

$$\not{p} \pm m = \begin{pmatrix} \pm m & 0 & p_0 - p_3 & -p_1 + ip_2 \\ 0 & \pm m & -p_1 - ip_2 & p_0 + p_3 \\ p_0 + p_3 & p_1 - ip_2 & \pm m & 0 \\ p_1 + ip_2 & p_0 - p_3 & 0 & \pm m \end{pmatrix}. \tag{A.46}$$

A.14 Matrix Elements

Throughout this work we normalize the nucleon spinor such that

$$\overline{u}_N(p)\, u_N(p) = 1. \tag{A.47}$$

A.14.1 Helicity matrix elements

The following results are matrix elements between the spinors $\overline{u}_+$ and u_+, needed for the spin-independent and spin-dependent quark distribution calculations in Chapter 4. The abbreviated notation used here is such that $\langle\Omega\rangle \Longrightarrow \overline{u}_+\Omega\, u_+$:

$$\langle\gamma^+\rangle = \frac{p^+}{M_N}, \qquad \langle\gamma^-\rangle = \frac{M_N^2 + p_1^2 + p_2^2}{2M_N\, p^+} = \frac{p^-}{M_N},$$
$$\langle\gamma^1\rangle = \frac{p^1}{M_N}, \qquad \langle\gamma^2\rangle = \frac{p^2}{M_N}, \qquad \langle\gamma_5\rangle = 0. \tag{A.48}$$

$$\langle\gamma^+\gamma^-\rangle = 1, \qquad \langle\gamma^+\gamma^1\rangle = 0, \qquad \langle\gamma^+\gamma^2\rangle = 0, \qquad \langle\gamma^+\gamma_5\rangle = \frac{p^+}{M_N}. \tag{A.49}$$

$$\langle\gamma^-\gamma^+\rangle = 1, \qquad \langle\gamma^-\gamma^1\rangle = i\,\frac{p^2}{p^+},$$
$$\langle\gamma^-\gamma^2\rangle = -i\,\frac{p^1}{p^+}, \qquad \langle\gamma^-\gamma_5\rangle = \frac{-M_N^2 + p_1^2 + p_2^2}{2M_N\, p^+}. \tag{A.50}$$

$$\langle\gamma^+\gamma^-\gamma_5\rangle = -1, \qquad \langle\gamma^+\gamma^1\gamma_5\rangle = 0, \qquad \langle\gamma^+\gamma^2\gamma_5\rangle = 0. \tag{A.51}$$

$$\langle\gamma^-\gamma^+\gamma_5\rangle = -\frac{p^1}{M_N}, \qquad \langle\gamma^-\gamma^1\gamma_5\rangle = \frac{p^1}{p^+}, \qquad \langle\gamma^-\gamma^2\gamma_5\rangle = -\frac{p^2}{p^+}. \tag{A.52}$$

A.14.2 Transverse matrix elements

Throughout this thesis the transverse polarization axis is always chosen in the x-direction. Therefore, transverse nucleon spinor are given by [29]

$$u_\uparrow^{(x)} = \frac{1}{\sqrt{2}}\left(u_+ + u_-\right), \qquad \text{and} \qquad u_\downarrow^{(x)} = \frac{1}{\sqrt{2}}\left(u_+ - u_-\right), \tag{A.53}$$

where u_+ and u_- are the positive and negative helicity spinors given in Eq. (A.43).

The following results are matrix elements between the spinors $\overline{u}_\uparrow^{(x)}$ and $u_\uparrow^{(x)}$, needed for the transversity quark distribution calculation in Chapter 4. The abbreviated notation used here is such that $\langle\Omega\rangle \implies \overline{u}_\uparrow^{(x)}\Omega\, u_\uparrow^{(x)}$:

$$\langle\gamma^+\rangle = \frac{p^+}{M_N}, \qquad \langle\gamma^-\rangle = \frac{M_N^2 + p_1^2 + p_2^2}{2M_N\, p^+},$$
$$\langle\gamma^1\rangle = \frac{p^1}{M_N}, \qquad \langle\gamma^2\rangle = \frac{p^2}{M_N}, \qquad \langle\gamma_5\rangle = 0. \tag{A.54}$$

$$\langle\gamma^+\gamma^-\rangle = \frac{M_N + i\,p^2}{M_N}, \qquad \langle\gamma^+\gamma^1\rangle = 0,$$
$$\langle\gamma^+\gamma^2\rangle = i\frac{p^+}{M_N}, \qquad \langle\gamma^+\gamma_5\rangle = 0. \tag{A.55}$$

$$\langle\gamma^-\gamma^+\rangle = \frac{M_N - i\,p^2}{M_N}, \qquad \langle\gamma^-\gamma^1\rangle = -i\,\frac{p^1p^2}{M_N\,p^+},$$
$$\langle\gamma^-\gamma^2\rangle = -i\left(\frac{M_N^2 - p_1^2 + p_2^2}{2M_N\,p^+}\right), \qquad \langle\gamma^-\gamma_5\rangle = \frac{p^1}{p^+}. \tag{A.56}$$

$$\langle\gamma^1\gamma^2\rangle = i\,\frac{p^1}{M_N}, \qquad \langle\gamma^1\gamma_5\rangle = 1, \qquad \langle\gamma^2\gamma_5\rangle = 0. \tag{A.57}$$

$$\langle\gamma^+\gamma^-\gamma_5\rangle = \frac{p^1}{M_N}, \qquad \langle\gamma^+\gamma^1\gamma_5\rangle = \frac{p^+}{M_N}, \qquad \langle\gamma^+\gamma^2\gamma_5\rangle = 0. \tag{A.58}$$

$$\langle\gamma^-\gamma^+\gamma_5\rangle = -\frac{p^1}{M_N}, \qquad \langle\gamma^-\gamma^1\gamma_5\rangle = \frac{M_N^2 - p_1^2 + p_2^2}{2M_N\,p^+},$$
$$\langle\gamma^-\gamma^2\gamma_5\rangle = -\frac{p^1\,p^2}{M_N\,p^+}. \tag{A.59}$$

$$\langle\gamma^1\gamma^2\gamma_5\rangle = -\frac{p^2}{M_N}. \tag{A.60}$$

$$\langle\gamma^+\gamma^-\gamma^2\rangle = \frac{1}{M_N}\left(p^2 - iM_N\right). \tag{A.61}$$

A.15 3j-symbols

The definition of the 3j-symbols is

$$\begin{pmatrix} j_1 & j_2 & j \\ m_1 & m_2 & m \end{pmatrix} = \frac{(-1)^{j_1-j_2-m_2}}{\sqrt{2j+1}} C^{j\,-m}_{j_1 m_1 j_2 m_2}, \tag{A.62}$$

where $C^{jm}_{j_1 m_1 j_2 m_2}$ is a Clebsch-Gordon coefficient. If a 3j-symbol does not satisfy the following constraints it is zero:

1. $j_1,\ j_2,\ j\ \geqslant 0$,
2. $m_1 \in (-|j_1|, \ldots, |j_1|)$, $m_2 \in (-|j_2|, \ldots, |j_2|)$, $m \in (-|j|, \ldots, |j|)$,
3. $m_1 + m_2 + m = 0$,
4. $|j_1 - j_2| \leqslant j \leqslant j_1 + j_2$,
5. $j_1 + j_2 + j$ is an integer.

Symmetries of the 3j-symbols:

$$\begin{pmatrix} j_1 & j_2 & j \\ m_1 & m_2 & m \end{pmatrix} = \underbrace{\begin{pmatrix} j & j_1 & j_2 \\ m & m_1 & m_2 \end{pmatrix} = \ldots}_{\text{cyclic permutations}}$$
$$= \underbrace{(-1)^{j_1+j_2+j} \begin{pmatrix} j_1 & j & j_2 \\ m_1 & m & m_2 \end{pmatrix} = \ldots}_{\text{column interchange}} = (-1)^{j_1+j_2+j} \begin{pmatrix} j_1 & j_2 & j \\ -m_1 & -m_2 & -m \end{pmatrix}. \tag{A.63}$$

Orthogonality relations

$$\sum_{j,m} (2j+1) \begin{pmatrix} j_1 & j_2 & j \\ m_1 & m_2 & m \end{pmatrix} \begin{pmatrix} j_1 & j_2 & j \\ m_1' & m_2' & m \end{pmatrix} = \delta_{m_1 m_1'} \delta_{m_2 m_2'}, \tag{A.64}$$

$$\sum_{m_1,m_2} (2j+1) \begin{pmatrix} j_1 & j_2 & j \\ m_1 & m_2 & m \end{pmatrix} \begin{pmatrix} j_1 & j_2 & j' \\ m_1 & m_2 & m' \end{pmatrix} = \delta_{jj'} \delta_{mm'}. \tag{A.65}$$

Useful identities

$$\begin{pmatrix} j_1 & j_2 & j \\ 0 & 0 & 0 \end{pmatrix} = 0 \qquad \text{if } j_1 + j_2 + j \text{ is odd.} \tag{A.66}$$

A.16 Spherical Harmonics

The spherical harmonic orthogonality relation is

$$\int_0^{2\pi}\int_0^{\pi} d\phi\, d\theta\, sin\theta\; Y^*_{\ell' m'}(\theta,\phi) Y_{\ell m}(\theta,\phi)$$
$$= \int_0^{2\pi}\int_{-1}^{1} d\phi\, d(\cos\theta)\, Y^*_{\ell' m'}(\theta,\phi) Y_{\ell m}(\theta,\phi) = \delta_{\ell'\ell}\delta_{m'm}. \quad \text{(A.67)}$$

B

Derivation of Lepton and Hadronic Tensors

The differential cross-section for inclusive scattering ($e\,P \to e'\,X$) is given by

$$d\sigma = \frac{1}{J}\frac{d^3k'}{2E'(2\pi)^3}\sum_X \prod_{i=1}^{n_X}\int \frac{d^3p_i}{(2\pi)^3 2p_{i0}} |\mathcal{A}|^2 (2\pi)^4 \delta^4(P+q-\sum_{i=1}^{n_X} p_i), \tag{B.1}$$

where $J = P \cdot k$ is a flux factor, which equals $J = 4\,M\,E$ in the nucleon rest frame. The sum runs over all hadronic final states X which are not observed, where each hadronic final state consists of n_X particles with momenta p_i, where $\sum_{i=1}^{n_X} p_i \equiv p_X$. The squared-amplitude $|\mathcal{A}|^2$, given by

$$|\mathcal{A}|^2 = \sum_{s'} \left| \bar{u}(k', s')\gamma^\mu u(k,s)\, \frac{ie^2\, g_{\mu\nu}}{q^2}\, \langle X|J^\nu(0)|P,s\rangle \right|^2, \tag{B.2}$$

can be separated into a leptonic ($L^{\mu\nu}$) and a hadronic ($W_{\mu\nu}$) tensor, such that

$$|\mathcal{A}|^2 = (4\pi)^2\, \frac{\alpha^2}{Q^4}\, L^{\mu\nu}\, W_{\mu\nu}, \tag{B.3}$$

where $\alpha = e^2/4\pi \sim 1/137$ is the electromagnetic fine structure constant.

B.1 The Lepton Tensor

The lepton tensor is given by

$$L^{\mu\nu} = \sum_{s'} \left|\bar{u}(k', s')\gamma^\mu u(k,s)\right|^2 = \sum_{s'} \left[\bar{u}(k', s')\gamma^\mu u(k,s)\right]^* \left[\bar{u}(k', s')\gamma^\nu u(k,s)\right]. \tag{B.4}$$

Now $[\bar{u}(k',s')\gamma^\mu u(k,s)]$ is just a complex number, therefore its complex conjugate is the same as the hermitian conjugate, therefore

$$\begin{aligned}
[\bar{u}(k',s')\gamma^\mu u(k,s)]^* ,&= [\bar{u}(k',s')\gamma^\mu u(k,s)]^\dagger ,\\
&= \left[u^\dagger(k',s')\gamma^0\gamma^\mu u(k,s)\right]^\dagger ,\\
&= \left[u^\dagger(k,s)(\gamma^\mu)^\dagger(\gamma^0)^\dagger u(k',s')\right] ,\\
&= \left[u^\dagger(k,s)(\gamma^\mu)^\dagger\gamma^0 u(k',s')\right] ,\\
&= \left[u^\dagger(k,s)\gamma^0\gamma^\mu u(k',s')\right] ,\\
&= [\bar{u}(k,s)\gamma^\mu u(k',s')] .
\end{aligned} \tag{B.5}$$

Where we have used the result $\gamma^{\mu\dagger}\gamma^0 = \gamma^0\gamma^\mu$. Therefore

$$L^{\mu\nu} = \sum_{s'} \bar{u}(k,s)\gamma^\mu u(k',s')\ \bar{u}(k',s')\gamma^\nu u(k,s). \tag{B.6}$$

To evaluate this expression we write the matrix indices explicitly, giving

$$L^{\mu\nu} = \sum_{s'} \bar{u}_\alpha(k,s)(\gamma^\mu)_{\alpha\beta}u_\beta(k',s')\ \bar{u}_\gamma(k',s')(\gamma^\nu)_{\gamma\delta}u_\delta(k,s). \tag{B.7}$$

Using

$$\sum_{s'} u_\beta(k',s')\,\bar{u}_\gamma(k',s') = \left(\not{k}' + m\right)_{\beta\gamma} , \tag{B.8}$$

we obtain

$$\begin{aligned}
L^{\mu\nu} &= \bar{u}_\alpha(k,s)(\gamma^\mu)_{\alpha\beta}\left(\not{k}' + m\right)_{\beta\gamma}(\gamma^\nu)_{\gamma\delta}u_\delta(k,s),\\
&= u_\delta(k,s)\bar{u}_\alpha(k,s)(\gamma^\mu)_{\alpha\beta}\left(\not{k}' + m\right)_{\beta\gamma}(\gamma^\nu)_{\gamma\delta}.
\end{aligned} \tag{B.9}$$

Now using

$$u_\delta(k,s)\,\bar{u}_\alpha(k,s) = \frac{1}{2}\left[(\not{k}+m)\left(1+\gamma_5\not{s}\right)\right]_{\delta\alpha}, \tag{B.10}$$

Therefore

$$\begin{aligned}
L^{\mu\nu} &= \frac{1}{2}\left[(\not{k}+m)\left(1+\gamma_5\not{s}\right)\right]_{\delta\alpha}(\gamma^\mu)_{\alpha\beta}\left(\not{k}' + m\right)_{\beta\gamma}(\gamma^\nu)_{\gamma\delta},\\
&= \frac{1}{2}\,\mathrm{Tr}\left[(\not{k}+m)\left(1+\gamma_5\not{s}\right)\gamma^\mu\left(\not{k}' + m\right)\gamma^\nu\right],\\
&= \frac{1}{2}\,\mathrm{Tr}\Big[\not{k}\,\gamma^\mu\not{k}' + m\not{k}\,\gamma^\mu\,\gamma^\nu + \not{k}\,\gamma_5\not{s}\,\gamma^\mu\not{k}'\gamma^\nu + m\not{k}\,\gamma_5\not{s}\,\gamma^\mu\,\gamma^\nu\\
&\qquad + m\,\gamma_5\not{s}\,\gamma^\mu\not{k}'\gamma^\nu + m^2\,\gamma_5\not{s}\,\gamma^\mu\,\gamma^\nu + m\,\gamma^\mu\not{k}'\gamma^\nu + m^2\,\gamma^\mu\,\gamma^\nu\Big],\\
&= k_\alpha\,k'_\beta\,\mathrm{Tr}\left[\gamma^\alpha\gamma^\mu\gamma^\beta\gamma^\nu\right] + m\,k_\alpha\,s_\sigma\,\mathrm{Tr}\left[\gamma^\alpha\gamma_5\gamma^\sigma\gamma^\mu\gamma^\nu\right]\\
&\qquad + m\,s_\sigma\,k'_\beta\,\mathrm{Tr}\left[\gamma_5\gamma^\sigma\gamma^\mu\gamma^\beta\gamma^\nu\right] + m^2\,\mathrm{Tr}\left[\gamma^\mu\gamma^\nu\right].
\end{aligned}$$

In the last step we used the fact that the trace of an odd number of gamma matrices is zero. Using the trace theorems and recalling $\{\gamma^\mu, \gamma_5\} = 0$, we obtain

$$L^{\mu\nu} = 2\, k_\alpha\, k_\beta \left[g^{\alpha\mu} g^{\beta\nu} - g^{\alpha\beta} g^{\mu\nu} + g^{\alpha\nu} g^{\mu\beta}\right] + \\ 2i\, m\, \varepsilon^{\alpha\sigma\mu\nu}\, k_\alpha\, s_\sigma - 2i\, m\, \varepsilon^{\sigma\mu\beta\nu} s_\sigma\, k'_\beta + m^2\, g^{\mu\nu}. \quad \text{(B.11)}$$

Therefore, the (summed over final spins) lepton tensor is given by

$$L^{\mu\nu} = 2\left(k^\mu\, k'^\nu + k^\nu\, k'^\mu\right) + 2\, g^{\mu\nu}\left(m^2 - k\cdot k'\right) + 2i\, m\, \varepsilon^{\mu\nu\lambda\sigma} q_\lambda\, s_\sigma. \quad \text{(B.12)}$$

B.2 The Hadronic Tensor

The Hadronic tensor is given by

$$W^{\mu\nu} = \frac{1}{2\pi} \sum_{X_i} \prod_{i=1}^{n_X} \int \frac{d^3 p_i}{(2\pi)^3 2E_i} \delta^4\left(P + q - p_X\right) \left|\langle X_i | J_\nu(0) | P, s\rangle\right|^2, \\ = \frac{1}{2\pi} \sum_{X} \prod_{i=1}^{n_X} \int \frac{d^3 p_i}{(2\pi)^3 2E_i} \delta^4\left(P + q - p_X\right) \langle P, s| J_\mu(0) | X_i\rangle \langle X_i | J_\nu(0) | P, s\rangle. \quad \text{(B.13)}$$

The hadronic tensor can be significantly simplified; first one rewrites the delta function as

$$(2\pi)^4\, \delta^4(P + q - p_X) = \int d^4\xi\, e^{i\,(P+q-p_X)\cdot\xi}, \quad \text{(B.14)}$$

then translational invariance implies

$$e^{i(P-p_X)\cdot\xi}\, \langle P, s| J_\mu(0) | X\rangle = \langle P, s| J_\mu(\xi) | X\rangle, \quad \text{(B.15)}$$

finally multi-particle completeness [14] gives

$$\sum_{X_i} \prod_{i=1}^{n_X} \int \frac{d^3 p_i}{(2\pi)^3 2E_i} |X_i\rangle\langle X_i| = 1, \quad \text{(B.16)}$$

hence

$$W^{\mu\nu} = \frac{1}{2\pi} \int d^4\xi\, e^{i\,q\cdot\xi}\, \langle P, s| J_\mu(\xi)\, J_\nu(0) | P, s\rangle, \\ = \frac{1}{2\pi} \int d^4\xi\, e^{i\,q\cdot\xi}\, \langle P, s| [J_\mu(\xi)\, J_\nu(0)] | P, s\rangle. \quad \text{(B.17)}$$

We obtain the current commutator in the last line of Eq. (B.17), because the term $J_\nu(0)\, J_\mu(\xi)$, gives a vanishing matrix element since it produces the delta function $\delta\,(q - P + p_X)$, which cannot be satisfied because of energy conservation. As the nucleon is the ground state baryon and there is no intermediate state with $E' = M - q_0 \leq M$. Note, for physical lepton scattering from a stable target $q_0 > 0$.

C

Solution to the NJL Faddeev Equation in the Static Approximation

C.1 The Nucleon Quark-Diquark Bubble Graphs

$$\begin{aligned}\Pi_N^{ab}(p) &= \int \frac{d^4k}{(2\pi)^4}\, \tau^{ab}(p-k)\, S(k), \\ &= \int \frac{d^4k}{(2\pi)^4} \begin{pmatrix} \tau_s(p-k) & 0 \\ 0 & \tau_a^{\mu\nu}(p-k) \end{pmatrix} S(k), \\ &= \begin{pmatrix} \Pi_{Ns}(p) & 0 \\ 0 & \Pi_{Na}^{\mu\nu}(p) \end{pmatrix}. \end{aligned} \tag{C.1}$$

Where

$$\Pi_{Ns}(p) = \int \frac{d^4k}{(2\pi)^4}\, \tau(p-k)\, S(k) = a_1 + \frac{\not{p}}{M}\, a_2, \tag{C.2}$$

$$a_1 = \frac{1}{16\pi^2} \int_{\frac{1}{(\Lambda_{UV})^2}}^{\frac{1}{(\Lambda_{IR})^2}} d\tau \left\{ \frac{4\, G_s\, M}{\tau^2}\, e^{-\tau M^2} + g_s\, M \int_0^1 d\alpha\, \frac{1}{\tau} e^{-\tau A} \right\}, \tag{C.3}$$

$$a_2 = \frac{g_s\, M}{16\pi^2} \int_0^1 d\alpha \int_{\frac{1}{(\Lambda_{UV})^2}}^{\frac{1}{(\Lambda_{IR})^2}} d\tau\, \frac{\alpha}{\tau} e^{-\tau A}, \tag{C.4}$$

and A is given by $A = (\alpha^2 - \alpha)p^2 + \alpha\, M_s^2 + (1-\alpha)M^2$. Also

$$\Pi_{Na}^{\mu\nu}(p) = \int \frac{d^4k}{(2\pi)^4}\, \tau^{\mu\nu}(p-k)\, S(k) = g^{\mu\nu} \left(b_1 + \frac{\not{p}}{M}\, b_2 \right), \tag{C.5}$$

$$b_1 = \frac{1}{16\pi^2} \int_{\frac{1}{(\Lambda_{UV})^2}}^{\frac{1}{(\Lambda_{IR})^2}} d\tau \left\{ \frac{4\,G_a\,M}{\tau^2}\, e^{-\tau\, M^2} + g_a\, M \int_0^1 d\alpha\, \frac{1}{\tau} e^{-\tau\, B} \right\}, \tag{C.6}$$

$$b_2 = \frac{g_a\, M}{16\pi^2} \int_0^1 d\alpha \int_{\frac{1}{(\Lambda_{UV})^2}}^{\frac{1}{(\Lambda_{IR})^2}} d\tau\, \frac{\alpha}{\tau} e^{-\tau\, B}, \tag{C.7}$$

where B is given by $B = (\alpha^2 - \alpha)p^2 + \alpha\, M_a^2 + (1-\alpha)M^2$.

C.2 The Faddeev Equation

The Faddeev equation for the nucleon vertex function $\Gamma^a(p)$ in operator form is given by

$$\Gamma^a(p) = Z^a{}_{a'}\, \Pi_N^{a'b}\, \Gamma_b(p) \equiv K^{ab}(p)\, \Gamma_b(p), \tag{C.8}$$

where

$$Z^a{}_{a'} = \frac{3}{M} \begin{pmatrix} 1 & \sqrt{3}\gamma_{\mu'}\gamma_5 \\ \sqrt{3}\gamma_5\gamma^\mu & -\gamma_{\mu'}\gamma^\mu \end{pmatrix}, \tag{C.9}$$

and $\Pi_N^{a'b}$ contains the nucleon quark-diquark bubble graphs. Therefore the Faddeev kernel has the form

$$K^{ab}(p) = \frac{3}{M} \begin{bmatrix} a_1 + \frac{\not p}{M}\, a_2 & \sqrt{3}\gamma^\nu\gamma_5 \left(b_1 + \frac{\not p}{M}\, b_2\right) \\ \sqrt{3}\gamma_5\gamma^\mu \left(a_1 + \frac{\not p}{M}\, a_2\right) & -\gamma^\nu\gamma^\mu \left(b_1 + \frac{\not p}{M}\, b_2\right) \end{bmatrix}. \tag{C.10}$$

The RHS of Eq. (C.8) becomes

$$K^{ab}(p)\Gamma_b(p) = \frac{3}{M} \begin{bmatrix} X \\ Y \end{bmatrix} u_N(p,s), \tag{C.11}$$

where

$$\begin{aligned} X &= \alpha_1 \left(a_1 + \frac{M_N}{M}\, a_2\right) + \alpha_2\sqrt{3}\left(b_1 - \frac{M_N}{M}\, b_2\right) - \alpha_3 2\sqrt{3}\left(2b_1 + \frac{M_N}{M}\, b_2\right), \\ Y &= \frac{p^\mu\gamma_5}{M_N}\left[-\alpha_2\, 2\left(b_1 - \frac{M_N}{M}\, b_2\right) - \alpha_3\, 4\frac{M_N}{M} b_2\right] \\ &\quad + \gamma^\mu\gamma_5 \left[-\alpha_1 \sqrt{3}\left(a_1 + \frac{M_N}{M}\, a_2\right) - \alpha_2\left(b_1 - \frac{M_N}{M}\, b_2\right) + \alpha_3\, 2b_1\right]. \end{aligned} \tag{C.12}$$

Therefore to satisfy the Faddeev equation, which can now be expressed as

$$\frac{3}{M}\begin{bmatrix}X\\Y\end{bmatrix}u_N(p,s)=\begin{bmatrix}\alpha_1\\ \alpha_2\,\frac{p^\mu}{M_N}\gamma_5\ +\alpha_3\,\gamma^\mu\gamma_5\end{bmatrix}u_N(p,s), \tag{C.13}$$

we must have

$$\alpha_1=\frac{3}{M}\left[\alpha_1\left(a_1+\frac{M_N}{M}a_2\right)\right.$$
$$\left.+\alpha_2\sqrt{3}\left(b_1-\frac{M_N}{M}b_2\right)-\alpha_3 2\sqrt{3}\left(2b_1+\frac{M_N}{M}b_2\right)\right], \tag{C.14}$$

$$\alpha_2=\frac{3}{M}\left[-\alpha_2\,2\left(b_1-\frac{M_N}{M}b_2\right)-\alpha_3\,4\frac{M_N}{M}b_2\right], \tag{C.15}$$

$$\alpha_3=\frac{3}{M}\left[-\alpha_1\sqrt{3}\left(a_1+\frac{M_N}{M}a_2\right)-\alpha_2\left(b_1-\frac{M_N}{M}b_2\right)+\alpha_3\,2b_1\right]. \tag{C.16}$$

These three equations can be written homogeneously as

$$\begin{pmatrix}M_{11}&M_{12}&M_{13}\\M_{21}&M_{22}&M_{23}\\M_{31}&M_{32}&M_{33}\end{pmatrix}\begin{pmatrix}\alpha_1\\\alpha_2\\\alpha_3\end{pmatrix}=M(p^2)\begin{pmatrix}\alpha_1\\\alpha_2\\\alpha_3\end{pmatrix}=0, \tag{C.17}$$

where

$$M_{11}=a_1+\frac{M_N}{M}a_2-\frac{M}{3},\qquad M_{12}=\sqrt{3}\left(b_1-\frac{M_N}{M}b_2\right),$$
$$M_{13}=-2\sqrt{3}\left(2b_1+\frac{M_N}{M}b_2\right), \tag{C.18}$$

$$M_{21}=0,\qquad M_{22}=-2\left(b_1-\frac{M_N}{M}b_2\right)-\frac{M}{3},\quad M_{23}=-4\frac{M_N}{M}b_2, \tag{C.19}$$

$$M_{31}=-\sqrt{3}\left(a_1+\frac{M_N}{M}a_2\right),\quad M_{32}=-b_1+\frac{M_N}{M}b_2,\qquad M_{23}=2b_1-\frac{M}{3}, \tag{C.20}$$

The nucleon mass then follows from the condition $\det M(p^2=M_N^2)=0$.

C.3 Normalization of the Nucleon Vertex Function

The T-matrix for the nucleon is defined as

$$T=Z+KT=Z+Z\,\Pi_N\,T. \tag{C.21}$$

In the lightcone normalization, the three-body T-matrix near a three-body bound state of of mass M_N, behaves as

$$T \longrightarrow \frac{\Gamma_N \overline{\Gamma}_N}{p_+ - \varepsilon_p}, \tag{C.22}$$

where $\varepsilon_p = \frac{M_N^2}{2p_-}$. Therefore near the T-matrix pole Eq. (C.21) becomes

$$\Gamma_N \overline{\Gamma}_N = (p_+ - \varepsilon_p)\, Z + Z\, \Pi_N\, \Gamma_N\, \overline{\Gamma}_N. \tag{C.23}$$

Taking $\frac{\partial}{\partial p_+}$ of the above equation, noting that $\Gamma_N^a \overline{\Gamma}_N^b$ and Z have no p_+ dependence, then taking the limit $p_+ \longrightarrow \varepsilon_p$, we obtain

$$0 = Z + Z \frac{\partial\, \Pi_N}{\partial p_+} \Gamma_N\, \overline{\Gamma}_N. \tag{C.24}$$

Removing the factor Z and multiplying by $\overline{\Gamma}_N$, we obtain

$$0 = \overline{\Gamma}_N + \left(\overline{\Gamma}_N \frac{\partial\, \Pi_N}{\partial p_+} \Gamma_N\right) \overline{\Gamma}_N. \tag{C.25}$$

This implies

$$\overline{\Gamma}_N \frac{\partial\, \Pi_N}{\partial p_+} \Gamma_N = -1. \tag{C.26}$$

Using $\Gamma_N = \sqrt{-Z_N \frac{M_N}{p_-}}\, \Gamma$, we obtain for the nucleon vertex normalization

$$Z_N = \frac{p_-}{M_N\, \overline{\Gamma}\, \frac{\partial \Pi_N}{\partial p_+}\, \Gamma}, \tag{C.27}$$

where we define $\overline{\Gamma}\Gamma = \alpha_1^2 + \alpha_2^2 - 2\alpha_2\alpha_3 + 4\alpha_3^2 = 1$.

Now

$$\frac{\partial}{\partial p_+} \Pi_N = \begin{pmatrix} \hat{a}_1 + \frac{\gamma^+}{M} a_2 + \frac{\not{p}}{M}\, \hat{a}_2 & 0 \\ 0 & \hat{b}_1 + \frac{\gamma^+}{M} b_2 + \frac{\not{p}}{M}\, \hat{b}_2 \end{pmatrix}, \tag{C.28}$$

where $\hat{x} \equiv \frac{\partial}{\partial p_+} x$. Therefore the denominator, D, is given by

$$\begin{aligned} \frac{1}{M_N} D = \overline{u}_N(p,s) &\left[\alpha_1 \quad \left(\alpha_2 \frac{p^\mu}{M_N} \gamma_5 \; + \alpha_3\, \gamma_5 \gamma^\mu\right)\right] \\ &\begin{pmatrix} \hat{a}_1 + \frac{\gamma^+}{M} a_2 + \frac{\not{p}}{M}\, \hat{a}_2 & 0 \\ 0 & \hat{b}_1 + \frac{\gamma^+}{M} b_2 + \frac{\not{p}}{M}\, \hat{b}_2 \end{pmatrix} \\ &\qquad\qquad \begin{bmatrix} \alpha_1 \\ \alpha_2 \frac{p_\mu}{M_N} \gamma_5 \; + \alpha_3\, \gamma_\mu \gamma_5 \end{bmatrix} u_N(p,s), \\ = I_1 + I_2. \end{aligned} \tag{C.29}$$

Using $\overline{u}_N\, u_N = 1$ and $\overline{u}_N\, \gamma^+\, u_N = \frac{p_-}{M_N}$, we find

$$I_1 = \alpha_1^2 \left(\hat{a}_1 + \frac{p_-}{M\, M_N} a_2 + \frac{M_N}{M}\, \hat{a}_2 \right),$$
$$I_2 = (\alpha_2^2 - 2\alpha_2\alpha_3 - 2\alpha_3^2) \left(\hat{b}_1 - \frac{p_-}{M\, M_N} b_2 - \frac{M_N}{M}\, \hat{b}_2 \right) + 6\alpha_3^2\, \hat{b}_1. \tag{C.30}$$

Therefore

$$Z_N = \frac{p_-}{M_N} \left[\alpha_1^2 \left(\hat{a}_1 + \frac{p_-}{M\, M_N} a_2 + \frac{M_N}{M}\, \hat{a}_2 \right) + (\alpha_2^2 - 2\alpha_2\alpha_3 - 2\alpha_3^2) \left(\hat{b}_1 - \frac{p_-}{M\, M_N} b_2 - \frac{M_N}{M}\, \hat{b}_2 \right) + 6\alpha_3^2\, \hat{b}_1 \right]^{-1}, \tag{C.31}$$

where

$$\hat{a}_1 = \frac{-g_s\, M}{8\pi^2} p_- \int_{\frac{1}{(\Lambda_{UV})^2}}^{\frac{1}{(\Lambda_{IR})^2}} d\tau \int_0^1 d\alpha\, (\alpha^2 - \alpha)\, e^{-\tau\, A}, \tag{C.32}$$

$$\hat{a}_2 = \frac{-g_s\, M}{8\pi^2} p_- \int_{\frac{1}{(\Lambda_{UV})^2}}^{\frac{1}{(\Lambda_{IR})^2}} d\tau \int_0^1 d\alpha\, \alpha\, (\alpha^2 - \alpha)\, e^{-\tau\, A}, \tag{C.33}$$

$$\hat{b}_1 = \frac{-g_a\, M}{8\pi^2} p_- \int_{\frac{1}{(\Lambda_{UV})^2}}^{\frac{1}{(\Lambda_{IR})^2}} d\tau \int_0^1 d\alpha\, (\alpha^2 - \alpha)\, e^{-\tau\, B}, \tag{C.34}$$

$$\hat{b}_2 = \frac{-g_a\, M}{8\pi^2} p_- \int_{\frac{1}{(\Lambda_{UV})^2}}^{\frac{1}{(\Lambda_{IR})^2}} d\tau \int_0^1 d\alpha\, \alpha\, (\alpha^2 - \alpha)\, e^{-\tau\, B}. \tag{C.35}$$

Recall

$$A = (\alpha^2 - \alpha)p^2 + \alpha\, M_s^2 + (1-\alpha)M^2, \tag{C.36}$$
$$B = (\alpha^2 - \alpha)p^2 + \alpha\, M_a^2 + (1-\alpha)M^2. \tag{C.37}$$

In order to reproduce the normalization for the case with scalar diquarks only, that is

$$Z_N = \left. \frac{-1}{\partial \Pi_N(p)/\partial \not{p}} \right|_{\not{p}=M_N}, \tag{C.38}$$

we require $\overline{\Gamma}\Gamma = 1$. Therefore the following condition for the coefficients of the nucleon vertex

$$\alpha_1^2 + \alpha_2^2 - 2\alpha_2\alpha_3 + 4\alpha_3^2 = 1, \tag{C.39}$$

must be satisfied.

D

Explicit Calculation of the Transversity Distributions

D.1 Transverse Feynman Diagrams

D.1.1 Transverse Scalar Quark Diagram

We have

$$\begin{aligned}\Delta_T q^{s}_{q/N}(x) &= i\,\overline{\Gamma}_N \int \frac{d^4k}{(2\pi)^4}\,\delta\Big(x-\frac{k_-}{p_-}\Big)\; iS(k)\, i\gamma^+\gamma^1\gamma_5\, iS(k)\tau_s(p-k)\,\Gamma_N, \\ &= -\frac{Z_N\,M_N}{p_-}\,\overline{u}_N \int \frac{d^4k}{(2\pi)^4}\,\delta\Big(x-\frac{k_-}{p_-}\Big)\; S(k)\,\gamma^+\gamma^1\gamma_5\,S(k)\tau_s(p-k)\,u_N,\end{aligned} \tag{D.1}$$

where Γ_N are the scalar transverse vertex function in the x direction. We evaluate the distribution using the moments where

$$\mathcal{A}_n = \int_0^1 dx\, x^{n-1}\, f(x). \tag{D.2}$$

Therefore

$$\begin{aligned}\mathcal{A}_n &= \overline{\Gamma}_N \int \frac{d^4k}{(2\pi)^4}\left(\frac{k_-}{p_-}\right)^{n-1} S(k)\,\gamma^+\gamma^1\gamma_5\,S(k)\tau_s(p-k)\,\Gamma_N, \\ &= \overline{\Gamma}_N \int \frac{d^4k}{(2\pi)^4}\left(\frac{k_-}{p_-}\right)^{n-1} \frac{(\not{k}+M)\gamma^+\gamma^1\gamma_5(\not{k}+M)}{(k^2-M^2+i\varepsilon)^2} \\ &\qquad\qquad \left[4i\,G_s - \frac{ig_s}{k^2+p^2-2k\cdot p-M_s^2+i\varepsilon}\right]\Gamma_N, \\ &= \mathcal{A}_n^A + \mathcal{A}_n^B.\end{aligned} \tag{D.3}$$

Using the result

$$\begin{aligned}(\not{k}+M)\gamma^+\gamma^1\gamma_5(\not{k}+M) &= 2\,k_-^2\,\gamma^-\gamma^1\gamma_5 + \left(k_2^2-k_1^2+M^2\right)\gamma^+\gamma^1\gamma_5 \\ &\quad - 2\,k_1\,k_2\,\gamma^+\gamma^2\gamma_5 - 2\,k_-\,k_2\,\gamma^1\gamma^2\gamma_5 \\ &\quad + 2\,k_-\,k_1\left(\gamma_5-\gamma^+\gamma^-\gamma_5\right) + 2M\,\left(k_-\gamma^1\gamma_5 + k_1\,\gamma^+\gamma_5\right),\end{aligned} \tag{D.4}$$

and the matrix elements in Section A.14 we have

$$\overline{u}_N\,(\not{k}+M)\gamma^+\gamma^1\gamma_5(\not{k}+M)\,u_N = \frac{M_N}{p_-}\,k_-^2 + \left(k_2^2 - k_1^2 + M^2\right)\frac{p_-}{M_N} + 2\,M\,k_-. \tag{D.5}$$

Therefore the numerator of $\mathcal{A}_n^A$ is given by

$$\mathcal{N}_n^A = \left(\frac{k_-}{p_-}\right)^{n-1}\left[\frac{M_N}{p_-}\,k_-^2 + \left(k_2^2 - k_1^2 + M^2\right)\frac{p_-}{M_N} + 2\,M\,k_-\right]. \tag{D.6}$$

Ignoring terms odd in k and using $g_{--} = g_{-1} = g_{-2} = 0$, the only non-zero term is

$$\mathcal{N}_1^A = \left(k_2^2 - k_1^2 + M^2\right)\frac{p_-}{M_N}. \tag{D.7}$$

Therefore

$$\mathcal{A}_1^A = -4i\,G_s\,Z_N \int \frac{d^4k}{(2\pi)^4}\frac{k_2^2 - k_1^2 + M^2}{(k^2 - M^2 + i\varepsilon)^2}. \tag{D.8}$$

Wick rotating where $k_1^2 = k_2^2 = \frac{1}{4}k_E^2$, introducing 4-d polars and the proper-time regularization gives

$$\mathcal{A}_1^A = \frac{G_s\,Z_N\,M^2}{4\pi^2}\int d\tau\,\tau \int_0^\infty dk_E^2\,k_E^2\,e^{-\tau(k_E^2+M^2)}. \tag{D.9}$$

Integrating over k_E^2 and using the fact that only the first moment is non-zero we have

$$\Delta_T q^A(x) = \delta(x)\,\frac{G_s\,Z_N\,M^2}{4\pi^2}\int d\tau\,\frac{1}{\tau}\,e^{-\tau\,M^2}. \tag{D.10}$$

Evaluating $\mathcal{A}_n^B$, we have

$$\mathcal{A}_n^B = ig_a\,\frac{Z_N\,M_N}{p_-}\int\frac{d^4k}{(2\pi)^4}\left(\frac{k_-}{p_-}\right)^{n-1} \frac{\frac{M_N}{p_-}\,k_-^2 + \left(k_2^2 - k_1^2 + M^2\right)\frac{p_-}{M_N} + 2\,M\,k_-}{(k^2 - M^2 + i\varepsilon)^2\,(k^2 + q^2 - 2k\cdot q - M_s^2 + i\varepsilon)}. \tag{D.11}$$

Using Eq. (A.14) and the fact that the k_1^2 and k_2^2 terms will cancel, we obtain

$$\mathcal{A}_n^B = ig_a\,\frac{Z_N\,M_N}{p_-}\int_0^1 d\alpha\,2(1-\alpha)\int\frac{d^4k}{(2\pi)^4}\left(\frac{k_- + \alpha\,p_-}{p_-}\right)^{n-1} \frac{\frac{M_N}{p_-}\,\left(k_- + \alpha p_-\right)^2 + M^2\frac{p_-}{M_N} + 2\,M\,\left(k_- + \alpha p_-\right)}{\left[k^2 - (\alpha^2 - \alpha)\,p^2 - \alpha M_s^2 - (1-\alpha)\,M^2 + i\varepsilon\right]^3}. \tag{D.12}$$

Ignoring terms odd in k and hence noting that terms like $\left(\frac{k_- + \alpha p_-}{p_-}\right)^n \longrightarrow \alpha^n$, gives

$$\mathcal{A}_n^B = i g_a \frac{Z_N M_N}{p_-} \int_0^1 d\alpha\, \alpha^{n-1} 2(1-\alpha)$$
$$\int \frac{d^4k}{(2\pi)^4} \frac{\frac{M_N}{p_-}\alpha^2 p_-^2 + M^2 \frac{p_-}{M_N} + 2\,M\,\alpha\, p_-}{\left[k^2 - (\alpha^2 - \alpha)\, p^2 - \alpha M_s^2 - (1-\alpha)\, M^2 + i\varepsilon\right]^3}. \quad \text{(D.13)}$$

Therefore from the definition of the moments we have

$$\Delta_T q^B(x) = i g_a\, Z_N\, 2(1-x)$$
$$\int \frac{d^4k}{(2\pi)^4} \frac{M_N^2\, x^2 + 2\,M\,M_N\,x + M^2}{\left[k^2 - (x^2 - x)\, p^2 - x M_s^2 - (1-x)\, M^2 + i\varepsilon\right]^3}. \quad \text{(D.14)}$$

Wick rotating, introducing 4-d polar coordinates and the proper-time regularization gives

$$\Delta_T q^B(x) = \frac{g_a\, Z_N}{16\pi^2} (1-x)\,(x\,M_N + M)^2$$
$$\int d\tau\, \tau^2 \int_0^\infty dk_E^2\; k_E^2\, e^{-\tau\left[k_E^2 + \left(x^2 - x\right)p^2 + x M_s^2 + (1-x) M^2\right]}. \quad \text{(D.15)}$$

Therefore

$$\Delta_T q^B(x) = \frac{g_a\, Z_N}{16\pi^2} (1-x)\,(x\,M_N + M)^2 \int d\tau\; e^{-\tau\left[\left(x^2 - x\right)p^2 + x M_s^2 + (1-x) M^2\right]}. \quad \text{(D.16)}$$

Hence the full transverse scalar quark diagram result is

$$\Delta_T q_{q/N}^{\mathrm{s}}(x) = \delta(x)\, \frac{G_s\, Z_N\, M^2}{4\pi^2} \int d\tau\, \frac{1}{\tau}\, e^{-\tau\, M^2}$$
$$+ \frac{g_a\, Z_N}{16\pi^2} (1-x)\,(x\,M_N + M)^2 \int d\tau\; e^{-\tau\left[\left(x^2 - x\right)p^2 + x M_s^2 + (1-x) M^2\right]}. \quad \text{(D.17)}$$

D.1.2 Transverse Axial-vector Quark Diagram

We have

$$\begin{aligned}\Delta_T q^{a}_{q/N}(x) &= i\,\overline{\Gamma}^{\mu}_N \int \frac{d^4k}{(2\pi)^4}\,\delta\left(x-\frac{k_-}{p_-}\right)\, iS(k)\, i\gamma^+\gamma^1\gamma_5\, iS(k)\tau_{\mu\nu}(p-k)\,\Gamma_N,\\ &= -\frac{Z_N\, M_N}{p_-}\,\overline{\Gamma}^{\mu}\int \frac{d^4k}{(2\pi)^4}\,\delta\left(x-\frac{k_-}{p_-}\right)\, S(k)\,\gamma^+\gamma^1\gamma_5\, S(k)\tau_{\mu\nu}(p-k)\,\Gamma^{\nu},\end{aligned} \tag{D.18}$$

where Γ^{ν} is the axial-vector transverse vertex function in the x direction. We evaluate the distribution using the moments, where

$$\mathcal{A}_n = \int_0^1 dx\, x^{n-1}\, f(x). \tag{D.19}$$

Therefore

$$\begin{aligned}\mathcal{A}_n &= \overline{\Gamma}^{\mu}_N \int \frac{d^4k}{(2\pi)^4}\left(\frac{k_-}{p_-}\right)^{n-1} S(k)\,\gamma^+\gamma^1\gamma_5\, S(k)\tau_{\mu\nu}(p-k)\,\Gamma^{\nu}_N,\\ &= -\frac{Z_N\, M_N}{p_-}\,\overline{\Gamma}^{\mu}\int \frac{d^4k}{(2\pi)^4}\left(\frac{k_-}{p_-}\right)^{n-1}\frac{(\not{k}+M)\gamma^+\gamma^1\gamma_5(\not{k}+M)}{(k^2-M^2+i\varepsilon)^2}\\ &\qquad\left[4i\,G_a - \frac{ig_a}{k^2+p^2-2k\cdot p-M_a^2+i\varepsilon}\right]\Gamma_{\mu},\\ &= \mathcal{A}_n^A + \mathcal{A}_n^B.\end{aligned} \tag{D.20}$$

Therefore we need

$$\overline{\Gamma}^{\mu}(\not{k}+M)\gamma^+\gamma^1\gamma_5(\not{k}+M)\Gamma_{\mu}, \tag{D.21}$$

where from the scalar quark diagram we have

$$\begin{aligned}(\not{k}+M)\gamma^+\gamma^1\gamma_5(\not{k}+M) &= 2\,k_-^2\,\gamma^-\gamma^1\gamma_5 + \left(k_2^2-k_1^2+M^2\right)\gamma^+\gamma^1\gamma_5\\ &\quad - 2\,k_1\,k_2\,\gamma^+\gamma^2\gamma_5 - 2\,k_-\,k_2\,\gamma^1\gamma^2\gamma_5 + 2\,k_-\,k_1\,\left(\gamma_5-\gamma^+\gamma^-\gamma_5\right)\\ &\quad + 2M\,\left(k_-\gamma^1\,\gamma_5 + k_1\,\gamma^+\gamma_5\right).\end{aligned} \tag{D.22}$$

Recall that

$$\Gamma_{\mu}(p,s) = \left(\alpha_2\,\frac{p_{\mu}}{M_N}\gamma_5 + \alpha_3\,\gamma_{\mu}\gamma_5\right)\,u_N(p,s), \tag{D.23}$$

$$\overline{\Gamma}^{\mu}(p,s) = \overline{u}_N(p,s)\,\left(\alpha_2\,\frac{p^{\mu}}{M_N}\gamma_5 + \alpha_3\,\gamma_5\gamma^{\mu}\right), \tag{D.24}$$

and hence it is easy to show

$$\overline{\Gamma}^{\mu}\Omega\Gamma_{\mu} = \overline{u}_N\left[\left(\alpha_2^2-2\alpha_2\alpha_3\right)\gamma_5\Omega\gamma_5 + \alpha_3^2\,\gamma_5\gamma^{\mu}\Omega\gamma_{\mu}\gamma_5\right]u_N. \tag{D.25}$$

Using the following results which are easily proven using the matrix elements in Section A.14

$$\begin{aligned}
\overline{\Gamma}^\mu \gamma^- \gamma^1 \gamma_5 \Gamma_\mu &= \left(\alpha_2^2 - 2\alpha_2\alpha_3\right) \frac{M_N}{2p_-}, & \overline{\Gamma}^\mu \gamma^+ \gamma^1 \gamma_5 \Gamma_\mu &= \left(\alpha_2^2 - 2\alpha_2\alpha_3\right) \frac{p_-}{M_N},\\
\overline{\Gamma}^\mu \gamma^+ \gamma^2 \gamma_5 \overline{\Gamma}^\mu &= 0, & \overline{\Gamma}^\mu \gamma^1 \gamma^2 \gamma_5 \Gamma_\mu &= 0,\\
\overline{\Gamma}^\mu \gamma^+ \gamma^- \gamma_5 \Gamma_\mu &= 0, & \overline{\Gamma}^\mu \gamma^1 \gamma_5 \Gamma_\mu &= -\left(\alpha_2^2 - 2\alpha_2\alpha_3 + 2\alpha_3^2\right),\\
\overline{\Gamma}^\mu \gamma^+ \gamma_5 \Gamma_\mu &= 0, & \overline{\Gamma}^\mu \gamma_5 \Gamma_\mu &= 0. \qquad \text{(D.26)}
\end{aligned}$$

Hence

$$\begin{aligned}
\overline{\Gamma}^\mu (\not{k} + M)\gamma^+ \gamma^1 \gamma_5 (\not{k} + M)\Gamma_\mu = \left(\alpha_2^2 - 2\alpha_2\alpha_3\right) &\left[\frac{M_N}{p_-} k_-^2\right.\\
&\left. + \left(k_2^2 - k_1^2 + M^2\right) \frac{p_-}{M_N} - 2M\, k_-\right] - 4M\, \alpha_3^2\, k_-. \quad \text{(D.27)}
\end{aligned}$$

Therefore the numerator of $\mathcal{A}_n^A$ is given by

$$\begin{aligned}
\mathcal{N}_n^A = \left(\frac{k_-}{p_-}\right)^{n-1} &\left\{ \left(\alpha_2^2 - 2\alpha_2\alpha_3\right) \left[\frac{M_N}{p_-} k_-^2\right.\right.\\
&\left.\left. + \left(k_2^2 - k_1^2 + M^2\right) \frac{p_-}{M_N} - 2M\, k_-\right] - 4M\, \alpha_3^2\, k_-\right\}. \quad \text{(D.28)}
\end{aligned}$$

Ignoring terms odd in k and using $g_{--} = g_{-1} = g_{-2} = 0$, the only non-zero term is

$$\mathcal{N}_1^A = \left(\alpha_2^2 - 2\alpha_2\alpha_3\right) \left[k_2^2 - k_1^2 + M^2\right] \frac{p_-}{M_N}. \quad \text{(D.29)}$$

Therefore

$$\mathcal{A}_1^A = -4i\, G_a\, Z_N \left(\alpha_2^2 - 2\alpha_2\alpha_3\right) \int \frac{d^4k}{(2\pi)^4} \frac{k_2^2 - k_1^2 + M^2}{(k^2 - M^2 + i\varepsilon)^2}. \quad \text{(D.30)}$$

Wick rotating where $k_1^2 = k_2^2 = \frac{1}{4}k_E^2$, introducing 4-d polars and the proper-time regularization gives

$$\mathcal{A}_1^A = \frac{G_a\, Z_N\, M^2}{4\pi^2} \left(\alpha_2^2 - 2\alpha_2\alpha_3\right) \int d\tau\, \tau \int_0^\infty dk_E^2\, k_E^2\, e^{-\tau(k_E^2 + M^2)}. \quad \text{(D.31)}$$

Integrating out k_E^2 and using the fact that only the first moment is non-zero, we have

$$\Delta_T q^A(x) = \delta(x)\, \frac{G_a\, Z_N\, M^2}{4\pi^2} \left(\alpha_2^2 - 2\alpha_2\alpha_3\right) \int d\tau\, \frac{1}{\tau}\, e^{-\tau M^2}. \quad \text{(D.32)}$$

Evaluating $\mathcal{A}_n^B$, we have

$$\mathcal{A}_n^B = i g_a \frac{Z_N\, M_N}{p_-} \int \frac{d^4k}{(2\pi)^4} \left(\frac{k_-}{p_-}\right)^{n-1} \frac{(\alpha_2^2 - 2\alpha_2\alpha_3)\left[\frac{M_N}{p_-} k_-^2 + (k_2^2 - k_1^2 + M^2)\frac{p_-}{M_N} - 2M\, k_-\right] - 4M\, \alpha_3^2\, k_-}{(k^2 - M^2 + i\varepsilon)^2\, (k^2 + q^2 - 2k\cdot q - M_a^2 + i\varepsilon)}. \quad \text{(D.33)}$$

Using Eq. (A.14) and the fact that the k_1^2 and k_2^2 terms will cancel, the numerator of $\mathcal{A}_n^B$ becomes

$$\mathcal{N}_n^B = \left(\frac{k_- + \alpha p_-}{p_-}\right)^{n-1} \left\{ (\alpha_2^2 - 2\alpha_2\alpha_3) \left[\frac{M_N}{p_-} \left(\frac{k_- + \alpha p_-}{p_-}\right)^2 p_-^2 + M^2 \frac{p_-}{M_N} - 2M \left(\frac{k_- + \alpha p_-}{p_-}\right) p_- \right] - 4M\, \alpha_3^2 \left(\frac{k_- + \alpha p_-}{p_-}\right) p_- \right\}. \quad \text{(D.34)}$$

Noting that terms like $\left(\frac{k_- + \alpha p_-}{p_-}\right)^n \to \alpha^n$, gives

$$\begin{aligned} \mathcal{N}_n^B &= \alpha^{n-1} \\ &\quad \left\{ (\alpha_2^2 - 2\alpha_2\alpha_3) \left[M_N\, \alpha^2\, p_- + M^2 \frac{p_-}{M_N} - 2M\, \alpha\, p_- \right] - 4M\, \alpha_3^2\, \alpha\, p_- \right\}, \\ &= \alpha^{n-1} \frac{p_-}{M_N} \left\{ (\alpha_2^2 - 2\alpha_2\alpha_3) \left[\alpha^2\, M_N^2 + M^2 - 2\alpha\, M\, M_N \right] - 4\, M\, M_N\, \alpha\, \alpha_3^2 \right\}. \end{aligned} \quad \text{(D.35)}$$

Therefore, from the definition of the moments we have

$$\Delta_T q^B(x) = i g_a\, Z_N\, 2(1-x) \int \frac{d^4k}{(2\pi)^4} \frac{(\alpha_2^2 - 2\alpha_2\alpha_3)\,[x\, M_N - M]^2 - 4\, \alpha_3^2\, M\, M_N\, x}{\left[k^2 - (x^2 - x)\, p^2 - x M_a^2 - (1-x)\, M^2 + i\varepsilon\right]^3}. \quad \text{(D.36)}$$

Wick rotating and introducing 4-d polar coordinates and the proper-time regularization gives

$$\Delta_T q^B(x) = \frac{g_a\, Z_N}{16\pi^2} (1-x) \left\{ (\alpha_2^2 - 2\alpha_2\alpha_3)\, [x\, M_N - M]^2 - 4\, \alpha_3^2\, M\, M_N\, x \right\} \int d\tau \tau^2 \int dk_E^2\; k_E^2\; e^{-\tau\left[k_E^2 + (x^2 - x)p^2 + x M_a^2 + (1-x) M^2\right]}. \quad \text{(D.37)}$$

Therefore

$$\Delta_T q^B(x) = \frac{g_a\, Z_N}{16\pi^2} (1-x) \left\{ (\alpha_2^2 - 2\alpha_2\alpha_3)\, [x\, M_N - M]^2 - 4\, \alpha_3^2\, M\, M_N\, x \right\} \int d\tau\; e^{-\tau\left[(x^2 - x)p^2 + x M_a^2 + (1-x) M^2\right]}. \quad \text{(D.38)}$$

Hence the full transverse axial-vector quark diagram result is

$$
\begin{aligned}
\Delta_T q^{\mathrm{a}}_{q/N}(x) = \delta(x)\, \frac{G_a\, Z_N\, M^2}{4\pi^2}\, \left(\alpha_2^2 - 2\alpha_2\alpha_3\right) \int d\tau\, \frac{1}{\tau}\, e^{-\tau\, M^2} \\
+ \frac{g_a\, Z_N}{16\pi^2}\, (1-x) \Big\{ \left(\alpha_2^2 - 2\alpha_2\alpha_3\right) [x\, M_N - M]^2 \\
- 4\, \alpha_3^2\, M\, M_N\, x \Big\} \int d\tau\ e^{-\tau\left[\left(x^2-x\right)p^2 + x M_a^2 + (1-x) M^2\right]} . \quad \text{(D.39)}
\end{aligned}
$$

Note also that

$$
\begin{aligned}
\left(\alpha_2^2 - 2\alpha_2\alpha_3\right) [x\, M_N - M]^2 - 4\, \alpha_3^2\, M\, M_N\, x \\
= \left(\alpha_2 - \alpha_3\right)^2 [x\, M_N - M]^2 - \alpha_3^2\, [x\, M_N + M]^2 . \quad \text{(D.40)}
\end{aligned}
$$

D.1.3 Transverse Axial-Vector Diquark Diagram

We have

$$\Delta_T f^{\mathrm{a}}_{q(D)/N}(x) = i\,\overline{\Gamma}^{\lambda}_N \int \frac{d^4q}{(2\pi)^4} \int \frac{d^4k}{(2\pi)^4}\,\delta\Big(x-\frac{k_-}{p_-}\Big)\, iS(p-q)\,\tau_{\lambda\mu}(q)$$
$$\left(-iC^{-1}\gamma^{\mu}\tau_i\tau_2\beta^A\right)_{\beta'\alpha'}\left(iS(k)\,i\gamma^+\gamma^1\gamma_5\,\tfrac{1}{2}\,(1\pm\tau_z)\,iS(k)\right)_{\alpha'\alpha}$$
$$\left(i\gamma^{\nu}C\tau_2\tau_j\beta^{A'}\right)_{\alpha\beta} iS(q-k)_{\beta'\beta}\,\tau_{\nu\sigma}(q)\,\Gamma^{\sigma}_N,$$
$$= i\overline{\Gamma}^{\lambda}_N \int \frac{d^4q}{(2\pi)^4} \int \frac{d^4k}{(2\pi)^4}\,\delta\Big(x-\frac{k_-}{p_-}\Big)\, S(p-q)\,\tau_{\lambda\mu}(q)$$
$$i\mathrm{Tr}\Big[\left(C^{-1}\gamma^{\mu}\tau_i\tau_2\beta^A\right)\left(S(k)\gamma^+\gamma^1\gamma_5\tfrac{1}{2}\,(1\pm\tau_z)\,S(k)\right)$$
$$\left(\gamma^{\nu}C\tau_2\tau_j\beta^{A'}\right)S^T(q-k)\Big]\,\tau_{\nu\sigma}(q)\,\Gamma^{\sigma}_N. \qquad \text{(D.41)}$$

We leave the isospin calculation until the end, but include a factor of 2 here that we will divide out later. Also using $CS^T(-q)C^{-1} = S(q)$ and $\mathrm{Tr}\{T^aT^b\} = \frac{1}{2}\delta_{ab}$ where $T^a = \frac{\lambda^a}{2}$, $\beta^A = \sqrt{\frac{3}{2}}\lambda^A$ and hence $\mathrm{Tr}\{\beta^A\beta^{A'}\} = \frac{3}{2}\mathrm{Tr}\{\lambda^A\lambda^{A'}\} = \frac{3}{2}\times 4\,\mathrm{Tr}\{T^AT^{A'}\} = 3\delta_{AA'}$. Therefore we obtain

$$\delta f^{\mathrm{a}}_{q(D)/N}(x) = i\overline{\Gamma}^{\lambda}_N \int \frac{d^4q}{(2\pi)^4} \int \frac{d^4k}{(2\pi)^4}\,\delta\Big(x-\frac{k_-}{p_-}\Big)\, S(p-q)$$
$$\tau_{\lambda\mu}(q)\,\tau_{\nu\sigma}(q)\Gamma^{\sigma}_N\,6i\,\mathrm{Tr}\left[\gamma^{\mu}S(k)\gamma^+\gamma^1\gamma_5 S(k)\gamma^{\nu}S(k-q)\right]. \qquad \text{(D.42)}$$

Inserting the identity in the form

$$\mathbb{1} = \int_0^1 dy \int_0^1 dz \int_{-\infty}^{\infty} dq_o^2\; \delta\Big(y-\frac{q_-}{p_-}\Big)\,\delta\Big(z-\frac{k_-}{q_-}\Big)\,\delta(q^2-q_o^2)\,, \qquad \text{(D.43)}$$

which implies $\delta\Big(x-\frac{k_-}{p_-}\Big) \longrightarrow \delta(x-yz)$, gives

$$\Delta_T f^{\mathrm{a}}_{q(D)/N}(x) = i\int_0^1 dy \int_0^1 dz\,\delta(x-yz)\int_{-\infty}^{\infty} dq_o^2\;\overline{\Gamma}^{\lambda}_N$$
$$\int \frac{d^4q}{(2\pi)^4}\,\delta\Big(y-\frac{q_-}{p_-}\Big)\,\delta(q^2-q_o^2)\,S(p-q)\,\tau_{\lambda\mu}(q)\,\tau_{\nu\sigma}(q)\Gamma^{\sigma}_N$$
$$6i\int \frac{d^4k}{(2\pi)^4}\,\delta\Big(z-\frac{k_-}{q_-}\Big)\;\mathrm{Tr}\left[\gamma^{\mu}S(k)\gamma^+\gamma^1\gamma_5 S(k)\gamma^{\nu}S(k-q)\right].$$
$$\text{(D.44)}$$

We define

$$\begin{aligned}\Delta_T\Pi^{\mu\nu}(z,q) &= \Delta_T\Pi^A(z,q^2)\varepsilon^{\mu+1\nu} + \Delta_T\Pi^B(z,q^2)\left(q_1 q_\sigma \varepsilon^{\sigma\mu+\nu} + q_- q_\sigma \varepsilon^{\sigma\mu 1\nu}\right)\\ &= 6i\int \frac{d^4k}{(2\pi)^4}\,\delta\!\left(z-\frac{k_-}{q_-}\right)\,\mathrm{Tr}\left[\gamma^\mu S(k)\gamma^+\gamma^1\gamma_5 S(k)\gamma^\nu S(k-q)\right], \quad \text{(D.45)}\end{aligned}$$

and

$$\Delta_T f^{\mathrm{a}}_{q(D)/N}(x) = \Delta_T f^A(x) + \Delta_T f^B(x). \quad \text{(D.46)}$$

We have

$$\begin{aligned}\varepsilon^{\mu+1\nu}\tau_{\lambda\mu}(q)\,\tau_{\nu\sigma}(q) &= \varepsilon^{\mu+1\nu}\left\{4\,i\,G_a\left[\frac{g_{\lambda\mu}+2G_a\Pi_a(q^2)\,\frac{q_\lambda q_\mu}{q^2}}{1+2G_a\Pi_a(q^2)}\right]\right\}\\ &\qquad\left\{4\,i\,G_a\left[\frac{g_{\nu\sigma}+2G_a\Pi_a(q^2)\,\frac{q_\nu q_\sigma}{q^2}}{1+2G_a\Pi_a(q^2)}\right]\right\},\\ &= \left(\frac{4\,i\,G_a}{1+2G_a\Pi_a(q^2)}\right)^2\varepsilon^{\mu+1\nu}\Big\{g_{\lambda\mu}g_{\nu\sigma} + X\,g_{\lambda\mu}q_\nu q_\sigma\\ &\qquad + X\,g_{\nu\sigma}q_\lambda q_\mu + X^2\,q_\lambda q_\mu q_\nu q_\sigma\Big\},\\ &= \tau_a(q)^2\left\{g_{-\lambda}g_{2\sigma} - g_{2\lambda}g_{-\sigma} + X\left[q_2\left(g_{-\lambda}q_\sigma - g_{-\sigma}q_\lambda\right) + q_-\left(g_{2\sigma}q_\lambda - g_{2\lambda}q_\sigma\right)\right]\right\}, \quad \text{(D.47)}\end{aligned}$$

where $X = 2G_a\,\Pi_a(q^2)/q^2$, $\varepsilon^{-+12}=1$ and we have defined

$$\tau_a(q) = \frac{4\,i\,G_a}{1+2G_a\Pi_a(q^2)}. \quad \text{(D.48)}$$

The term proportional to X are discussed in section D.1.3 From the spin-dependent axial-vector diquark diagram we also have the results

$$\begin{aligned}q_\sigma\varepsilon^{\sigma\mu+\nu}\tau_{\lambda\mu}(q)\,\tau_{\nu\sigma}(q) &= \tau_a(q)^2\Big\{q_-\left[g_{2\lambda}g_{1\sigma} - g_{1\lambda}g_{2\sigma}\right]\\ &\qquad + q_1\left[g_{-\lambda}g_{2\sigma} - g_{2\lambda}g_{-\sigma}\right] + q_2\left[g_{1\lambda}g_{-\sigma} - g_{-\lambda}g_{1\sigma}\right]\Big\}, \quad \text{(D.49)}\\ q_\sigma\varepsilon^{\sigma\mu 1\nu}\tau_{\lambda\mu}(q)\,\tau_{\nu\sigma}(q) &= \tau_a(q)^2\Big\{q_-\left[g_{+\lambda}g_{2\sigma} - g_{2\lambda}g_{+\sigma}\right]\\ &\qquad + q_+\left[g_{2\lambda}g_{-\sigma} - g_{-\lambda}g_{2\sigma}\right] + q_2\left[g_{-\lambda}g_{+\sigma} - g_{+\lambda}g_{-\sigma}\right]\Big\}. \quad \text{(D.50)}\end{aligned}$$

Using the identity

$$\tau_a(q)^2 = -\frac{i}{q_-}\left(\frac{\partial\Pi_a(q^2)}{\partial q^2}\right)^{-1}\frac{\partial}{\partial q_+}\tau_a(q) = \frac{i}{2q_-}\,g_a(q^2)\,\frac{\partial}{\partial q_+}\tau_a(q), \quad \text{(D.51)}$$

we have

$$\Delta_T f^I(x) = \int_0^1 \int_0^1 \delta(x - yz) \int_{-\infty}^{\infty} dq_o^2 \, g_a(q_o^2) \Delta\Pi_a^I(z, q_o^2)$$
$$\frac{-1}{2yp_-} \overline{\Gamma}_N^\lambda \int \frac{d^4q}{(2\pi)^4} \delta\left(y - \frac{q_-}{p_-}\right) \delta(q^2 - q_o^2)\, S(p-q) \frac{\partial \tau_a(q^2)}{\partial q_+} \, G_{\lambda\sigma}^I(q)\, \Gamma_N^\sigma, \quad \text{(D.52)}$$

where $I \in (A, B)$. Defining

$$\Delta_T f^I_{q/D_a}(z, q_o^2) = i g_a(q_o^2) \Delta\Pi_a^I(z, q_o^2), \quad \text{(D.53)}$$
$$\Delta_T f^I_{D_a/N}(y, q_o^2) = \frac{i}{2yp_-} \overline{\Gamma}_N^\lambda \int \frac{d^4q}{(2\pi)^4} \delta\left(y - \frac{q_-}{p_-}\right) \delta(q^2 - q_o^2)$$
$$S(p-q) \frac{\partial \tau_a(q)}{\partial q_+} G_{\lambda\sigma}^I(q)\, \Gamma_N^\sigma, \quad \text{(D.54)}$$

where we have introduced one in the form $-i\,i = 1$. We now simplify $\Delta f^{aI}_{D/N}(y, q_o^2)$. Integrating by parts in q_+ gives

$$\Delta_T f^{aI}_{D/N}(y, q_o^2) = -\frac{i}{2yp_-} \overline{\Gamma}_N^\lambda \int \frac{d^4q}{(2\pi)^4} \delta\left(y - \frac{q_-}{p_-}\right)$$
$$\frac{\partial}{\partial q_+} \left\{ \delta(q^2 - q_o^2)\, S(p-q) G_{\lambda\sigma}^I(q) \right\} \tau_a(q)\, \Gamma_N^\sigma,$$
$$= \frac{i}{y} \overline{\Gamma}_N^\lambda \left(y \frac{\partial}{\partial q_o^2} + \frac{1}{2p_-} \frac{\partial}{\partial p_+} \right)$$
$$\int \frac{d^4q}{(2\pi)^4} \delta\left(y - \frac{q_-}{p_-}\right) \delta(q^2 - q_o^2)\, S(p-q) \tau_a(q)\, G_{\lambda\sigma}^I(q)\, \Gamma_N^\sigma$$
$$- i \frac{1}{2yp_-} \overline{\Gamma}_N^\lambda \int \frac{d^4q}{(2\pi)^4} \delta\left(y - \frac{q_-}{p_-}\right) \delta(q^2 - q_o^2)\, S(p-q) \tau_a(q) \frac{\partial}{\partial q_+} G_{\lambda\sigma}^I(q)\, \Gamma_N^\sigma. \quad \text{(D.55)}$$

Therefore the spin-dependent axial-vector diquark diagram is given by

$$\Delta_T f^{a}_{q(D)/N}(x) = \sum_I \int_0^1 \int_0^1 \delta(x - yz) \int_{-\infty}^{\infty} dq_o^2 \, \Delta_T f^I_{q/D_a}(z, q_o^2)\, \Delta_T f^I_{D_a/N}(y, q_o^2), \quad \text{(D.56)}$$

where

$$\Delta_T f^I_{q/D_a}(z, q_o^2) = i g_a(q_o^2)\, \Delta_T \Pi^I_a(z, q_o^2), \tag{D.57}$$

$$\begin{aligned}
\Delta_T f^I_{D_a/N}(y, q_o^2) = &-\frac{i}{y}\frac{Z_N M_N}{p_-}\,\overline{\Gamma}^\lambda \left(y\frac{\partial}{\partial q_o^2} + \frac{1}{2p_-}\frac{\partial}{\partial p_+}\right) \\
&\int \frac{d^4q}{(2\pi)^4}\,\delta\!\left(y - \frac{q_-}{p_-}\right) \delta\!\left(q^2 - q_o^2\right) S(p-q)\tau_a(q)\, G^I_{\lambda\sigma}(q)\, \Gamma^\sigma \\
&+ \frac{i}{2yp_-}\frac{Z_N M_N}{p_-}\overline{\Gamma}^\lambda \int \frac{d^4q}{(2\pi)^4}\,\delta\!\left(y - \frac{q_-}{p_-}\right) \\
&\qquad \delta\!\left(q^2 - q_o^2\right) S(p-q)\tau_a(q)\, \frac{\partial}{\partial q_+} G^I_{\lambda\sigma}(q)\, \Gamma^\sigma,
\end{aligned} \tag{D.58}$$

and

$$\begin{aligned}
G^A_{\lambda\sigma} &= g_{-\lambda} g_{2\sigma} - g_{2\lambda} g_{-\sigma}, \\
G^B_{\lambda\sigma} &= q_1\Big(q_-\left[g_{2\lambda}g_{1\sigma} - g_{1\lambda}g_{2\sigma}\right] + q_1\left[g_{-\lambda}g_{2\sigma} - g_{2\lambda}g_{-\sigma}\right] + q_2\left[g_{1\lambda}g_{-\sigma} - g_{-\lambda}g_{1\sigma}\right]\Big) \\
&+ q_-\Big(q_-\left[g_{+\lambda}g_{2\sigma} - g_{2\lambda}g_{+\sigma}\right] + q_+\left[g_{2\lambda}g_{-\sigma} - g_{-\lambda}g_{2\sigma}\right] + q_2\left[g_{-\lambda}g_{+\sigma} - g_{+\lambda}g_{-\sigma}\right]\Big).
\end{aligned} \tag{D.59, D.60}$$

If we make the on-shell approximation, the transverse axial-vector diquark diagram reduces to

$$\Delta_T f^{\mathrm{a}}_{q(D)/N}(x) = \sum_I \int_0^1 \int_0^1 \delta(x - yz)\, \Delta_T f^I_{q/D_a}(z)\, \Delta_T f^I_{D_a/N}(y), \tag{D.61}$$

where

$$\begin{aligned}
\Delta_T f^I_{q/D_a}(z) &= i g_a(q_o^2)\, \Delta_T \Pi^I_a(z, q_o^2)\Big|_{q_o^2 = M_a^2}, \\
\Delta f^I_{D_a/N}(y) &= -\frac{i}{2yp_-}\frac{Z_N M_N}{p_-} \\
&\qquad \overline{\Gamma}^\lambda \frac{\partial}{\partial p_+} \int \frac{d^4q}{(2\pi)^4}\,\delta\!\left(y - \frac{q_-}{p_-}\right) S(p-q)\tau_a(q)\, G^I_{\lambda\sigma}(q)\, \Gamma^\sigma \\
&+ \frac{i}{2yp_-}\frac{Z_N M_N}{p_-}\,\overline{\Gamma}^\lambda \int \frac{d^4q}{(2\pi)^4}\,\delta\!\left(y - \frac{q_-}{p_-}\right) S(p-q)\tau_a(q)\, \frac{\partial}{\partial q_+} G^I_{\lambda\sigma}(q)\, \Gamma^\sigma,
\end{aligned} \tag{D.62}$$

and $I \in [A, B]$.

Determining $\Delta_T f^I_{q/D_a}(z)$.

Recall

$$\Delta_T f^I_{q/D_a}(z) = ig_a(q_o^2)\Delta_T \Pi^I_a(z,q_o^2)\Big|_{q_o^2=M_a^2}, \tag{D.63}$$

where $I \in (A, B)$ and

$$\begin{aligned}\Delta_T\Pi^A(z,q^2)\varepsilon^{\mu+1\nu} &+ \Delta_T\Pi^B(z,q^2)\left(q_1 q_\sigma \varepsilon^{\sigma\mu+\nu} + q_- q_\sigma \varepsilon^{\sigma\mu 1\nu}\right)\\ &= 6i\int \frac{d^4k}{(2\pi)^4}\,\delta\!\left(z - \frac{k_-}{q_-}\right)\,\mathrm{Tr}\left[\gamma^\mu S(k)\gamma^+\gamma^1\gamma_5 S(k)\gamma^\nu S(k-q)\right].\end{aligned} \tag{D.64}$$

Using the moments and the result

$$\begin{aligned}&\mathrm{Tr}\left[\gamma^\mu(\not k + M)\gamma^+\gamma^1\gamma_5(\not k + M)\gamma^\nu(\not k - \not q + M)\right]\\ &\quad = -4iM\Big[\left(k^2 - M^2\right)\varepsilon^{\mu+1\nu} + 2k_-\, q_\sigma\varepsilon^{\sigma\mu1\nu} + 2k_1\, q_\sigma\varepsilon^{\sigma\mu+\nu}\Big],\end{aligned} \tag{D.65}$$

we have

$$\begin{aligned}A_n^{\mu\nu} = 24M\int \frac{d^4k}{(2\pi)^4}\left(\frac{k_-}{q_-}\right)^{n-1}\\ \Bigg\{\frac{\varepsilon^{\mu+1\nu}}{(k^2 - M^2 + i\varepsilon)\,(k^2 + q^2 - 2k\cdot q - M^2 + i\varepsilon)}\\ + \frac{2k_-\, q_\sigma\varepsilon^{\sigma\mu1\nu} + 2k_1\, q_\sigma\varepsilon^{\sigma\mu+\nu}}{(k^2 - M^2 + i\varepsilon)^2\,(k^2 + q^2 - 2k\cdot q - M^2 + i\varepsilon)}\Bigg\}.\end{aligned} \tag{D.66}$$

Using the Feynman parametrization results of section A.5 we obtain

$$\begin{aligned}A_n^{\mu\nu} = 24M\int_0^1 d\alpha\int \frac{d^4k}{(2\pi)^4}\left(\frac{k_- + \alpha q_-}{q_-}\right)^{n-1}\\ \Bigg\{\frac{\varepsilon^{\mu+1\nu}}{\left[k^2 - (\alpha^2-\alpha)\,q^2 - M^2 + i\varepsilon\right]^2}\\ + \frac{4(1-\alpha)\left[(k_- + \alpha q_-)\,q_\sigma\varepsilon^{\sigma\mu1\nu} + (k_1 + \alpha q_1)\,q_\sigma\varepsilon^{\sigma\mu+\nu}\right]}{\left[k^2 - (\alpha^2-\alpha)\,q^2 - M^2 + i\varepsilon\right]^3}\Bigg\}.\end{aligned} \tag{D.67}$$

Using

$$\left(\frac{k_- + \alpha q_-}{q_-}\right)^{n-1} = \alpha^{n-1} + (n-1)\alpha^{n-2}\frac{k_-}{q_-} + \ldots \tag{D.68}$$

and that $g_{--} = g_{-1} = 0$ and ignoring terms odd in k we have

$$\begin{aligned}A_n^{\mu\nu} = 24M\int_0^1 d\alpha\alpha^{n-1}\int \frac{d^4k}{(2\pi)^4}\\ \Bigg\{\frac{\varepsilon^{\mu+1\nu}}{\left[k^2 - (\alpha^2-\alpha)\,q^2 - M^2 + i\varepsilon\right]^2} + \frac{4\alpha(1-\alpha)\left[q_-\, q_\sigma\varepsilon^{\sigma\mu1\nu} + q_1\, q_\sigma\varepsilon^{\sigma\mu+\nu}\right]}{\left[k^2 - (\alpha^2-\alpha)\,q^2 - M^2 + i\varepsilon\right]^3}\Bigg\}.\end{aligned} \tag{D.69}$$

From the definition of the moments we have

$$\Delta_T \Pi^A(z,q^2) = 24M \int \frac{d^4k}{(2\pi)^4} \frac{1}{\left[k^2 - (z^2 - z)\, q^2 - M^2 + i\varepsilon\right]^2}, \tag{D.70}$$

$$\Delta_T \Pi^B(z,q^2) = 96M\, z(1-z) \int \frac{d^4k}{(2\pi)^4} \frac{1}{\left[k^2 - (z^2 - z)\, q^2 - M^2 + i\varepsilon\right]^3}. \tag{D.71}$$

Wick rotating and introducing polar coordinates we obtain

$$\Delta_T \Pi^A(z,q^2) = i\frac{3M}{2\pi^2} \int_0^\infty dk_E^2 \frac{k_E^2}{\left[k_E^2 + (z^2 - z)\, q^2 + M^2\right]^2}, \tag{D.72}$$

$$\Delta_T \Pi^B(z,q^2) = -i\,\frac{6M}{\pi^2}\, z(1-z) \int_0^\infty dk_E^2 \frac{k_E^2}{\left[k_E^2 + (z^2 - z)\, q^2 + M^2\right]^3}. \tag{D.73}$$

Introducing the proper-time regularization gives

$$\Delta_T \Pi^A(z,q^2) = i\frac{3M}{2\pi^2} \int d\tau\, \tau \int_0^\infty dk_E^2\, k_E^2\, e^{-\tau\left[k_E^2 + (z^2 - z) q^2 + M^2\right]}, \tag{D.74}$$

$$\Delta_T \Pi^B(z,q^2) = -i\,\frac{3M}{\pi^2}\, z(1-z) \int d\tau\, \tau^2 \int_0^\infty dk_E^2\, k_E^2\, e^{-\tau\left[k_E^2 + (z^2 - z) q^2 + M^2\right]}. \tag{D.75}$$

Integrating over k_E^2 gives

$$\Delta_T \Pi^A(z,q^2) = i\frac{3M}{2\pi^2} \int d\tau\, \frac{1}{\tau}\, e^{-\tau\left[(z^2 - z) q^2 + M^2\right]}, \tag{D.76}$$

$$\Delta_T \Pi^B(z,q^2) = -i\,\frac{3M}{\pi^2}\, z(1-z) \int d\tau\, e^{-\tau\left[(z^2 - z) q^2 + M^2\right]}. \tag{D.77}$$

Therefore

$$\Delta_T f^A(z) = -g_a\, \frac{3M}{2\pi^2} \int d\tau\, \frac{1}{\tau}\, e^{-\tau\left[(z^2 - z) M_a^2 + M^2\right]}, \tag{D.78}$$

$$\Delta_T f^B(z) = g_a\, \frac{3M}{\pi^2}\, z(1-z) \int d\tau\, e^{-\tau\left[(z^2 - z) M_a^2 + M^2\right]}. \tag{D.79}$$

Determining $\Delta_T f^A_{D_a/N}(y)$.

Recall

$$\Delta f^A_{D_a/N}(y) = -\frac{i}{2yp_-}\frac{Z_N M_N}{p_-} \overline{\Gamma}^\lambda \frac{\partial}{\partial p_+}\int \frac{d^4q}{(2\pi)^4}\,\delta\!\left(y-\frac{q_-}{p_-}\right) S(p-q)\tau_a(q)\,G^A_{\lambda\sigma}(q)\,\Gamma^\sigma + \frac{i}{2yp_-}\frac{Z_N\,M_N}{p_-}\,\overline{\Gamma}^\lambda\int\frac{d^4q}{(2\pi)^4}\,\delta\!\left(y-\frac{q_-}{p_-}\right) S(p-q)\tau_a(q)\,\frac{\partial}{\partial q_+}G^A_{\lambda\sigma}(q)\,\Gamma^\sigma.$$

Since $G^A_{\lambda\sigma} = (g_{-\lambda}g_{2\sigma} - g_{2\lambda}g_{-\sigma})$, we have $\frac{\partial}{\partial q_+}G^A_{\lambda\sigma} = 0$ and hence

$$\Delta f^A_{D_a/N}(y) = \frac{-i}{2yp_-}\frac{Z_N M_N}{p_-}\,\overline{\Gamma}^\lambda\,\frac{\partial}{\partial p_+}\int\frac{d^4q}{(2\pi)^4}\,\delta\!\left(y-\frac{q_-}{p_-}\right) S(p-q)\tau_a(q)\,G^A_{\lambda\sigma}\,\Gamma^\sigma. \tag{D.80}$$

Let

$$\begin{aligned} I^A &= \frac{\partial}{\partial p_+}\int\frac{d^4q}{(2\pi)^4}\,\delta\!\left(y-\frac{q_-}{p_-}\right) S(p-q)\tau_a(q), \\ &= \frac{\partial}{\partial p_+}\int\frac{d^4q}{(2\pi)^4}\delta\!\left(y-\frac{q_-}{p_-}\right) \frac{\not p - \not q + M}{q^2+p^2-2p\cdot q - M^2 + i\varepsilon}\left[4i\,G_a - \frac{i\,g_a}{q^2 - M_a^2 + i\varepsilon}\right], \\ &\equiv I^{A1} + I^{A2}. \end{aligned} \tag{D.81}$$

Using the moments to evaluate I^{A1} we have

$$\begin{aligned} \mathcal{A}^{A1}_n &= 4i\,G_a\frac{\partial}{\partial p_+}\int\frac{d^4q}{(2\pi)^4}\left(\frac{q_-}{p_-}\right)^{n-1}\frac{\not p - \not q + M}{q^2+p^2-2p\cdot q - M^2 + i\varepsilon}, \\ &\overset{q\to q+p}{=} 4i\,G_a\frac{\partial}{\partial p_+}\int\frac{d^4q}{(2\pi)^4}\left(\frac{q_- + p_-}{p_-}\right)^{n-2}\frac{M-\not q}{q^2 - M^2 + i\varepsilon}, \\ &= 0, \end{aligned} \tag{D.82}$$

because there is no p_+ dependence. Hence

$$I^{A1} = 0. \tag{D.83}$$

Taking the moments of I^{A2} and using Eq. (A.13) gives

$$\mathcal{A}^{A2}_n = -i\,g_a\frac{\partial}{\partial p_+}\int_0^1 d\alpha\int\frac{d^4q}{(2\pi)^4}\left(\frac{q_- + \alpha p_-}{p_-}\right)^{n-1} \frac{(1-\alpha)\not p - \not q + M}{[q^2 - (\alpha^2-\alpha)\,p^2 - (1-\alpha)\,M_a^2 - \alpha M^2 + i\varepsilon]^2}. \tag{D.84}$$

Ignoring terms odd in k and using $g^{--} = g^{1-} = g^{2-} = 0$ gives

$$\mathcal{A}_n^{A2} = -i\, g_a \frac{\partial}{\partial p_+} \int_0^1 d\alpha$$
$$\int \frac{d^4q}{(2\pi)^4} \frac{\alpha^{n-1}\left[(1-\alpha)\not{p} + M\right] - q_- q_+ \frac{\gamma^+}{p_-}\frac{d}{d\alpha}\alpha^{n-1}}{\left[q^2 - (\alpha^2-\alpha)\,p^2 - (1-\alpha)\,M_a^2 - \alpha M^2 + i\varepsilon\right]^2}. \quad \text{(D.85)}$$

Integrating by parts in $d\alpha$ and noting that the surface term is zero as it has no p_+ dependence and using the definition of the moments we have

$$I^{A2} = -i\, g_a \frac{\partial}{\partial p_+} \int \frac{d^4q}{(2\pi)^4} \frac{\left[(1-\alpha)\not{p} + M\right] + q_- q_+ \frac{\gamma^+}{p_-}\frac{d}{d\alpha}}{\left[q^2 - (\alpha^2-\alpha)\,p^2 - (1-\alpha)\,M_a^2 - \alpha M^2 + i\varepsilon\right]^2}. \quad \text{(D.86)}$$

Using the result for the spin-dependent axial-vector diquark diagram

$$I^A = \frac{g_a}{16\pi^2} \int d\tau \Big\{ \gamma^+ \left[\frac{y}{\tau} - (y^2-y)\left[(2y-1)\,p^2 - M_a^2 + M^2\right]\right]$$
$$- 2p_-\left(y^2-y\right)\left[(1-y)\not{p} + M\right]\Big\} e^{-\tau\left[(y^2-y)p^2 + (1-y)M_a^2 + yM^2\right]}. \quad \text{(D.87)}$$

Now

$$\begin{aligned}
\Delta f^A_{D_a/N}(y) &= -\frac{i}{2yp_-}\frac{Z_N M_N}{p_-}\,\overline{\Gamma}^\lambda I^A\, G^A_{\lambda\sigma}\,\Gamma^\sigma, \\
&= -\frac{i}{2yp_-}\frac{Z_N M_N}{p_-}\,\overline{\Gamma}^\lambda I^A\,(g_{-\lambda}g_{2\sigma} - g_{2\lambda}g_{-\sigma})\,\Gamma^\sigma, \\
&= -\frac{i}{2yp_-}\frac{Z_N M_N}{p_-}\,\left\{\overline{\Gamma}_- I^A\,\Gamma_2 - \overline{\Gamma}_2\, I^A\,\Gamma_-\right\}. \quad \text{(D.88)}
\end{aligned}$$

Therefore we need to determine $\overline{\Gamma}_-\Gamma_2 - \overline{\Gamma}_2\Gamma_-$, $\overline{\Gamma}_-\,\gamma^+\,\Gamma_2 - \overline{\Gamma}_2\,\gamma^+\,\Gamma_-$ and $\overline{\Gamma}_-\not{p}\,\Gamma_2 - \overline{\Gamma}_2\not{p}\,\Gamma_-$. In general we have

$$\overline{\Gamma}_-\,\Omega\,\Gamma_2 - \overline{\Gamma}_2\,\Omega\,\Gamma_- = \overline{u}_N\Big\{\alpha_2\alpha_3\Big[\frac{p_-}{M_N}\gamma_5\left(\Omega\gamma_2 - \gamma_2\Omega\right)\gamma_5$$
$$+ \frac{p_2}{M_N}\gamma_5\left(\gamma_-\Omega - \Omega\gamma_-\right)\gamma_5\Big] + \alpha_3^2\gamma_5\left(\gamma_-\Omega\gamma_2 - \gamma_2\Omega\gamma_-\right)\gamma_5\Big\}u_N. \quad \text{(D.89)}$$

Therefore

$$\begin{aligned}
\overline{\Gamma}_-\Gamma_2 - \overline{\Gamma}_2\Gamma_- &= \overline{u}_N\left\{\alpha_3^2\left(\gamma_-\gamma_2 - \gamma_2\gamma_-\right)\right\}u_N \\
&= -2\alpha_3^2\overline{u}_N\gamma^+\gamma^2 u_N = -2i\,\alpha_3^2\,\frac{p^+}{M_N}, \quad \text{(D.90)}
\end{aligned}$$

$$\overline{\Gamma}_-\gamma^+\Gamma_2 - \overline{\Gamma}_2\gamma^+\Gamma_- = \alpha_2\alpha_3\frac{p_-}{M_N}\overline{u}_N\left(\gamma^+\gamma_2 - \gamma_2\gamma^+\right)u_N$$
$$= 2\alpha_2\alpha_3\frac{p^+}{M_N}\overline{u}_N\gamma^+\gamma_2 u_N = -2i\alpha_2\alpha_3\frac{p^+p^+}{M_N^2}, \quad \text{(D.91)}$$

$$\overline{\Gamma}_-\not{p}\,\Gamma_2 \;-\; \overline{\Gamma}_2\not{p}\,\Gamma_- \;=\; -\alpha_3^2\overline{u}_N\left(\gamma_-\not{p}\gamma_2 - \gamma_2\not{p}\gamma_-\right)u_N \;=\; -2i\,\alpha_3^2\,p^+. \quad \text{(D.92)}$$

Therefore the final result is

$$\Delta f^A_{D_a/N}(y) = -\frac{g_a\,Z_N}{16\pi^2}\int d\tau\left\{\frac{\alpha_2\alpha_3}{M_N}\left[\frac{1}{\tau} + (1-y)\left[(2y-1)\,p^2 - M_a^2 + M^2\right]\right]\right.$$
$$\left. + \,2\alpha_3^2\,(1-y)\left[(1-y)M_N + M\right]\right\}e^{-\tau\left[\left(y^2-y\right)p^2+(1-y)M_a^2+yM^2\right]}. \quad \text{(D.93)}$$

Determining $\Delta_T f^{A'}_{D_a/N}(y)$.

The diquark in the nucleon part of the diagram has the general form

$$\begin{aligned}\Delta_T f^{I}_{D_a/N}(y) = &-\frac{i}{2yp_-}\frac{Z_N M_N}{p_-} \\ &\overline{\Gamma}^{\lambda}\frac{\partial}{\partial p_+}\int\frac{d^4q}{(2\pi)^4}\,\delta\left(y-\frac{q_-}{p_-}\right)S(p-q)\tau_a(q)\,G^{I}_{\lambda\sigma}(q)\,\Gamma^{\sigma} \\ &+\frac{i}{2yp_-}\frac{Z_N\,M_N}{p_-}\,\overline{\Gamma}^{\lambda}\int\frac{d^4q}{(2\pi)^4}\,\delta\left(y-\frac{q_-}{p_-}\right)S(p-q)\tau_a(q)\,\frac{\partial}{\partial q_+}G^{I}_{\lambda\sigma}(q)\,\Gamma^{\sigma},\end{aligned} \tag{D.94}$$

where in this part we have

$$\begin{aligned}G^{I}_{\lambda\sigma} &= X\left[q_2\left(g_{-\lambda}q_\sigma - g_{-\sigma}q_\lambda\right)+q_-\left(g_{2\sigma}q_\lambda - g_{2\lambda}q_\sigma\right)\right] \\ &= \frac{2G_a\,\Pi_a(q^2)}{q^2}\left[q_2\left(g_{-\lambda}q_\sigma - g_{-\sigma}q_\lambda\right)+q_-\left(g_{2\sigma}q_\lambda - g_{2\lambda}q_\sigma\right)\right].\end{aligned} \tag{D.95}$$

If we make the pole approximation to the diquark t-matrix from the beginning this term does not contribute. However if we keep the full t-matrix until the end, which is the normal practice, then these term will contribute. In the on-shell approximation the $X(q^2)$ term moves outside the integral and becomes $X(M_a^2)$, where $2G_a\,\Pi_a(M_a^2) = -1$, hence we have

$$\begin{aligned}\Delta_T f^{A'}_{D_a/N}(y) = &-\frac{i}{2yp_-}\frac{Z_N M_N}{p_-}\frac{-1}{M_a^2} \\ &\overline{\Gamma}^{\lambda}\frac{\partial}{\partial p_+}\int\frac{d^4q}{(2\pi)^4}\,\delta\left(y-\frac{q_-}{p_-}\right)S(p-q)\tau_a(q)\,G^{A'}_{\lambda\sigma}(q)\,\Gamma^{\sigma} \\ &+\frac{i}{2yp_-}\frac{Z_N\,M_N}{p_-}\frac{-1}{M_a^2}\,\overline{\Gamma}^{\lambda}\int\frac{d^4q}{(2\pi)^4}\,\delta\left(y-\frac{q_-}{p_-}\right)S(p-q)\tau_a(q)\,\frac{\partial}{\partial q_+}G^{A'}_{\lambda\sigma}(q)\,\Gamma^{\sigma},\end{aligned} \tag{D.96}$$

where

$$G^{A'}_{\lambda\sigma} = \left[q_2\left(g_{-\lambda}q_\sigma - g_{-\sigma}q_\lambda\right)+q_-\left(g_{2\sigma}q_\lambda - g_{2\lambda}q_\sigma\right)\right]. \tag{D.97}$$

If we just consider the matrix element part we have

$$\overline{\Gamma}^{\lambda}\,G^{A'}_{\lambda\sigma}\,\Gamma^{\sigma} = \overline{\Gamma}^{\lambda}\,\Omega\left\{\left[q_2\left(g_{-\lambda}q_\sigma - g_{-\sigma}q_\lambda\right)+q_-\left(g_{2\sigma}q_\lambda - g_{2\lambda}q_\sigma\right)\right]\right\}\Gamma^{\sigma}, \tag{D.98}$$

where Ω is some Dirac structure. Summing over the indices gives

$$\begin{aligned}\overline{\Gamma}^{\lambda}\, G^{A'}_{\lambda\sigma}\, \Gamma^{\sigma} = &\Big\{q_2\Big[q_+\overline{\Gamma}_-\Omega\Gamma^+ + q_-\overline{\Gamma}_-\Omega\Gamma^- + q_1\overline{\Gamma}_-\Omega\Gamma^1 + q_2\overline{\Gamma}_-\Omega\Gamma^2 \\ &\qquad - q_+\overline{\Gamma}^+\Omega\Gamma_- - q_-\overline{\Gamma}^-\Omega\Gamma_- - q_1\overline{\Gamma}^1\Omega\Gamma_- - q_2\overline{\Gamma}^2\Omega\Gamma_-\Big]\Big\} \\ &+\Big\{q_-\Big[q_+\overline{\Gamma}^+\Omega\Gamma_2 + q_-\overline{\Gamma}^-\Omega\Gamma_2 + q_1\overline{\Gamma}^1\Omega\Gamma_2 + q_2\overline{\Gamma}^2\Omega\Gamma_2 \\ &\qquad - q_+\overline{\Gamma}_2\Omega\Gamma^+ - q_-\overline{\Gamma}_2\Omega\Gamma^- - q_1\overline{\Gamma}_2\Omega\Gamma^1 - q_2\overline{\Gamma}_2\Omega\Gamma^2\Big]\Big\}.\end{aligned} \tag{D.99}$$

Cancelling and grouping terms gives

$$\begin{aligned}\overline{\Gamma}^{\lambda}\, G^{A'}_{\lambda\sigma}\, \Gamma^{\sigma} = &\Big\{q_2\Big[q_-\left(\overline{\Gamma}_-\Omega\Gamma_+ - \overline{\Gamma}_+\Omega\Gamma_-\right) \\ &\qquad + q_1\left(\overline{\Gamma}_1\Omega\Gamma_- - \overline{\Gamma}_-\Omega\Gamma_1\right) + q_2\left(\overline{\Gamma}_2\Omega\Gamma_- - \overline{\Gamma}_-\Omega\Gamma_2\right)\Big]\Big\} \\ &+\Big\{q_-\Big[q_+\left(\overline{\Gamma}_-\Omega\Gamma_2 - \overline{\Gamma}_2\Omega\Gamma_-\right) \\ &\qquad + q_-\left(\overline{\Gamma}_+\Omega\Gamma_2 - \overline{\Gamma}_2\Omega\Gamma_+\right) + q_1\left(\overline{\Gamma}_2\Omega\Gamma_1 - \overline{\Gamma}_1\Omega\Gamma_2\right)\Big]\Big\}.\end{aligned} \tag{D.100}$$

Therefore $\Delta_T f^{A'}_{D_a/N}(y)$ has seven terms. Letting

$$I = \frac{\partial}{\partial p_+}\int \frac{d^4q}{(2\pi)^4}\,\delta\!\left(y - \frac{q_-}{p_-}\right) S(p-q)\tau_a(q), \tag{D.101}$$

$$I' = \int \frac{d^4q}{(2\pi)^4}\,\delta\!\left(y - \frac{q_-}{p_-}\right) S(p-q)\tau_a(q), \tag{D.102}$$

these are

$$\Delta_T f^{A'1}(y) = -\frac{i}{2yp_-}\frac{Z_N M_N}{p_-}\frac{-1}{M_a^2}\left\{\overline{\Gamma}_-\, I\, q_- q_2\, \Gamma_+ - \overline{\Gamma}_+\, I\, q_- q_2 \Gamma_-\right\}, \tag{D.103}$$

$$\Delta_T f^{A'2}(y) = -\frac{i}{2yp_-}\frac{Z_N M_N}{p_-}\frac{-1}{M_a^2}\left\{\overline{\Gamma}_1\, I\, q_1 q_2\, \Gamma_- - \overline{\Gamma}_-\, I\, q_- q_2 \Gamma_1\right\}, \tag{D.104}$$

$$\Delta_T f^{A'3}(y) = -\frac{i}{2yp_-}\frac{Z_N M_N}{p_-}\frac{-1}{M_a^2}\left\{\overline{\Gamma}_2\, I\, q_2^2\, \Gamma_- - \overline{\Gamma}_-\, I\, q_2^2 \Gamma_2\right\}, \tag{D.105}$$

$$\Delta_T f^{A'4}(y) = -\frac{i}{2yp_-}\frac{Z_N M_N}{p_-}\frac{-1}{M_a^2}\left\{\overline{\Gamma}_-\, I\, q_+ q_-\, \Gamma_2 - \overline{\Gamma}_2\, I\, q_+ q_- \Gamma_-\right\}, \tag{D.106}$$

$$\Delta_T f^{A'5}(y) = -\frac{i}{2yp_-}\frac{Z_N M_N}{p_-}\frac{-1}{M_a^2}\left\{\overline{\Gamma}_+\, I\, q_-^2\, \Gamma_2 - \overline{\Gamma}_2\, I\, q_-^2 \Gamma_+\right\}, \tag{D.107}$$

$$\Delta_T f^{A'6}(y) = -\frac{i}{2yp_-}\frac{Z_N M_N}{p_-}\frac{-1}{M_a^2}\left\{\overline{\Gamma}_2\, I\, q_1 q_-\, \Gamma_1 - \overline{\Gamma}_1\, I\, q_1 q_- \Gamma_2\right\}, \tag{D.108}$$

$$\Delta_T f^{A'7}(y) = \frac{i}{2yp_-}\frac{Z_N M_N}{p_-}\frac{-1}{M_a^2}\left\{\overline{\Gamma}_-\, I'\, q_-\, \Gamma_2 - \overline{\Gamma}_2\, I'\, q_- \Gamma_-\right\}. \tag{D.109}$$

We now evaluate each of these terms.

Determining $\Delta_T f^{A'1}_{Da/N}(y)$

$$\Delta f^{A'1}_{Da/N}(y) = -\frac{i}{2yp_-}\frac{Z_N M_N}{p_-}\frac{-1}{M_a^2}$$
$$\overline{\Gamma}^\lambda \frac{\partial}{\partial p_+}\int \frac{d^4q}{(2\pi)^4}\,\delta\!\left(y-\frac{q_-}{p_-}\right) S(p-q)\tau_a(q)\, q_- q_2\left[g_{-\lambda}g_{+\sigma}-g_{+\lambda}g_{-\sigma}\right]\Gamma^\sigma. \quad \text{(D.110)}$$

From the δ-function we have $q_- \to yp_-$, therefore

$$\Delta f^{A'1}_{Da/N}(y) = -\frac{i}{2}\frac{Z_N M_N}{p_-}\overline{\Gamma}^\lambda \frac{\partial}{\partial p_+}\int \frac{d^4q}{(2\pi)^4}$$
$$\delta\!\left(y-\frac{q_-}{p_-}\right) S(p-q)\tau_a(q)\, q_2\left[g_{-\lambda}g_{+\sigma}-g_{+\lambda}g_{-\sigma}\right]\Gamma^\sigma. \quad \text{(D.111)}$$

From the $\Delta f^{B6}_{Da/N}(y)$ calculation we have

$$\Delta f^{A'1}_{Da/N}(y) = \frac{i}{2}\frac{Z_N M_N}{p_-}\frac{1}{M_a^2}\frac{g_a}{16\pi^2}\,y(1-y)p_-\,\gamma^2$$
$$\int d\tau\,\frac{1}{\tau}\,e^{-\tau\left[\left(y^2-y\right)p^2+(1-y)M_a^2+yM^2\right]}, \quad \text{(D.112)}$$

where

$$\overline{\Gamma}_-\gamma^2\Gamma_+ - \overline{\Gamma}_+\gamma^2\Gamma_- = 2i\,\alpha_3\left(\alpha_2-\alpha_3\right). \quad \text{(D.113)}$$

Therefore

$$\Delta f^{A'1}_{Da/N}(y) = \frac{g_a\,Z_N\,M_N}{16\pi^2\,M_a^2}\,y(1-y)\,\alpha_3\left(\alpha_3-\alpha_2\right)$$
$$\int d\tau\,\frac{1}{\tau}\,e^{-\tau\left[\left(y^2-y\right)p^2+(1-y)M_a^2+yM^2\right]}. \quad \text{(D.114)}$$

Determining $\Delta_T f^{A'2}_{Da/N}(y)$

$$\Delta f^{A'2}_{Da/N}(y) = -\frac{i}{2yp_-}\frac{Z_N M_N}{p_-}\frac{-1}{M_a^2}\overline{\Gamma}^\lambda \frac{\partial}{\partial p_+}\int \frac{d^4q}{(2\pi)^4}$$
$$\delta\!\left(y-\frac{q_-}{p_-}\right) S(p-q)\tau_a(q)\, q_- q_2\left[g_{1\lambda}g_{-\sigma}-g_{-\lambda}g_{1\sigma}\right]\Gamma^\sigma. \quad \text{(D.115)}$$

From the $\Delta f^{B3}_{Da/N}(y)$ calculation we have

$$\Delta f^{A'2}_{Da/N}(y) = 0. \quad \text{(D.116)}$$

Determining $\Delta_T f^{A'3}_{Da/N}(y)$

$$\Delta f^{A'3}_{D_a/N}(y) = -\frac{i}{2yp_-}\frac{Z_N M_N}{p_-}\frac{-1}{M_a^2}\overline{\Gamma}^\lambda \frac{\partial}{\partial p_+}\int \frac{d^4q}{(2\pi)^4}$$
$$\delta\left(y - \frac{q_-}{p_-}\right) S(p-q)\tau_a(q)\, q_2^2 \left[g_{2\lambda} g_{-\sigma} - g_{-\lambda} g_{2\sigma}\right] \Gamma^\sigma. \quad \text{(D.117)}$$

From the $\Delta f^{B2}_{D_a/N}(y)$ calculation we have

$$\Delta f^{A'3}_{D_a/N}(y) = \frac{g_a\, Z_N}{32\pi^2\, M_a^2}\int d\tau\, \frac{1}{\tau^2}\; e^{-\tau\left[(y^2-y)p^2+(1-y)M_a^2+yM^2\right]}$$
$$\left\{\frac{\alpha_2\alpha_3}{M_N}\left[1+\tau\,(1-y)\left[(2y-1)p^2 - M_a^2 + M^2\right]\right]\right.$$
$$\left. + 2\tau\alpha_3^2\,(1-y)\left[(1-y)M_N + M\right]\right\}. \quad \text{(D.118)}$$

Determining $\Delta_T f^{A'4}_{D_a/N}(y)$

$$\Delta f^{A'4}_{D_a/N}(y) = -\frac{i}{2yp_-}\frac{Z_N M_N}{p_-}\frac{-1}{M_a^2}\overline{\Gamma}^\lambda \frac{\partial}{\partial p_+}\int \frac{d^4q}{(2\pi)^4}$$
$$\delta\left(y - \frac{q_-}{p_-}\right) S(p-q)\tau_a(q)\, q_- q_+ \left[g_{-\lambda} g_{2\sigma} - g_{2\lambda} g_{-\sigma}\right] \Gamma^\sigma. \quad \text{(D.119)}$$

From the δ-function we have $q_- \to yp_-$, therefore

$$\Delta f^{A'4}_{D_a/N}(y) = -\frac{i}{2}\frac{Z_N M_N}{p_-}\frac{-1}{M_a^2}\overline{\Gamma}^\lambda \frac{\partial}{\partial p_+}\int \frac{d^4q}{(2\pi)^4}$$
$$\delta\left(y - \frac{q_-}{p_-}\right) S(p-q)\tau_a(q)\, q_+ \left[g_{-\lambda} g_{2\sigma} - g_{2\lambda} g_{-\sigma}\right] \Gamma^\sigma. \quad \text{(D.120)}$$

From the $\Delta f^{B5}_{D_a/N}(y)$ calculation we have

$$\Delta_T f^{A'4}_{D_a/N}(y) = \Delta_T f_1^{A'4}(y) + \Delta_T f_{2a}^{A'4}(y) + \Delta_T f_{2b}^{A'4}(y), \quad \text{(D.121)}$$

where

$$\Delta_T f_1^{A'4}(y) = \frac{G_a\, Z_N}{8\pi^2\, M_a^2} \int d\tau\, \frac{1}{\tau^2} \left[2\, M\, \alpha_3^2\, \delta(y-1) - \frac{\alpha_2\alpha_3}{\tau\, M_N}\, \frac{d}{dy}\, \delta(y-1)\right] e^{-\tau\, M^2}, \tag{D.122}$$

$$\Delta_T f_{2a}^{A'4}(y) = -\frac{g_a\, \alpha_3^2\, Z_N}{32\pi^2\, M_a^2\, M_N} \int d\tau\, \frac{1}{\tau^2} \left[\delta(y-1) e^{-\tau\, M^2} + \delta(y)\, e^{-\tau\, M_a^2}\right], \tag{D.123}$$

$$\Delta_T f_{2b}^{A'4}(y) = -\frac{g_a\, Z_N}{16\pi^2\, M_a^2} \int d\tau\, \frac{1}{\tau} \left\{\alpha_3^2\, (1-y)\Big[1 - \tau\, y\, \left[(y-1)\, p^2 - M_a^2 + M^2\right]\Big] \left[(1-y) M_N + M\right] - \frac{\alpha_2\alpha_3}{M_N}\left[\frac{y}{2}\,(3y-2) M_N^2 - \frac{1}{\tau} - \frac{1}{2}\Big[1 - 2y + \tau\, y (y^2 - y) p^2\Big] \left[(2y-1)\, p^2 - M_a^2 + M^2\right]\right]\right\} e^{-\tau\, A}, \tag{D.124}$$

where $A = (y^2 - y)\, M_N^2 + (1-y)\, M_a^2 + y M^2$.

Determining $\Delta_T f_{D_a/N}^{A'5}(y)$

$$\Delta f_{D_a/N}^{A'5}(y) = -\frac{i}{2yp_-}\,\frac{Z_N M_N}{p_-}\,\frac{-1}{M_a^2}\,\overline{\Gamma}^{\lambda}\,\frac{\partial}{\partial p_+} \int \frac{d^4q}{(2\pi)^4}\, \delta\!\left(y - \frac{q_-}{p_-}\right) S(p-q)\tau_a(q)\, q_-^2\, \left[g_{+\lambda} g_{2\sigma} - g_{2\lambda} g_{+\sigma}\right] \Gamma^{\sigma}. \tag{D.125}$$

From the δ-function we have $q_- \longrightarrow y p_-$, therefore

$$\Delta f_{D_a/N}^{A'5}(y) = -\frac{i}{2} Z_N M_N\, y\, \frac{-1}{M_a^2}\,\overline{\Gamma}^{\lambda}\,\frac{\partial}{\partial p_+} \int \frac{d^4q}{(2\pi)^4}\, \delta\!\left(y - \frac{q_-}{p_-}\right) S(p-q)\tau_a(q)\, \left[g_{+\lambda} g_{2\sigma} - g_{2\lambda} g_{+\sigma}\right] \Gamma^{\sigma}. \tag{D.126}$$

From the $\Delta f^{B4}_{D_a/N}(y)$ calculation we have

$$\Delta f^{A'5}_{D_a/N}(y) = -\frac{g_a\, Z_N\, M_N}{32\pi^2\, M_a^2}\, y^2 \int d\tau\, e^{-\tau\left[\left(y^2-y\right)M_N^2+(1-y)M_a^2+yM^2\right]}$$
$$\left\{\alpha_2\alpha_3 \left[\frac{1}{\tau} + (1-y)\left[(2y-1)\,M_N^2 - M_a^2 + M^2\right]\right]\right.$$
$$\left. - \alpha_3^2\,(1-y)\left[(M_N+M)^2 - M_a^2\right]\right\}. \quad \text{(D.127)}$$

Determining $\Delta_T f^{A'6}_{D_a/N}(y)$

$$\Delta f^{A'6}_{D_a/N}(y) = -\frac{i}{2yp_-}\frac{Z_N M_N}{p_-}\frac{-1}{M_a^2}\overline{\Gamma}^\lambda \frac{\partial}{\partial p_+}\int \frac{d^4q}{(2\pi)^4}$$
$$\delta\!\left(y - \frac{q_-}{p_-}\right) S(p-q)\tau_a(q)\, q_1 q_- \left[g_{2\lambda}g_{1\sigma} - g_{1\lambda}g_{2\sigma}\right]\Gamma^\sigma,$$
$$= -\frac{i}{2yp_-}\frac{Z_N M_N}{p_-}\, yp_-\, \overline{\Gamma}^\lambda \frac{\partial}{\partial p_+}\int \frac{d^4q}{(2\pi)^4}$$
$$\delta\!\left(y - \frac{q_-}{p_-}\right) S(p-q)\tau_a(q)\, q_1 \left[g_{2\lambda}g_{1\sigma} - g_{1\lambda}g_{2\sigma}\right]\Gamma^\sigma. \quad \text{(D.128)}$$

From the δ-function we have $q_- \longrightarrow yp_-$, therefore

$$\Delta f^{A'6}_{D_a/N}(y) = -\frac{i}{2yp_-}\frac{Z_N M_N}{p_-}\, yp_-\, \frac{-1}{M_a^2}\overline{\Gamma}^\lambda \frac{\partial}{\partial p_+}$$
$$\int \frac{d^4q}{(2\pi)^4}\,\delta\!\left(y - \frac{q_-}{p_-}\right) S(p-q)\tau_a(q)\, q_1 \left[g_{2\lambda}g_{1\sigma} - g_{1\lambda}g_{2\sigma}\right]\Gamma^\sigma. \quad \text{(D.129)}$$

From the $\Delta f^{B1}_{D_a/N}(y)$ calculation we have

$$\Delta f^{A'6}_{D_a/N}(y) = -p_1^2\, \frac{g_a\, Z_N}{16\pi^2\, M_a^2\, M_N}\,\alpha_2\alpha_3\, y\,(1-y)$$
$$\int d\tau\, \frac{1}{\tau}\, e^{-\tau\left[\left(y^2-y\right)p^2+(1-y)M_a^2+\alpha M^2\right]},$$
$$\longrightarrow 0. \quad \text{(D.130)}$$

Determining $\Delta_T f^{A'7}_{D_a/N}(y)$

$$\Delta f^{B7}_{D_a/N}(y) = \frac{i}{2yp_-}\frac{Z_N M_N}{p_-}\frac{-1}{M_a^2}\overline{\Gamma}^\lambda \int \frac{d^4q}{(2\pi)^4}$$
$$\delta\!\left(y - \frac{q_-}{p_-}\right) S(p-q)\tau_a(q)\, q_- \left[g_{-\lambda}g_{2\sigma} - g_{2\lambda}g_{-\sigma}\right]\Gamma^\sigma. \quad \text{(D.131)}$$

From the δ-function we have $q_- \to yp_-$, therefore

$$\Delta f^{B7}_{D_a/N}(y) = \frac{i}{2}\frac{Z_N M_N}{p_-}\frac{-1}{M_a^2}\overline{\Gamma}^\lambda \int \frac{d^4q}{(2\pi)^4} \delta\left(y - \frac{q_-}{p_-}\right) S(p-q)\tau_a(q)\,[g_{-\lambda}g_{2\sigma} - g_{2\lambda}g_{-\sigma}]\,\Gamma^\sigma. \quad \text{(D.132)}$$

From the $\Delta f^{B7}_{D_a/N}(y)$ calculation we have

$$\Delta f^{B7}_{D_a/N}(y) = -\frac{G_a\,Z_N}{8\pi^2\,M_a^2}\int d\tau\,\frac{1}{\tau^2} \left[2\,M\,\alpha_3^2\,\delta(y-1) - \frac{\alpha_2\alpha_3}{\tau\,M_N}\,\frac{d}{dy}\,\delta(y-1)\right]e^{-\tau\,M^2} - \frac{g_a\,Z_N}{16\pi^2\,M_a^2}\int d\tau\,\frac{1}{\tau}e^{-\tau\left[(y^2-y)p^2+(1-y)M_a^2+yM^2\right]} \left\{\alpha_3^2\,[(1-y)M_N + M] + \frac{\alpha_2\alpha_3}{2M_N}\left[(2y-1)p^2 - M_a^2 + M^2\right]\right\}. \quad \text{(D.133)}$$

Summary of Results for $\Delta_T f^{A'}_{D_a/N}(y)$

We have

$$\begin{aligned}\Delta_T f^{A'}_{D_a/N}(y) &= \Delta_T f^{A'1} + \Delta_T f^{A'2} + \Delta_T f^{A'3} + \Delta_T f^{A'4} + \Delta_T f^{A'5} + \Delta_T f^{A'6} + \Delta_T f^{A'7},\\ &= \Delta_T f^{A'1} + \Delta_T f^{A'2} + \Delta_T f^{A'3} + \Delta_T f^{A'4} + \Delta_T f_1^{A'5} + \Delta_T f_{2a}^{A'5} + \Delta_T f_{2b}^{A'5} + \Delta_T f^{A'6} + \Delta_T f_1^{A'7} + \Delta_T f_2^{A'7}.\end{aligned} \quad \text{(D.134)}$$

where

$$\Delta f^{A'1}(y) = \frac{g_a\,Z_N\,M_N}{16\pi^2\,M_a^2}\,y(1-y)\,\alpha_3\,(\alpha_2-\alpha_3) \int d\tau\,\frac{1}{\tau}\,e^{-\tau\left[(y^2-y)p^2+(1-y)M_a^2+yM^2\right]}, \quad \text{(D.135)}$$

$$\Delta f^{A'2}(y) = 0, \quad \text{(D.136)}$$

$$\Delta f^{A'3}(y) = \frac{g_a\,Z_N}{32\pi^2\,M_a^2}\int d\tau\,\frac{1}{\tau^2}\,e^{-\tau\left[(y^2-y)p^2+(1-y)M_a^2+yM^2\right]}$$

$$\left\{ \frac{\alpha_2\alpha_3}{M_N} \left[1 + \tau \left(y^2 - y\right) \left[(2y-1)p^2 - M_a^2 + M^2\right]\right] \right.$$

$$\left. + 2\tau\alpha_3^2 (1-y) \left[(1-y)M_N + M\right] \right\}, \tag{D.137}$$

$$\Delta_T f_1^{A'4}(y) = -\frac{G_a\, Z_N}{8\pi^2\, M_a^2} \int d\tau\, \frac{1}{\tau^2}$$

$$\left[2\, M\, \alpha_3^2\, \delta(y-1) - \frac{\alpha_2\alpha_3}{\tau\, M_N} \frac{d}{dy}\, \delta(y-1)\right] e^{-\tau\, M^2}, \tag{D.138}$$

$$\Delta_T f_{2a}^{A'4}(y) = \frac{g_a\, \alpha_3^2\, Z_N}{32\pi^2\, M_a^2\, M_N} \int d\tau\, \frac{1}{\tau^2} \left[\delta(y-1)e^{-\tau\, M^2} + \delta(y)\, e^{-\tau\, M_a^2}\right], \tag{D.139}$$

$$\Delta_T f_{2b}^{A'4}(y) = \frac{g_a\, Z_N}{16\pi^2\, M_a^2} \int d\tau\, \frac{1}{\tau}\, e^{-\tau\left[\left(y^2-y\right)M_N^2 + (1-y)M_a^2 + yM^2\right]}$$

$$\left\{ \alpha_3^2\, (1-y)\left[1 - \tau\, y\, \left[(y-1)\, p^2 - M_a^2 + M^2\right]\right] \left[(1-y)M_N + M\right] \right.$$

$$+ \frac{\alpha_2\alpha_3}{M_N} \left[\frac{y}{2}\, (3y-2)M_N^2 - \frac{1}{\tau} - \frac{1}{2}\left[1 - 2y + \tau\, y(y^2-y)p^2\right]\right.$$

$$\left.\left.\left[(2y-1)\, p^2 - M_a^2 + M^2\right]\right]\right\}, \tag{D.140}$$

$$\Delta f^{A'5}(y) = \frac{g_a\, Z_N\, M_N}{32\pi^2\, M_a^2}\, y^2 \int d\tau\;\; e^{-\tau\left[\left(y^2-y\right)M_N^2 + (1-y)M_a^2 + yM^2\right]}$$

$$\left\{ \alpha_2\alpha_3 \left[\frac{1}{\tau} + (1-y)\, \left[(2y-1)\, M_N^2 - M_a^2 + M^2\right]\right] \right.$$

$$\left. - \alpha_3^2\, (1-y)\, \left[(M_N + M)^2 - M_a^2\right] \right\}, \tag{D.141}$$

$$\Delta f^{A'6}(y) = 0, \tag{D.142}$$

$$\Delta f_1^{A'7}(y) = \frac{G_a\, Z_N}{8\pi^2\, M_a^2} \int d\tau\, \frac{1}{\tau^2}$$

$$\left[2\, M\, \alpha_3^2\, \delta(y-1) - \frac{\alpha_2\alpha_3}{\tau\, M_N} \frac{d}{dy}\, \delta(y-1)\right] e^{-\tau\, M^2}, \tag{D.143}$$

$$\Delta f_2^{A'7}(y) = \frac{g_a\, Z_N}{16\pi^2\, M_a^2} \int d\tau\, \frac{1}{\tau}\, e^{-\tau\left[\left(y^2-y\right)p^2 + (1-y)M_a^2 + yM^2\right]}$$

$$\left\{ \alpha_3^2\, \left[(1-y)M_N + M\right] + \frac{\alpha_2\alpha_3}{2M_N}\left[(2y-1)p^2 - M_a^2 + M^2\right] \right\}. \tag{D.144}$$

Note $\Delta_T f_1^{A'4}(y)$ and $\Delta f_1^{A'7}(y)$ cancel.

Determining $\Delta_T f^B_{D_a/N}(y)$

Recall

$$\Delta f^B_{D_a/N}(y) = -\frac{i}{2yp_-}\frac{Z_N M_N}{p_-}\,\overline{\Gamma}^\lambda \frac{\partial}{\partial p_+}\int \frac{d^4q}{(2\pi)^4} \delta\left(y-\frac{q_-}{p_-}\right) S(p-q)\tau_a(q)\, G^B_{\lambda\sigma}(q)\,\Gamma^\sigma$$
$$+\frac{i}{2yp_-}\frac{Z_N\, M_N}{p_-}\,\overline{\Gamma}^\lambda \int \frac{d^4q}{(2\pi)^4}\,\delta\left(y-\frac{q_-}{p_-}\right) S(p-q)\tau_a(q)\,\frac{\partial}{\partial q_+} G^B_{\lambda\sigma}(q)\,\Gamma^\sigma, \quad \text{(D.145)}$$

where

$$G^B_{\lambda\sigma} = q_1\Big(q_-\,[g_{2\lambda}g_{1\sigma} - g_{1\lambda}g_{2\sigma}] + q_1\,[g_{-\lambda}g_{2\sigma} - g_{2\lambda}g_{-\sigma}] + q_2\,[g_{1\lambda}g_{-\sigma} - g_{-\lambda}g_{1\sigma}]\Big)$$
$$+\,q_-\Big(q_-\,[g_{+\lambda}g_{2\sigma} - g_{2\lambda}g_{+\sigma}] + q_+\,[g_{2\lambda}g_{-\sigma} - g_{-\lambda}g_{2\sigma}] + q_2\,[g_{-\lambda}g_{+\sigma} - g_{+\lambda}g_{-\sigma}]\Big),$$
$$\equiv G^{B1}_{\lambda\sigma} + G^{B2}_{\lambda\sigma} + \ldots + G^{B6}_{\lambda\sigma}, \quad \text{(D.146)}$$

and hence

$$\frac{\partial}{\partial q_+} G^B_{\lambda\sigma} = q_-\,[g_{2\lambda}g_{-\sigma} - g_{-\lambda}g_{2\sigma}] \equiv G^{B7}_{\lambda\sigma}. \quad \text{(D.147)}$$

Therefore

$$\Delta f^{B1\ldots B6}_{D_a/N}(y) = -\frac{i}{2yp_-}\frac{Z_N M_N}{p_-}\,\overline{\Gamma}^\lambda \frac{\partial}{\partial p_+}\int \frac{d^4q}{(2\pi)^4} \delta\left(y-\frac{q_-}{p_-}\right) S(p-q)\tau_a(q)\, G^{B1\ldots B6}_{\lambda\sigma}\,\Gamma^\sigma,$$
$$\Delta f^{B7}_{D_a/N}(y) = \frac{i}{2yp_-}\frac{Z_N\, M_N}{p_-}\,\overline{\Gamma}^\lambda \int \frac{d^4q}{(2\pi)^4}\,\delta\left(y-\frac{q_-}{p_-}\right) S(p-q)\tau_a(q)\, G^{B7}_{\lambda\sigma}\,\Gamma^\sigma. \quad \text{(D.148)}$$

Determining $\Delta_T f^{B1}_{D_a/N}(y)$

$$\Delta f^{B1}_{D_a/N}(y) = -\frac{i}{2yp_-}\frac{Z_N M_N}{p_-}\,\overline{\Gamma}^\lambda \frac{\partial}{\partial p_+}\int \frac{d^4q}{(2\pi)^4} \delta\left(y-\frac{q_-}{p_-}\right) S(p-q)\tau_a(q)\, q_1 q_-\,[g_{2\lambda}g_{1\sigma} - g_{1\lambda}g_{2\sigma}]\,\Gamma^\sigma,$$
$$= -\frac{i}{2yp_-}\frac{Z_N M_N}{p_-}\,yp_-\,\overline{\Gamma}^\lambda \frac{\partial}{\partial p_+}\int \frac{d^4q}{(2\pi)^4} \delta\left(y-\frac{q_-}{p_-}\right) S(p-q)\tau_a(q)\, q_1\,[g_{2\lambda}g_{1\sigma} - g_{1\lambda}g_{2\sigma}]\,\Gamma^\sigma. \quad \text{(D.149)}$$

Let

$$\begin{aligned} I^{B1} &= \frac{\partial}{\partial p_+} \int \frac{d^4q}{(2\pi)^4}\, \delta\!\left(y - \frac{q_-}{p_-}\right) S(p-q)\tau_a(q)\, q_1, \\ &= \frac{\partial}{\partial p_+} \int \frac{d^4q}{(2\pi)^4} \delta\!\left(y - \frac{q_-}{p_-}\right) \frac{\not p - \not q + M}{q^2 + p^2 - 2p\cdot q - M^2 + i\varepsilon} \\ &\qquad\qquad \left[4i\, G_a - \frac{i\, g_a}{q^2 - M_a^2 + i\varepsilon}\right] q_1, \\ &\equiv I_1^{B1} + I_2^{B1}. \end{aligned} \tag{D.150}$$

The p_+ dependence of I_1^{B1} can be removed via the shift $q \to q + p$ hence

$$I_1^{B1} = 0. \tag{D.151}$$

Taking the moments of I_2^{B1} and introducing Feynman parametrization gives

$$\begin{aligned} \mathcal{A}_{2n}^{B1} &= -i\, g_a \frac{\partial}{\partial p_+} \int_0^1 d\alpha \int \frac{d^4q}{(2\pi)^4} \left(\frac{q_- + \alpha p_-}{p_-}\right)^{n-1} \\ &\qquad \frac{\left[(1-\alpha)\not p - \not q + M\right] q_1}{\left[q^2 - (\alpha^2 - \alpha)\, p^2 - (1-\alpha)\, M_a^2 - \alpha M^2 + i\varepsilon\right]^2}, \\ &= -i\, g_a \frac{\partial}{\partial p_+} \int_0^1 d\alpha\, \alpha^{n-1} \\ &\qquad \int \frac{d^4q}{(2\pi)^4} \frac{-q_1^2\, \gamma^1}{\left[q^2 - (\alpha^2 - \alpha)\, p^2 - (1-\alpha)\, M_a^2 - \alpha M^2 + i\varepsilon\right]^2}. \end{aligned} \tag{D.152}$$

Using the definition of the moments, Wick rotating (noting $q_1^2 \to \frac{1}{4} q_E^2$), introducing 4-d polars and the proper-time regularization gives

$$\begin{aligned} I_2^{B1} &= \frac{g_a}{16\pi^2} \frac{\partial}{\partial p_+} \int d\tau\, \tau \int_0^\infty dq_E^2\, q_E^2 \left(-\tfrac{1}{4} q_E^2\right) \gamma^1\; e^{-\tau\left[q_E^2 + (y^2 - y)p^2 + (1-y)M_a^2 + \alpha M^2\right]}, \\ &= -\frac{g_a}{32\pi^2} \frac{\partial}{\partial p_+} \int d\tau\, \frac{1}{\tau^2}\, \gamma^1\; e^{-\tau\left[(y^2-y)p^2 + (1-y)M_a^2 + \alpha M^2\right]}, \\ &= \frac{g_a}{16\pi^2}\, (y^2 - y)\, p_- \int d\tau\, \frac{1}{\tau^2} \gamma^1\; e^{-\tau\left[(y^2-y)p^2 + (1-y)M_a^2 + \alpha M^2\right]}. \end{aligned} \tag{D.153}$$

Therefore we need the matrix element

$$\overline{\Gamma}_2\, \gamma^1\, \Gamma_1 - \overline{\Gamma}_1\, \gamma^1\, \Gamma_2 = 2\alpha_1\alpha_2 \frac{p_1}{M_N}\, \overline{u}_N \gamma^1 \gamma^2 u_N = -2i\alpha_2\alpha_3 \frac{p_1^2}{M_N^2}. \tag{D.154}$$

Hence

$$\begin{aligned} \Delta f_{D_a/N}^{B1}(y) &= -\frac{i}{2} \frac{Z_N M_N}{p_-} \frac{g_a}{16\pi^2} \left(-2i\alpha_2\alpha_3 \frac{p_1^2}{M_N^2}\right) (y^2 - y)\, p_- \\ &\qquad \int d\tau\, \frac{1}{\tau}\; e^{-\tau\left[(y^2-y)p^2 + (1-y)M_a^2 + \alpha M^2\right]}, \end{aligned} \tag{D.155}$$

which simplifies to

$$\Delta f^{B1}_{D_a/N}(y) = p_1^2 \, \frac{g_a \, Z_N}{16\pi^2 \, M_N} \alpha_2 \alpha_3 \, y \, (1-y) \int d\tau \, \frac{1}{\tau} \, e^{-\tau\left[(y^2-y)p^2+(1-y)M_a^2+\alpha M^2\right]}. \tag{D.156}$$

Determining $\Delta_T f^{B2}_{D_a/N}(y)$

$$\Delta f^{B2}_{D_a/N}(y) = -\frac{i}{2yp_-} \frac{Z_N M_N}{p_-} \, \overline{\Gamma}^\lambda \frac{\partial}{\partial p_+} \int \frac{d^4q}{(2\pi)^4} \delta\left(y - \frac{q_-}{p_-}\right) S(p-q)\tau_a(q) \, q_1^2 \left[g_{-\lambda} g_{2\sigma} - g_{2\lambda} g_{-\sigma}\right] \Gamma^\sigma. \tag{D.157}$$

Let

$$\begin{aligned} I^{B2} &= \frac{\partial}{\partial p_+} \int \frac{d^4q}{(2\pi)^4} \delta\left(y - \frac{q_-}{p_-}\right) S(p-q)\tau_a(q) \, q_1^2, \\ &= \frac{\partial}{\partial p_+} \int \frac{d^4q}{(2\pi)^4} \delta\left(y - \frac{q_-}{p_-}\right) \frac{\not p - \not q + M}{q^2 + p^2 - 2p\cdot q - M^2 + i\varepsilon} \\ &\qquad \left[4i \, G_a - \frac{i \, g_a}{q^2 - M_a^2 + i\varepsilon}\right] q_1^2, \\ &\equiv I_1^{B2} + I_2^{B2}. \end{aligned} \tag{D.158}$$

The p_+ dependence of I_1^{B2} can be removed via the shift $q \longrightarrow q + p$ hence

$$I_1^{B2} = 0. \tag{D.159}$$

Taking the moments of I_2^{B2} and introducing Feynman parametrization gives

$$\begin{aligned} \mathcal{A}^{B2}_{2n} &= -i \, g_a \frac{\partial}{\partial p_+} \int_0^1 d\alpha \int \frac{d^4q}{(2\pi)^4} \left(\frac{q_- + \alpha p_-}{p_-}\right)^{n-1} \\ &\qquad \frac{\left[(1-\alpha)\not p - \not q + M\right] q_1^2}{\left[q^2 - (\alpha^2-\alpha)\,p^2 - (1-\alpha)\,M_a^2 - \alpha M^2 + i\varepsilon\right]^2}, \\ &= -i \, g_a \frac{\partial}{\partial p_+} \int_0^1 d\alpha \\ &\qquad \int \frac{d^4q}{(2\pi)^4} \frac{\alpha^{n-1}\left[(1-\alpha)\not p + M\right] q_1^2 - \frac{1}{p_-} q_1^2 \, q_- q_+ \gamma^+ \, \frac{d}{d\alpha} \alpha^{n-1}}{\left[q^2 - (\alpha^2-\alpha)\,p^2 - (1-\alpha)\,M_a^2 - \alpha M^2 + i\varepsilon\right]^2}. \end{aligned} \tag{D.160}$$

Integrating by parts in $d\alpha$, noting the surface term has no p_+ dependence and using the definition of the moments we obtain

$$I_2^{B2} = -i \, g_a \frac{\partial}{\partial p_+} \int \frac{d^4q}{(2\pi)^4} \frac{\left[(1-y)\not p + M\right] q_1^2 + \frac{1}{p_-} q_1^2 \, q_- q_+ \gamma^+ \, \frac{d}{dy}}{\left[q^2 - (y^2-y)\,p^2 - (1-y)\,M_a^2 - yM^2 + i\varepsilon\right]^2}. \tag{D.161}$$

Wick rotating, noting $q_1^2 \to \frac{1}{4}q_E^2$ and $q_1^2 q_- q_+ \to -\frac{1}{24}q_E^4$, introducing 4-d polars and the proper-time regularization gives

$$
\begin{aligned}
I_2^{B2} &= \frac{g_a}{64\pi^2}\frac{\partial}{\partial p_+}\int d\tau\,\tau \int_0^\infty dq_E^2\, q_E^2 \\
&\quad \left\{\left[(1-y)\not{p}+M\right] q_E^2 - \frac{\gamma^+}{6p_-}q_E^4\,\frac{d}{dy}\right\} e^{-\tau\left[q_E^2+\left(y^2-y\right)p^2+(1-y)M_a^2+yM^2\right]}, \\
&= \frac{g_a}{32\pi^2}\int d\tau\,\frac{1}{\tau^2}\left\{\gamma^+\left[y-\tau\left(y^2-y\right)\left[(2y-1)p^2-M_a^2+M^2\right]\right]\right. \\
&\quad \left. - 2\tau p_-\left(y^2-y\right)\left[(1-y)\not{p}+M\right]\right\} e^{-\tau\left[\left(y^2-y\right)p^2+(1-y)M_a^2+yM^2\right]}.
\end{aligned}
\tag{D.162}
$$

The required matrix elements are the same as $\Delta_T f_{D_a/N}(y)$ and are

$$\overline{\Gamma}_-\Gamma_2 - \overline{\Gamma}_2\Gamma_- = -2i\,\alpha_3^2\,\frac{p^+}{M_N}, \tag{D.163}$$

$$\overline{\Gamma}_-\gamma^+\Gamma_2 - \overline{\Gamma}_2\gamma^+\Gamma_- = -2i\alpha_2\alpha_3\frac{p^+p^+}{M_N^2}, \tag{D.164}$$

$$\overline{\Gamma}_-\not{p}\,\Gamma_2 - \overline{\Gamma}_2\not{p}\,\Gamma_- = -2i\,\alpha_3^2\,p^+. \tag{D.165}$$

Therefore

$$
\begin{aligned}
\Delta f^{B2}_{D_a/N}(y) &= -\frac{g_a\,Z_N}{32\pi^2}\int d\tau\,\frac{1}{\tau^2}\,e^{-\tau\left[\left(y^2-y\right)p^2+(1-y)M_a^2+yM^2\right]} \\
&\quad \left\{\frac{\alpha_2\alpha_3}{M_N}\left[1+\tau\,(1-y)\left[(2y-1)p^2-M_a^2+M^2\right]\right]\right. \\
&\quad \left. + 2\tau\alpha_3^2\,(1-y)\left[(1-y)M_N+M\right]\right\}.
\end{aligned}
\tag{D.166}
$$

Determining $\Delta_T f^{B3}_{D_a/N}(y)$

$$
\begin{aligned}
\Delta f^{B3}_{D_a/N}(y) &= -\frac{i}{2yp_-}\frac{Z_N M_N}{p_-}\,\overline{\Gamma}^\lambda\frac{\partial}{\partial p_+}\int\frac{d^4q}{(2\pi)^4}\,\delta\!\left(y-\frac{q_-}{p_-}\right) \\
&\quad S(p-q)\tau_a(q)\,q_1q_2\left[g_{1\lambda}g_{-\sigma}-g_{-\lambda}g_{1\sigma}\right]\Gamma^\sigma.
\end{aligned}
\tag{D.167}
$$

Let

$$I^{B3} = \frac{\partial}{\partial p_+} \int \frac{d^4q}{(2\pi)^4}\, \delta\Big(y - \frac{q_-}{p_-}\Big)\, S(p-q)\tau_a(q)\, q_1 q_2,$$
$$= \frac{\partial}{\partial p_+} \int \frac{d^4q}{(2\pi)^4} \delta\Big(y - \frac{q_-}{p_-}\Big)\, \frac{\not p - \not q + M}{q^2 + p^2 - 2p\cdot q - M^2 + i\varepsilon}$$
$$\left[4i\, G_a - \frac{i\, g_a}{q^2 - M_a^2 + i\varepsilon}\right] q_1 q_2,$$
$$\equiv I_1^{B3} + I_2^{B3}. \tag{D.168}$$

The p_+ dependence of I_1^{B3} can be removed via the shift $q \longrightarrow q + p$ hence

$$I_1^{B3} = 0. \tag{D.169}$$

Taking the moments of I_2^{B2} and introducing Feynman parametrization gives

$$\mathcal{A}_{2n}^{B2} = -i\, g_a \frac{\partial}{\partial p_+} \int_0^1 d\alpha \int \frac{d^4q}{(2\pi)^4} \left(\frac{q_- + \alpha p_-}{p_-}\right)^{n-1}$$
$$\frac{\left[(1-\alpha)\not p - \not q + M\right] q_1 q_2}{\left[q^2 - (\alpha^2 - \alpha)\, p^2 - (1-\alpha)\, M_a^2 - \alpha M^2 + i\varepsilon\right]^2}. \tag{D.170}$$

Since $g^{12} = g^{-1} = g^{-2} = 0$ we have

$$I_2^{B3} = 0, \tag{D.171}$$

and hence

$$\Delta f_{D_a/N}^{B3}(y) = 0. \tag{D.172}$$

Determining $\Delta_T f_{D_a/N}^{B4}(y)$

$$\Delta f_{D_a/N}^{B4}(y) = -\frac{i}{2yp_-} \frac{Z_N M_N}{p_-}\, \overline{\Gamma}^\lambda \frac{\partial}{\partial p_+} \int \frac{d^4q}{(2\pi)^4}\, \delta\Big(y - \frac{q_-}{p_-}\Big)$$
$$S(p-q)\tau_a(q)\, q_-^2\, \left[g_{+\lambda} g_{2\sigma} - g_{2\lambda} g_{+\sigma}\right] \Gamma^\sigma. \tag{D.173}$$

From the δ-function we have $q_- \longrightarrow yp_-$, therefore

$$\Delta f_{D_a/N}^{B4}(y) = -\frac{i}{2} Z_N M_N\, y\, \overline{\Gamma}^\lambda \frac{\partial}{\partial p_+} \int \frac{d^4q}{(2\pi)^4}\, \delta\Big(y - \frac{q_-}{p_-}\Big)$$
$$S(p-q)\tau_a(q)\, \left[g_{+\lambda} g_{2\sigma} - g_{2\lambda} g_{+\sigma}\right] \Gamma^\sigma. \tag{D.174}$$

Let

$$
\begin{aligned}
I^{B4} &= \frac{\partial}{\partial p_+} \int \frac{d^4 q}{(2\pi)^4}\, \delta\left(y - \frac{q_-}{p_-}\right) S(p-q)\tau_a(q), \\
&= \frac{\partial}{\partial p_+} \int \frac{d^4 q}{(2\pi)^4} \delta\left(y - \frac{q_-}{p_-}\right) \frac{\not p - \not q + M}{q^2 + p^2 - 2p\cdot q - M^2 + i\varepsilon} \\
&\qquad\qquad \left[4i\, G_a - \frac{i\, g_a}{q^2 - M_a^2 + i\varepsilon}\right], \\
&\equiv I_1^{B4} + I_2^{B4}.
\end{aligned} \tag{D.175}
$$

The p_+ dependence of I_1^{B4} can be removed via the shift $q \to q + p$ hence

$$
I_1^{B4} = 0. \tag{D.176}
$$

Taking the moments of I_2^{B4} and introducing Feynman parametrization gives

$$
\begin{aligned}
\mathcal{A}_{2n}^{B4} = -i\, g_a \frac{\partial}{\partial p_+} \int_0^1 d\alpha \int \frac{d^4 q}{(2\pi)^4} \left(\frac{q_- + \alpha p_-}{p_-}\right)^{n-1} \\
\frac{\left[(1-\alpha)\not p - \not q + M\right]}{\left[q^2 - (\alpha^2 - \alpha)\, p^2 - (1-\alpha)\, M_a^2 - \alpha M^2 + i\varepsilon\right]^2}.
\end{aligned} \tag{D.177}
$$

From the same calculation in $\Delta_T f^A_{D_a/N}(y)$ we have

$$
\begin{aligned}
I_2^{B4} = \frac{g_a}{16\pi^2} \int d\tau\, \frac{1}{\tau} \Big\{ \gamma^+ \Big[y + \tau\, y\,(1-y)\, \left[(2y-1)\, p^2 - M_a^2 + M^2\right] \Big] \\
+ 2p_- \tau\, y\,(1-y)\, \left[(1-y)\not p + M\right] \Big\} e^{-\tau\left[(y^2-y)p^2 + (1-y)M_a^2 + yM^2\right]}.
\end{aligned} \tag{D.178}
$$

Therefore we need the matrix elements

$$
\begin{aligned}
\overline{\Gamma}_+ \Gamma_2 - \overline{\Gamma}_2 \Gamma_+ &= \overline{u}_N \left\{\alpha_3^2 \left(\gamma_+ \gamma_2 - \gamma_2 \gamma_+\right)\right\} u_N \\
&= 2\alpha_3^2 \overline{u}_N \gamma^2 \gamma^- u_N = i\, \alpha_3^2\, \frac{M_N^2 - p_1^2 + p_2^2}{M_N\, p^+} \overset{\vec p_\perp = 0}{=} i\, \alpha_3^2\, \frac{M_N}{p^+}.
\end{aligned} \tag{D.179}
$$

$$
\begin{aligned}
\overline{\Gamma}_+ \gamma^+ \Gamma_2 - \overline{\Gamma}_2 \gamma^+ \Gamma_+ &= \frac{2}{M_N} \alpha_2 \alpha_3\, \overline{u}_N \left(p_+ \gamma^2 \gamma^+\right) u_N \\
&\qquad + 2\alpha_3^2\, \overline{u}_N \left(\gamma^2 - \gamma^2 \gamma^+ \gamma^-\right) u_N, \\
&= i\alpha_3\, (2\alpha_3 - \alpha_2)\,.
\end{aligned} \tag{D.180}
$$

$$
\overline{\Gamma}_+ \not p \Gamma_2 - \overline{\Gamma}_2 \not p \Gamma_+ = i\, \alpha_3^2\, \frac{M_N^2}{p^+}. \tag{D.181}
$$

Therefore

$$I_2^{B4} = i\frac{g_a\, y}{16\pi^2} \int d\tau\, e^{-\tau\left[(y^2-y)p^2+(1-y)M_a^2+yM^2\right]}$$
$$\Big\{2\alpha_3^2\Big[\frac{1}{\tau} + (1-y)\left[(2y-1)\,p^2 - M_a^2 + M^2 + (1-y)M_N^2 + M\,M_N\right]\Big]$$
$$- \alpha_2\alpha_3\Big[\frac{1}{\tau} + (1-y)\left[(2y-1)\,p^2 - M_a^2 + M^2\right]\Big]\Big\}. \quad \text{(D.182)}$$

Therefore

$$\Delta f_{D_a/N}^{B4}(y) = \frac{g_a\, Z_N\, M_N}{32\pi^2}\, y^2 \int d\tau\, e^{-\tau\left[(y^2-y)p^2+(1-y)M_a^2+yM^2\right]}$$
$$\Big\{2\alpha_3^2\Big[\frac{1}{\tau} + (1-y)\left[y\,p^2 + M\,M_N + M^2 - M_a^2\right]\Big]$$
$$- \alpha_2\alpha_3\Big[\frac{1}{\tau} + (1-y)\left[(2y-1)\,p^2 - M_a^2 + M^2\right]\Big]\Big\}. \quad \text{(D.183)}$$

Determining $\Delta_T f_{D_a/N}^{B5}(y)$

$$\Delta f_{D_a/N}^{B5}(y) = -\frac{i}{2yp_-}\frac{Z_N M_N}{p_-}\,\overline{\Gamma}^\lambda \frac{\partial}{\partial p_+} \int \frac{d^4q}{(2\pi)^4}\,\delta\Big(y - \frac{q_-}{p_-}\Big)$$
$$S(p-q)\tau_a(q)\, q_- q_+ \left[g_{2\lambda}g_{-\sigma} - g_{-\lambda}g_{2\sigma}\right]\Gamma^\sigma. \quad \text{(D.184)}$$

From the δ-function we have $q_- \longrightarrow yp_-$, therefore

$$\Delta f_{D_a/N}^{B5}(y) = -\frac{i}{2}\frac{Z_N M_N}{p_-}\,\overline{\Gamma}^\lambda \frac{\partial}{\partial p_+} \int \frac{d^4q}{(2\pi)^4}\,\delta\Big(y - \frac{q_-}{p_-}\Big)$$
$$S(p-q)\tau_a(q)\, q_+ \left[g_{2\lambda}g_{-\sigma} - g_{-\lambda}g_{2\sigma}\right]\Gamma^\sigma. \quad \text{(D.185)}$$

Let

$$\begin{aligned} I^{B5} &= \frac{\partial}{\partial p_+} \int \frac{d^4q}{(2\pi)^4}\,\delta\Big(y - \frac{q_-}{p_-}\Big)\, S(p-q)\tau_a(q), \\ &= \frac{\partial}{\partial p_+} \int \frac{d^4q}{(2\pi)^4}\delta\Big(y - \frac{q_-}{p_-}\Big)\, \frac{\not p - \not q + M}{q^2 + p^2 - 2p\cdot q - M^2 + i\varepsilon} \\ &\qquad \left[4i\,G_a - \frac{i\,g_a}{q^2 - M_a^2 + i\varepsilon}\right] q_+, \\ &\equiv I_1^{B5} + I_2^{B5}. \end{aligned} \quad \text{(D.186)}$$

Performing the shift $q \rightarrow q + p$ and taking the moments of I_1^{B5} gives

$$\begin{aligned} \mathcal{A}_{1n}^{B5} &= 4i\,G_a \frac{\partial}{\partial p_+} \int \frac{d^4q}{(2\pi)^4} \left(\frac{q_- + p_-}{p_-}\right)^{n-1} \frac{(M - \not q)\,(q_+ + p_+)}{q^2 - M^2 + i\varepsilon}, \\ &= 4i\,G_a \int \frac{d^4q}{(2\pi)^4} \left(\frac{q_- + p_-}{p_-}\right)^{n-1} \frac{(M - \not q)}{q^2 - M^2 + i\varepsilon}. \end{aligned} \quad \text{(D.187)}$$

Using

$$\left(\frac{q_- + p_-}{p_-}\right)^{n-1} = 1 + (n-1)\frac{q_-}{p_-} + \ldots, \tag{D.188}$$

and ignoring terms odd in k and using $g^{--} = g^{-1} = g^{2-} = 0$ we obtain

$$\mathcal{A}_{1n}^{B5} = 4i\, G_a \int \frac{d^4q}{(2\pi)^4} \frac{M - (n-1)\frac{\gamma^+}{p_-} q_- q_+}{q^2 - M^2 + i\varepsilon}. \tag{D.189}$$

Wick rotating, introducing 4-d polars and the proper-time regularization gives

$$\begin{aligned}\mathcal{A}_{1n}^{B5} &= -\frac{G_a}{4\pi^2} \int d\tau \int_0^\infty dq_E^2\, q_E^2 \left[M + (n-1)\frac{\gamma^+}{4p_-} q_E^2\right] e^{-\tau\left[q_E^2 + M^2\right]}, \\ &= -\frac{G_a}{4\pi^2} \int d\tau\, \frac{1}{\tau^2} \left[M + (n-1)\, \frac{\gamma^+}{2\tau\, p_-}\right] e^{-\tau M^2}. \end{aligned} \tag{D.190}$$

The distribution can be obtained from the moments via the formula

$$f(x) = \frac{1}{2\pi\, i} \lim_{\varepsilon \to 0^+} \Big[F(x - i\varepsilon) - F(x + i\varepsilon)\Big], \tag{D.191}$$

where

$$F(x) = \sum_{n=1}^{\infty} \frac{\mathcal{A}_n}{x^n}. \tag{D.192}$$

Therefore using the results

$$\sum_{n=1}^{\infty} \frac{1}{x^n} = \frac{1}{x-1}, \qquad \text{and} \qquad \sum_{n=1}^{\infty} \frac{n-1}{x^n} = \frac{1}{(x-1)^2}, \tag{D.193}$$

we have

$$F_{1n}^{B5}(y) = -\frac{G_a}{4\pi^2} \int d\tau\, \frac{1}{\tau^2} \left[\frac{M}{y-1} + \frac{1}{(y-1)^2} \frac{\gamma^+}{2\tau\, p_-}\right] e^{-\tau M^2}. \tag{D.194}$$

Now

$$\frac{1}{2\pi\, i} \lim_{\varepsilon \to 0^+} \left[\frac{1}{y - 1 - i\varepsilon} - \frac{1}{y - 1 + i\varepsilon}\right] = \delta(y-1), \tag{D.195}$$

$$\begin{aligned}&\frac{1}{2\pi\, i} \lim_{\varepsilon \to 0^+} \left[\frac{1}{(y - 1 - i\varepsilon)^2} - \frac{1}{(y - 1 + i\varepsilon)^2}\right] \\ &\quad = -\frac{1}{2\pi\, i} \frac{d}{dy} \lim_{\varepsilon \to 0^+} \left[\frac{1}{y - 1 - i\varepsilon} - \frac{1}{y - 1 + i\varepsilon}\right] = -\frac{d}{dy}\, \delta(y-1). \end{aligned} \tag{D.196}$$

If we also use the matrix element results from $\Delta_T f_{D_a/N}^{B2}(y)$, that is

$$\overline{\Gamma}_2 \Gamma_- - \overline{\Gamma}_- \Gamma_2 = 2i\, \alpha_3^2\, \frac{p^+}{M_N}, \tag{D.197}$$

$$\overline{\Gamma}_2 \gamma^+ \Gamma_- - \overline{\Gamma}_- \gamma^+ \Gamma_2 = 2i\alpha_2\alpha_3 \frac{p^+ p^+}{M_N^2}, \tag{D.198}$$

we obtain

$$I_1^{B5} = -i\frac{G_a}{4\pi^2}\frac{p_-}{M_N}\int d\tau\,\frac{1}{\tau^2}\left[2\,M\,\alpha_3^2\,\delta(y-1) - \frac{\alpha_2\alpha_3}{\tau\,M_N}\frac{d}{dy}\,\delta(y-1)\right]e^{-\tau\,M^2}. \tag{D.199}$$

We now consider I_2^{B5}, taking the moments and introducing Feynman parametrization gives

$$\mathcal{A}_{2n}^{B5} = -ig_a\frac{\partial}{\partial p_+}\int_0^1 d\alpha\int\frac{d^4q}{(2\pi)^4}\left(\frac{q_-+\alpha p_-}{p_-}\right)^{n-1} \frac{\left[(1-\alpha)\not{p} - \not{q} + M\right]\left[q_+ + \alpha p_+\right]}{\left[q^2-(\alpha^2-\alpha)\,p^2-(1-\alpha)\,M_a^2-\alpha M^2+i\varepsilon\right]^2}. \tag{D.200}$$

The numerator of I_2^{B5} becomes

$$\begin{aligned}
\mathcal{N}_{2n}^{B5} &= \alpha^{n-1}\Big\{q_+\left[-q_-\gamma^-\right] + \alpha p_+\left[(1-\alpha)\not{p}+M\right]\Big\} \\
&\quad + \frac{q_-}{p_-}\Big\{q_+\left[(1-\alpha)\not{p}+M\right] + \alpha p_+\left[-q_+\gamma^+\right]\Big\}\frac{d}{d\alpha}\alpha^{n-1} \\
&\quad + \frac{1}{2}\frac{q_-^2}{p_-^2}\left(-\gamma^+ q_+ q_+\right)\frac{d^2}{d\alpha^2}\alpha^{n-1}, \\
&= \alpha^{n-1}\Big\{\alpha p_+\left[(1-\alpha)\not{p}+M\right] - q_+q_-\gamma^-\Big\} + \alpha^{n-1}\frac{q_-q_+}{p_-}\Big\{\not{p}+p_+\gamma^+\Big\} \\
&\quad - \alpha^{n-1}\frac{q_-q_+}{p_-}\Big\{(1-\alpha)\not{p}+M-\alpha p_+\gamma^+\Big\}\frac{d}{d\alpha} + \mathcal{N}_{2n}^{B5-\text{surface:1}} \\
&\quad + \alpha^{n-1}\frac{1}{2}\frac{q_-^2}{p_-^2}\left(-\gamma^+ q_+ q_+\right)\frac{d^2}{d\alpha^2} + \mathcal{N}_{2n}^{B5-\text{surface:2}}.
\end{aligned} \tag{D.201}$$

We first evaluate the surface term, which is

$$\begin{aligned}
&\mathcal{A}_{2n}^{B5-\text{surface:1}} \\
&= -ig_a\frac{\partial}{\partial p_+}\int\frac{d^4q}{(2\pi)^4}\frac{\frac{q_-q_+}{p_-}\left[(1-\alpha)\not{p}+M-\alpha p_+\gamma^+\right]\alpha^{n-1}}{\left[q^2-(\alpha^2-\alpha)\,p^2-(1-\alpha)\,M_a^2-\alpha M^2+i\varepsilon\right]^2}\Bigg|_{\alpha=0}^{1} \\
&= -ig_a\frac{\partial}{\partial p_+}\int\frac{d^4q}{(2\pi)^4}\frac{q_-q_+}{p_-}\left\{\frac{M-p_+\gamma^+}{\left[q^2-M^2+i\varepsilon\right]^2} - \lim_{\varepsilon\to0^+}\frac{(\not{p}+M)\,\varepsilon^{n-1}}{\left[q^2-M_a^2+i\varepsilon\right]^2}\right\}, \\
&= \frac{g_a}{32\pi^2}\frac{\gamma^+}{p_-}\int d\tau\,\frac{1}{\tau^2}\left[e^{-\tau\,M^2} + \lim_{\varepsilon\to0^+}\varepsilon^{n-1}e^{-\tau\,M_a^2}\right].
\end{aligned} \tag{D.202}$$

Using earlier results we have

$$F_{2n}^{B5-\text{surface:1}} = \frac{g_a}{32\pi^2}\frac{\gamma^+}{p_-}\int d\tau\,\frac{1}{\tau^2}\left[\frac{1}{y-1}e^{-\tau\,M^2} + \frac{1}{y}e^{-\tau\,M_a^2}\right]. \tag{D.203}$$

Therefore

$$I_{2n}^{B5-\text{surface:1}} = i\,\frac{g_a\,\alpha_2\alpha_3}{16\pi^2}\,\frac{p_-}{M_N^2}\int d\tau\;\frac{1}{\tau^2}\left[\delta(y-1)e^{-\tau M^2}+\delta(y)\,e^{-\tau M_a^2}\right]. \quad \text{(D.204)}$$

We now evaluate the second surface term, we have

$$\mathcal{A}_{2n}^{B5-\text{surface:2}} = -ig_a\,\frac{\gamma^+}{2\,p_-^2}\,\frac{\partial}{\partial p_+}$$
$$\int\frac{d^4q}{(2\pi)^4}\frac{q_-q_-q_+q_+\,\alpha^{n-1}\,\frac{d}{d\alpha}}{\left[q^2-(\alpha^2-\alpha)\,p^2-(1-\alpha)\,M_a^2-\alpha M^2+i\varepsilon\right]^2}\Bigg|_{\alpha=0}^{1}. \quad \text{(D.205)}$$

Using

$$q^\mu q^\nu q^\rho q^\sigma \longrightarrow \frac{1}{24}\,q^4\left(g^{\mu\nu}g^{\rho\sigma}+g^{\mu\rho}g^{\nu\sigma}+g^{\mu\sigma}g^{\nu\rho}\right)$$
$$\Longrightarrow\quad q_-q_-q_+q_+ \longrightarrow \frac{1}{24}\,q^4\left(g^{--}g^{++}+g^{-+}g^{-+}+g^{-+}g^{-+}\right)=\frac{1}{12}\,q^4, \quad \text{(D.206)}$$

we have

$$\mathcal{A}_{2n}^{B5-\text{surface:2}} = -ig_a\,\frac{\gamma^+}{24\,p_-^2}\,\frac{\partial}{\partial p_+}$$
$$\int\frac{d^4q}{(2\pi)^4}\frac{q^4\,2\left[(2\alpha-1)p^2-M_a^2+M^2\right]\alpha^{n-1}}{\left[q^2-(\alpha^2-\alpha)\,p^2-(1-\alpha)\,M_a^2-\alpha M^2+i\varepsilon\right]^3}\Bigg|_{\alpha=0}^{1},$$
$$= -ig_a\,\frac{\gamma^+}{6\,p_-}\int\frac{d^4q}{(2\pi)^4}\left\{\frac{q^4}{\left[q^2-M^2+i\varepsilon\right]^3}+\lim_{\varepsilon\to0^+}\frac{q^4\varepsilon^{n-1}}{\left[q^2-M_a^2+i\varepsilon\right]^3}\right\}. \quad \text{(D.207)}$$

Wicking rotating and introducing the proper-time regularization gives

$$\mathcal{A}_{2n}^{B5-\text{surface:2}} = -g_a\,\frac{\gamma^+}{32\pi^2\,p_-}\int d\tau\;\frac{1}{\tau^2}\left[e^{-\tau M^2}+\lim_{\varepsilon\to0^+}\varepsilon^{n-1}e^{-\tau M_a^2}\right]. \quad \text{(D.208)}$$

From $\mathcal{A}_{2n}^{B5-\text{surface:1}}$ we have

$$I_{2n}^{B5-\text{surface:2}} = -i\,\frac{g_a\,\alpha_2\alpha_3}{16\pi^2}\,\frac{p_-}{M_N^2}\int d\tau\;\frac{1}{\tau^2}\left[\delta(y-1)e^{-\tau M^2}+\delta(y)\,e^{-\tau M_a^2}\right], \quad \text{(D.209)}$$

and hence the two surface terms cancel. We now evaluate the second last term of Eq. (D.201), we have

$$I_{2n}^{B5c} = ig_a\,\frac{\gamma^+}{2\,p_-^2}\,\frac{\partial}{\partial p_+}\int\frac{d^4q}{(2\pi)^4}\frac{q_-q_-q_+q_+\,\frac{d^2}{dy^2}}{\left[q^2-(y^2-y)\,p^2-(1-y)\,M_a^2-yM^2+i\varepsilon\right]^2}. \quad \text{(D.210)}$$

Using

$$q_- q_- q_+ q_+ \longrightarrow \frac{1}{12}\, q^4. \tag{D.211}$$

Therefore, Wick rotating and introducing the proper-time regularization gives

$$\begin{aligned}
I_{2n}^{B5c} &= -\frac{g_a}{384\pi^2}\frac{\gamma^+}{p_-^2}\frac{\partial}{\partial p_+}\int d\tau\,\tau\int_0^\infty dq_E^2 q_E^6 \frac{d^2}{dy^2} e^{-\tau\left[q_E^2+(y^2-y)p^2+(1-y)M_a^2+yM^2\right]}, \\
&= -\frac{g_a}{64\pi^2}\frac{\gamma^+}{p_-^2}\frac{\partial}{\partial p_+}\int d\tau\,\frac{1}{\tau^3}\frac{d^2}{dy^2} e^{-\tau\left[(y^2-y)p^2+(1-y)M_a^2+yM^2\right]}, \\
&= \frac{g_a}{32\pi^2}\frac{\gamma^+}{p_-}\int d\tau\,\frac{1}{\tau}\Bigg\{\left[\frac{2}{\tau}-2\,(2y-1)\left[(2y-1)\,p^2-M_a^2+M^2\right]\right] \\
&\qquad -\left(y^2-y\right)\left[2p^2-\tau\left[(2y-1)\,p^2-M_a^2+M^2\right]^2\right]\Bigg\}e^{-\tau A}.
\end{aligned} \tag{D.212}$$

Using the matrix element result

$$\overline{\Gamma}_2\gamma^+\Gamma_- - \overline{\Gamma}_-\gamma^+\Gamma_2 = 2i\alpha_2\alpha_3\frac{p^+p^+}{M_N^2}, \tag{D.213}$$

we obtain

$$\begin{aligned}
I_{2n}^{B5c} &= i\frac{g_a\,p_-}{16\pi^2\,M_N^2}\,\alpha_2\alpha_3\int d\tau\,\frac{1}{\tau}\Bigg\{\left[\frac{2}{\tau}-2\,(2y-1)\left[(2y-1)\,p^2-M_a^2+M^2\right]\right] \\
&\qquad -\left(y^2-y\right)\left[2p^2-\tau\left[(2y-1)\,p^2-M_a^2+M^2\right]^2\right]\Bigg\}e^{-\tau A}.
\end{aligned} \tag{D.214}$$

We now continue with the evaluation of the remainder of I_{2n}^{B5}, from the definition of the moments we have

$$\begin{aligned}
I_{2n}^{B5} &= -ig_a\frac{\partial}{\partial p_+}\int\frac{d^4q}{(2\pi)^4}\Bigg\{yp_+\left[(1-y)\not{p}+M\right] \\
&\quad +\frac{q_-q_+}{p_-}\left[\not{p}+p_+\gamma^+-p_-\gamma^-\right]-\frac{q_-q_+}{p_-}\left[(1-y)\not{p}+M-yp_+\gamma^+\right]\frac{d}{dy}\Bigg\} \\
&\qquad \left[q^2-\left(y^2-y\right)p^2-(1-y)\,M_a^2-yM^2+i\varepsilon\right]^{-2}.
\end{aligned} \tag{D.215}$$

Wick rotating and introducing 4-d polars gives

$$\begin{aligned}
I_{2n}^{B5} &= \frac{g_a}{16\pi^2}\frac{\partial}{\partial p_+}\int_0^\infty dq_E^2\, q_E^2 \\
&\quad \frac{yp_+\left[(1-y)\not{p}+M\right]-\frac{1}{2p_-}q_E^2\,p_+\gamma^+ + \frac{1}{4p_-}q_E^2\left[(1-y)\not{p}+M-yp_+\gamma^+\right]\frac{d}{dy}}{\left[q_E^2+(y^2-y)\,p^2+(1-y)\,M_a^2+yM^2\right]^2}.
\end{aligned} \tag{D.216}$$

Introducing the proper-time regularization gives

$$I_{2n}^{B5} = \frac{g_a}{16\pi^2}\frac{\partial}{\partial p_+}\int d\tau\,\tau\int_0^\infty dq_E^2\,q_E^2 e^{-\tau\left[q_E^2+\left(y^2-y\right)p^2+(1-y)M_a^2+yM^2\right]}$$
$$\Big\{yp_+\left[(1-y)\not p+M\right]-\frac{1}{2p_-}q_E^2\,p_+\gamma^+$$
$$-\frac{\tau}{4p_-}q_E^2\left[(1-y)\not p+M-yp_+\gamma^+\right]\left[(2y-1)\,p^2-M_a^2+M^2\right]\Big\}. \quad (D.217)$$

Integrating over q_E^2 gives

$$I_{2n}^{B5} = \frac{g_a}{16\pi^2}\frac{\partial}{\partial p_+}\int d\tau\,\frac{1}{\tau}\;e^{-\tau\left[\left(y^2-y\right)p^2+(1-y)M_a^2+yM^2\right]}$$
$$\Big\{yp_+\left[(1-y)\not p+M\right]-\frac{1}{\tau\,p_-}\,p_+\gamma^+$$
$$-\frac{\tau}{2\tau\,p_-}\left[(1-y)\not p+M-yp_+\gamma^+\right]\left[(2y-1)\,p^2-M_a^2+M^2\right]\Big\}. \quad (D.218)$$

Performing the partial derivative gives

$$I_{2n}^{B5} = \frac{g_a}{16\pi^2}\int d\tau\,\frac{1}{\tau}e^{-\tau\left[(y^2-y)p^2+(1-y)M_a^2+yM^2\right]}$$
$$\Big\{(1-y)\Big[1-\tau\,y\left[(y-1)\,p^2-M_a^2+M^2\right]\Big]\left[(1-y)\not p+M\right]$$
$$+\gamma^+\Big[y\,p_+(3y-2)-\frac{1}{\tau\,p_-}-\frac{1}{2p_-}\Big[1-2y+\tau\,y(y^2-y)p^2\Big]$$
$$\left[(2y-1)\,p^2-M_a^2+M^2\right]\Big]\Big\}. \quad (D.219)$$

Using the matrix element results

$$\overline{\Gamma}_2\Gamma_- - \overline{\Gamma}_-\Gamma_2 = 2i\,\alpha_3^2\,\frac{p^+}{M_N}, \quad (D.220)$$
$$\overline{\Gamma}_2\gamma^+\Gamma_- - \overline{\Gamma}_-\gamma^+\Gamma_2 = 2i\alpha_2\alpha_3\frac{p^+p^+}{M_N^2}, \quad (D.221)$$
$$\overline{\Gamma}_2\not p\Gamma_- - \overline{\Gamma}_-\not p\Gamma_2 = 2i\,\alpha_3^2\,p^+, \quad (D.222)$$

we obtain

$$I_{2n}^{B5} = i\frac{g_a}{8\pi^2}\frac{p^+}{M_N}\int d\tau\,\frac{1}{\tau}e^{-\tau\left[(y^2-y)p^2+(1-y)M_a^2+yM^2\right]}$$
$$\Bigg\{\alpha_3^2\,(1-y)\Big[1-\tau\,y\,\big[(y-1)\,p^2-M_a^2+M^2\big]\Big]\,[(1-y)M_N+M]$$
$$+\frac{\alpha_2\alpha_3}{M_N}\left[\frac{y}{2}\,(3y-2)M_N^2-\frac{1}{\tau}-\frac{1}{2}\Big[1-2y+\tau\,y(y^2-y)p^2\Big]\right.$$
$$\left.\big[(2y-1)\,p^2-M_a^2+M^2\big]\right]\Bigg\}. \tag{D.223}$$

Therefore the full result for $\Delta_T f_{D_a/N}^{B5}(y)$ is a sum of five terms, a contact term ($\propto\ 4iG_a$), two surface term which cancel and two regular terms, that is

$$\Delta_T f_{D_a/N}^{B5}(y) = \Delta_T f_1^{B5}(y) + \Delta_T f_{2s1}^{B5}(y) + \Delta_T f_{2s2}^{B5}(y) + \Delta_T f_{2a}^{B5}(y) + \Delta_T f_{2b}^{B5}(y), \tag{D.224}$$

where

$$\Delta_T f_1^{B5}(y) = -\frac{G_a\,Z_N}{8\pi^2}\int d\tau\,\frac{1}{\tau^2}$$
$$\left[2\,M\,\alpha_3^2\,\delta(y-1)-\frac{\alpha_2\alpha_3}{\tau\,M_N}\,\frac{d}{dy}\,\delta(y-1)\right]e^{-\tau\,M^2}, \tag{D.225}$$

$$\Delta_T f_{2s1}^{B5}(y) = \frac{g_a\,\alpha_2\alpha_3\,Z_N}{32\pi^2\,M_N}\int d\tau\;\frac{1}{\tau^2}\left[\delta(y-1)e^{-\tau\,M^2}+\delta(y)\,e^{-\tau\,M_a^2}\right], \tag{D.226}$$

$$\Delta_T f_{2s2}^{B5}(y) = -\frac{g_a\,\alpha_2\alpha_3\,Z_N}{32\pi^2\,M_N}\int d\tau\;\frac{1}{\tau^2}\left[\delta(y-1)e^{-\tau\,M^2}+\delta(y)\,e^{-\tau\,M_a^2}\right], \tag{D.227}$$

$$\Delta_T f_{2(a+b)}^{B5}(y) = \frac{g_a\,Z_N}{16\pi^2}\int d\tau\,\frac{1}{\tau}e^{-\tau\left[(y^2-y)p^2+(1-y)M_a^2+yM^2\right]}$$
$$\Bigg\{\alpha_3^2\,(1-y)\Big[1-\tau\,y\,\big[(y-1)\,p^2-M_a^2+M^2\big]\Big]\,[(1-y)M_N+M]$$
$$+\frac{\alpha_2\alpha_3}{2M_N}\Big(y^2M_N^2-\Big[2y-1+\tau\,y(1-y)\,\big[(y-1)\,p^2-M_a^2+M^2\big]\Big]$$
$$\big[(2y-1)\,p^2-M_a^2+M^2\big]\Big)\Bigg\}. \tag{D.228}$$

Determining $\Delta_T f_{D_a/N}^{B6}(y)$

$$\Delta f^{B6}_{D_a/N}(y) = -\frac{i}{2yp_-}\frac{Z_N M_N}{p_-}\,\overline{\Gamma}^{\lambda}\frac{\partial}{\partial p_+}\int\frac{d^4q}{(2\pi)^4}\,\delta\Big(y-\frac{q_-}{p_-}\Big)$$
$$S(p-q)\tau_a(q)\,q_-q_2\,[g_{-\lambda}g_{+\sigma}-g_{+\lambda}g_{-\sigma}]\,\Gamma^{\sigma}. \quad \text{(D.229)}$$

From the δ-function we have $q_- \to yp_-$, therefore

$$\Delta f^{B6}_{D_a/N}(y) = -\frac{i}{2}\frac{Z_N M_N}{p_-}\,\overline{\Gamma}^{\lambda}\frac{\partial}{\partial p_+}\int\frac{d^4q}{(2\pi)^4}\,\delta\Big(y-\frac{q_-}{p_-}\Big)$$
$$S(p-q)\tau_a(q)\,q_2\,[g_{-\lambda}g_{+\sigma}-g_{+\lambda}g_{-\sigma}]\,\Gamma^{\sigma}. \quad \text{(D.230)}$$

Let

$$\begin{aligned} I^{B6} &= \frac{\partial}{\partial p_+}\int\frac{d^4q}{(2\pi)^4}\,\delta\Big(y-\frac{q_-}{p_-}\Big)\,S(p-q)\tau_a(q)\,q_2,\\ &= \frac{\partial}{\partial p_+}\int\frac{d^4q}{(2\pi)^4}\delta\Big(y-\frac{q_-}{p_-}\Big)\,\frac{\not p-\not q+M}{q^2+p^2-2p\cdot q-M^2+i\varepsilon}\\ &\qquad\qquad\Big[4i\,G_a-\frac{i\,g_a}{q^2-M_a^2+i\varepsilon}\Big]\,q_2,\\ &\equiv I^{B6}_1+I^{B6}_2. \end{aligned} \quad \text{(D.231)}$$

The p_+ dependence of I^{B6}_1 can be removed via the shift $q \to q+p$ hence

$$I^{B6}_1 = 0. \quad \text{(D.232)}$$

Taking the moments of I^{B6}_2 and introducing Feynman parametrization gives

$$\mathcal{A}^{B6}_{2n} = -i\,g_a\,\frac{\partial}{\partial p_+}\int_0^1 d\alpha\int\frac{d^4q}{(2\pi)^4}\Big(\frac{q_-+\alpha p_-}{p_-}\Big)^{n-1}$$
$$\frac{[(1-\alpha)\not p-\not q+M]\,q_2}{[q^2-(\alpha^2-\alpha)\,p^2-(1-\alpha)\,M_a^2-\alpha M^2+i\varepsilon]^2}. \quad \text{(D.233)}$$

Ignoring terms odd in q and noting $g^{--}=g^{-1}=g^{-2}=0$ we obtain

$$\mathcal{A}^{B6}_{2n} = -i\,g_a\,\frac{\partial}{\partial p_+}\int_0^1 d\alpha\,\alpha^{n-1}$$
$$\int\frac{d^4q}{(2\pi)^4}\frac{-q_2^2\,\gamma^2}{[q^2-(\alpha^2-\alpha)\,p^2-(1-\alpha)\,M_a^2-\alpha M^2+i\varepsilon]^2}. \quad \text{(D.234)}$$

Using the definition of the moments, Wick rotating, introducing 4-d polar coordinates and the proper-time regularization gives

$$I_2^{B6} = \frac{g_a}{16\pi^2}\frac{\partial}{\partial p_+}\int d\tau\,\tau\int dq_E^2\,q_E^2\left(-\frac{1}{4}q_E^2\right)\gamma^2\,e^{-\tau\left[q_E^2+(y^2-y)p^2+(1-y)M_a^2+yM^2\right]},$$
$$= -\frac{g_a}{32\pi^2}\frac{\partial}{\partial p_+}\int d\tau\,\frac{1}{\tau^2}\gamma^2\,e^{-\tau\left[(y^2-y)p^2+(1-y)M_a^2+yM^2\right]},$$
$$= -\frac{g_a}{16\pi^2}\,y(1-y)p_-\gamma^2\int d\tau\,\frac{1}{\tau}\,e^{-\tau\left[(y^2-y)p^2+(1-y)M_a^2+yM^2\right]}. \qquad \text{(D.235)}$$

The matrix element we need is $\overline{\Gamma}_-\gamma^2\Gamma_+ - \overline{\Gamma}_+\gamma^2\Gamma_-$ and has the value

$$\overline{\Gamma}_-\gamma^2\Gamma_+ - \overline{\Gamma}_+\gamma^2\Gamma_- = \overline{u}_N\bigg\{\frac{2\alpha_2\alpha_3}{M_N}\left[p_+\gamma^+\gamma^2 - p_-\gamma^-\gamma^2\right]$$
$$-\alpha_3^2\left[\gamma^+\gamma^2\gamma^- - \gamma^-\gamma^2\gamma^+\right]\bigg\}u_N = 2i\,\alpha_3\,(\alpha_2-\alpha_3)\,. \qquad \text{(D.236)}$$

Therefore

$$\Delta f_{D_a/N}^{B6}(y) = \alpha_3\,(\alpha_3-\alpha_2)\,\frac{g_a\,Z_N\,M_N}{16\pi^2}\,y(1-y)$$
$$\int d\tau\,\frac{1}{\tau}\,e^{-\tau\left[(y^2-y)p^2+(1-y)M_a^2+yM^2\right]}. \qquad \text{(D.237)}$$

Determining $\Delta_T f_{D_a/N}^{B7}(y)$

$$\Delta f_{D_a/N}^{B7}(y) = \frac{i}{2yp_-}\frac{Z_N M_N}{p_-}\,\overline{\Gamma}^\lambda\int\frac{d^4q}{(2\pi)^4}\,\delta\!\left(y-\frac{q_-}{p_-}\right)$$
$$S(p-q)\tau_a(q)\,q_-\left[g_{2\lambda}g_{-\sigma} - g_{-\lambda}g_{2\sigma}\right]\Gamma^\sigma. \qquad \text{(D.238)}$$

From the δ-function we have $q_- \to yp_-$, therefore

$$\Delta f_{D_a/N}^{B7}(y) = \frac{i}{2}\frac{Z_N M_N}{p_-}\,\overline{\Gamma}^\lambda\int\frac{d^4q}{(2\pi)^4}\,\delta\!\left(y-\frac{q_-}{p_-}\right)$$
$$S(p-q)\tau_a(q)\,\left[g_{2\lambda}g_{-\sigma} - g_{-\lambda}g_{2\sigma}\right]\Gamma^\sigma. \qquad \text{(D.239)}$$

Let

$$I^{B5} = \int\frac{d^4q}{(2\pi)^4}\,\delta\!\left(y-\frac{q_-}{p_-}\right)S(p-q)\tau_a(q),$$
$$= \int\frac{d^4q}{(2\pi)^4}\delta\!\left(y-\frac{q_-}{p_-}\right)\frac{\not p - \not q + M}{q^2+p^2-2p\cdot q - M^2 + i\varepsilon}$$
$$\left[4i\,G_a - \frac{i\,g_a}{q^2-M_a^2+i\varepsilon}\right],$$
$$\equiv I_1^{B7} + I_2^{B7}. \qquad \text{(D.240)}$$

Performing the shift $q \to q + p$ and taking the moments of I_1^{B5} gives

$$\mathcal{A}_{1n}^{B7} = 4i\, G_a \int \frac{d^4q}{(2\pi)^4} \left(\frac{q_- + p_-}{p_-}\right)^{n-1} \frac{(M - \not{q})}{q^2 - M^2 + i\varepsilon}. \tag{D.241}$$

From a similar calculation in $\Delta_T f_{D_a/N}^{B5}$ we have

$$I_1^{B7} = -i\frac{G_a}{4\pi^2}\frac{p_-}{M_N} \int d\tau \, \frac{1}{\tau^2} \left[2\, M\, \alpha_3^2\, \delta(y-1) - \frac{\alpha_2\alpha_3}{\tau\, M_N}\frac{d}{dy}\delta(y-1)\right] e^{-\tau\, M^2}. \tag{D.242}$$

We now determine I_2^{B7}, we have

$$I_2^{B7} = \int \frac{d^4q}{(2\pi)^4}\delta\left(y - \frac{q_-}{p_-}\right) \frac{\not{p} - \not{q} + M}{q^2 + p^2 - 2p\cdot q - M^2 + i\varepsilon}\left[-\frac{i\, g_a}{q^2 - M_a^2 + i\varepsilon}\right]. \tag{D.243}$$

From $\Delta_T f_{D_a/N}^{A}$ we obtain

$$I_2^{B7} = \frac{g_a}{16\pi^2}\int d\tau \, \frac{1}{\tau} e^{-\tau\left[(y^2-y)p^2 + (1-y)M_a^2 + yM^2\right]} \left\{(1-y)\not{p} + M + \frac{\gamma^+}{2p_-}\left[(2y-1)p^2 - M_a^2 + M^2\right]\right\}. \tag{D.244}$$

Using the matrix elements from $\Delta_T f_{D_a/N}^{B5}$ gives

$$I_2^{B7} = i\frac{g_a}{8\pi^2}\frac{p_-}{M_N}\int d\tau \, \frac{1}{\tau}\, e^{-\tau\left[(y^2-y)p^2 + (1-y)M_a^2 + yM^2\right]} \left\{\alpha_3^2\left[(1-y)M_N + M\right] + \frac{\alpha_2\alpha_3}{2M_N}\left[(2y-1)p^2 - M_a^2 + M^2\right]\right\}. \tag{D.245}$$

However we must also include the a surface term, which did not contribute to $\Delta_T f_{D_a/N}^{A}$ because of p_+ derivative. This term has the form

$$\begin{aligned}\mathcal{A}_n^{B7-\text{surface}} &= i\, g_a \frac{\gamma^+}{p_-} \\ &\quad \int \frac{d^4q}{(2\pi)^4}\frac{q_- q_+ \alpha^{n-1}}{\left[q^2 - (\alpha^2 - \alpha)\, p^2 - (1-\alpha)\, M_a^2 - \alpha M^2 + i\varepsilon\right]^2}\Bigg|_0^1, \\ &= i\, g_a \frac{\gamma^+}{p_-}\int \frac{d^4q}{(2\pi)^4}\left\{\frac{q_- q_+}{\left[q^2 - M^2 + i\varepsilon\right]^2} - \lim_{\varepsilon\to 0^+}\frac{q_- q_+\, \varepsilon^{n-1}}{\left[q^2 - M_a^2 + i\varepsilon\right]^2}\right\}.\end{aligned} \tag{D.246}$$

Using the results from $\mathcal{A}_{2n}^{B7-\text{surface}}$ we obtain

$$I^{B7-\text{surface}} = i\, \frac{g_a\, \alpha_2\alpha_3}{16\pi^2}\frac{p_-}{M_N^2}\int d\tau \, \frac{1}{\tau^2}\left[\delta(y-1)e^{-\tau\, M^2} + \delta(y)\, e^{-\tau\, M_a^2}\right]. \tag{D.247}$$

Therefore

$$\Delta f^{B7}_{Da/N}(y) = \frac{G_a\, Z_N}{8\pi^2} \int d\tau\, \frac{1}{\tau^2} \left[2\, M\, \alpha_3^2\, \delta(y-1) - \frac{\alpha_2\alpha_3}{\tau\, M_N} \frac{d}{dy}\, \delta(y-1)\right] e^{-\tau\, M^2}$$
$$- \frac{g_a\, Z_N}{16\pi^2} \int d\tau\, \frac{1}{\tau} e^{-\tau\left[(y^2-y)p^2+(1-y)M_a^2+yM^2\right]}$$
$$\left\{\alpha_3^2\left[(1-y)M_N + M\right] + \frac{\alpha_2\alpha_3}{2M_N}\left[(2y-1)p^2 - M_a^2 + M^2\right]\right\}$$
$$+ \frac{g_a\, \alpha_2\alpha_3\, Z_N}{32\pi^2\, M_N} \int d\tau\, \frac{1}{\tau^2}\left[\delta(y-1)e^{-\tau\, M^2} + \delta(y)\, e^{-\tau\, M_a^2}\right]. \quad \text{(D.248)}$$

Summary of Results for $\Delta_T f^B_{Da/N}(y)$

The full result for $\Delta_T f^B_{Da/N}(y)$ contains seven terms, that is

$$\Delta_T f^B_{Da/N}(y) = \Delta_T f^{B1} + \Delta_T f^{B2} + \Delta_T f^{B3}$$
$$+ \Delta_T f^{B4} + \Delta_T f^{B5} + \Delta_T f^{B6} + \Delta_T f^{B7}. \quad \text{(D.249)}$$

Both $\Delta_T f^{B5}(y)$ and $\Delta f^{B7}(y)$ contain one contact term, however these terms cancel, $\Delta f^{B7}(y)$ also contains a surface term which we give below as $\Delta f^{B7}_s(y)$. The full result is

$$\Delta f^{B1}(y) = 0, \quad \text{(D.250)}$$
$$\Delta f^{B2}(y) = -\frac{g_a\, Z_N}{32\pi^2} \int d\tau\, \frac{1}{\tau^2}\; e^{-\tau\left[(y^2-y)p^2+(1-y)M_a^2+yM^2\right]}$$
$$\left\{\frac{\alpha_2\alpha_3}{M_N}\left[1 + \tau\,(1-y)\left[(2y-1)p^2 - M_a^2 + M^2\right]\right]\right.$$
$$\left. + 2\tau\alpha_3^2\,(1-y)\left[(1-y)M_N + M\right]\right\}, \quad \text{(D.251)}$$

$$\Delta f^{B3}(y) = 0, \quad \text{(D.252)}$$
$$\Delta f^{B4}(y) = \frac{g_a\, Z_N\, M_N}{32\pi^2}\, y^2 \int d\tau\; e^{-\tau\left[(y^2-y)p^2+(1-y)M_a^2+yM^2\right]}$$
$$\left\{2\alpha_3^2\left[\frac{1}{\tau} + (1-y)\left[y\, p^2 + M\, M_N + M^2 - M_a^2\right]\right]\right.$$
$$\left. - \alpha_2\alpha_3\left[\frac{1}{\tau} + (1-y)\left[(2y-1)\, p^2 - M_a^2 + M^2\right]\right]\right\}, \quad \text{(D.253)}$$
$$\Delta_T f^{B5}(y) = \frac{g_a\, Z_N}{16\pi^2} \int d\tau\, \frac{1}{\tau}\; e^{-\tau\left[(y^2-y)p^2+(1-y)M_a^2+yM^2\right]}$$
$$\left\{\alpha_3^2\,(1-y)\left[1 - \tau\, y\left[(y-1)\, p^2 - M_a^2 + M^2\right]\right]\left[(1-y)M_N + M\right]\right.$$

$$+\frac{\alpha_2\alpha_3}{2M_N}\left[y^2M_N^2-\left(2y-1+\tau\,y(1-y)\left[(y-1)\,p^2-M_a^2+M^2\right]\right)\right.$$

$$\left.\left.\left[(2y-1)\,p^2-M_a^2+M^2\right]\right]\right\}, \qquad \text{(D.254)}$$

$$\Delta f^{B6}(y)=\alpha_3\,(\alpha_3-\alpha_2)\,\frac{g_a\,Z_N\,M_N}{16\pi^2}\,y(1-y)$$

$$\int d\tau\,\frac{1}{\tau}\,e^{-\tau\left[(y^2-y)p^2+(1-y)M_a^2+yM^2\right]}, \qquad \text{(D.255)}$$

$$\Delta f^{B7}(y)=-\frac{g_a\,Z_N}{16\pi^2}\int d\tau\,\frac{1}{\tau}e^{-\tau\left[(y^2-y)p^2+(1-y)M_a^2+yM^2\right]}$$

$$\left\{\alpha_3^2\left[(1-y)M_N+M\right]+\frac{\alpha_2\alpha_3}{2M_N}\left[(2y-1)p^2-M_a^2+M^2\right]\right\}, \qquad \text{(D.256)}$$

$$\Delta f_s^{B7}(y)=\frac{g_a\,\alpha_2\alpha_3\,Z_N}{32\pi^2\,M_N}\int d\tau\,\frac{1}{\tau^2}\left[\delta(y-1)e^{-\tau\,M^2}+\delta(y)\,e^{-\tau\,M_a^2}\right]. \qquad \text{(D.257)}$$

D.1.4 Transverse Mixed Diquark Diagram

In the calculation below we calculate the two diquark mixing diagrams together. That is, the diagram where we have an axial-vector diquark → operator insertion → scalar diquark and the opposite diagram scalar diquark → operator insertion → axial-vector diquark. We have

$$\begin{aligned}\Delta_T f_{q(D_m)/N}(x) &= i\,\overline{\Gamma}_N \int \frac{d^4q}{(2\pi)^4} \int \frac{d^4k}{(2\pi)^4}\,\delta\Big(x - \frac{k_-}{p_-}\Big)\, S(p-q)\,\tau_{\sigma\mu}(q)\tau_s(q)\,\Gamma_N^\sigma \\ &i\mathrm{Tr}\Big[\big(C^{-1}\gamma_5\tau_2\beta^A\big)\big(S(k)\gamma^+\gamma^1\gamma_5\,\tfrac{1}{2}\,(1\pm\tau_z)\,S(k)\big)\Big(\gamma^\mu C\tau_j\tau_2\beta^{A'}\Big)\,S^T(q-k)\Big] \\ &+ i\,\overline{\Gamma}_N^\sigma \int \frac{d^4q}{(2\pi)^4} \int \frac{d^4k}{(2\pi)^4}\,\delta\Big(x - \frac{k_-}{p_-}\Big)\, S(p-q)\,\tau_s(q)\tau_{\mu\sigma}(q)\,\Gamma_N \\ &i\mathrm{Tr}\Big[\big(C^{-1}\gamma^\mu\tau_2\tau_i\beta^A\big)\big(S(k)\gamma^+\gamma^1\gamma_5\tfrac{1}{2}\,(1\pm\tau_z)\,S(k)\big)\Big(\gamma_5 C\tau_2\beta^{A'}\Big)\,S^T(q-k)\Big]. \end{aligned} \tag{D.258}$$

Using $CS^T(-q)C^{-1} = S(q)$ and $\mathrm{Tr}\{T^aT^b\} = \frac{1}{2}\delta_{ab}$ where $T^a = \frac{\lambda^a}{2}$, $\beta^A = \sqrt{\frac{3}{2}}\lambda^A$ and hence $\mathrm{Tr}\{\beta^A\beta^{A'}\} = \frac{3}{2}\mathrm{Tr}\{\lambda^A\lambda^{A'}\} = \frac{3}{2}\times 4\,\mathrm{Tr}\{T^AT^{A'}\} = 3\delta_{AA'}$. Also the isospin trace for each diagram gives, respectively

$$\tfrac{1}{2}\mathrm{Tr}\left[\tau_2\,(1\pm\tau_z)\,\tau_i\tau_2\right] = \tfrac{1}{2}\mathrm{Tr}\left[\tau_2\tau_i\tau_2\right] \pm \tfrac{1}{2}\mathrm{Tr}\left[\tau_2\,\tau_z\,\tau_i\tau_2\right] = \tfrac{1}{2} \pm \mathrm{Tr}\left[\tau_z\tau_i\right] = \pm\delta_{iz}, \tag{D.259}$$

$$\tfrac{1}{2}\mathrm{Tr}\left[\tau_2\tau_i\,(1\pm\tau_z)\,\tau_2\right] = \tfrac{1}{2}\mathrm{Tr}\left[\tau_2\tau_i\tau_2\right] \pm \tfrac{1}{2}\mathrm{Tr}\left[\tau_2\tau_i\,\tau_z\,\tau_2\right] = \pm\tfrac{1}{2}\mathrm{Tr}\left[\tau_i\tau_z\right] = \pm\delta_{iz}. \tag{D.260}$$

Therefore we obtain

$$\begin{aligned}\Delta_T f_{q(D_m)/N}(x) &= i\overline{\Gamma}_N \int \frac{d^4q}{(2\pi)^4} \int \frac{d^4k}{(2\pi)^4}\,\delta\Big(x - \frac{k_-}{p_-}\Big)\, S(p-q)\,\tau_{\sigma\mu}(q) \\ &\qquad 6i\mathrm{Tr}\left[\gamma_5 S(k)\gamma^+\gamma^1\gamma_5\,S(k)\gamma^\mu S(k-q)\right]\,\tau_s(q)\,\Gamma_N^\sigma \\ &+ i\overline{\Gamma}_N^\sigma \int \frac{d^4q}{(2\pi)^4} \int \frac{d^4k}{(2\pi)^4}\,\delta\Big(x - \frac{k_-}{p_-}\Big)\, S(p-q)\,\tau_s(q) \\ &\qquad 6i\mathrm{Tr}\left[\gamma^\mu S(k)\gamma^+\gamma^1\gamma_5 S(k)\gamma_5 S(k-q)\right]\,\tau_{\mu\sigma}(q)\,\Gamma_N. \end{aligned} \tag{D.261}$$

We have dropped the isospin part, as this coefficient will be evaluated later and inserted an extra factor of 2 which will be cancelled via the final isospin factor. Using

$$\begin{aligned}&\mathrm{Tr}\left[\gamma_5 S(k)\gamma^+\gamma^1\gamma_5\,S(k)\gamma^\mu S(k-q)\right] \\ &= -\mathrm{Tr}\left[\gamma^\mu S(k)\gamma^+\gamma^1\gamma_5 S(k)\gamma_5 S(k-q)\right] + 2\,(k^\mu - q^\mu)\,\mathrm{Tr}\left[\gamma_5 S(k)\gamma^+\gamma^1\gamma_5 S(k)\right] \\ &= -\mathrm{Tr}\left[\gamma^\mu S(k)\gamma^+\gamma^1\gamma_5 S(k)\gamma_5 S(k-q)\right], \end{aligned} \tag{D.262}$$

since $g^{+1} = 0$, we obtain

$$\Delta_T f_{q(D_m)/N}(x) = -i \int \frac{d^4q}{(2\pi)^4} \int \frac{d^4k}{(2\pi)^4} \delta\left(x - \frac{k_-}{p_-}\right) \tau_{\sigma\mu}(q)\tau_s(q)$$
$$\left\{\overline{\Gamma}_N^\sigma\, S(p-q)\,\Gamma_N - \overline{\Gamma}_N S(p-q)\,\Gamma_N^\sigma\right\} 6i\mathrm{Tr}\left[\gamma_5 S(k)\gamma^+\gamma^1\gamma_5\, S(k)\gamma^\mu S(k-q)\right], \tag{D.263}$$

where in the last line we used $\tau_{\sigma\mu} = \tau_{\mu\sigma}$ and $\tau_{\sigma\mu}\tau_s = \tau_s\tau_{\sigma\mu}$. Inserting the identity in the form $\mathbb{1} = \int_0^1 dy \int_0^1 dz\, \delta\left(y - \frac{q_-}{p_-}\right)\delta\left(z - \frac{k_-}{q_-}\right)$, which implies $\delta\left(x - \frac{k_-}{p_-}\right) \longrightarrow \delta(x - yz)$, we obtain

$$\Delta_T f_{q(D_m)/N}(x) = -i \int_0^1 dy \int_0^1 dz\ \delta(x - yz)$$
$$\int \frac{d^4q}{(2\pi)^4}\delta\left(y - \frac{q_-}{p_-}\right) \tau_{\sigma\mu}(q)\tau_s(q) \left\{\overline{\Gamma}_N^\sigma\, S(p-q)\,\Gamma_N - \overline{\Gamma}_N S(p-q)\,\Gamma_N^\sigma\right\}$$
$$6i \int \frac{d^4k}{(2\pi)^4}\delta\left(z - \frac{k_-}{q_-}\right) \mathrm{Tr}\left[\gamma_5 S(k)\gamma^+\gamma^1\gamma_5\, S(k)\gamma^\mu S(k-q)\right]. \tag{D.264}$$

We define

$$\Delta_T f_{q/D_m}(z, q^2)\ \left[q^1 g^{\mu+} - q^+ g^{\mu 1}\right] = 6i \int \frac{d^4k}{(2\pi)^4}\delta\left(z - \frac{k_-}{q_-}\right)$$
$$\mathrm{Tr}\left[\gamma_5 S(k)\gamma^+\gamma^1\gamma_5\, S(k)\gamma^\mu S(k-q)\right], \tag{D.265}$$

$$\Delta_T f_{D_m/N}(y, p^2) = -i \int \frac{d^4q}{(2\pi)^4}\delta\left(y - \frac{q_-}{p_-}\right) \tau_{\sigma\mu}(q)\tau_s(q)$$
$$\left\{\overline{\Gamma}_N^\sigma\, S(p-q)\,\Gamma_N - \overline{\Gamma}_N S(p-q)\,\Gamma_N^\sigma\right\} \left[q^1 g^{\mu+} - q^+ g^{\mu 1}\right]. \tag{D.266}$$

Therefore

$$\Delta_T f_{q(D_m)/N}(x) = \int_0^1 dy \int_0^1 dz\ \delta(x - yz)\ \ \Delta_T f_{D_m/N}(y, p^2)\ \ \Delta_T f_{q/D_m}(z, q^2). \tag{D.267}$$

If we make the on-shell approximation for the diquark we have

$$\Delta_T f_{q(D_m)/N}(x) = \int_0^1 dy \int_0^1 dz\ \delta(x - yz)\ \ \Delta_T f_{D_m/N}(y, p^2)\ \ \Delta_T f_{q/D_m}(z, M_D^2). \tag{D.268}$$

Determining the quark in the diquark: $\Delta_T f_{q/D_m}(z, M_D^2)$

We have

$$\Delta_T f_{q/D_m}(z, q^2)\ \left[q^1 g^{\mu +} - q^+ g^{\mu 1}\right] = 6i \int \frac{d^4k}{(2\pi)^4}$$
$$\delta\!\left(z - \frac{k_-}{q_-}\right) \mathrm{Tr}\left[\gamma_5 S(k)\gamma^+\gamma^1\gamma_5\, S(k)\gamma^\mu S(k-q)\right]. \quad \text{(D.269)}$$

Using the result

$$\mathrm{Tr}\left[\gamma_5(\not{k} + M)\gamma^+\gamma^1\gamma_5\,(\not{k} + M)\gamma^\mu(\not{k} - \not{q} + M)\right]$$
$$= 8\Big[\left(k^1\, g^{\mu +} - k^+\, g^{\mu 1}\right) k\cdot q + \left(k^+ q^1 - k^1 q^+\right) k^\mu\Big]$$
$$+ 4\left(k^2 - M^2\right)\left[\left(k^+ + q^+\right) g^{\mu 1} - \left(k^1 + q^1\right) g^{\mu +}\right], \quad \text{(D.270)}$$

where we have used $g^{+1} = 0$ in the last line. Letting

$$\Delta_T f_{q/D_m}(z, q^2) = \Delta_T f^A(z, q^2) + \Delta_T f^B(z, q^2), \quad \text{(D.271)}$$

where

$$\Delta_T f^A(z, q^2)\left[q^1 g^{\mu +} - q^+ g^{\mu 1}\right] = 48i \int \frac{d^4k}{(2\pi)^4}$$
$$\delta\!\left(z - \frac{k_-}{q_-}\right) \frac{\left(k^1\, g^{\mu +} - k^+\, g^{\mu 1}\right) k\cdot q + \left(k^+ q^1 - k^1 q^+\right) k^\mu}{\left(k^2 - M^2 + i\varepsilon\right)^2\left(k^2 + q^2 - 2\,k\cdot q - M^2 + i\varepsilon\right)}, \quad \text{(D.272)}$$

$$\Delta_T f^B(z, q^2)\left[q^1 g^{\mu +} - q^+ g^{\mu 1}\right] = 24i \int \frac{d^4k}{(2\pi)^4}$$
$$\delta\!\left(z - \frac{k_-}{q_-}\right) \frac{\left(k^2 - M^2\right)\left[\left(k^+ + q^+\right) g^{\mu 1} - \left(k^1 + q^1\right) g^{\mu +}\right]}{\left(k^2 - M^2 + i\varepsilon\right)^2\left(k^2 + q^2 - 2\,k\cdot q - M^2 + i\varepsilon\right)}. \quad \text{(D.273)}$$

Using the Feynman parametrization results of section A.5 and taking the moments gives

$$\mathcal{A}_n^A\left[q^1 g^{\mu +} - q^+ g^{\mu 1}\right] = 96i \int_0^1 d\alpha(1-\alpha) \int \frac{d^4k}{(2\pi)^4}\left(\frac{k_- + \alpha q_-}{q_-}\right)^{n-1}$$
$$\Big\{\left[\left(k^1 + \alpha q^1\right) g^{\mu +} - \left(k^+ + \alpha q^+\right) g^{\mu 1}\right]\left[k\cdot q + \alpha\, q^2\right]$$
$$+ \left[\left(k^+ + \alpha q^+\right) q^1 - \left(k^1 + \alpha q^1\right) q^+\right]\left[k^\mu + \alpha q^\mu\right]\Big\}$$
$$\left[k^2 - \left(\alpha^2 - \alpha\right) q^2 - M^2 + i\varepsilon\right]^{-3}. \quad \text{(D.274)}$$

Considering just the numerator, ignoring terms odd in k and using $g^{--} = g^{-1} = g^{-2} = 0$ we have

$$\mathcal{N}_n^A \left[q^1 g^{\mu+} - q^+ g^{\mu 1}\right] = (1-\alpha)\alpha^{n-1}\Big\{\left[k^1 k^1 q_1 + q^1(\alpha q)^2\right] g^{\mu+} - \left[k^+ k^- q_- + q^+(\alpha q)^2\right] g^{\mu 1} + k^+ k^\mu q^1 + \alpha^2 q^1 q^\mu q^+ - k^1 k^\mu q^+ - \alpha^2 q^1 q^\mu q^+\Big\} + (1-\alpha)\frac{k_-}{q_-}\Big\{\alpha\, q^1\, k_+ q_-\, g^{\mu+} - \alpha\, q^+\, k_+ q_-\, g^{\mu 1} + \alpha q^1 q^+ k^\mu - \alpha q^1 q^+ k^\mu\Big\}\frac{d}{d\alpha}\alpha^{n-1}. \tag{D.275}$$

Cancelling terms and integrating by parts in $d\alpha$ gives

$$\begin{aligned}\mathcal{N}_n^A \left[q^1 g^{\mu+} - q^+ g^{\mu 1}\right] &= (1-\alpha)\alpha^{n-1}\Big\{k^1 k^1 q_1\, g^{\mu+} - k^1 k^\mu q^+ \\ &\quad + k^+ k^\mu q^1 - k^+ k^- q_- g^{\mu 1} + (\alpha q)^2\left[q^1 g^{\mu+} - q^+ g^{\mu 1}\right]\Big\} \\ &\quad - \alpha^{n-1}\frac{d}{d\alpha}(1-\alpha)\alpha\, k_+ k_-\left[q^1\, g^{\mu+} - q^+\, g^{\mu 1}\right] \\ &\quad + (1-\alpha)\alpha^{n-1}\alpha\, k_+ k_-\left[q^1\, g^{\mu+} - q^+\, g^{\mu 1}\right]\Bigg|_0^1,\end{aligned} \tag{D.276}$$

where the surface term is zero. Using the relation

$$\int \frac{d^4k}{(2\pi)^4}\frac{k^\mu k^\nu}{(k^2 - A + i\varepsilon)^n} = \frac{1}{4}g^{\mu\nu}\int \frac{d^4k}{(2\pi)^4}\frac{k^2}{(k^2 - A + i\varepsilon)^n}, \tag{D.277}$$

and $g^{11} = -1$ and $g^{-+} = 1$, we obtain

$$\mathcal{N}_n^A = (1-\alpha)\alpha^{n-1}\left[\frac{k^2}{4} + \frac{k^2}{4} + (\alpha q)^2 - \frac{k^2}{4} - \alpha\frac{k^2}{4}\frac{d}{d\alpha}\right] + \alpha^{n-1}\alpha\frac{k^2}{4}. \tag{D.278}$$

Therefore from the definition of the moments we have

$$\Delta_T f^A(z, q^2) = 96i\int \frac{d^4k}{(2\pi)^4}\frac{(1-z)\left[z^2 q^2 + \frac{k^2}{4} - z\frac{k^2}{4}\frac{d}{dz}\right] + z\frac{k^2}{4}}{\left[k^2 - (z^2 - z)\,q^2 - M^2 + i\varepsilon\right]^3}. \tag{D.279}$$

Wick rotating, introducing 4d-polars, then the proper-time regularization gives

$$\begin{aligned}\Delta_T f^A(z, q^2) &= \frac{6}{\pi^2}\int_0^\infty dk_E^2\, k_E^2\,\frac{(1-z)\left[z^2 q^2 - \frac{k_E^2}{4} + z\frac{k_E^2}{4}\frac{d}{dz}\right] - z\frac{k_E^2}{4}}{\left[k_E^2 + (z^2 - z)\,q^2 + M^2\right]^3}, \\ &= \frac{3}{\pi^2}\int d\tau\left\{(1-z)\left[z^2 q^2 - \frac{1}{2\tau} - \frac{1}{2}z\,(2z-1)q^2\right] - \frac{z}{2\tau}\right\} e^{-\tau\left[(z^2 - z)q^2 + M^2\right]}.\end{aligned} \tag{D.280}$$

Therefore

$$\Delta_T f^A(z,q^2) = \frac{3}{2\pi^2}\int d\tau \, \left[z(1-z)q^2 - \frac{1}{\tau}\right] e^{-\tau\left[(z^2-z)q^2+M^2\right]}. \tag{D.281}$$

We now evaluate $\Delta_T f^B(z,q^2)$, taking the moments we have

$$\mathcal{A}_n^B\left[q^1 g^{\mu +} - q^+ g^{\mu 1}\right] = 24i\int_0^1 d\alpha \int \frac{d^4k}{(2\pi)^4}\left(\frac{k_- + \alpha q_-}{q_-}\right)^{n-1} \frac{\left[\left[k^+ + (1+\alpha)q^+\right]g^{\mu 1} - \left[k^1 + (1+\alpha)q^1\right]g^{\mu +}\right]}{\left[k^2 - (\alpha^2-\alpha)\, q^2 - M^2 + i\varepsilon\right]^2}. \tag{D.282}$$

Ignoring terms odd in q and noting $g^{--} = g^{-1} = g^{-2} = 0$ we obtain

$$\mathcal{A}_n^B\left[q^1 g^{\mu +} - q^+ g^{\mu 1}\right] = -24i\int_0^1 d\alpha \, \alpha^{n-1} \int \frac{d^4k}{(2\pi)^4}\frac{(1+\alpha)}{\left[k^2 - (\alpha^2-\alpha)\, q^2 - M^2 + i\varepsilon\right]^2}\left[q^1 g^{\mu +} - q^+ g^{\mu 1}\right]. \tag{D.283}$$

Therefore from the definition of the moments we have

$$\Delta_T f^B(z,q^2) = -24i\int \frac{d^4k}{(2\pi)^4}\frac{(1+z)}{\left[k^2 - (z^2-z)\, q^2 - M^2 + i\varepsilon\right]^2}. \tag{D.284}$$

Wick rotating, introducing 4d-polars and the proper-time regularization gives

$$\Delta_T f^B(z,q^2) = \frac{3}{2\pi^2}(1+z)\int d\tau\, \tau \int_0^\infty dk_E^2 \, k_E^2 \, e^{-\tau\left[k_E^2 + (z^2-z)q^2 + M^2\varepsilon\right]}. \tag{D.285}$$

Therefore

$$\Delta_T f^B(z,q^2) = \frac{3}{2\pi^2}(1+z)\int d\tau \, \frac{1}{\tau}\, e^{-\tau\left[(z^2-z)q^2+M^2\right]}. \tag{D.286}$$

Therefore the final result is

$$\Delta_T f_{q/D_m}(z,q^2) = \frac{3}{2\pi^2}\, z\int d\tau \, \left[(1-z)q^2 + \frac{1}{\tau}\right] e^{-\tau\left[(z^2-z)q^2+M^2\right]}. \tag{D.287}$$

Determining the diquark in the nucleon: $\Delta_T f_{D_m/N}(y, p^2)$

We have

$$\begin{aligned}\Delta_T f_{D_m/N}(y,p^2) &= -i \int \frac{d^4q}{(2\pi)^4}\,\delta\left(y - \frac{q_-}{p_-}\right)\tau_{\sigma\mu}(q)\tau_s(q) \\ &\quad \left\{\overline{\Gamma}^\sigma_N\, S(p-q)\,\Gamma_N - \overline{\Gamma}_N S(p-q)\,\Gamma^\sigma_N\right\}\left[q^1 g^{\mu+} - q^+ g^{\mu 1}\right], \\ &= i\,\alpha_1 \frac{Z_N\, M_N}{p_-}\int \frac{d^4q}{(2\pi)^4}\,\delta\left(y - \frac{q_-}{p_-}\right)\tau_a(q)\tau_s(q) \\ &\quad \left\{q^1\left[\overline{\Gamma}^+ S(p-q)\,\Gamma - \overline{\Gamma} S(p-q)\,\Gamma^+\right] - q^+\left[\overline{\Gamma}^1 S(p-q)\,\Gamma - \overline{\Gamma} S(p-q)\,\Gamma^1\right]\right\}.\end{aligned} \tag{D.288}$$

We define

$$I^A = \int \frac{d^4q}{(2\pi)^4}\,\delta\left(y - \frac{q_-}{p_-}\right)\tau_a(q)\tau_s(q) S(p-q)\, q^1, \tag{D.289}$$

$$I^B = \int \frac{d^4q}{(2\pi)^4}\,\delta\left(y - \frac{q_-}{p_-}\right)\tau_a(q)\tau_s(q) S(p-q)\, q^+, \tag{D.290}$$

therefore

$$\begin{aligned}\Delta_T f_{D_m/N}(y,p^2) &= i\,\alpha_1 \frac{Z_N\, M_N}{p_-} \\ &\quad \left\{\left[\overline{\Gamma}^+ I^A\,\Gamma - \overline{\Gamma}\, I^A\,\Gamma^+\right] - \left[\overline{\Gamma}^1 I^B\,\Gamma - \overline{\Gamma}\, I^B\,\Gamma^1\right]\right\} \equiv \Delta_T f^A - \Delta_T f^B.\end{aligned} \tag{D.291}$$

Using the result

$$\begin{aligned}\tau_a(q)\tau_s(q) &= \left[4i\,G_s - \frac{i\,g_a}{q^2 - M_a - i\varepsilon}\right]\left[4i\,G_s - \frac{i\,g_a}{q^2 - M_s - i\varepsilon}\right], \\ &= -16 G_a\, G_s + \left[4\,G_a\, g_s + \frac{g_a\, g_s}{M_a^2 - M_s^2}\right]\frac{1}{q^2 - M_s^2 + i\varepsilon} \\ &\quad + \left[4\,G_s\, g_a - \frac{g_a\, g_s}{M_a^2 - M_s^2}\right]\frac{1}{q^2 - M_a^2 + i\varepsilon},\end{aligned} \tag{D.292}$$

we have

$$I^A = I^{A1} + I^{A2} + I^{A3}, \qquad I^B = I^{B1} + I^{B2} + I^{B3}, \tag{D.293}$$

and hence

$$\Delta_T f^A = \Delta_T f^{A1} + \Delta_T f^{A2} + \Delta_T f^{A3}, \quad \Delta_T f^B = \Delta_T f^{B1} + \Delta_T f^{B2} + \Delta_T f^{B3}. \tag{D.294}$$

Determining $\Delta_T f^A(y, M_D^2)$:

We first determine the individual parts of I^A, we have

$$I^{A1} = -16 G_a\, G_s \int \frac{d^4q}{(2\pi)^4}\, \delta\left(y - \frac{q_-}{p_-}\right) \frac{\not p - \not q + M}{q^2 + p^2 - 2q\cdot p - M^2 + i\varepsilon}\, q^1. \quad \text{(D.295)}$$

Taking the moments and performing the shift $q \longrightarrow q + p$, we obtain

$$\mathcal{A}_n^{A1} = 16 G_a\, G_s \int \frac{d^4q}{(2\pi)^4} \left(\frac{q_- + p_-}{p_-}\right)^{n-1} \frac{q_1\,(M - \not q)}{q^2 - M^2 + i\varepsilon}. \quad \text{(D.296)}$$

Ignoring terms odd in q and noting $g^{-1} = g^{--} = 0$ we obtain

$$\mathcal{A}_n^{A1} = 16 G_a\, G_s \int \frac{d^4q}{(2\pi)^4} \frac{-q_1^2\,\gamma^1}{q^2 - M^2 + i\varepsilon}. \quad \text{(D.297)}$$

Wick rotating, introducing 4d-polars and the proper-time regularization gives

$$\begin{aligned}\mathcal{A}_n^{A1} &= i\,\frac{G_a\, G_s}{\pi^2}\,\gamma^1 \int d\tau \int dq_E^2\, q_E^2\, \left(\tfrac{1}{4} q_E^2\right) e^{-\tau\left[q_E^2 + M^2\right]} \\ &= i\,\frac{G_a\, G_s}{2\pi^2}\,\gamma^1 \int d\tau\, \frac{1}{\tau^3}\, e^{-\tau M^2}. \end{aligned} \quad \text{(D.298)}$$

Using the following method to obtain the distribution from the moments

$$f(x) = \frac{1}{2\pi\, i} \lim_{\varepsilon \to 0+} \left[F(x - i\varepsilon) - F(x + i\varepsilon)\right], \quad \text{(D.299)}$$

where

$$F(x) = \sum_0^\infty \frac{\mathcal{A}_n}{x^n}, \quad \text{(D.300)}$$

we obtain

$$I^{A1}(y) = i\,\delta(y-1)\,\frac{G_a\, G_s}{2\pi^2}\,\gamma^1 \int d\tau\, \frac{1}{\tau^3}\, e^{-\tau M^2}. \quad \text{(D.301)}$$

Therefore we need the matrix element $\overline{\Gamma}^+ \gamma^1\, \Gamma - \overline{\Gamma}\gamma^1\, \Gamma^+$, where in general we have

$$\overline{\Gamma}^\mu \Omega\, \Gamma - \overline{\Gamma}\Omega\, \Gamma^\mu = \overline{u}_N \left[\alpha_2\, \frac{p^\mu}{M_N} \left(\gamma_5 \Omega - \Omega \gamma_5\right) + \alpha_3 \left(\gamma_5 \gamma^\mu \Omega - \Omega \gamma^\mu \gamma_5\right)\right] u_N. \quad \text{(D.302)}$$

Therefore

$$\overline{\Gamma}^+ \gamma^1\, \Gamma - \overline{\Gamma}\gamma^1\, \Gamma^+ = 2\alpha_2 \frac{p^+}{M_N}\, \overline{u}_N \gamma_5 \gamma^1 u_N + 2\alpha_3\, \overline{u}_N \gamma_5 \gamma^+ \gamma^1 u_N = 2\, \frac{p^+}{M_N}\, (\alpha_3 - \alpha_2)\,. \quad \text{(D.303)}$$

Hence

$$\Delta_T f^{A1}(y) \;=\; \delta(y\;-\;1)\,\alpha_1 \frac{G_a\,G_s\,Z_N}{\pi^2}\;(\alpha_2-\alpha_3)\int d\tau\;\frac{1}{\tau^3}\;e^{-\tau\,M^2}. \quad (D.304)$$

Evaluating I^{A2}, we have

$$I^{A2}(y) = \left[4\,G_a\,g_s + \frac{g_a\,g_s}{M_a^2-M_s^2}\right] \int \frac{d^4q}{(2\pi)^4}\,\delta\left(y-\frac{q_-}{p_-}\right)\frac{1}{q^2-M_s^2+i\varepsilon}\,\frac{\not p-\not q+M}{q^2+p^2-2q\cdot p-M^2+i\varepsilon}\,q^1. \quad (D.305)$$

Taking the moments and introducing Feynman parametrization we obtain

$$\mathcal{A}_n^{A2} = \left[4\,G_a\,g_s + \frac{g_a\,g_s}{M_a^2-M_s^2}\right]\int_0^1 d\alpha \int \frac{d^4q}{(2\pi)^4}\left(\frac{q_-+\alpha p_-}{p_-}\right)^{n-1} \frac{\left[(1-\alpha)\not p-\not q+M\right]q^1}{\left[q^2-(\alpha^2-\alpha)p^2-(1-\alpha)M_s^2-\alpha M^2+i\varepsilon\right]^2}. \quad (D.306)$$

Ignoring terms odd in q and using $g^{-1}=g^{--}=0$ we obtain

$$\mathcal{A}_n^{A2} = \left[4\,G_a\,g_s + \frac{g_a\,g_s}{M_a^2-M_s^2}\right]\int_0^1 d\alpha\,\alpha^{n-1}\int \frac{d^4q}{(2\pi)^4}\,\frac{q_1^2\,\gamma^1}{\left[q^2-(\alpha^2-\alpha)p^2-(1-\alpha)M_s^2-\alpha M^2+i\varepsilon\right]^2}. \quad (D.307)$$

Using the definition of the moments, then Wick rotating, introducing 4d-polar coordinates and the proper-time regularization gives

$$I^{A2}(y) = \left[4\,G_a\,g_s + \frac{g_a\,g_s}{M_a^2-M_s^2}\right]\frac{i\,\gamma^1}{16\pi^2}\int d\tau\;\tau \int_0^\infty dq_E^2\,q_E^2\left(\frac{1}{4}q_E^2\right)\;e^{-\tau\left[q_E^2+(y^2-y)p^2+(1-y)M_s^2+yM^2\right]}. \quad (D.308)$$

Therefore integrating over q_E^2 we obtain

$$I^{A2}(y) = \left[4\,G_a\,g_s + \frac{g_a\,g_s}{M_a^2-M_s^2}\right] \frac{i\,\gamma^1}{32\pi^2}\int d\tau\;\frac{1}{\tau^2}\,e^{-\tau\left[(y^2-y)p^2+(1-y)M_s^2+yM^2\right]}. \quad (D.309)$$

Therefore using the previous matrix element results we have

$$\Delta_T f^{A2}(y) = \left[4\, G_a\, g_s + \frac{g_a\, g_s}{M_a^2 - M_s^2}\right] \alpha_1 \frac{Z_N\,(\alpha_2 - \alpha_3)}{16\pi^2} \int d\tau\; \frac{1}{\tau^2}\; e^{-\tau\left[(y^2-y)p^2+(1-y)M_s^2+yM^2\right]}. \quad (D.310)$$

Therefore clearly

$$\Delta_T f^{A3}(y) = \left[4\, G_s\, g_a - \frac{g_a\, g_s}{M_a^2 - M_s^2}\right] \alpha_1 \frac{Z_N\,(\alpha_2 - \alpha_3)}{16\pi^2} \int d\tau\; \frac{1}{\tau^2}\; e^{-\tau\left[(y^2-y)p^2+(1-y)M_a^2+yM^2\right]}. \quad (D.311)$$

Ignoring contact terms gives

$$\Delta_T f^{A}(y) = \frac{g_a\, g_s}{M_a^2 - M_s^2} \alpha_1 \frac{Z_N\,(\alpha_2 - \alpha_3)}{16\pi^2} \int d\tau\; \frac{1}{\tau^2}\; \left[e^{-\tau(1-y)M_s^2} - e^{-\tau(1-y)M_a^2}\right] e^{-\tau\left[(y^2-y)p^2+yM^2\right]}. \quad (D.312)$$

Determining $\Delta_T f^B(y, M_D^2)$:

We first determine the individual parts of I^B, we have

$$\begin{aligned} I^{B1} &= -16 G_a\, G_s \int \frac{d^4q}{(2\pi)^4}\, \delta\left(y - \frac{q_-}{p_-}\right) \frac{\not{p} - \not{q} + M}{q^2 + p^2 - 2q\cdot p - M^2 + i\varepsilon}\, q_-, \\ &= -16 G_a\, G_s\, y p_- \int \frac{d^4q}{(2\pi)^4}\, \delta\left(y - \frac{q_-}{p_-}\right) \frac{\not{p} - \not{q} + M}{q^2 + p^2 - 2q\cdot p - M^2 + i\varepsilon}. \end{aligned} \tag{D.313}$$

Taking the moments, where we temporarily drop the factor y to avoid confusion with the sum over moments, and performing the shift $q \to q + p$, gives

$$\mathcal{A}_n^{B1} = -16 G_a\, G_s\, p_- \int \frac{d^4q}{(2\pi)^4} \left(\frac{q_- + p_-}{p_-}\right)^{n-1} \frac{M - \not{q}}{q^2 - M^2 + i\varepsilon}. \tag{D.314}$$

Ignoring terms odd in q and noting $g^{-1} = g^{--} = 0$ we obtain

$$\mathcal{A}_n^{B1} = -16 G_a\, G_s\, p_- \int \frac{d^4q}{(2\pi)^4} \frac{M - (n-1) q_- q_+ \frac{\gamma^+}{p_-}}{q^2 - M^2 + i\varepsilon}. \tag{D.315}$$

Wick rotating, introducing 4d-polars and the proper-time regularization gives

$$\begin{aligned} \mathcal{A}_n^{B1} &= -i\, \frac{G_a\, G_s}{\pi^2}\, p_- \int d\tau \int_0^\infty dq_E^2\, q_E^2 \left[M + (n-1) q_E^2\, \frac{\gamma^+}{4p_-}\right] e^{-\tau\left[q_E^2 + M^2\right]}, \\ &= -i\, \frac{G_a\, G_s}{\pi^2}\, p_- \int d\tau\, \frac{1}{\tau^2} \left[M + (n-1)\, \frac{\gamma^+}{2\tau\, p_-}\right] e^{-\tau M^2}. \end{aligned} \tag{D.316}$$

Using the following method to obtain the distribution from the moments

$$f(x) = \frac{1}{2\pi i} \left[F(x - i\varepsilon) - F(x + i\varepsilon)\right], \qquad \text{where} \qquad F(x) = \sum_0^\infty \frac{\mathcal{A}_n}{x^n}, \tag{D.317}$$

we obtain

$$I^{B1}(y) = -i\, \frac{G_a\, G_s}{\pi^2}\, y p_- \int d\tau\, \frac{1}{\tau^2} \left[M\, \delta(y-1) - \frac{\gamma^+}{2\tau\, p_-} \frac{d}{dy} \delta(y-1)\right] e^{-\tau M^2}, \tag{D.318}$$

where we have reinserted the factor of y. Therefore we need the matrix elements $\overline{\Gamma}^1\, \Gamma - \overline{\Gamma}\, \Gamma^1$ and $\overline{\Gamma}^1 \gamma^+\, \Gamma - \overline{\Gamma} \gamma^+\, \Gamma^1$, where in general we have

$$\overline{\Gamma}^\mu \Omega\, \Gamma - \overline{\Gamma} \Omega\, \Gamma^\mu = \overline{u}_N \left[\alpha_2\, \frac{p^\mu}{M_N} (\gamma_5 \Omega - \Omega \gamma_5) + \alpha_3\, (\gamma_5 \gamma^\mu \Omega - \Omega \gamma^\mu \gamma_5)\right] u_N. \tag{D.319}$$

Therefore

$$\overline{\Gamma}^1\, \Gamma - \overline{\Gamma}\, \Gamma^1 = -2\alpha_3, \tag{D.320}$$

$$\overline{\Gamma}^1 \gamma^+\, \Gamma - \overline{\Gamma} \gamma^+\, \Gamma^1 = -2\alpha_3\, \frac{p^+}{M_N}, \tag{D.321}$$

and hence

$$\Delta_T f^{B1}(y) = \alpha_1 \alpha_3 \frac{G_a\, G_s\, Z_N}{\pi^2}\, y$$
$$\int d\tau\, \frac{1}{\tau^2} \left[\frac{1}{\tau} \frac{d}{dy} \delta(y-1) - 2\, M\, M_N\, \delta(y-1) \right] e^{-\tau\, M^2}. \quad \text{(D.322)}$$

We now evaluate I^{B2}

We have

$$I^{B2}(y) = \left[4\,G_a\,g_s - \frac{g_a\,g_s}{M_a^2 - M_s^2}\right] y\,p_- \int \frac{d^4q}{(2\pi)^4}\,\delta\left(y - \frac{q_-}{p_-}\right) \frac{1}{q^2 - M_s^2 + i\varepsilon}\,\frac{\not{p} - \not{q} + M}{q^2 + p^2 - 2q\cdot p - M^2 + i\varepsilon}. \quad (D.323)$$

Taking the moments (again temporarily removing the factor y) and introducing Feynman parametrization we obtain

$$\mathcal{A}_n^{B2} = \left[4\,G_a\,g_s + \frac{g_a\,g_s}{M_a^2 - M_s^2}\right] p_- \int_0^1 d\alpha \int \frac{d^4q}{(2\pi)^4} \left(\frac{q_- + \alpha p_-}{p_-}\right)^{n-1} \frac{[(1-\alpha)\not{p} - \not{q} + M]}{[q^2 - (\alpha^2 - \alpha)p^2 - (1-\alpha)M_s^2 - \alpha M^2 + i\varepsilon]^2}. \quad (D.324)$$

Ignoring term odd in q and using $g^{-1} = g^{--} = 0$ we obtain

$$\begin{aligned}
\mathcal{A}_n^{B2} &= \left[4\,G_a\,g_s + \frac{g_a\,g_s}{M_a^2 - M_s^2}\right] p_- \int_0^1 d\alpha \\
&\quad \int \frac{d^4q}{(2\pi)^4}\,\frac{\alpha^{n-1}\left[(1-\alpha)\not{p} + M\right] - \frac{\gamma^+}{p_-}\,q_- q_+ \frac{d}{d\alpha}\alpha^{n-1}}{[q^2 - (\alpha^2 - \alpha)p^2 - (1-\alpha)M_s^2 - \alpha M^2 + i\varepsilon]^2}, \\
&= \left[4\,G_a\,g_s + \frac{g_a\,g_s}{M_a^2 - M_s^2}\right] p_- \int_0^1 d\alpha\,\alpha^{n-1} \\
&\quad \int \frac{d^4q}{(2\pi)^4}\,\frac{(1-\alpha)\not{p} + M + \frac{\gamma^+}{p_-}\,q_- q_+ \frac{d}{d\alpha}}{[q^2 - (\alpha^2 - \alpha)p^2 - (1-\alpha)M_s^2 - \alpha M^2 + i\varepsilon]^2} \\
&\quad + \left[4\,G_a\,g_s + \frac{g_a\,g_s}{M_a^2 - M_s^2}\right] p_- \\
&\quad \int \frac{d^4q}{(2\pi)^4}\,\left.\frac{-\frac{\gamma^+}{p_-}\,q_- q_+ \alpha^{n-1}}{[q^2 - (\alpha^2 - \alpha)p^2 - (1-\alpha)M_s^2 - \alpha M^2 + i\varepsilon]^2}\right|_0^1.
\end{aligned} \quad (D.325)$$

We first determine the surface term, we have

$$\mathcal{A}_n^{B2:\mathrm{surface}} = -\left[4\,G_a\,g_s + \frac{g_a\,g_s}{M_a^2 - M_s^2}\right] \gamma^+ \int \frac{d^4q}{(2\pi)^4}\,q_- q_+ \left\{\frac{1}{[q^2 - M^2 + i\varepsilon]^2} - \frac{\varepsilon^{n-1}}{[q^2 - M_s^2 + i\varepsilon]^2}\right\}. \quad (D.326)$$

Wick rotating, introducing 4d-polars and the proper-time regularization gives

$$\mathcal{A}_n^{B2:\text{surface}} = i\left[4\,G_a\,g_s + \frac{g_a\,g_s}{M_a^2 - M_s^2}\right]\frac{\gamma^+}{32\pi^2}\int d\tau\,\frac{1}{\tau^2}\left\{e^{-\tau M^2} - \varepsilon^{n-1}e^{-\tau M_s^2}\right\}. \tag{D.327}$$

Summing over the moments and reinserting the factor y gives the result

$$I^{B2:\text{surface}} = i\left[4\,G_a\,g_s + \frac{g_a\,g_s}{M_a^2 - M_s^2}\right]\frac{y\,\gamma^+}{32\pi^2} \int d\tau\,\frac{1}{\tau^2}\left\{\delta(y-1)e^{-\tau M^2} - \delta(y)e^{-\tau M_s^2}\right\}. \tag{D.328}$$

Noting $\lim_{y\to 0}\, y\delta(y) = 0$ and using the earlier matrix element results, we obtain

$$\Delta_T f^{B2:\text{surface}}(y) = \left[4\,G_a\,g_s + \frac{g_a\,g_s}{M_a^2 - M_s^2}\right]\delta(y-1)\,\alpha_1\alpha_3\frac{Z_N}{16\pi^2}\int d\tau\,\frac{1}{\tau^2}e^{-\tau M^2}. \tag{D.329}$$

We now continue with the regular part of I^{B2}. Using the definition of the moments Wick rotating and introducing 4d-polars gives

$$I^{B2}(y) = i\left[4\,G_a\,g_s + \frac{g_a\,g_s}{M_a^2 - M_s^2}\right]\frac{y\,p_-}{16\pi^2} \int dq_E^2\,q_E^2\,\frac{(1-y)\not{p} + M - \frac{\gamma^+}{4p_-}\,q_E^2\frac{d}{dy}}{\left[q_E^2 + (y^2-y)p^2 - (1-y)M_s^2 - yM^2\right]^2}. \tag{D.330}$$

Introducing the proper-time regularization, then integrating over q_E^2 gives

$$I^{B2}(y) = i\left[4\,G_a\,g_s + \frac{g_a\,g_s}{M_a^2 - M_s^2}\right]\frac{y\,p_-}{16\pi^2} \int d\tau\,\frac{1}{\tau}\left[(1-y)\not{p} + M - \frac{\gamma^+}{2\tau\,p_-}\frac{d}{dy}\right]e^{-\tau\left[(y^2-y)p^2+(1-y)M_s^2+yM^2\right]}. \tag{D.331}$$

Using earlier matrix element results and

$$\overline{\Gamma}^1\not{p}\,\Gamma - \overline{\Gamma}\not{p}\,\Gamma^1 = 2\alpha_3\,M_N\,\overline{u}_N\gamma_5\gamma^1 u_N = -2\alpha_3\,M_N, \tag{D.332}$$

we obtain

$$I^{B2}(y) = -i\alpha_3\left[4\,G_a\,g_s + \frac{g_a\,g_s}{M_a^2 - M_s^2}\right]\frac{y\,p_-}{16\pi^2} \int d\tau\,\frac{1}{\tau}\left[2(1-y)M_N + 2M + \frac{p^2}{M_N}(2y-1)\right]e^{-\tau\left[(y^2-y)p^2+(1-y)M_s^2+yM^2\right]}. \tag{D.333}$$

Therefore

$$I^{B2}(y) = -i\alpha_3 \left[4\, G_a\, g_s + \frac{g_a\, g_s}{M_a^2 - M_s^2}\right] \frac{y\, p_-}{16\pi^2} \left[M_N + 2M\right]$$
$$\int d\tau\, \frac{1}{\tau} e^{-\tau\left[(y^2-y)p^2+(1-y)M_s^2+yM^2\right]}. \quad \text{(D.334)}$$

Hence, the full $\Delta_T f^B(y)$ result is

$$\Delta_T f^{B1}(y) = \alpha_1\alpha_3 \frac{G_a\, G_s\, Z_N}{\pi^2}\, y$$
$$\int d\tau\, \frac{1}{\tau^2} \left[\frac{1}{\tau}\frac{d}{dy}\delta(y-1) - 2\, M\, M_N\, \delta(y-1)\right] e^{-\tau\, M^2}. \quad \text{(D.335)}$$

$$\Delta_T f^{B2}(y) = \left[4\, G_a\, g_s + \frac{g_a\, g_s}{M_a^2 - M_s^2}\right] \alpha_1\alpha_3 \frac{Z_N\, M_N}{16\pi^2} \left[M_N + 2M\right] y$$
$$\int d\tau\, \frac{1}{\tau} e^{-\tau\left[(y^2-y)p^2+(1-y)M_s^2+yM^2\right]}$$
$$+ \left[4\, G_a\, g_s + \frac{g_a\, g_s}{M_a^2 - M_s^2}\right] \delta(y-1)\, \alpha_1\alpha_3\, \frac{Z_N}{16\pi^2} \int d\tau\, \frac{1}{\tau^2} e^{-\tau\, M^2}.$$
$$\text{(D.336)}$$

Therefore

$$\Delta_T f^{B3}(y) = \left[4\, G_s\, g_a - \frac{g_a\, g_s}{M_a^2 - M_s^2}\right] \alpha_1\alpha_3 \frac{Z_N\, M_N}{16\pi^2} \left[M_N + 2M\right] y$$
$$\int d\tau\, \frac{1}{\tau} e^{-\tau\left[(y^2-y)p^2+(1-y)M_a^2+yM^2\right]}$$
$$+ \left[4\, G_s\, g_a - \frac{g_a\, g_s}{M_a^2 - M_s^2}\right] \delta(y-1)\, \alpha_1\alpha_3\, \frac{Z_N}{16\pi^2} \int d\tau\, \frac{1}{\tau^2} e^{-\tau\, M^2}.$$
$$\text{(D.337)}$$

Ignoring contact terms we find

$$\Delta_T f^B(y) = \frac{g_a\, g_s}{M_a^2 - M_s^2} \alpha_1\alpha_3 \frac{Z_N\, M_N}{16\pi^2} \left[M_N + 2M\right] y$$
$$\int d\tau\, \frac{1}{\tau} \left[e^{-\tau(1-y)M_s^2} - e^{-\tau(1-y)M_a^2}\right] e^{-\tau\left[(y^2-y)p^2+yM^2\right]}. \quad \text{(D.338)}$$

Summary of $\Delta_T f_{D_m/N}(y, M_D^2)$

We have

$$\Delta_T f_{D_m/N}(y, M_D^2) = \Delta_T f^A(y) - \Delta_T f^B(y)$$
$$= \Delta_T f^{A1} + \Delta_T f^{A2} + \Delta_T f^{A3} - \Delta_T f^{B1} - \Delta_T f^{B2} - \Delta_T f^{B3}. \quad \text{(D.339)}$$

where

$$\Delta_T f^{A1}(y) = \delta(y-1)\,\frac{G_a\,G_s\,Z_N}{\pi^2}\;\alpha_1\,(\alpha_2-\alpha_3)\int d\tau\;\frac{1}{\tau^3}\;e^{-\tau\,M^2}, \quad \text{(D.340)}$$

$$\Delta_T f^{A2}(y) = \left[4\,G_a\,g_s + \frac{g_a\,g_s}{M_a^2 - M_s^2}\right]\frac{Z_N\,\alpha_1\,(\alpha_2-\alpha_3)}{16\pi^2}$$
$$\int d\tau\;\frac{1}{\tau^2}\;e^{-\tau\left[(y^2-y)p^2+(1-y)M_s^2+yM^2\right]}, \quad \text{(D.341)}$$

$$\Delta_T f^{A3}(y) = \left[4\,G_s\,g_a - \frac{g_a\,g_s}{M_a^2 - M_s^2}\right]\frac{Z_N\,\alpha_1\,(\alpha_2-\alpha_3)}{16\pi^2}$$
$$\int d\tau\;\frac{1}{\tau^2}\;e^{-\tau\left[(y^2-y)p^2+(1-y)M_a^2+yM^2\right]}, \quad \text{(D.342)}$$

$$\Delta_T f^{B1}(y) = \alpha_1\alpha_3\frac{G_a\,G_s\,Z_N}{\pi^2}\,y$$
$$\int d\tau\,\frac{1}{\tau^2}\left[\frac{1}{\tau}\,\frac{d}{dy}\delta(y-1) - 2\,M\,M_N\,\delta(y-1)\right]e^{-\tau\,M^2}, \quad \text{(D.343)}$$

$$\Delta_T f^{B2}(y) = \left[4\,G_a\,g_s + \frac{g_a\,g_s}{M_a^2 - M_s^2}\right]$$
$$\alpha_1\alpha_3\frac{Z_N\,M_N}{16\pi^2}\,[M_N + 2M]\;y\int d\tau\;\frac{1}{\tau}e^{-\tau\left[(y^2-y)p^2+(1-y)M_s^2+yM^2\right]}$$
$$+\,\alpha_1\alpha_3\,\delta(y-1)\,\frac{Z_N\,G_a\,g_s}{4\pi^2}\int d\tau\;\frac{1}{\tau^2}e^{-\tau\,M^2}, \quad \text{(D.344)}$$

$$\Delta_T f^{B3}(y) = \left[4\,G_s\,g_a - \frac{g_a\,g_s}{M_a^2 - M_s^2}\right]$$
$$\alpha_1\alpha_3\frac{Z_N\,M_N}{16\pi^2}\,[M_N + 2M]\;y\int d\tau\;\frac{1}{\tau}e^{-\tau\left[(y^2-y)p^2+(1-y)M_a^2+yM^2\right]}$$
$$+\,\alpha_1\alpha_3\,\delta(y-1)\,\frac{Z_N\,G_s\,g_a}{4\pi^2}\int d\tau\;\frac{1}{\tau^2}e^{-\tau\,M^2}, \quad \text{(D.345)}$$

where we have canceled terms between $\Delta_T f^{B2}(y)$ and $\Delta_T f^{B3}(y)$.

D.2 Summary of All Feynman Diagram Results

D.2.1 Scalar Quark Diagrams

Spin-Independent

$$f^{\mathrm{s}}_{q/N}(x) = \frac{\alpha_1^2\, Z_N\, g_s}{16\pi^2}\,(1-x) \int d\tau \left\{\frac{1}{\tau} + x\left[(M_N + M)^2 - M_s^2\right]\right\} e^{-\tau\left[(x^2-x)M_N^2 + xM_s^2 + (1-x)M^2\right]}. \quad \text{(D.346)}$$

Spin-Dependent

$$\Delta f^{\mathrm{s}}_{q/N}(x) = \delta(x)\,\frac{\alpha_1^2\, G_s\, Z_N}{16\pi^2} \int d\tau\, \frac{1}{\tau}\, e^{-\tau M^2} + \frac{\alpha_1^2\, g_s\, Z_N}{16\pi^2}(1-x) \int d\tau \left[(x\, M_N + M)^2 - \frac{1}{\tau}\right] e^{-\tau\left[(x^2-x)M_N^2 + xM_s^2 + (1-x)M^2\right]}. \quad \text{(D.347)}$$

Transversity

$$\Delta_T f^{\mathrm{s}}_{q/N}(x) = \delta(x)\, \frac{\alpha_1^2\, G_s\, Z_N\, M^2}{4\pi^2} \int d\tau\, \frac{1}{\tau}\, e^{-\tau M^2} + \frac{\alpha_1^2\, g_a\, Z_N}{16\pi^2}\,(1-x)\,(x\, M_N + M)^2 \int d\tau\; e^{-\tau\left[(x^2-x)M_N^2 + xM_s^2 + (1-x)M^2\right]}. \quad \text{(D.348)}$$

D.2.2 Axial-Vector Quark Diagrams

Spin-Independent

$$f^{\mathrm{a}}_{q/N}(x) = -\frac{g_a\, Z_N}{16\pi^2}\,(1-x) \int d\tau\, e^{-\tau\left[(x^2-x)M_N^2 + xM_s^2 + (1-x)M^2\right]} \left\{\left(\alpha_2^2 - 2\alpha_2\alpha_3 - 2\alpha_3^2\right)\left[\frac{1}{\tau} + x\,\left[(M_N - M)^2 - M_a^2\right]\right] - 12\alpha_3^2\, x\, M\, M_N\right\}. \quad \text{(D.349)}$$

Spin-Dependent

$$\Delta f^{a}_{q/N}(x) = -\delta(x)\,\frac{G_s\,Z_N}{16\pi^2}\,\left(\alpha_2^2 - 2\alpha_2\alpha_3 + 2\alpha_3^2\right)\int d\tau\,\frac{1}{\tau}\,e^{-\tau\,M^2}$$
$$+\,\frac{g_s\,Z_N}{16\pi^2}\,(1-x)\int d\tau\,e^{-\tau\left[(x^2-x)M_N^2 + xM_s^2 + (1-x)M^2\right]}$$
$$\left\{\left(\alpha_2^2 - 2\alpha_2\alpha_3 + 2\alpha_3^2\right)\left[\frac{1}{\tau} - (xM_N - M)^2\right] - 4MM_N\,x\,\alpha_3^2\right\}. \quad \text{(D.350)}$$

Transversity

$$\Delta_T f^{a}_{q/N}(x) = \delta(x)\,\frac{G_a\,Z_N\,M^2}{4\pi^2}\,\left(\alpha_2^2 - 2\alpha_2\alpha_3\right)\int d\tau\,\frac{1}{\tau}\,e^{-\tau\,M^2}$$
$$+\,\frac{g_a\,Z_N}{16\pi^2}\,(1-x)\left\{\left(\alpha_2^2 - 2\alpha_2\alpha_3\right)[x\,M_N - M]^2 - 4\,\alpha_3^2\,M\,M_N\,x\right\}$$
$$\int d\tau\;e^{-\tau\left[(x^2-x)p^2 + xM_a^2 + (1-x)M^2\right]}. \quad \text{(D.351)}$$

D.2.3 Scalar Diquark Diagrams

Spin-Independent

$$f^{s}_{q(D)/N}(x) \quad = \quad \int_0^1 dy \int_0^1 dz\,\delta(x - yz)\,f^{s}_{q/D}(z) f^{s}_{q/N}(1 \quad - \quad y), \quad \text{(D.352)}$$

where

$$f^{s}_{q/D}(z) = \frac{3}{4\pi^2}\,g_s(M_s)\int_{\frac{1}{(\Lambda_{UV})^2}}^{\frac{1}{(\Lambda_{IR})^2}} d\tau\,\left[\frac{1}{\tau} - (x^2 - x)M_s^2\right]\,e^{-\tau\left[(x^2-x)M_s^2 + M^2\right]}, \quad \text{(D.353)}$$

and $f^{s}_{q/N}(1-y)$ is just the spin-independent scalar quark diagram.

Spin-Dependent

$$\Delta f^{s}_{q(D)/N}(x) = 0. \quad \text{(D.354)}$$

Transversity

$$\Delta_T f^{s}_{q(D)/N}(x) = 0. \quad \text{(D.355)}$$

D.2.4 Axial-Vector Diquark Diagrams

Spin-Independent

$$f^{\mathrm{a}}_{q(D)/N}(x) = \int_0^1 dy \int_0^1 dz\, \delta(x - yz)\, f^{\mathrm{a}}_{q/D}(z) f^{\mathrm{a}}_{q/N}(1-y), \tag{D.356}$$

where

$$f^{\mathrm{a}}_{q/D}(z) = \frac{3\, g_a}{\pi^2}\,(z^2 - z) \int d\tau \left[M_a^2(z^2 - z) - \frac{1}{\tau}\right] e^{-\tau\left[(z^2-z)M_a^2 + M^2\right]}, \tag{D.357}$$

and $f^{\mathrm{a}}_{q/N}(1-y)$ is just the spin-independent axial-vector quark diagram.

Spin-Dependent

$$\Delta f^{\mathrm{a}}_{q(D)/N}(x) = \int_0^1 dy \int_0^1 dz\, \delta(x - yz)\, \Delta f^{\mathrm{a}}_{q/D}(z) \Delta f^{\mathrm{a}}_{D/N}(y), \tag{D.358}$$

where

$$\Delta f^{\mathrm{a}}_{q/D}(z) = -\frac{3\, g_a}{2\pi^2} \int d\tau \left[\frac{(1-2z)}{\tau} - z\,(1-z) M_a^2\right] e^{-\tau\left[(z^2-z)M_a^2 + M^2\right]}, \tag{D.359}$$

$$\Delta f^{\mathrm{a}}_{D/N}(y) = \frac{\alpha_3^2\, g_a\, Z_N}{16\pi^2}\, y \int d\tau$$
$$\left\{\frac{1}{\tau} + (1-y)\left[(M_N + M)^2 - M_a^2\right]\right\} e^{-\tau\left[(y^2-y)p^2 + (1-y)M_a^2 + yM^2\right]}. \tag{D.360}$$

Transversity

$$\Delta_T f^{\mathrm{a}}_{q(D)/N}(x) = \sum_{I \in A,B} \int_0^1 \int_0^1 \delta(x - yz)\, \Delta_T f^{I}_{q/D_a}(z)\, \Delta_T f^{I}_{D_a/N}(y), \tag{D.361}$$

where

$$\Delta_T f^{A}_{q/D_a}(z) = -g_a\, \frac{3M}{2\pi^2} \int d\tau\, \frac{1}{\tau}\, e^{-\tau\left[(z^2-z)M_a^2 + M^2\right]}, \tag{D.362}$$

$$\Delta_T f^{B}_{q/D_a}(z) = g_a\, \frac{3M}{\pi^2}\, z(1-z) \int d\tau\, e^{-\tau\left[(z^2-z)M_a^2 + M^2\right]}, \tag{D.363}$$

$$\Delta_T f^A_{D_a/N}(y) = -\frac{g_a\, Z_N}{16\pi^2} \int d\tau\; e^{-\tau\left[\left(y^2-y\right)p^2+(1-y)M_a^2+yM^2\right]}$$
$$\left\{\frac{\alpha_2\alpha_3}{M_N}\left[\frac{1}{\tau}+(1-y)\left[(2y-1)\,p^2-M_a^2+M^2\right]\right]\right.$$
$$\left. +\,2\alpha_3^2\,(1-y)\left[(1-y)M_N+M\right]\right\}, \quad \text{(D.364)}$$

$$\Delta_T f^B_{D_a/N}(y) = -\frac{g_a\, Z_N}{16\pi^2} \int d\tau\;\frac{1}{\tau}\; \epsilon^{-\tau\left[\left(y^2-y\right)p^2+(1-y)M_a^2+yM^2\right]}$$
$$\left\{\frac{\alpha_2\alpha_3}{2M_N}\left[\frac{1}{\tau}+2y(1-y)M_N^2+\left[(2y-1)M_N^2-M_a^2+M^2\right]\right.\right.$$
$$\left.\left[1+y+\tau\, y(1-y)\left[(2y-1)M_N^2-M_a^2+M^2\right]\right]\right]$$
$$-\,\alpha_3^2\left[(2y-1)M_N-M+\tau y(1-y)\right.$$
$$\left.\left.\left[2y^2M_N^3-\left[(2y-1)M_N-M\right]\left(M_N^2+M_a^2-M^2\right)\right]\right]\right\}. \quad \text{(D.365)}$$

The function $\Delta f^B_{D_a/N}(y)$ also has a surface term of the form

$$\Delta_T f^{B\text{:surface}}_{D_a/N}(y) = \frac{g_a\,\alpha_2\alpha_3\,Z_N}{32\pi^2\,M_N}$$
$$\int d\tau\;\frac{1}{\tau^2}\left[\delta(y-1)e^{-\tau M^2}+\delta(y)\,e^{-\tau M_a^2}\right]. \quad \text{(D.366)}$$

D.2.5 Mixed Diquark Diagrams

Spin-Independent

$$f^{\mathrm{m}}_{q(D)/N}(x) = 0. \quad \text{(D.367)}$$

Spin-Dependent

$$\Delta f^{\mathrm{m}}_{q(D)/N}(x) = \sum_{I\in A,B}\int_0^1\!\!\int_0^1 \delta(x-yz)\,\Delta f^I_{q/D_m}(z)\,\Delta f^I_{D_m/N}(y), \quad \text{(D.368)}$$

where

$$f^A_{q/D_m}(z,q^2) = \frac{3M}{\pi^2}\, z(1-z) \int d\tau\, e^{-\tau\left[(z^2-z)q^2+M^2\right]}, \tag{D.369}$$

$$f^B_{q/D_m}(z,q^2) = -\frac{3M}{2\pi^2} \int d\tau\, \left[\frac{1}{\tau} + 2z(1-z)q^2\right] e^{-\tau\left[(z^2-z)q^2+M^2\right]}. \tag{D.370}$$

The diquark term has the form

$$\Delta f^I_{D_m/N}(y) = \Delta f^{I1}(y) + \Delta f^{I2}(y) + \Delta f^{I3}(y) + \Delta f^{I\text{surface}}(y), \tag{D.371}$$

where

$$\Delta f^{A1}(y) = \alpha_1 \frac{G_a\, G_s\, Z_N}{2\pi^2}\, y \int d\tau \frac{1}{\tau^3}\Big[2\left[\alpha_2\, M_N - \alpha_3\,(M_N+M)\right] - \alpha_2 \frac{2}{M_N\,\tau}\frac{d}{dy}\Big] \frac{d}{dy}\,\delta(y-1)\, e^{-\tau\, M^2}, \tag{D.372}$$

$$\Delta f^{A2}(y) = \left[4\, G_a\, g_s + \frac{g_a\, g_s}{M_a^2 - M_s^2}\right] \frac{\alpha_1 Z_N}{16\pi^2}\, y \left\{\frac{\alpha_2}{2\, M_N}\,\left[M_N^2 + M_s^2 - M^2\right] - \alpha_3\left[M_N + M\right]\right\} \left[(2y-1)M_N^2 - M_s^2 + M^2\right] \int d\tau\, \frac{1}{\tau} e^{-\tau\left[(y^2-y)p^2+(1-y)M_s^2+yM^2\right]}, \tag{D.373}$$

$$\Delta f^{A3}(y) = \left[4\, G_s\, g_a - \frac{g_a\, g_s}{M_a^2 - M_s^2}\right] \frac{\alpha_1 Z_N}{16\pi^2}\, y \left\{\frac{\alpha_2}{2\, M_N}\,\left[M_N^2 + M_a^2 - M^2\right] - \alpha_3\left[M_N + M\right]\right\} \left[(2y-1)M_N^2 - M_a^2 + M^2\right] \int d\tau\, \frac{1}{\tau} e^{-\tau\left[(y^2-y)p^2+(1-y)M_a^2+yM^2\right]}, \tag{D.374}$$

$$\Delta f^{A\text{surface}}(y) = \delta(y-1)\,(G_a\, g_s + G_s\, g_a) \frac{\alpha_1\, Z_N}{4\pi^2} \int d\tau \frac{1}{\tau^2}\, \left[\alpha_3\, M + (\alpha_3 - \alpha_2) M_N + \frac{\alpha_2}{3\tau}\right] e^{-\tau\, M^2} + \delta(y)\, \frac{Z_N}{96\pi^2}\, \alpha_1\alpha_2 \int d\tau\, \frac{1}{\tau^2} \left\{\left[4\, G_a\, g_s + \frac{g_a\, g_s}{M_a^2 - M_s^2}\right] e^{-\tau\, M_s^2} + \left[4\, G_s\, g_a - \frac{g_a\, g_s}{M_a^2 - M_s^2}\right] e^{-\tau\, M_a^2}\right\}. \tag{D.375}$$

$$\Delta f^{B1}(y) = -\frac{\alpha_1\, Z_N\, G_a\, G_s}{\pi^2}$$
$$\int d\tau\, \frac{1}{\tau^2} \left[2\alpha_3\, M\, \delta(y-1) - \frac{\alpha_2}{\tau M_N}\frac{d}{dy}\delta(y-1)\right] e^{-\tau\, M^2}, \tag{D.376}$$

$$\Delta f^{B2} = \left[4\, G_a\, g_s + \frac{g_a\, g_s}{M_a^2 - M_s^2}\right] \frac{\alpha_1 Z_N}{8\pi^2}$$
$$\left\{\alpha_3\left[(1-y)M_N + M\right] + \frac{\alpha_2}{2M_N}\left[(2y-1)M_N^2 - M_s^2 + M^2\right]\right\}$$
$$\int d\tau\, \frac{1}{\tau} e^{-\tau\left[(y^2-y)p^2+(1-y)M_s^2+yM^2\right]}, \tag{D.377}$$

$$\Delta f^{B3} = \left[4\, G_s\, g_a - \frac{g_a\, g_s}{M_a^2 - M_s^2}\right] \frac{\alpha_1 Z_N}{8\pi^2}$$
$$\left\{\alpha_3\left[(1-y)M_N + M\right] + \frac{\alpha_2}{2M_N}\left[(2y-1)M_N^2 - M_a^2 + M^2\right]\right\}$$
$$\int d\tau\, \frac{1}{\tau} e^{-\tau\left[(y^2-y)p^2+(1-y)M_a^2+yM^2\right]}, \tag{D.378}$$

$$\Delta f^{B\mathrm{surface}}(y) = \delta(y-1)\left[4\, G_a\, g_s + 4\, G_a\, g_s\right] \frac{Z_N\, \alpha_1\alpha_2}{16\pi^2\, M_N} \int d\tau \frac{1}{\tau^2} e^{-\tau\, M^2}$$
$$+\, \delta(y)\, \frac{Z_N\, \alpha_1\alpha_2}{16\pi^2\, M_N} \int d\tau\, \frac{1}{\tau^2}\left\{\left[4\, G_a\, g_s + \frac{g_a\, g_s}{M_a^2 - M_s^2}\right] e^{-\tau\, M_s^2}\right.$$
$$\left. + \left[4\, G_s\, g_a - \frac{g_a\, g_s}{M_a^2 - M_s^2}\right] e^{-\tau\, M_a^2}\right\}. \tag{D.379}$$

Transversity

$$\Delta_T f^{\mathrm{m}}_{q(D)/N}(x) = \int_0^1 \int_0^1 \delta(x - yz)\, \Delta_T f_{q/D_m}(z)\, \Delta_T f_{D_m/N}(y), \tag{D.380}$$

where

$$\Delta_T f_{q/D_m}(z, q^2) = \frac{3}{2\pi^2}\, z \int d\tau\ \left[(1-z)q^2 + \frac{1}{\tau}\right] e^{-\tau\left[(z^2-z)q^2+M^2\right]}, \tag{D.381}$$

and $\Delta_T f_{D_m/N}(y)$ has the form

$$\begin{aligned}\Delta_T f_{D_m/N}(y) &= \Delta_T f^A_{D_m/N}(y) - \Delta_T f^B_{D_m/N}(y)\\ &= \Delta_T f^{A1}(y) + \Delta_T f^{A2}(y) + \Delta_T f^{A3}(y)\\ &\quad - \Delta_T f^{B1}(y) - \Delta_T f^{B2}(y) - \Delta_T f^{B3}(y) - \Delta f^{B\text{surface}}(y),\end{aligned} \tag{D.382}$$

where

$$\Delta_T f^{A1}(y) = \delta(y-1)\,\frac{G_a\,G_s\,Z_N}{\pi^2}\,\alpha_1\,(\alpha_2-\alpha_3)\int d\tau\,\frac{1}{\tau^3}\,e^{-\tau\,M^2}, \tag{D.383}$$

$$\begin{aligned}\Delta_T f^{A2}(y) = &\left[4\,G_a\,g_s + \frac{g_a\,g_s}{M_a^2-M_s^2}\right]\\ &\frac{Z_N\,\alpha_1\,(\alpha_2-\alpha_3)}{16\pi^2}\int d\tau\,\frac{1}{\tau^2}\,e^{-\tau\left[(y^2-y)p^2+(1-y)M_s^2+yM^2\right]},\end{aligned} \tag{D.384}$$

$$\begin{aligned}\Delta_T f^{A3}(y) = &\left[4\,G_s\,g_a - \frac{g_a\,g_s}{M_a^2-M_s^2}\right]\\ &\frac{Z_N\,\alpha_1\,(\alpha_2-\alpha_3)}{16\pi^2}\int d\tau\,\frac{1}{\tau^2}\,e^{-\tau\left[(y^2-y)p^2+(1-y)M_a^2+yM^2\right]},\end{aligned} \tag{D.385}$$

$$\begin{aligned}\Delta_T f^{B1}(y) = &\,\alpha_1\alpha_3\frac{G_a\,G_s\,Z_N}{\pi^2}\,y\\ &\int d\tau\,\frac{1}{\tau^2}\left[\frac{1}{\tau}\frac{d}{dy}\delta(y-1) - 2\,M\,M_N\,\delta(y-1)\right]e^{-\tau\,M^2},\end{aligned} \tag{D.386}$$

$$\begin{aligned}\Delta_T f^{B2}(y) = &\left[4\,G_a\,g_s + \frac{g_a\,g_s}{M_a^2-M_s^2}\right]\\ &\alpha_1\alpha_3\frac{Z_N\,M_N}{16\pi^2}\,[M_N+2M]\;y\int d\tau\,\frac{1}{\tau}e^{-\tau\left[(y^2-y)p^2+(1-y)M_s^2+yM^2\right]},\end{aligned} \tag{D.387}$$

$$\begin{aligned}\Delta_T f^{B3}(y) = &\left[4\,G_s\,g_a - \frac{g_a\,g_s}{M_a^2-M_s^2}\right]\\ &\alpha_1\alpha_3\frac{Z_N\,M_N}{16\pi^2}\,[M_N+2M]\;y\int d\tau\,\frac{1}{\tau}e^{-\tau\left[(y^2-y)p^2+(1-y)M_a^2+yM^2\right]},\end{aligned} \tag{D.388}$$

$$\Delta f^{B\text{surface}}(y) = \delta(y-1)\,\frac{\alpha_1\alpha_3\,Z_N}{4\pi^2}\,(G_a\,g_s + G_s\,g_a)\int d\tau\,\frac{1}{\tau^2}e^{-\tau\,M^2}. \tag{D.389}$$

Ignoring contact terms we find

$$\Delta_T f^A_{D_m/N}(y) = \frac{g_a\, g_s}{M_a^2 - M_s^2}\alpha_1 \frac{Z_N\,(\alpha_2 - \alpha_3)}{16\pi^2}$$
$$\int d\tau\ \frac{1}{\tau^2}\left[e^{-\tau(1-y)M_s^2} - e^{-\tau(1-y)M_a^2}\right] e^{-\tau\left[(y^2-y)p^2+yM^2\right]}, \tag{D.390}$$

$$\Delta_T f^B_{D_m/N}(y) = \frac{g_a\, g_s}{M_a^2 - M_s^2}\alpha_1\alpha_3 \frac{Z_N\, M_N}{16\pi^2}\,[M_N + 2M]\ y$$
$$\int d\tau\ \frac{1}{\tau}\left[e^{-\tau(1-y)M_s^2} - e^{-\tau(1-y)M_a^2}\right] e^{-\tau\left[(y^2-y)p^2+yM^2\right]}. \tag{D.391}$$

E

Derivation of the Infinite Nuclear Matter Distribution Function

We begin with Eq. (5.26) which has the form

$$f_{N/A}(y_A) = -i\frac{\sqrt{2}}{\rho}\int \frac{d^4p}{(2\pi)^4}\delta\left(y_A - \frac{\sqrt{2}\,p_-}{\varepsilon_F}\right)\mathrm{Tr}\left[\gamma^+ S_{ND}(p)\right], \tag{E.1}$$

where

$$S_{ND}(p) = i\pi\,\frac{\not p - 3\not V + M_N}{E_p}\,\delta\left(p_0 - 3V_0 - E_p\right)\Theta\left(p_F - |\vec{p}\,|\right). \tag{E.2}$$

Evaluating the trace gives

$$\mathrm{Tr}\left[\gamma^+ S_{ND}(p)\right] = 4i\pi\,\delta\left(p_0 - 3V_0 - E_p\right)\Theta\left(p_F - |\vec{p}\,|\right)\frac{p^+ - 3V^+}{E_p}. \tag{E.3}$$

Using the delta function to remove the p_0 integration in Eq. (E.1) we obtain

$$f_{N/A}(y_A) = \frac{2}{\rho}\int \frac{d^3\vec{p}}{(2\pi)^3}\delta\left(y_A - \frac{E_p + 3V_0 + p^3}{\varepsilon_F}\right)\Theta\left(p_F - |\vec{p}\,|\right)\frac{E_p + p^3}{E_p}. \tag{E.4}$$

Making the change of variables

$$\xi = E_p + p^3, \qquad \Longrightarrow \qquad d\xi = \frac{E_p + p^3}{E_p}\,dp^3. \tag{E.5}$$

Therefore Eq. (E.4) becomes

$$f_{N/A}(y_A) = \frac{2}{\rho}\int \frac{d^2\vec{p}_\perp}{(2\pi)^3}\,d\xi\;\delta\left(y_A - \frac{\xi + 3V_0}{\varepsilon_F}\right)\Theta\left(p_F - |\vec{p}\,|\right). \tag{E.6}$$

The constraint imposed by the Θ-function can be re-expressed as

$$\Theta\left(p_F - |\vec{p}\,|\right) \quad\longrightarrow\quad \Theta\left[p_F^2 - \vec{p}_\perp^{\,2} - (\xi - E_F)^2\right]. \tag{E.7}$$

Therefore, using the remaining delta function to remove the ξ integration, Eq. (E.6) becomes

$$\begin{aligned} f_{N/A}(y_A) &= \frac{2}{\rho}\int \frac{d^2\vec{p}_\perp}{(2\pi)^3}\,\varepsilon_F\,\Theta\left[p_F^2 - \vec{p}_\perp^{\,2} - (\varepsilon_F\,y_A - 3V_0 - E_F)^2\right], \\ &= \frac{1}{4\pi^3\,\rho}\int d^2\vec{p}_\perp\,\varepsilon_F\,\Theta\left[p_F^2 - \vec{p}_\perp^{\,2} - (\varepsilon_F\,y_A - \varepsilon_F)^2\right]. \end{aligned} \tag{E.8}$$

Using

$$\int d^2\vec{p}_\perp \to 2\pi \int dp \to \pi \int dp^2 \qquad \text{and} \qquad p_\perp^2 \to \frac{1}{2}p^2, \tag{E.9}$$

we obtain

$$\begin{aligned} f_{N/A}(y_A) &= \frac{1}{4\pi^2\,\rho} \int dp^2\ \varepsilon_F\ \Theta\left[p_F^2 - \frac{1}{2}p^2 - \varepsilon_F^2\,(1-y_A)^2\right], \\ &= \frac{1}{2\pi^2\,\rho}\varepsilon_F\ \left[p_F^2 - \varepsilon_F^2\,(1-y_A)^2\right]. \end{aligned} \tag{E.10}$$

The density is related to the Fermi momentum via

$$\rho = \frac{2}{3\pi^2}\,p_F^2. \tag{E.11}$$

Therefore we obtain the final result

$$f_{N/A}(y_A) = \frac{3}{4}\left(\frac{\varepsilon_F}{p_F}\right)^3 \left[\left(\frac{p_F}{\varepsilon_F}\right)^2 - (1-y_A)^2\right]. \tag{E.12}$$

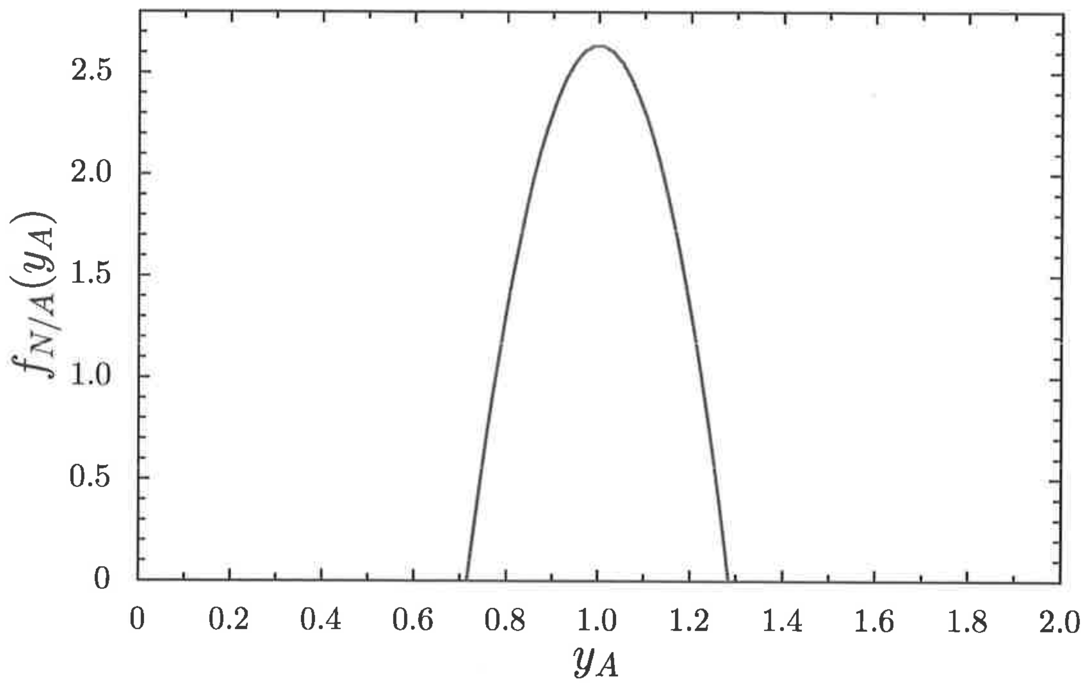

Figure E.1: Plot of Eq. (E.12) with values for the Fermi energy and Fermi momentum taken from chapter 5, namely $\varepsilon_F = 924.3\,\text{MeV}$ and $p_F = 263\,\text{MeV}$.

F

Dirac Equation with Scalar and Vector Potentials

F.1 Coordinate Space Derivation

The Dirac equation with spherically symmetric scalar, $V_s(r)$ and vector, $V^\mu = (V_v(r), \vec{0}\,)$, potentials has the form

$$\left[-i\,\vec{\alpha}\cdot\vec{\nabla} + \beta\,[M(r) - V_s(r)] + V_v(r)\right]\psi(r) = E\,\psi(r), \tag{F.1}$$

where

$$\vec{\alpha} = \begin{pmatrix} 0 & \vec{\sigma} \\ \vec{\sigma} & 0 \end{pmatrix}, \qquad \beta = \begin{pmatrix} \mathbb{1} & 0 \\ 0 & -\mathbb{1} \end{pmatrix}. \tag{F.2}$$

It is easy to show that the operators $\boldsymbol{J}^2$, $\boldsymbol{J}_z$ and $\boldsymbol{\mathcal{P}} = \gamma_0 \boldsymbol{P}$ commute with the Hamiltonian, and hence their eigenvalues are constants of the motion. Simultaneous eigenfunctions of these operators can be written as

$$\psi_{j\ell m}(\vec{r}\,) = \begin{pmatrix} \psi^A_{j\ell m} \\ \psi^B_{j\ell m} \end{pmatrix} = \begin{pmatrix} F(r)\,\Omega_{\ell s j m}(\theta,\phi) \\ iG(r)\,\Omega_{\tilde{\ell} s j m}(\theta,\phi) \end{pmatrix}, \tag{F.3}$$

where the spherical two-spinor has the form

$$\Omega_{\ell s j m}(\theta,\phi) = \sum_{m_\ell, m_s} \langle \ell\, m_\ell\, s\, m_s | j\, m\rangle\, Y_{\ell m_\ell}(\theta,\phi)\; \chi_{s m_s}. \tag{F.4}$$

The spin vectors are given by $\chi_{\frac{1}{2}\frac{1}{2}} = \binom{1}{0}$ and $\chi_{\frac{1}{2}-\frac{1}{2}} = \binom{0}{1}$. Recall that the parity operator acting on the spherical harmonics gives

$$\boldsymbol{P}\,Y_{\ell m}(\theta,\phi) = Y_{\ell m}(\pi-\theta, \phi+\pi) = (-1)^\ell\, Y_{\ell m}(\theta,\phi), \tag{F.5}$$

hence

$$\boldsymbol{\mathcal{P}}\psi_{j\ell m}(\vec{r}\,) = \begin{pmatrix} (-1)^\ell\; F(r)\,\Omega_{\ell s j m}(\theta,\phi) \\ -(-1)^{\tilde{\ell}}\; iG(r)\,\Omega_{\tilde{\ell} s j m}(\theta,\phi) \end{pmatrix}. \tag{F.6}$$

Therefore if $\psi_{jm}(r)$ is to be an eigenstate of parity we must have $\tilde{\ell} = \ell \pm 1$. Now if ℓ and s couple such that $j = \ell + \frac{1}{2}$, in order for $\tilde{\ell}$ and s to couple to give the same j we must have $\tilde{\ell} = \ell + 1$. Similarly if ℓ and s couple such that $j = \ell - \frac{1}{2}$ we must have $\tilde{\ell} = \ell - 1$. Therefore in summary

$$\tilde{\ell} = \begin{cases} \ell + 1 & \text{for} \;\; j = \ell + \frac{1}{2}, \\ \ell - 1 & \text{for} \;\; j = \ell - \frac{1}{2}. \end{cases} \tag{F.7}$$

In relativistic systems it is convenient to introduce another operator that also commutes with the Hamiltonian, $\boldsymbol{K} = \beta\,(\boldsymbol{\sigma}\cdot\boldsymbol{L} + 1)$, which satisfies the eigenvalue equation $\boldsymbol{K}\psi_{j\ell m} = -\kappa\,\psi_{j\ell m}$ and is sometimes called the eccentricity or Runge-Lenz operator. Evaluating the eigenvalue equation we have

$$\begin{aligned} \boldsymbol{K}\psi_{j\ell m} &= \begin{pmatrix} \boldsymbol{\sigma}\cdot\boldsymbol{L}+1 & 0 \\ 0 & -[\boldsymbol{\sigma}\cdot\boldsymbol{L}+1] \end{pmatrix} \begin{pmatrix} \psi^A_{j\ell m} \\ \psi^B_{j\ell m} \end{pmatrix}, \\ &= \begin{pmatrix} \boldsymbol{J}^2 - \boldsymbol{L}^2 - \boldsymbol{S}^2 + 1 & 0 \\ 0 & -\left[\boldsymbol{J}^2 - \boldsymbol{L}^2 - \boldsymbol{S}^2 + 1\right] \end{pmatrix} \begin{pmatrix} \psi^A_{j\ell m} \\ \psi^B_{j\ell m} \end{pmatrix}, \\ &= \begin{pmatrix} j(j+1) - \ell(\ell+1) + \frac{1}{4} & 0 \\ 0 & -\left[j(j+1) - \tilde{\ell}(\tilde{\ell}+1) + \frac{1}{4}\right] \end{pmatrix} \begin{pmatrix} \psi^A_{j\ell m} \\ \psi^B_{j\ell m} \end{pmatrix}. \end{aligned} \tag{F.8}$$

If $j = \ell + \frac{1}{2}$, which implies $\ell = j - \frac{1}{2}$ and $\tilde{\ell} = j + \frac{1}{2}$ we have

$$\boldsymbol{K}\psi_{j\ell m} = \left(j + \tfrac{1}{2}\right)\psi_{j\ell m} = -\kappa\psi_{j\ell m}, \tag{F.9}$$

hence if $\kappa < 0$, j, ℓ and $\tilde{\ell}$ must satisfy the above conditions. Similarly if $j = \ell - \frac{1}{2}$, which implies $\ell = j + \frac{1}{2}$ and $\tilde{\ell} = j - \frac{1}{2}$ we have

$$\boldsymbol{K}\psi_{j\ell m} = -\left(j + \tfrac{1}{2}\right)\psi_{j\ell m} = -\kappa\psi_{j\ell m}, \tag{F.10}$$

which implies $\kappa > 0$. Therefore the sign and magnitude of κ determines both j, ℓ and hence $\tilde{\ell}$. In summary we have

$$\begin{aligned} \kappa < 0 \quad &\Longrightarrow \quad \kappa = -\left(j + \tfrac{1}{2}\right), \quad j = \ell + \tfrac{1}{2} = -\kappa - \tfrac{1}{2}, \\ &\qquad\qquad \longrightarrow \quad \ell = -\left(\kappa + 1\right), \qquad \tilde{\ell} = \ell + 1 = -\kappa, \end{aligned} \tag{F.11}$$

$$\begin{aligned} \kappa > 0 \quad &\Longrightarrow \quad \kappa = +\left(j + \tfrac{1}{2}\right), \quad j = \ell - \tfrac{1}{2} = \kappa - \tfrac{1}{2}, \\ &\qquad\qquad \longrightarrow \quad \ell = \kappa, \qquad \tilde{\ell} = \ell - 1 = \kappa - 1, \end{aligned} \tag{F.12}$$

note in both cases we have $j = |\kappa| - \frac{1}{2}$. We can therefore label our states with the more compact notation $\Omega_{\kappa m} \equiv \Omega_{j\ell m}$. Therefore the complete states can be labeled

$$\psi_{n\kappa m}(\vec{r}) = \begin{pmatrix} F_{n\kappa}(r)\,\Omega_{\kappa m}(\theta,\phi) \\ iG_{n\kappa}(r)\,\Omega_{-\kappa m}(\theta,\phi) \end{pmatrix}, \tag{F.13}$$

where we have also included the radial quantum number, n, for completeness. Note the spherical two-spinors satisfy the orthogonality relation

$$\int_0^{\pi} d\theta \, \sin\theta \int_0^{2\pi} d\phi \; \Omega^{\dagger}_{\kappa' m'}(\theta,\phi)\Omega_{\kappa m}(\theta,\phi)$$
$$= \int_{-1}^{1} d\left(\cos\theta\right) \int_0^{2\pi} d\phi \; \Omega^{\dagger}_{\kappa' m'}(\theta,\phi)\Omega_{\kappa m}(\theta,\phi) = \delta_{\kappa'\kappa}\delta_{m'm}. \quad \text{(F.14)}$$

The states are normalized such that

$$\int d^3r \; \psi^{\dagger}_{\kappa m}(\vec{r}) \, \psi_{\kappa m}(\vec{r}) = 1, \quad \text{(F.15)}$$

which using Eq. (F.14) reduces to

$$\int_0^{\infty} dr \, r^2 \left[F_{\kappa}(r)^2 + G_{\kappa}(r)^2\right] = 1. \quad \text{(F.16)}$$

Assuming the complete solution of the Dirac equation is of the form $\psi(x) = \psi_{n\kappa m}(\vec{r}) \, e^{iEt}$, we obtain

$$\begin{pmatrix} M - V_s + V_v & -i\,\vec{\sigma}\cdot\vec{\nabla} \\ -i\,\vec{\sigma}\cdot\vec{\nabla} & V_v - M + V_s \end{pmatrix} \begin{pmatrix} F_{n\kappa}(r)\,\Omega_{\kappa m}(\theta,\phi) \\ iG_{n\kappa}(r)\,\Omega_{-\kappa m}(\theta,\phi) \end{pmatrix}$$
$$= E \begin{pmatrix} F_{n\kappa}(r)\,\Omega_{\kappa m}(\theta,\phi) \\ iG_{n\kappa}(r)\,\Omega_{-\kappa m}(\theta,\phi) \end{pmatrix}. \quad \text{(F.17)}$$

To simplify this equation we note

$$\vec{\sigma}\cdot\vec{\nabla} = \frac{\vec{\sigma}\cdot\vec{r}}{r^2}\left(\vec{\sigma}\cdot\vec{r}\,\vec{\sigma}\cdot\vec{\nabla}\right). \quad \text{(F.18)}$$

Using the identity

$$\vec{\sigma}\cdot\vec{a}\,\vec{\sigma}\cdot\vec{b} = \vec{a}\cdot\vec{b} + i\vec{\sigma}\cdot\left(\vec{a}\times\vec{b}\right), \quad \text{(F.19)}$$

we have

$$\vec{\sigma}\cdot\vec{\nabla} = \frac{\vec{\sigma}\cdot\vec{r}}{r^2}\left(\vec{r}\cdot\vec{\nabla} + i\vec{\sigma}\cdot\left(\vec{r}\times\vec{\nabla}\right)\right) = \frac{\vec{\sigma}\cdot\vec{r}}{r^2}\left(r\frac{\partial}{\partial r} - \vec{\sigma}\cdot\vec{L}\right). \quad \text{(F.20)}$$

To simplify further we need the following results

$$\boldsymbol{\sigma}\cdot\boldsymbol{L}\,\Omega_{\kappa m} = \left(\boldsymbol{J}^2 - \boldsymbol{L}^2 - \boldsymbol{S}^2\right)\,\Omega_{\kappa m} = -\left(\kappa + 1\right)\,\Omega_{\kappa m}, \quad \text{(F.21)}$$
$$\boldsymbol{\sigma}\cdot\hat{r}\,\Omega_{\kappa m} = -\Omega_{-\kappa m}, \quad \text{(F.22)}$$

the first of which is easily derived using previous results (see Eq. (F.8)). The second is obtained by noting that the quantity $\boldsymbol{\sigma} \cdot \hat{r}\, \Omega_{\kappa m}$ has the same quantum numbers j and m, but opposite parity to $\Omega_{\kappa m}$, then an explicit calculation shows that the proportionality constant is -1. Using these results we obtain

$$\vec{\sigma} \cdot \vec{\nabla}\, \Omega_{\kappa m} = -\left(\frac{\partial}{\partial r} + \frac{1+\kappa}{r}\right) \Omega_{-\kappa m}. \tag{F.23}$$

Substituting the above result into Eq. (F.17), we find that the Dirac equation reduces to two coupled first order partial differential equations given by

$$\left(\frac{\partial}{\partial r} + \frac{1+\kappa}{r}\right) F_{n\kappa}(r) = (M + E - V)\, G_{n\kappa}, \tag{F.24}$$

$$\left(\frac{\partial}{\partial r} + \frac{1-\kappa}{r}\right) G_{n\kappa}(r) = (M - E - \Delta)\, F_{n\kappa}, \tag{F.25}$$

where we have defined $V = V_s + V_v$ and $\Delta = V_s - V_v$. These equations can be rearranged to give

$$F_\kappa(r) = \frac{1}{M - E - \Delta(r)} \left(G'_\kappa(r) + \frac{1-\kappa}{r}\, G_\kappa(r)\right), \tag{F.26}$$

$$G_\kappa(r) = \frac{1}{M + E - V(r)} \left(F'_\kappa(r) + \frac{1-\kappa}{r}\, F_\kappa(r)\right). \tag{F.27}$$

It is then trivial to decouple Eqs. (F.24) and (F.25), giving

$$F''_\kappa + \frac{2}{r} F'_\kappa + \frac{1-\kappa^2}{r} F_\kappa + \frac{\Delta'}{M - E - \Delta}\left(F'_\kappa + \frac{1-\kappa}{r} F_\kappa\right) - (M - E - \Delta)(M + E - V)\, F_\kappa = 0, \tag{F.28}$$

$$G''_\kappa + \frac{2}{r} G'_\kappa + \frac{1-\kappa^2}{r} G_\kappa + \frac{\Delta'}{M - E - \Delta}\left(G'_\kappa + \frac{1-\kappa}{r} G_\kappa\right) - (M - E - \Delta)(M + E - V)\, G_\kappa = 0. \tag{F.29}$$

From Eqs. (F.26) and (F.27) it is easy to derive the relation

$$r^2 F_\kappa(r) \cdot G_\kappa(r) = \frac{\frac{\partial}{\partial r}\left(r^2\left[F_\kappa(r)^2 + G_\kappa(r)^2\right]\right)}{4M^*} - \frac{\kappa\, r}{2M^*}\left[F_\kappa(r)^2 - G_\kappa(r)^2\right], \tag{F.30}$$

where $M^* = M - V_s(r)$, which is useful if one wishes to take the non-relativistic limit.

F.2 Momentum space solutions

For the present application, that is nuclear structure functions, we require momentum space solutions to the Dirac equation, $\phi_{\kappa m}(\vec{p})$, which can be obtained from $\psi_{\kappa m}(\vec{r})$ via Fourier transform, therefore

$$\phi_{\kappa m}(\vec{p}) = \int d^3r\, e^{-i\vec{p}\cdot\vec{r}}\, \psi_{\kappa m}(\vec{r}). \tag{F.31}$$

If we consider the upper component first we have

$$\phi^{A}_{\kappa m}(\vec{p}) = \int d^3r\, e^{-i\vec{p}\cdot\vec{r}}\, F_\kappa(r)\Omega_{\kappa m}(\theta,\phi)\,. \tag{F.32}$$

Using

$$\begin{aligned} e^{-i\vec{p}\cdot\vec{r}} &= 4\pi \sum_{L=0}^{\infty}\sum_{m=-L}^{L} (-i)^L j_L(pr)\, Y^*_{LM}(\Omega_r)\, Y_{LM}(\Omega_p) \\ &= 4\pi \sum_{L=0}^{\infty}\sum_{m=-L}^{L} (-i)^L j_L(pr)\, Y^*_{LM}(\Omega_p)\, Y_{LM}(\Omega_r)\,, \end{aligned} \tag{F.33}$$

where Ω_p are the angles (θ,ϕ) for $\vec{p}$ and Ω_r the angles for $\vec{r}$, we obtain

$$\begin{aligned} \phi^{A}_{\kappa m}(\vec{p}) &= 4\pi \int d^3r \sum_{L,M} (-i)^L j_L(pr)\, Y^*_{LM}(\Omega_r)\, Y_{LM}(\Omega_p)\; F_\kappa(r)\, \Omega_{\kappa m}(\theta,\phi)\,, \\ &= 4\pi \int dr\, r^2 \sum_{L,M} (-i)^L j_L(pr)\, F_\kappa(r) \\ &\qquad \left(\int d\Omega_r Y^*_{LM}(\Omega_r)\; \Omega_{\kappa m}(\theta_r,\phi_r)\right) Y_{LM}(\Omega_p)\,, \\ &= 4\pi \int dr\, r^2 \sum_{L,M} (-i)^L j_L(pr)\, F_\kappa(r) \\ &\qquad \sum_{m_\ell, m_s} \langle \ell\, m_\ell\, s\, m_s | j\, m\rangle \left(\int d\Omega_r Y^*_{LM}(\Omega_r)\; Y_{\ell m_\ell}(\Omega_r)\right) Y_{LM}(\Omega_p)\,, \\ &= 4\pi \int dr\, r^2 \sum_{L,M} (-i)^L j_L(pr)\, F_\kappa(r) \\ &\qquad \sum_{m_\ell, m_s} \langle \ell\, m_\ell\, s\, m_s | j\, m\rangle\, (\delta_{L\ell}\delta_{M m_\ell})\, Y_{LM}(\Omega_p)\,, \\ &= 4\pi \int dr\, r^2\, (-i)^\ell j_\ell(pr)\, F_\kappa(r) \sum_{m_\ell, m_s} \langle \ell\, m_\ell\, s\, m_s | j\, m\rangle\, Y_{\ell m_\ell}(\Omega_p)\,, \end{aligned}$$

$$
\begin{aligned}
&= (-i)^\ell \left(4\pi \int dr\, r^2\, j_\ell\,(pr)\, F_\kappa(r)\right) \Omega_{\kappa m}(\Omega_p)\,, \\
&\equiv (-i)^\ell F(p)\, \Omega_{\kappa m}(\theta,\phi)\,.
\end{aligned}
\tag{F.34}
$$

Similarly, for the lower component we find

$$
\phi^B_{\kappa m}(\vec{p}) = i(-i)^{\tilde{\ell}} \left(4\pi \int dr\, r^2\, j_{\tilde{\ell}}\,(pr)\, G_\kappa(r)\right) \Omega_{\kappa m}(\Omega_p)\,. \tag{F.35}
$$

Now

$$
i(-i)^{\tilde{\ell}} = i(-i)^{\ell\pm 1} = \begin{cases} i(-i)^{\ell+1} = (-i)^\ell & \text{for } \tilde{\ell} = \ell + 1 \iff \kappa < 0, \\ i(-i)^{\ell-1} = -(-i)^\ell & \text{for } \tilde{\ell} = \ell - 1 \iff \kappa > 0, \end{cases} \tag{F.36}
$$

hence

$$
i(-i)^{\tilde{\ell}} = -\mathrm{sign}(\kappa)\,(-i)^\ell. \tag{F.37}
$$

Therefore, the lower component of $\phi\,(\vec{p})$ becomes

$$
\begin{aligned}
\phi^B_{\kappa m}(\vec{p}) &= -\mathrm{sign}(\kappa)\,(-i)^\ell \left(4\pi \int dr\, r^2\, j_{\tilde{\ell}}\,(pr)\, G_\kappa(r)\right) \Omega_{\kappa m}(\Omega_p)\,, \\
&\equiv i^\ell\, G(p)\, \Omega_{\kappa m}(\theta,\phi)\,.
\end{aligned}
\tag{F.38}
$$

Hence the momentum space solutions to the Dirac equation have the general form

$$
\phi_{jm}(\vec{p}) = \begin{pmatrix} \phi^A_{jm} \\ \phi^B_{jm} \end{pmatrix} = (-i)^\ell \begin{pmatrix} F(p)\, \Omega_{\ell s j m}(\theta,\phi) \\ G(p)\, \Omega_{\tilde{\ell} s j m}(\theta,\phi) \end{pmatrix}, \tag{F.39}
$$

where

$$
F(p) = 4\pi \int_0^\infty dr\, r^2\, j_\ell\,(pr)\, F_\kappa(r), \tag{F.40}
$$

$$
G(p) = -4\pi\, \mathrm{sign}(\kappa) \int_0^\infty dr\, r^2\, j_{\tilde{\ell}}\,(pr)\, G_\kappa(r). \tag{F.41}
$$

The inverse relations are

$$
F(r) = \frac{1}{4\pi} \int_0^\infty dp\, \frac{p}{r}\, j_\ell\,(pr)\, F_\kappa(p), \tag{F.42}
$$

$$
G(r) = -\frac{1}{4\pi}\, \mathrm{sign}(\kappa) \int_0^\infty dp\, \frac{p}{r}\, j_{\tilde{\ell}}\,(pr)\, G_\kappa(p), \tag{F.43}
$$

which are easily proven using the identities

$$
\int_0^\infty dr\, r\, j_\ell\,(pr)\, j_\ell\,(p'r) = \frac{\delta(p-p')}{p}, \tag{F.44}
$$

$$
\int_0^\infty dp\, p\, j_\ell\,(pr)\, j_\ell\,(pr') = \frac{\delta(r-r')}{r}. \tag{F.45}
$$

In momentum space the normalization condition for the Dirac wavefunctions is

$$\int \frac{d^3p}{(2\pi)^3}\, \phi^\dagger_{\kappa m}\phi_{\kappa m} = 1, \tag{F.46}$$

which becomes

$$\int_0^\infty \frac{d^3p}{(2\pi)^3}\, p^2 \left[F_\kappa(p)^2 + G_\kappa(p)^2\right] = 1. \tag{F.47}$$

G

Multipole Formulas

The multipole expansions have the form

$$f^{(jk)}(y) = \sum_{m=-j,\ldots,j} (-1)^{j-m} \sqrt{2k+1} \begin{pmatrix} j & j & k \\ m & -m & 0 \end{pmatrix} f^{jm}(y), \quad k = 0, 2, \ldots, 2j, \tag{G.1}$$

$$\Delta f^{(jk)}(y) = \sum_{m=-j,\ldots,j} (-1)^{j-m} \sqrt{2k+1} \begin{pmatrix} j & j & k \\ m & -m & 0 \end{pmatrix} \Delta f^{jm}(y), \; k = 1, 3, \ldots, 2j, \tag{G.2}$$

where $f^{jm}(y)$ is the spin-independent result and $\Delta f_{jm}(y)$ the spin-dependent expression. The inverse relations are

$$f^{jm}(y) = (-1)^{j-m} \sum_{k=0,2,\ldots,2j} \sqrt{2k+1} \begin{pmatrix} j & j & k \\ m & -m & 0 \end{pmatrix} f^{(jk)}(y), \tag{G.3}$$

$$\Delta f^{jm}(y) = (-1)^{j-m} \sum_{k=1,3,\ldots,2j} \sqrt{2k+1} \begin{pmatrix} j & j & k \\ m & -m & 0 \end{pmatrix} \Delta f^{(jk)}(y). \tag{G.4}$$

Examples of the multipole transformations are given in the following sections.

G.1 $J = 0$

$$f^{(00)}(y) = f^{00}(y), \tag{G.5}$$

(G.6)

G.2 $J = \frac{1}{2}$

$$f^{(\frac{1}{2}0)}(y) = \sqrt{2}\, f^{\frac{1}{2}\frac{1}{2}}(y), \tag{G.7}$$

$$\Delta f^{(\frac{1}{2}1)}(y) = \sqrt{2}\, \Delta f^{\frac{1}{2}\frac{1}{2}}(y). \tag{G.8}$$

G.3 $J = 1$

$$f^{(1\,0)}(y) = \frac{1}{\sqrt{3}}\left[2f^{1\,1}(y) + f^{1\,0}(y)\right], \tag{G.9}$$

$$f^{(1\,2)}(y) = \sqrt{\frac{2}{3}}\left[f^{1\,1}(y) - f^{1\,0}(y)\right] \tag{G.10}$$

$$\Delta f^{(1\,1)}(y) = \sqrt{2}\,\Delta f^{1\,1}(y). \tag{G.11}$$

G.4 $J = \frac{3}{2}$

$$f^{(\frac{3}{2}\,0)}(y) = f^{\frac{3}{2}\,\frac{3}{2}}(y) + f^{\frac{3}{2}\,\frac{1}{2}}(y), \tag{G.12}$$

$$f^{(\frac{3}{2}\,2)}(y) = f^{\frac{3}{2}\,\frac{3}{2}}(y) - f^{\frac{3}{2}\,\frac{1}{2}}(y), \tag{G.13}$$

$$\Delta f^{(\frac{3}{2}\,1)}(y) = \frac{1}{\sqrt{5}}\left[3\,\Delta f^{\frac{3}{2}\,\frac{3}{2}}(y) + \Delta f^{\frac{3}{2}\,\frac{1}{2}}(y)\right], \tag{G.14}$$

$$\Delta f^{(\frac{3}{2}\,3)}(y) = \frac{1}{\sqrt{5}}\left[\Delta f^{\frac{3}{2}\,\frac{3}{2}}(y) - 3\,\Delta f^{\frac{3}{2}\,\frac{1}{2}}(y)\right]. \tag{G.15}$$

G.5 $J = \frac{5}{2}$

$$f^{(\frac{5}{2}\,0)}(y) = \sqrt{\frac{2}{3}}\left[f^{\frac{5}{2}\,\frac{5}{2}}(y) + f^{\frac{5}{2}\,\frac{3}{2}}(y) + f^{\frac{5}{2}\,\frac{1}{2}}(y)\right], \tag{G.16}$$

$$f^{(\frac{5}{2}\,2)}(y) = \frac{1}{\sqrt{21}}\left[5\,f^{\frac{5}{2}\,\frac{5}{2}}(y) - f^{\frac{5}{2}\,\frac{3}{2}}(y) - 4\,f^{\frac{5}{2}\,\frac{1}{2}}(y)\right], \tag{G.17}$$

$$f^{(\frac{5}{2}\,4)}(y) = \frac{1}{\sqrt{7}}\left[f^{\frac{5}{2}\,\frac{5}{2}}(y) - 3\,f^{\frac{5}{2}\,\frac{3}{2}}(y) + 2\,f^{\frac{5}{2}\,\frac{1}{2}}(y)\right], \tag{G.18}$$

$$\Delta f^{(\frac{5}{2}\,1)}(y) = \sqrt{\frac{2}{35}}\left[5\,\Delta f^{\frac{5}{2}\,\frac{5}{2}}(y) + 3\,\Delta f^{\frac{5}{2}\,\frac{3}{2}}(y) + \Delta f^{\frac{5}{2}\,\frac{1}{2}}(y)\right], \tag{G.19}$$

$$\Delta f^{(\frac{5}{2}\,3)}(y) = \frac{1}{3\sqrt{5}}\left[5\,\Delta f^{\frac{5}{2}\,\frac{5}{2}}(y) - 7\,\Delta f^{\frac{5}{2}\,\frac{3}{2}}(y) - 4\,\Delta f^{\frac{5}{2}\,\frac{1}{2}}(y)\right], \tag{G.20}$$

$$\Delta f^{(\frac{5}{2}\,5)}(y) = \frac{1}{3\sqrt{7}}\left[\Delta f^{\frac{5}{2}\,\frac{5}{2}}(y) - 5\,\Delta f^{\frac{5}{2}\,\frac{3}{2}}(y) + 10\,\Delta f^{\frac{5}{2}\,\frac{1}{2}}(y)\right]. \tag{G.21}$$

H

Explicit Calculation of the Nucleon Distribution Functions in the Nucleus.

H.1 Spin-Dependent Nucleon Distribution

In the convolution formalism the spin-dependent quark distribution in a nucleus is given by

$$\Delta q_A^{JH}(x_A) = \sum_{\alpha,\kappa m} C^{JH}_{\alpha,\kappa m} \int_0^A dy_A \int_0^1 dx \delta(x_A - y_A x) \Delta q_{\alpha,\kappa}(x) \; \Delta f_{\kappa m}(y_A) , \quad \text{(H.1)}$$

where J and H are the angular quantum numbers of the nucleus and

$$\Delta f_{\kappa m}(y_A) = \frac{\sqrt{2}\,\overline{M}_N}{A} \int \frac{d^3p}{(2\pi)^3} \sum_\lambda \delta\left(p^3 + \varepsilon_\kappa - \overline{M}_N\, y_A\right) \overline{\Psi}_\kappa(\vec{p}) \; \gamma^+ \gamma_5 \, \Psi_\lambda(\vec{p}) . \quad \text{(H.2)}$$

For the spin-dependent case we consider only A-odd nuclei, with only one particle or hole outside and a closed spin zero core. In this case J and H are simply the quantum number j and m of the valence level and the sum over λ includes just this single energy level, where $\lambda \equiv (\ell s j m)$.

In momentum space the Dirac wavefunction for a central potential has the form

$$\Psi_{\kappa m}(\vec{p}) = (-i)^\ell \begin{pmatrix} F_\lambda(p)\,|\ell s j m; \Omega_p\rangle \\ G_\lambda(p)\,|\tilde{\ell} s j m; \Omega_p\rangle \end{pmatrix} , \quad \text{(H.3)}$$

where

$$|\ell s j m; \Omega_p\rangle \equiv \sum_{\ell_z, s_z} (\ell s \ell_z s_z | j m) \; Y_{\ell \ell_z}(\Omega_p)\, |s s_z\rangle . \quad \text{(H.4)}$$

We have also introduced the quantum number κ, which is defined by

$$\kappa = \pm\left(j + \frac{1}{2}\right) = \begin{cases} -(\ell+1) & \text{for} \quad j = \ell + \frac{1}{2}, \quad \text{where} \quad \tilde{\ell} = \ell + 1, \\ \ell & \text{for} \quad j = \ell - \frac{1}{2}, \quad \text{where} \quad \tilde{\ell} = \ell - 1, \end{cases} \quad \text{(H.5)}$$

We now wish to evaluate Eq. (H.2). Consider

$$\overline{\Psi}\,\gamma^+\gamma_5\,\Psi = \Psi^\dagger\,\gamma^0\gamma^+\gamma_5\,\Psi = \frac{1}{\sqrt{2}}\Psi^\dagger\,\left(\mathbb{1}+\gamma^0\gamma^3\right)\gamma_5\,\Psi = \frac{1}{\sqrt{2}}\Psi^\dagger\begin{pmatrix}\sigma^3 & 1\\ 1 & \sigma^3\end{pmatrix}\Psi, \tag{H.6}$$

where we are using the Dirac representation for the gamma matrices. Using the expression for the Dirac wavefunction given in Eq. (H.3), and noting $\left(i^\ell\right)^* i^\ell = 1$ we have

$$\begin{aligned}\overline{\Psi}\,\gamma^+\gamma_5\,\Psi &= \frac{1}{\sqrt{2}}\Big(\langle \ell sjm|F(p),\,\langle\tilde{\ell}sjm|G(p)\Big)\begin{pmatrix}\sigma^3 & 1\\ 1 & \sigma^3\end{pmatrix}\begin{pmatrix}F(p)\,|\ell sjm\rangle\\ G(p)\,|\tilde{\ell}sjm\rangle\end{pmatrix},\\ &= \frac{1}{\sqrt{2}}\Big\{F(p)G(p)\Big(\langle\ell sjm|\tilde{\ell}sjm\rangle+\langle\tilde{\ell}sjm|\ell sjm\rangle\Big)\\ &\qquad + F(p)^2\langle\ell sjm|\sigma^3|\ell sjm\rangle + G(p)^2\langle\tilde{\ell}sjm|\sigma^3|\tilde{\ell}sjm\rangle\Big\}.\end{aligned} \tag{H.7}$$

To evaluate the above matrix elements it is advantageous to use the Wigner-Echart theorem, which states

$$\begin{aligned}\langle\tau JM|T_q^{(K)}|\tau' J' M'\rangle &= \frac{(-1)^{2K}}{\sqrt{2J+1}}\langle J'KM'q|JM\rangle\langle\tau J||T_q^{(K)}||\tau' J'\rangle\\ &= (-1)^{J-M}\begin{pmatrix}J & K & J'\\ -M & q & M'\end{pmatrix}\langle\tau J||T^{(K)}||\tau' J'\rangle,\end{aligned} \tag{H.8}$$

where $T_q^{(K)}$ is a component of the irreducible tensor operator $T^{(K)}$ and $\langle\tau J||T^{(K)}||\tau' J'\rangle$ is called the reduced matrix element.

To utilize this theorem we introduce unity in the form

$$1 = \sum_{L,L_z} Y^*_{LL_z}(\Omega_p)Y_{LL_z}(\Omega_p), \tag{H.9}$$

and obtain

$$\begin{aligned}\Delta f_{\kappa m}(y_A) = \frac{\overline{M}_N}{A}\int\frac{d^3p}{(2\pi)^3}\,\delta\!\left(p^3+\varepsilon_\kappa-\overline{M}_N\,y_A\right)\sum_{L,L_z}Y^*_{LL_z}(\Omega_p)\\ \Big\{F(p)G(p)\Big(\langle\ell sjm|Y_{LL_z}|\tilde{\ell}sjm\rangle+\langle\tilde{\ell}sjm|Y_{LL_z}|\ell sjm\rangle\Big)\\ + F(p)^2\langle\ell sjm|Y_{LL_z}\sigma^3|\ell sjm\rangle + G(p)^2\langle\tilde{\ell}sjm|Y_{LL_z}\sigma^3|\tilde{\ell}sjm\rangle\Big\}.\end{aligned} \tag{H.10}$$

We can now evaluate the matrix elements using the Wigner-Echart theorem and various reduced matrix element identities. Consider

$$\langle\ell sjm|Y_{LL_z}|\tilde{\ell}sjm\rangle = (-1)^{j-m}\begin{pmatrix}j & L & j\\ -m & L_z & m\end{pmatrix}\langle\ell sj||Y^{(L)}||\tilde{\ell}sj\rangle. \tag{H.11}$$

Using C.89 of Ref. [166], which states

$$\langle \tau_1\tau_2 J_1 J_2 J \| T^{(k)} \| \tau_1'\tau_2' J_1' J_2' J'\rangle = \delta_{\tau_2\tau_2'}\delta_{J_2 J_2'} (-1)^{J'+J_1+J_2+k} \sqrt{(2J+1)(2J'+1)} \begin{Bmatrix} J_1 & k & J_1' \\ J' & J_2 & J \end{Bmatrix} \langle \tau_1\tau_2 J_1 \| T^{(k)} \| \tau_1'\tau_2' J_1\rangle. \quad \text{(H.12)}$$

Therefore

$$\langle \ell sjm | Y_{LL_z} | \tilde{\ell} sjm\rangle = (-1)^{j-m}(-1)^{j+\ell+s+L}(2j+1) \begin{pmatrix} j & L & j \\ -m & L_z & m \end{pmatrix} \begin{Bmatrix} \ell & L & \tilde{\ell} \\ j & s & j \end{Bmatrix} \langle \ell \| Y^{(L)} \| \tilde{\ell}\rangle. \quad \text{(H.13)}$$

Now

$$\langle \ell_1 \| Y^{(L)} \| \ell_2\rangle = (-1)^{\ell_1} \sqrt{\frac{(2\ell_1+1)(2L+1)(2\ell_2+1)}{4\pi}} \begin{pmatrix} \ell_1 & L & \ell_2 \\ 0 & 0 & 0 \end{pmatrix}. \quad \text{(H.14)}$$

Therefore

$$\langle \ell sjm | Y_{LL_z} | \tilde{\ell} sjm\rangle = (-1)^{j-m}(2j+1)\sqrt{\frac{2L+1}{4\pi}}(-1)^{j+\ell+s+L}(-1)^{\ell} \sqrt{(2\ell+1)(2\tilde{\ell}+1)} \begin{pmatrix} j & L & j \\ -m & L_z & m \end{pmatrix} \begin{pmatrix} \ell & L & \tilde{\ell} \\ 0 & 0 & 0 \end{pmatrix} \begin{Bmatrix} \ell & L & \tilde{\ell} \\ j & s & j \end{Bmatrix}. \quad \text{(H.15)}$$

Now $\left(\begin{smallmatrix} \ell & L & \tilde{\ell} \\ 0 & 0 & 0 \end{smallmatrix}\right) = 0$ if $\ell + L + \tilde{\ell}$ is odd, therefore since $\tilde{\ell} = \ell \pm 1$, only terms where L is odd contribute, hence

$$\langle \ell sjm | Y_{LL_z} | \tilde{\ell} sjm\rangle = (-1)^{j-m}(2j+1)\sqrt{\frac{2L+1}{4\pi}}(-1)(-1)^{j+s} \sqrt{(2\ell+1)(2\tilde{\ell}+1)} \begin{pmatrix} j & L & j \\ -m & L_z & m \end{pmatrix} \begin{pmatrix} \ell & L & \tilde{\ell} \\ 0 & 0 & 0 \end{pmatrix} \begin{Bmatrix} \ell & L & \tilde{\ell} \\ j & s & j \end{Bmatrix}. \quad \text{(H.16)}$$

Since $s = \frac{1}{2}$, we have

$$\langle \ell sjm | Y_{LL_z} | \tilde{\ell} sjm\rangle = (-1)^{j-m}(2j+1)\sqrt{\frac{2L+1}{4\pi}}(-1)^{j-\frac{1}{2}} \sqrt{(2\ell+1)(2\tilde{\ell}+1)} \begin{pmatrix} j & L & j \\ -m & L_z & m \end{pmatrix} \begin{pmatrix} \ell & L & \tilde{\ell} \\ 0 & 0 & 0 \end{pmatrix} \begin{Bmatrix} \ell & L & \tilde{\ell} \\ j & s & j \end{Bmatrix}. \quad \text{(H.17)}$$

The above equation is symmetric in $\ell \to \tilde{\ell}$, hence

$$\langle \ell sjm | Y_{LL_z} | \tilde{\ell} sjm\rangle = \langle \tilde{\ell} sjm | Y_{LL_z} | \ell sjm\rangle. \quad \text{(H.18)}$$

To evaluate the third matrix element in Eq. (H.7) we first couple Y and σ to an irreducible tensor of rank $K = L, L \pm 1$, giving

$$Y_{LL_z}\sigma^3 \equiv Y^{(L)}_{L_z}\sigma^{(1)}_0 = \sum_{K,K_z} \sqrt{2K+1}\,(-1)^{L-1+K_z} \begin{pmatrix} L & 1 & K \\ L_z & 0 & -K_z \end{pmatrix} \left[Y^{(L)} \otimes \sigma^{(1)}\right]^{(K)}_{K_z}. \tag{H.19}$$

Using C.88 of Ref. [166], which states

$$\langle \tau_1\tau_2 J_1 J_2 J \| V^{(K)} \| \tau_1'\tau_2' J_1' J_2' J' \rangle = \sqrt{(2J+1)\,(2K+1)\,(2J'+1)} \begin{Bmatrix} J_1' & J_2' & J' \\ k_1 & k_2 & K \\ J_1 & J_2 & J \end{Bmatrix} \langle \tau_1 J_1 \| T^{(k_1)} \| \tau_1' J_1' \rangle \langle \tau_2 J_2 \| U^{(k_2)} \| \tau_2' J_2' \rangle, \tag{H.20}$$

where $V^{(K)} = \left[T^{(k_1)} \otimes U^{(k_2)}\right]^{(K)}$ and the Wigner-Echart theorem, we obtain

$$\begin{aligned}\langle \ell s j m | Y_{LL_z}\sigma^3 | \ell s j m \rangle &= (-1)^{j-m} \sum_{K,K_z} \sqrt{2K+1}\,(-1)^{L-1+K_z} \begin{pmatrix} L & 1 & K \\ L_z & 0 & -K_z \end{pmatrix} \begin{pmatrix} j & K & j \\ -m & K_z & m \end{pmatrix} \left\langle lsj \left\| \left[Y^{(L)} \otimes \sigma^{(1)}\right]^{(K)} \right\| lsj \right\rangle, \\ &= (-1)^{j-m}\,(2j+1) \sum_{K,K_z} (-1)^{L-1+K_z}\,(2K+1)\,, \\ &\begin{pmatrix} L & 1 & K \\ L_z & 0 & -K_z \end{pmatrix} \begin{pmatrix} j & K & j \\ -m & K_z & m \end{pmatrix} \begin{Bmatrix} \ell & s & j \\ L & 1 & K \\ \ell & s & j \end{Bmatrix} \langle \ell \| Y^{(L)} \| \ell \rangle \, \langle s \| \sigma^{(1)} \| s \rangle .\end{aligned} \tag{H.21}$$

Using Eq. (H.14) and $\langle s \| \sigma^{(1)} \| s \rangle = \sqrt{6}$ we have

$$\begin{aligned}\langle \ell s j m | Y_{LL_z}\sigma^3 | \ell s j m \rangle &= (-1)^{j-m}\,(2j+1) \sqrt{\frac{2L+1}{4\pi}} \sqrt{6} \sum_{K,K_z} (-1)^{L-1+K_z}\,(-1)^{\ell}\,(2K+1)\,(2\ell+1) \\ &\begin{pmatrix} \ell & L & \ell \\ 0 & 0 & 0 \end{pmatrix} \begin{pmatrix} L & 1 & K \\ L_z & 0 & -K_z \end{pmatrix} \begin{pmatrix} j & K & j \\ -m & K_z & m \end{pmatrix} \begin{Bmatrix} \ell & s & j \\ L & 1 & K \\ \ell & s & j \end{Bmatrix}.\end{aligned} \tag{H.22}$$

Now because of the Φ integration in $\Delta f_{\kappa m}(y_A)$ only the $L_z = 0$ terms are non-zero, hence we must also have $K_z = 0$. Further, in analogy with a similar earlier argument, L must be even for $\left(\begin{smallmatrix}\ell & L & \ell\\ 0 & 0 & 0\end{smallmatrix}\right)$ to be non-zero and hence K must be odd because of $\left(\begin{smallmatrix}L & 1 & K\\ 0 & 0 & 0\end{smallmatrix}\right)$. Therefore

$$\langle \ell s j m | Y_{LL_z} \sigma^3 | \ell s j m \rangle = (-1)^{j-m}\,(2j+1)\sqrt{\frac{2L+1}{4\pi}}\,(-1)\,\sqrt{6}\sum_K (-1)^{\ell}$$
$$(2K+1)\,(2\ell+1)\begin{pmatrix}\ell & L & \ell\\ 0 & 0 & 0\end{pmatrix}\begin{pmatrix}L & 1 & K\\ 0 & 0 & 0\end{pmatrix}\begin{pmatrix}j & K & j\\ -m & 0 & m\end{pmatrix}\begin{Bmatrix}\ell & s & j\\ L & 1 & K\\ \ell & s & j\end{Bmatrix}. \tag{H.23}$$

Therefore clearly

$$\langle \tilde{\ell} s j m | Y_{LL_z} \sigma^3 | \tilde{\ell} s j m \rangle$$
$$= (-1)^{j-m}\,(2j+1)\sqrt{\frac{2L+1}{4\pi}}\,(-1)\,\sqrt{6}\sum_K (-1)^{\tilde{\ell}}\,(2K+1)\,(2\tilde{\ell}+1)$$
$$\begin{pmatrix}\tilde{\ell} & L & \tilde{\ell}\\ 0 & 0 & 0\end{pmatrix}\begin{pmatrix}L & 1 & K\\ 0 & 0 & 0\end{pmatrix}\begin{pmatrix}j & K & j\\ -m & 0 & m\end{pmatrix}\begin{Bmatrix}\tilde{\ell} & s & j\\ L & 1 & K\\ \tilde{\ell} & s & j\end{Bmatrix},$$
$$= (-1)^{j-m}\,(2j+1)\sqrt{\frac{2L+1}{4\pi}}\sqrt{6}\sum_K (-1)^{\ell}\,(2K+1)\,(2\tilde{\ell}+1)$$
$$\begin{pmatrix}\tilde{\ell} & L & \tilde{\ell}\\ 0 & 0 & 0\end{pmatrix}\begin{pmatrix}L & 1 & K\\ 0 & 0 & 0\end{pmatrix}\begin{pmatrix}j & K & j\\ -m & 0 & m\end{pmatrix}\begin{Bmatrix}\tilde{\ell} & s & j\\ L & 1 & K\\ \tilde{\ell} & s & j\end{Bmatrix}. \tag{H.24}$$

Therefore

$$\Delta f_{\kappa m}(y_A) = (-1)^{j-m}\,(2j+1)\,\frac{\overline{M}_N}{\sqrt{4\pi}\,A}\int \frac{d^3p}{(2\pi)^3}\,\delta(p^3+\varepsilon_\kappa-\overline{M}_N\, y_A)$$
$$\sum_L \sqrt{2L+1}\; Y^*_{L0}(\Omega_p)\left\{\; 2F_\lambda(p)G_\lambda(p)(-1)^{j-\frac{1}{2}}\sqrt{(2\ell+1)(2\tilde{\ell}+1)}\right.$$
$$\begin{pmatrix}j & j & L\\ m & -m & 0\end{pmatrix}\begin{pmatrix}\ell & L & \tilde{\ell}\\ 0 & 0 & 0\end{pmatrix}\begin{Bmatrix}\ell & L & \tilde{\ell}\\ j & s & j\end{Bmatrix}$$
$$-\sqrt{6}\sum_K (-1)^{\ell}\,(2K+1)\begin{pmatrix}L & 1 & K\\ 0 & 0 & 0\end{pmatrix}\begin{pmatrix}j & j & K\\ m & -m & 0\end{pmatrix}$$

$$\left[F_\lambda(p)^2(2\ell+1)\begin{pmatrix}\ell & L & \ell\\ 0 & 0 & 0\end{pmatrix}\begin{Bmatrix}\ell & s & j\\ L & 1 & K\\ \ell & s & j\end{Bmatrix}\right.$$
$$\left.\left. - G_\lambda(p)^2(2\tilde{\ell}+1)\begin{pmatrix}\tilde{\ell} & L & \tilde{\ell}\\ 0 & 0 & 0\end{pmatrix}\begin{Bmatrix}\tilde{\ell} & s & j\\ L & 1 & K\\ \tilde{\ell} & s & j\end{Bmatrix}\right]\right\}. \tag{H.25}$$

A significant simplification can be made if we expand $\Delta f_{\kappa m}$ $(m = -j, \ldots, j)$ in terms of the multipole distributions $\Delta f_{\kappa k}$ $(k = -1, 3, \ldots, 2j)$, defined by

$$\Delta f_{\kappa m} \equiv \sum_{k=1,3,\ldots,2j} A_m^{jk}\,\Delta f_{\kappa k} = (-1)^{j-m} \sum_{k=1,3,\ldots,2j} \sqrt{2k+1}\begin{pmatrix}j & j & k\\ m & -m & 0\end{pmatrix}\Delta f_{\kappa k}. \tag{H.26}$$

The inverse relationship is

$$\Delta f_{\kappa k} \equiv \sum_{m=-j,\ldots,j} A_m^{jk}\,\Delta f_{\kappa m} = \sum_{m=-j,\ldots,j} (-1)^{j-m}\sqrt{2k+1}\begin{pmatrix}j & j & k\\ m & -m & 0\end{pmatrix}\Delta f_{\kappa m}, \tag{H.27}$$

which is easily proven using the orthogonality relation

$$\sum_{j,m}(2j+1)\begin{pmatrix}j_1 & j_2 & j\\ m_1 & m_2 & m\end{pmatrix}\begin{pmatrix}j_1 & j_2 & j\\ m_1' & m_2' & m\end{pmatrix} = \delta_{m_1 m_1'}\delta_{m_2 m_2'}. \tag{H.28}$$

Another orthogonality relation is given by

$$\sum_{m_1,m_2}(2j+1)\begin{pmatrix}j_1 & j_2 & j\\ m_1 & m_2 & m\end{pmatrix}\begin{pmatrix}j_1 & j_2 & j'\\ m_1 & m_2 & m'\end{pmatrix} = \delta_{jj'}\delta_{mm'}, \tag{H.29}$$

with a special case being

$$\sum_{m}\begin{pmatrix}j & j & J\\ m & -m & 0\end{pmatrix}\begin{pmatrix}j & j & J'\\ m & -m & 0\end{pmatrix} = \frac{\delta_{JJ'}}{2J+1}. \tag{H.30}$$

Using Eq. (H.30) we obtain for the multipole distributions

$$\Delta f_{\kappa k}(y_A) = (2j+1)\,\frac{\overline{M}_N}{\sqrt{4\pi}\,A}\int \frac{d^3p}{(2\pi)^3}\,\delta\big(p^3+\varepsilon_\kappa-\overline{M}_N\,y_A\big)$$
$$\Bigg\{\; 2Y_{k0}(\Omega_p)F_\lambda(p)G_\lambda(p)(-1)^{j-\frac{1}{2}}\sqrt{(2\ell+1)(2\tilde{\ell}+1)}\begin{pmatrix}\ell & k & \tilde{\ell}\\ 0 & 0 & 0\end{pmatrix}\begin{Bmatrix}\ell & k & \tilde{\ell}\\ j & s & j\end{Bmatrix}$$
$$-\sqrt{6}\sqrt{2k+1}\,(-1)^{\ell}\sum_{L=k-1,k+1}\sqrt{2L+1}\,Y_{L0}(\Omega_p)\begin{pmatrix}L & 1 & k\\ 0 & 0 & 0\end{pmatrix}$$
$$\Bigg[F_\lambda(p)^2(2\ell+1)\begin{pmatrix}\ell & L & \ell\\ 0 & 0 & 0\end{pmatrix}\begin{Bmatrix}\ell & s & j\\ L & 1 & k\\ \ell & s & j\end{Bmatrix}$$
$$-\,G_\lambda(p)^2(2\tilde{\ell}+1)\begin{pmatrix}\tilde{\ell} & L & \tilde{\ell}\\ 0 & 0 & 0\end{pmatrix}\begin{Bmatrix}\tilde{\ell} & s & j\\ L & 1 & k\\ \tilde{\ell} & s & j\end{Bmatrix}\Bigg]\Bigg\}. \tag{H.31}$$

Note the sum over L in the second term includes only the $k-1$ and $k+1$ components, because $\left(\begin{smallmatrix}L & 1 & k\\ 0 & 0 & 0\end{smallmatrix}\right)$ is zero otherwise. To evaluate Eq. (H.31) we note that

$$Y_{L0}(\Omega_p) = \sqrt{\frac{2L+1}{4\pi}}\,P_L\left(\cos\theta\right), \tag{H.32}$$

where P_L are Legendre polynomials of degree L. We also introduce polar coordinates, where

$$\begin{aligned}
&\int d^3p\;\delta\big(p^3+\varepsilon_\kappa-\overline{M}_N\,y_A\big)\;\Gamma\left(p,\cos\theta\right)\\
&= \int_0^{2\pi} d\phi \int_{-1}^{1} d\cos\theta \int_0^\infty dp\,p^2\;\delta(p\cos\theta+\varepsilon_\kappa-\overline{M}_N\,y_A)\,\Gamma\left(p,\cos\theta\right),\\
&= 2\pi\int_{-1}^{1} d\cos\theta\int_0^\infty dp\,p^2\,\frac{1}{p}\,\delta\Big(\cos\theta-\frac{\overline{M}_N\,y_A-\varepsilon_\kappa}{p}\Big)\,\Gamma\left(p,\cos\theta\right),\\
&= 2\pi\int_\Lambda^\infty dp\,p\,\Gamma\Big(p,\frac{\overline{M}_N\,y_A-\varepsilon_\kappa}{p}\Big).
\end{aligned} \tag{H.33}$$

Where in order to satisfy the delta function we must have $p > |\overline{M}_N\,y_A-\varepsilon_\kappa|$, hence $\Lambda = |\overline{M}_N\, y_A - \varepsilon_\kappa|$. Therefore

$$\Delta f_{\kappa k}(y_A) = (2j+1)\sqrt{2k+1}\frac{\overline{M}_N}{16\pi^3 A}\int_\Lambda^\infty dp\, p$$
$$\left\{ 2P_k\left(\frac{\overline{M}_N\, y_A - \varepsilon_\kappa}{p}\right) F_\lambda(p) G_\lambda(p) (-1)^{j-\frac{1}{2}} \right.$$
$$\sqrt{(2\ell+1)(2\tilde{\ell}+1)}\begin{pmatrix}\ell & k & \tilde{\ell}\\ 0 & 0 & 0\end{pmatrix}\begin{Bmatrix}\ell & k & \tilde{\ell}\\ j & s & j\end{Bmatrix}$$
$$-\sqrt{6}\,(-1)^\ell \sum_{L=k-1,k+1} (2L+1)\,P_L\left(\frac{\overline{M}_N\, y_A - \varepsilon_\kappa}{p}\right)\begin{pmatrix}L & 1 & k\\ 0 & 0 & 0\end{pmatrix}$$
$$\left[F_\lambda(p)^2 (2\ell+1)\begin{pmatrix}\ell & L & \ell\\ 0 & 0 & 0\end{pmatrix}\begin{Bmatrix}\ell & s & j\\ L & 1 & k\\ \ell & s & j\end{Bmatrix}\right.$$
$$\left.\left. -G_\lambda(p)^2(2\tilde{\ell}+1)\begin{pmatrix}\tilde{\ell} & L & \tilde{\ell}\\ 0 & 0 & 0\end{pmatrix}\begin{Bmatrix}\tilde{\ell} & s & j\\ L & 1 & k\\ \tilde{\ell} & s & j\end{Bmatrix}\right]\right\}. \qquad \text{(H.34)}$$

The first few Legendre polynomials are

$$P_0(x) = 1, \qquad P_1(x) = x,$$
$$P_2(x) = \frac{1}{2}\left(3x^2 - 1\right), \qquad P_3(x) = \frac{1}{2}\left(5x^3 - 3x\right),$$
$$P_4(x) = \frac{1}{8}\left(35x^4 - 30x^2 + 3\right), \qquad P_5(x) = \frac{1}{8}\left(63x^5 - 70x^3 + 15x\right),$$
$$P_6(x) = \frac{1}{16}\left(231x^6 - 315x^4 + 105x^2 - 5\right),$$
$$P_7(x) = \frac{1}{16}\left(429x^7 - 693x^5 + 315x^3 - 35x\right). \qquad \text{(H.35)}$$

Transforming back, our final result is

$$\Delta f_{\kappa m}(y_A) = (2j+1)\,(-1)^{j-m}\,\frac{\overline{M}_N}{16\pi^3 A}\sum_{k=1,3,\ldots,2j}(2k+1)\begin{pmatrix}j & j & k\\ m & -m & 0\end{pmatrix}\int_\Lambda^\infty dp$$

$$\Bigg\{ 2P_k\left(\frac{\overline{M}_N\, y_A - \varepsilon_\kappa}{p}\right) F_\lambda(p) G_\lambda(p) (-1)^{j-\frac{1}{2}}$$

$$\sqrt{(2\ell+1)(2\tilde{\ell}+1)} \begin{pmatrix} \ell & k & \tilde{\ell} \\ 0 & 0 & 0 \end{pmatrix} \begin{Bmatrix} \ell & k & \tilde{\ell} \\ j & s & j \end{Bmatrix}$$

$$- \sqrt{6}\,(-1)^{\ell} \sum_{L=k-1,k+1} (2L+1)\, P_L \left(\frac{\overline{M}_N\, y_A - \varepsilon_\kappa}{p}\right) \begin{pmatrix} L & 1 & k \\ 0 & 0 & 0 \end{pmatrix}$$

$$\left[F_\lambda(p)^2 (2\ell+1) \begin{pmatrix} \ell & L & \ell \\ 0 & 0 & 0 \end{pmatrix} \begin{Bmatrix} \ell & s & j \\ L & 1 & k \\ \ell & s & j \end{Bmatrix} \right.$$

$$\left. \left. - G_\lambda(p)^2 (2\tilde{\ell}+1) \begin{pmatrix} \tilde{\ell} & L & \tilde{\ell} \\ 0 & 0 & 0 \end{pmatrix} \begin{Bmatrix} \tilde{\ell} & s & j \\ L & 1 & k \\ \tilde{\ell} & s & j \end{Bmatrix} \right] \right\} . \qquad \text{(H.36)}$$

The conventions for the angular momentum is given by

$$\begin{aligned} \kappa < 0 \quad &\Longrightarrow \quad \kappa = -\left(j+\tfrac{1}{2}\right), \quad \ell = j - \tfrac{1}{2}, \quad \tilde{\ell} = \ell + 1, \\ \kappa > 0 \quad &\Longrightarrow \quad \kappa = j + \tfrac{1}{2}, \qquad\quad \ell = j + \tfrac{1}{2}, \quad \tilde{\ell} = \ell - 1. \end{aligned} \qquad \text{(H.37)}$$

Recall for every j, there are $\frac{1}{2}(2j+1)$ multipole distributions, $\Delta f_{\kappa k}$, where $k = (1, \ldots, 2j)$.

H.1.1 Moments

We first calculate the moments of the multipole distribution functions and from these we can reconstruct - via the multipole expansion - the moments of the usual distribution functions. We have

$$\int_0^A dy_A\, \Delta f_{\kappa k}(y_A) = (2j+1)\frac{1}{\sqrt{4\pi}}\int_0^A dy_A \int \frac{d^3p}{(2\pi)^3}\,\delta\Big(y_A - \frac{p\cos\theta + \varepsilon_\kappa}{M_N}\Big)$$
$$\Bigg\{2Y_{k0}(\Omega_p)F_\lambda(p)G_\lambda(p)(-1)^{j-\frac{1}{2}}\sqrt{(2\ell+1)(2\tilde{\ell}+1)}\begin{pmatrix}\ell & k & \tilde{\ell}\\ 0 & 0 & 0\end{pmatrix}\begin{Bmatrix}\ell & k & \tilde{\ell}\\ j & s & j\end{Bmatrix}$$
$$-\sqrt{6}\sqrt{2k+1}\,(-1)^\ell \sum_{L=k-1,k+1}\sqrt{2L+1}\,Y_{L0}(\Omega_p)\begin{pmatrix}L & 1 & k\\ 0 & 0 & 0\end{pmatrix}$$
$$\Bigg[F_\lambda(p)^2(2\ell+1)\begin{pmatrix}\ell & L & \ell\\ 0 & 0 & 0\end{pmatrix}\begin{Bmatrix}\ell & s & j\\ L & 1 & k\\ \ell & s & j\end{Bmatrix}$$
$$-G_\lambda(p)^2(2\tilde{\ell}+1)\begin{pmatrix}\tilde{\ell} & L & \tilde{\ell}\\ 0 & 0 & 0\end{pmatrix}\begin{Bmatrix}\tilde{\ell} & s & j\\ L & 1 & k\\ \tilde{\ell} & s & j\end{Bmatrix}\Bigg]\Bigg\}. \tag{H.38}$$

From the orthogonality relation for the spherical harmonics, for the first term in the curly brackets to be non-zero we must have $k=0$, however for the multipole moments $k=1,3,\ldots,2j$, hence this term is zero. Similarly, for the second term only the $L=0$ term is non-zero, and hence we have $k=0$. Therefore

$$\int_0^A dy_A\, \Delta f_{\kappa k}(y_A) = \delta_{k1}\,(2j+1)\frac{1}{\sqrt{4\pi}\,A}\int \frac{d^3p}{(2\pi)^3}$$
$$\Bigg\{-\sqrt{6}\sqrt{3}\,(-1)^\ell\; Y_{00}(\Omega_p)\begin{pmatrix}0 & 1 & 1\\ 0 & 0 & 0\end{pmatrix}$$
$$\Bigg[F_\lambda(p)^2(2\ell+1)\begin{pmatrix}\ell & 0 & \ell\\ 0 & 0 & 0\end{pmatrix}\begin{Bmatrix}\ell & s & j\\ 0 & 1 & 1\\ \ell & s & j\end{Bmatrix}$$
$$-G_\lambda(p)^2(2\tilde{\ell}+1)\begin{pmatrix}\tilde{\ell} & 0 & \tilde{\ell}\\ 0 & 0 & 0\end{pmatrix}\begin{Bmatrix}\tilde{\ell} & s & j\\ 0 & 1 & 1\\ \tilde{\ell} & s & j\end{Bmatrix}\Bigg]\Bigg\}. \tag{H.39}$$

Using the results

$$Y_{00}(\Omega_p) = \frac{1}{\sqrt{4\pi}}, \qquad \begin{pmatrix} 0 & 1 & 1 \\ 0 & 0 & 0 \end{pmatrix} = -\frac{1}{\sqrt{3}},$$
$$\begin{pmatrix} \ell & 0 & \ell \\ 0 & 0 & 0 \end{pmatrix} = \frac{(-1)^{\ell}}{\sqrt{2\ell+1}}, \qquad (-1)^{\tilde{\ell}} = -(-1)^{\ell}, \quad \text{(H.40)}$$

and

$$\begin{Bmatrix} a & b & J \\ c & d & J \\ K & K & 0 \end{Bmatrix} = \frac{(-1)^{b+c+J+K}}{\sqrt{(2J+1)\,(2K+1)}} \begin{Bmatrix} a & b & J \\ d & c & K \end{Bmatrix}, \quad \text{(H.41)}$$

giving

$$\begin{Bmatrix} \ell & s & j \\ 0 & 1 & 1 \\ \ell & s & j \end{Bmatrix} = \begin{Bmatrix} j & s & \ell \\ j & s & \ell \\ 1 & 1 & 0 \end{Bmatrix} = \frac{(-1)^{j+\ell+s+1}}{\sqrt{3}\sqrt{2\ell+1}} \begin{Bmatrix} j & s & \ell \\ s & j & 1 \end{Bmatrix}$$
$$= \frac{(-1)^{j+\ell+s+1}}{\sqrt{3}\sqrt{2\ell+1}} \frac{2(-1)^{j+\ell+s+1}\left[j(j+1)+s(s+1)-\ell(\ell+1)\right]}{\sqrt{2j(2j+1)(2j+2)2s(2s+1)(2s+2)}}, \quad \text{(H.42)}$$

substituting $s = \frac{1}{2}$ we have

$$\begin{Bmatrix} \ell & s & j \\ 0 & 1 & 1 \\ \ell & s & j \end{Bmatrix} = \frac{\sqrt{2}\left[j(j+1)-\ell(\ell+1)+\frac{3}{4}\right]}{3\sqrt{2\ell+1}\sqrt{2j(2j+1)(2j+2)}}. \quad \text{(H.43)}$$

Therefore the first moment becomes

$$\int_0^A dy_A\,\Delta f_{\kappa k}(y_A) = \delta_{k1}\,(2j+1)\,\frac{1}{4\pi}\frac{2}{\sqrt{3}\sqrt{2j(2j+1)(2j+2)}}$$
$$\int \frac{d^3p}{(2\pi)^3}\left\{F_\lambda(p)^2\left[j(j+1)-\ell(\ell+1)+\tfrac{3}{4}\right]\right.$$
$$\left.+\,G_\lambda(p)^2\left[j(j+1)-\tilde{\ell}(\tilde{\ell}+1)+\tfrac{3}{4}\right]\right\}. \quad \text{(H.44)}$$

Using the normalization condition, the first moment of the multipole distribution is

$$\int_0^A dy_A\,\Delta f_{\kappa k}(y_A) = \delta_{k1}\sqrt{\frac{2}{3}}\sqrt{\frac{2j+1}{j(2j+2)}}$$
$$\left\{j(j+1)+\tfrac{3}{4}-\int\frac{dp}{(2\pi)^3}\left[\ell(\ell+1)\,p^2\,F_\lambda(p)^2+\tilde{\ell}(\tilde{\ell}+1)\,p^2\,G_\lambda(p)^2\right]\right\}. \quad \text{(H.45)}$$

Using the multipole expansion and the result

$$\begin{pmatrix} j & j & 1 \\ m & -m & 0 \end{pmatrix} = \frac{(-1)^{j-m}\, m}{\sqrt{j(2j+1)(j+1)}}, \tag{H.46}$$

we obtain

$$\int_0^A dy_A\, \Delta f_{\kappa m}(y_A) = \frac{m}{j(j+1)}$$
$$\left\{ j(j+1) + \tfrac{3}{4} - \int \frac{dp}{(2\pi)^3} \left[\ell(\ell+1)\, p^2\, F_\lambda(p)^2 + \tilde{\ell}(\tilde{\ell}+1)\, p^2\, G_\lambda(p)^2 \right] \right\}. \tag{H.47}$$

Some explicit examples are

- $\kappa = -1 \quad \Longrightarrow \quad j = \frac{1}{2},\ \ell = 0$ and $\tilde{\ell} = 1$

$$\int_0^A dy_A\, g_{\frac{1}{2}k}(y_A) = \delta_{k1} \frac{\sqrt{2}}{A} \left\{ 1 - \frac{4}{3} \int \frac{dp}{(2\pi)^3}\, p^2\, G_\lambda(p)^2 \right\}, \tag{H.48}$$

$$\int_0^A dy_A\, g^{\frac{1}{2}m}(y_A) = \frac{2\,m}{A} \left\{ 1 - \frac{4}{3} \int \frac{dp}{(2\pi)^3} p^2\, G_\lambda(p)^2 \right\}. \tag{H.49}$$

- $\kappa = -2 \quad \Longrightarrow \quad j = \frac{3}{2},\ \ell = 1$ and $\tilde{\ell} = 2$

$$\int_0^A dy_A\, g_{\frac{1}{2}k}(y_A) = \delta_{k1} \frac{2\sqrt{5}}{3\,A} \left\{ 1 - \frac{8}{5} \int \frac{dp}{(2\pi)^3}\, p^2\, G_\lambda(p)^2 \right\}, \tag{H.50}$$

$$\int_0^A dy_A\, g^{\frac{3}{2}m}(y_A) = \frac{2\,m}{3\,A} \left\{ 1 - \frac{8}{5} \int \frac{dp}{(2\pi)^3}\, p^2\, G_\lambda(p)^2 \right\}. \tag{H.51}$$

- $\kappa = 1 \quad \Longrightarrow \quad j = \frac{1}{2},\ \ell = 1$ and $\tilde{\ell} = 0$

$$\int_0^A dy_A\, g_{\frac{1}{2}k}(y_A) = \delta_{k1} \frac{\sqrt{2}}{A} \left\{ 1 - \frac{4}{3} \int \frac{dp}{(2\pi)^3}\, p^2\, F_\lambda(p)^2 \right\}, \tag{H.52}$$

$$\int_0^A dy_A\, g^{\frac{1}{2}m}(y_A) = \frac{2\,m}{A} \left\{ 1 - \frac{4}{3} \int \frac{dp}{(2\pi)^3} p^2\, F_\lambda(p)^2 \right\}. \tag{H.53}$$

H.2 Spin-Independent Nucleon Distribution

In the convolution formalism the spin-independent quark distribution in a nucleus is given by

$$q_A^{JH}(x_A) = \sum_{\alpha,\kappa m} C_{\alpha,\kappa m}^{JH} \int_0^A dy_A \int_0^1 dx\ \delta(x_A - y_A\, x)\, q_{\alpha,\kappa}(x)\ f_{\kappa m}(y_A), \qquad \text{(H.54)}$$

where

$$f_{\kappa m}(y_A) = \sqrt{2}\,\overline{M}_N \int \frac{d^3p}{(2\pi)^3}\ \delta\big(p^3 + \varepsilon_\kappa - \overline{M}_N\, y_A\big)\, \overline{\Psi}_{\kappa m}(\vec{p})\ \gamma^+\, \Psi_{\kappa m}(\vec{p})\,. \qquad \text{(H.55)}$$

In order to evaluate Eq. (H.55) we first consider

$$\overline{\Psi}\,\gamma^+\,\Psi = \Psi^\dagger\,\gamma^0\gamma^+\,\Psi = \frac{1}{\sqrt{2}}\Psi^\dagger\ \big(\mathbb{1} + \gamma^0\gamma^3\big)\ \Psi = \frac{1}{\sqrt{2}}\Psi^\dagger \begin{pmatrix} 1 & \sigma^3 \\ \sigma^3 & 1 \end{pmatrix} \Psi, \qquad \text{(H.56)}$$

where we are using the Dirac representation for the gamma matrices. Using the expression for the Dirac wavefunction given in Eq. (H.3), and noting $\big[(-i)^\ell\big]^*\,(-i)^\ell = 1$ we have

$$\begin{aligned}\overline{\Psi}\,\gamma^+\,\Psi &= \frac{1}{\sqrt{2}}\Big(\langle \ell sjm|F(p),\, \langle\tilde{\ell} sjm|G(p)\Big)\begin{pmatrix} 1 & \sigma^3 \\ \sigma^3 & 1 \end{pmatrix}\begin{pmatrix} F_\kappa(p)\,|\ell sjm\rangle \\ G_\kappa(p)\,|\tilde{\ell} sjm\rangle \end{pmatrix}, \\ &= \frac{1}{\sqrt{2}}\Big\{F(p)_{\kappa m}G_\kappa(p)\,\Big(\langle \ell sjm|\sigma^3|\tilde{\ell} sjm\rangle + \langle\tilde{\ell} sjm|\sigma^3|\ell sjm\rangle\Big) \\ &\qquad + F_\kappa(p)^2\langle \ell sjm|\ell sjm\rangle + G_\kappa(p)^2\langle\tilde{\ell} sjm|\tilde{\ell} sjm\rangle\Big\}. \end{aligned} \qquad \text{(H.57)}$$

Using the result

$$|\tilde{\ell} sjm\rangle = -\vec{\sigma}\cdot\hat{p}\,|\ell sjm\rangle, \qquad \text{(H.58)}$$

and hence

$$\begin{aligned}&\langle \ell sjm|\sigma^3|\tilde{\ell} sjm\rangle + \langle\tilde{\ell} sjm|\sigma^3|\ell sjm\rangle \\ &\qquad = -\langle \ell sjm|\big\{\sigma^3, \vec{\sigma}\cdot\hat{p}\big\}|\ell sjm\rangle = -\frac{2p^3}{p}\langle \ell sjm|\ell sjm\rangle. \end{aligned} \qquad \text{(H.59)}$$

Therefore

$$\begin{aligned} f_{\kappa m}(y_A) = \overline{M}_N \int \frac{d^3p}{(2\pi)^3}\ \delta\big(p^3 + \varepsilon_\kappa - \overline{M}_N\, y_A\big) \\ \Big\{F_\kappa(p)^2 + G_\kappa(p)^2 - \frac{2p^3}{p}F_\kappa(p)G_\kappa(p)\Big\}\ \langle \ell sjm|\ell sjm\rangle. \end{aligned} \qquad \text{(H.60)}$$

To evaluate Eq. (H.60) we first introduce unity in the form

$$1 = \sum_{L,L_z} Y^*_{LL_z}(\Omega_p) Y_{LL_z}(\Omega_p), \tag{H.61}$$

and obtain

$$f_{\kappa m}(y_A) = \overline{M}_N \int \frac{d^3p}{(2\pi)^3}\, \delta\big(p^3 + \varepsilon_\kappa - \overline{M}_N\, y_A\big) \sum_{L,L_z} Y^*_{LL_z}(\Omega_p)$$
$$\left\{ F_\kappa(p)^2 + G_\kappa(p)^2 - \frac{2p^3}{p} F_\kappa(p) G_\kappa(p) \right\} \langle \ell sjm | Y_{LL_z} | \ell sjm \rangle. \tag{H.62}$$

We now consider in matrix element $\langle \ell sjm | Y_{LL_z} | \ell sjm \rangle$, from Eq. (H.13)

$$\langle \ell sjm | Y_{LL_z} | \ell sjm \rangle$$
$$= (-1)^{j-m} (-1)^{j+\ell+s+L} (2j+1) \begin{pmatrix} j & L & j \\ -m & L_z & m \end{pmatrix} \begin{Bmatrix} \ell & L & \ell \\ j & s & j \end{Bmatrix} \langle \ell \| Y^{(L)} \| \ell \rangle,$$
$$= (-1)^{j-m} (2j+1) (-1)^{j+\ell+s+L} (-1)^\ell \sqrt{\frac{2L+1}{4\pi}}\, (2\ell+1)$$
$$\begin{pmatrix} \ell & L & \ell \\ 0 & 0 & 0 \end{pmatrix} \begin{pmatrix} j & L & j \\ -m & L_z & m \end{pmatrix} \begin{Bmatrix} \ell & L & \ell \\ j & s & j \end{Bmatrix}. \tag{H.63}$$

Now $L_z = 0$ and L is even, therefore the matrix element is given by

$$\langle \ell sjm | Y_{LL_z} | \ell sjm \rangle = (-1)^{j-m} (2j+1) (-1)^{j+\frac{1}{2}}$$
$$\sqrt{\frac{2L+1}{4\pi}}\, (2\ell+1) \begin{pmatrix} \ell & L & \ell \\ 0 & 0 & 0 \end{pmatrix} \begin{pmatrix} j & L & j \\ -m & 0 & m \end{pmatrix} \begin{Bmatrix} \ell & L & \ell \\ j & s & j \end{Bmatrix}. \tag{H.64}$$

Therefore

$$f_{\kappa m}(y_A) = (-1)^{j-m} (-1)^{j+\frac{1}{2}} \frac{(2j+1)}{\sqrt{4\pi}} (2\ell+1)\, \overline{M}_N$$
$$\int \frac{d^3p}{(2\pi)^3} \delta\big(p^3 + \varepsilon_\kappa - \overline{M}_N\, y_A\big) \sum_L \sqrt{2L+1}\; Y^*_{L0}(\Omega_p)$$
$$\left[F_\kappa(p)^2 + G_\kappa(p)^2 - \frac{2p^3}{p} F_\kappa(p) G_\kappa(p) \right]$$
$$\begin{pmatrix} j & L & j \\ -m & 0 & m \end{pmatrix} \begin{pmatrix} \ell & L & \ell \\ 0 & 0 & 0 \end{pmatrix} \begin{Bmatrix} \ell & L & \ell \\ j & s & j \end{Bmatrix}. \tag{H.65}$$

We now expand $f_{\kappa m}(y_A)$ into multipole distributions $f_{\kappa k}(y_A)$. Using the identity

$$\sum_m \begin{pmatrix} j & j & J \\ m & -m & 0 \end{pmatrix} \begin{pmatrix} j & j & J' \\ m & -m & 0 \end{pmatrix} = \frac{\delta_{JJ'}}{2J+1}, \tag{H.66}$$

we obtain

$$f_{jk}(y_A) = (-1)^{j+\frac{1}{2}}\,(2j+1)\,(2\ell+1)\,\sqrt{2k+1}\begin{pmatrix}\ell & k & \ell\\ 0 & 0 & 0\end{pmatrix}\begin{Bmatrix}\ell & k & \ell\\ j & s & j\end{Bmatrix}$$
$$\frac{\overline{M}_N}{16\pi^3}\int_\Lambda^\infty dp\;p\Big[F_\kappa(p)^2+G_\kappa(p)^2$$
$$+\frac{2}{p}\left(\varepsilon_\kappa-\overline{M}_N\,y_A\right)F_\kappa(p)G_\kappa(p)\Big]P_k\left(\frac{\overline{M}_N\,y_A-\varepsilon_\kappa}{p}\right), \quad \text{(H.67)}$$

where we have introduced the Legendre form for the spherical harmonics.

H.2.1 Baryon Number Sum Rule

Our result for the spin-independent distribution given in Eq. (H.65) must obey the baryon number sum rule, that is

$$\int_0^A dy_A\,f_{\kappa m}(y_A)=1, \qquad \Longrightarrow \qquad \sum_{\kappa m}\int_0^A dy_A\,f_{\kappa m}(y_A)=A. \quad \text{(H.68)}$$

We have

$$\int_0^A dy_A\,f_{\kappa m}(y_A)=(-1)^{j-m}\,(-1)^{j+\frac{1}{2}}\,\frac{(2j+1)}{\sqrt{4\pi}}\,(2\ell+1)\,\overline{M}_N$$
$$\int_0^A dy_A\int\frac{d^3p}{(2\pi)^3}\delta(p^3+\varepsilon_\kappa-\overline{M}_N\,y_A)\sum_L\sqrt{2L+1}\;Y^*_{L0}(\Omega_p)$$
$$\left[F_\kappa(p)^2+G_\kappa(p)^2-\frac{2p^3}{p}F_\kappa(p)G_\kappa(p)\right]$$
$$\begin{pmatrix}j & L & j\\ -m & 0 & m\end{pmatrix}\begin{pmatrix}\ell & L & \ell\\ 0 & 0 & 0\end{pmatrix}\begin{Bmatrix}\ell & L & \ell\\ j & s & j\end{Bmatrix}. \quad \text{(H.69)}$$

Noting that $p^3 = p\cos\theta$ and $\cos\theta = \sqrt{\frac{4\pi}{3}}\,Y_{10}$, the orthogonality condition for the spherical harmonics

$$\int_0^\pi d\phi\int_0^{2\pi} d\theta\sin\theta\;Y^*_{\ell m}(\theta,\phi)=\sqrt{4\pi}\;\delta_{\ell 0}\delta_{m0}, \quad \text{(H.70)}$$

implies that $L = 0$ for the F^2 and G^2 terms and $L = 1$ for the FG term. However $\left(\begin{smallmatrix}\ell & 1 & \ell\\ 0 & 0 & 0\end{smallmatrix}\right)=0$, therefore

$$\int_0^A dy_A\,f_{\kappa m}(y_A)=(-1)^{j-m}\,(-1)^{j+\frac{1}{2}}\,\frac{(2j+1)}{4\pi}\,(2\ell+1)$$
$$\int\frac{d^3p}{(2\pi)^3}\left[F_\kappa(p)^2+G_\kappa(p)^2\right]\begin{pmatrix}j & 0 & j\\ -m & 0 & m\end{pmatrix}\begin{pmatrix}\ell & 0 & \ell\\ 0 & 0 & 0\end{pmatrix}\begin{Bmatrix}\ell & 0 & \ell\\ j & s & j\end{Bmatrix}. \quad \text{(H.71)}$$

Using the results

$$\begin{pmatrix} j & j & 0 \\ m & -m & 0 \end{pmatrix} = \frac{(-1)^{j-m}}{\sqrt{2j+1}}, \qquad \begin{pmatrix} \ell & 0 & \ell \\ 0 & 0 & 0 \end{pmatrix} = \frac{(-1)^{\ell}}{\sqrt{2\ell+1}},$$

$$\begin{Bmatrix} \ell & 0 & \ell \\ j & s & j \end{Bmatrix} = \frac{(-1)^{j+\ell+s}}{\sqrt{2j+1}\sqrt{2\ell+1}}, \tag{H.72}$$

we obtain

$$\int_0^A dy_A\, f_{\kappa m}(y_A) = \frac{1}{4\pi}\int \frac{d^3p}{(2\pi)^3}\left[F_\kappa(p)^2 + G_\kappa(p)^2\right] = 1, \tag{H.73}$$

as required.

H.2.2 Momentum Sum Rule

The momentum sum rule

$$\sum_{\kappa m} \int_0^A dy_A \, y_A \, f_{\kappa m}(y_A) = A, \tag{H.74}$$

is used to determine the mass per nucleon $\overline{M}_N$. From Eq. (H.65) we have

$$\begin{aligned}\int_0^A dy_A \, y_A \, f_{\kappa m}(y_A) &= (-1)^{j-m} (-1)^{j+\frac{1}{2}} \frac{(2j+1)}{\sqrt{4\pi}} (2\ell+1) \overline{M}_N \\ &\int_0^A dy_A \, y_A \int \frac{d^3p}{(2\pi)^3} \delta(p^3 + \varepsilon_\kappa - \overline{M}_N y_A) \sum_L \sqrt{2L+1} \, Y^*_{L0}(\Omega_p) \\ &\left[F_\kappa(p)^2 + G_\kappa(p)^2 - \frac{2p^3}{p} F_\kappa(p) G_\kappa(p) \right] \\ &\begin{pmatrix} j & L & j \\ -m & 0 & m \end{pmatrix} \begin{pmatrix} \ell & L & \ell \\ 0 & 0 & 0 \end{pmatrix} \begin{Bmatrix} \ell & L & \ell \\ j & s & j \end{Bmatrix}. \end{aligned} \tag{H.75}$$

Using the delta function to remove the dy_A integration we obtain

$$\begin{aligned}\int_0^A dy_A \, y_A \, f_{\kappa m}(y_A) &= (-1)^{j-m} (-1)^{j+\frac{1}{2}} \frac{(2j+1)}{\sqrt{4\pi}} (2\ell+1) \\ &\int \frac{d^3p}{(2\pi)^3} \frac{p^3 + \varepsilon_\kappa}{\overline{M}_N} \sum_L \sqrt{2L+1} \, Y^*_{L0}(\Omega_p) \\ &\left[F_\kappa(p)^2 + G_\kappa(p)^2 - \frac{2p^3}{p} F_\kappa(p) G_\kappa(p) \right] \\ &\begin{pmatrix} j & L & j \\ -m & 0 & m \end{pmatrix} \begin{pmatrix} \ell & L & \ell \\ 0 & 0 & 0 \end{pmatrix} \begin{Bmatrix} \ell & L & \ell \\ j & s & j \end{Bmatrix}. \end{aligned} \tag{H.76}$$

The terms proportional to ε_κ and p^3 are analogous to the baryon number sum rule, however the term proportional to $(p^3)^2$ is new. Therefore

$$\begin{aligned}\int_0^A dy_A \, y_A \, f_{\kappa m}(y_A) &= \frac{\varepsilon_\kappa}{\overline{M}_N} + (-1)^{j-m} (-1)^{j+\frac{1}{2}} \frac{(2j+1)}{\sqrt{4\pi}} (2\ell+1) \\ &\frac{1}{\overline{M}_N} \int \frac{d^3p}{(2\pi)^3} \sum_L \sqrt{2L+1} \, Y^*_{L0}(\Omega_p) \left[-\frac{2(p^3)^2}{p} F_\kappa(p) G_\kappa(p) \right] \\ &\begin{pmatrix} j & L & j \\ -m & 0 & m \end{pmatrix} \begin{pmatrix} \ell & L & \ell \\ 0 & 0 & 0 \end{pmatrix} \begin{Bmatrix} \ell & L & \ell \\ j & s & j \end{Bmatrix}. \end{aligned} \tag{H.77}$$

Using $\cos^2\theta = \frac{4}{3}\sqrt{\frac{\pi}{5}}\,Y_{20} + \frac{1}{3}$ we obtain

$$\begin{aligned}
\int_0^A dy_A\, y_A\, f_{\kappa m}(y_A) &= \frac{\varepsilon_\kappa}{\overline{M}_N} - \frac{2}{12\pi\,\overline{M}_N}\int \frac{d^3p}{(2\pi)^3}\, p\, F_\kappa(p)G_\kappa(p) \\
&\quad - (-1)^{j-m}\,(-1)^{j+\frac{1}{2}}\,(2j+1)\,(2\ell+1) \\
\frac{4}{3\overline{M}_N}\int \frac{d^3p}{(2\pi)^3}\, p\, F_\kappa(p)G_\kappa(p) &\begin{pmatrix} j & 2 & j \\ -m & 0 & m \end{pmatrix}\begin{pmatrix} \ell & 2 & \ell \\ 0 & 0 & 0 \end{pmatrix}\begin{Bmatrix} \ell & 2 & \ell \\ j & s & j \end{Bmatrix}. \qquad \text{(H.78)}
\end{aligned}$$

I

Further Finite Nuclei Results

In this appendix we present many results for the finite nuclei multipole quark distributions, not included in Chapter 6. The nuclei we include are ^{7}Li, ^{11}B, ^{12}C, ^{15}N, ^{16}O, ^{27}Al and ^{28}Si. We also illustrate our results for the EMC effect in ^{12}C, ^{16}O and ^{28}Si, which where not presented in Chapter 6. For more complete figure captions see analogous figures in Chapter 6.

I.1 ^{7}Li

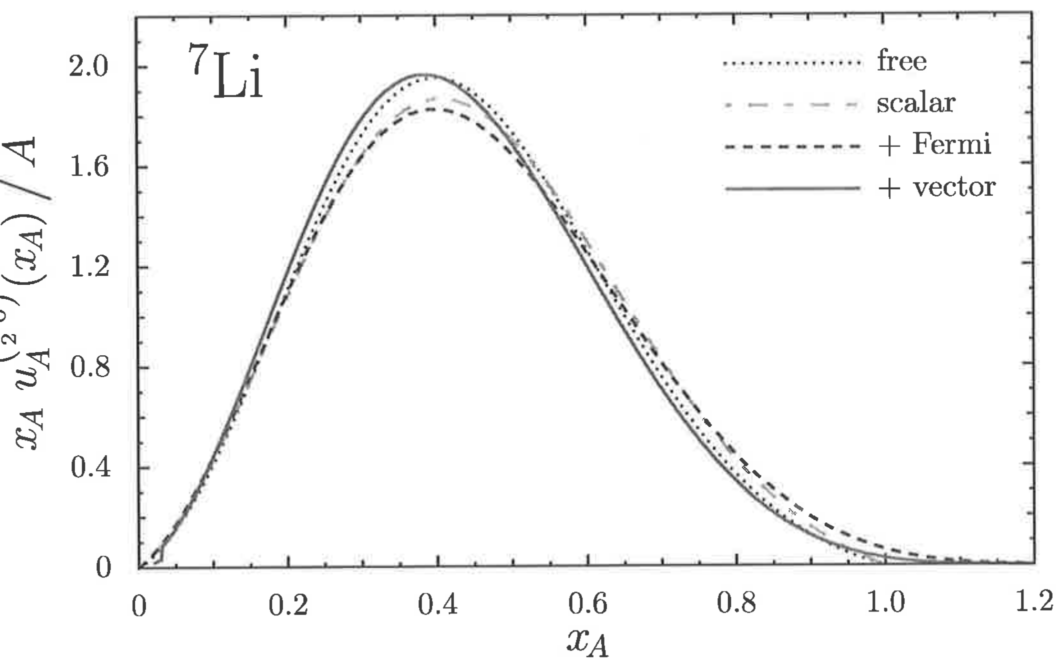

Figure I.1: Spin-independent 1$^{\text{st}}$ ($K = 0$) multipole u-quark distributions in ^{7}Li.

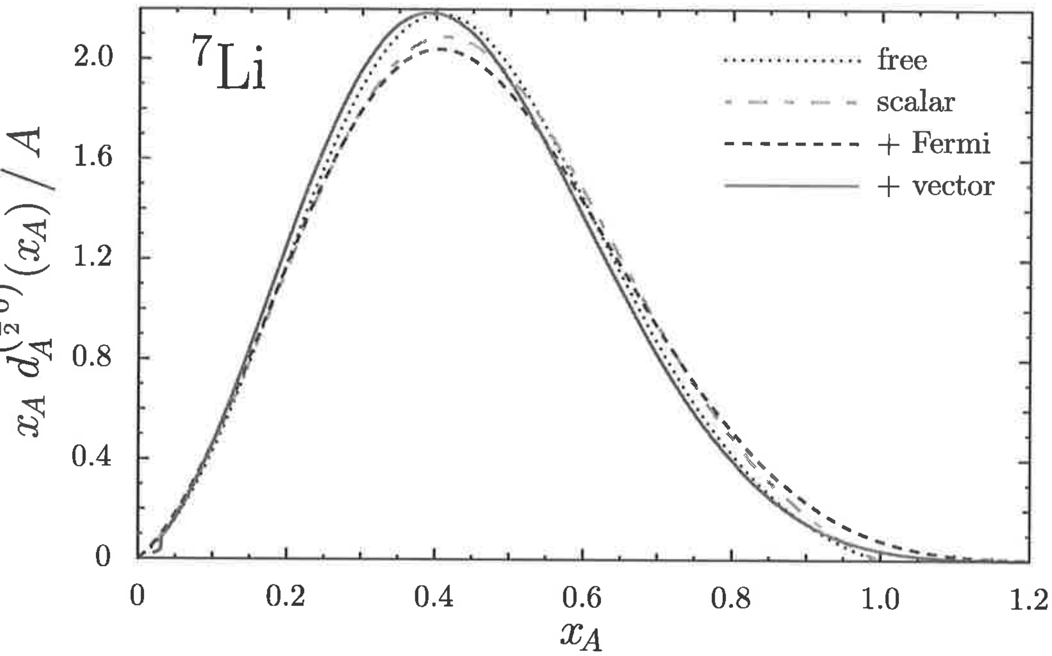

Figure I.2: Spin-independent 1$^{\text{st}}$ ($K = 0$) multipole d-quark distributions in ^{7}Li.

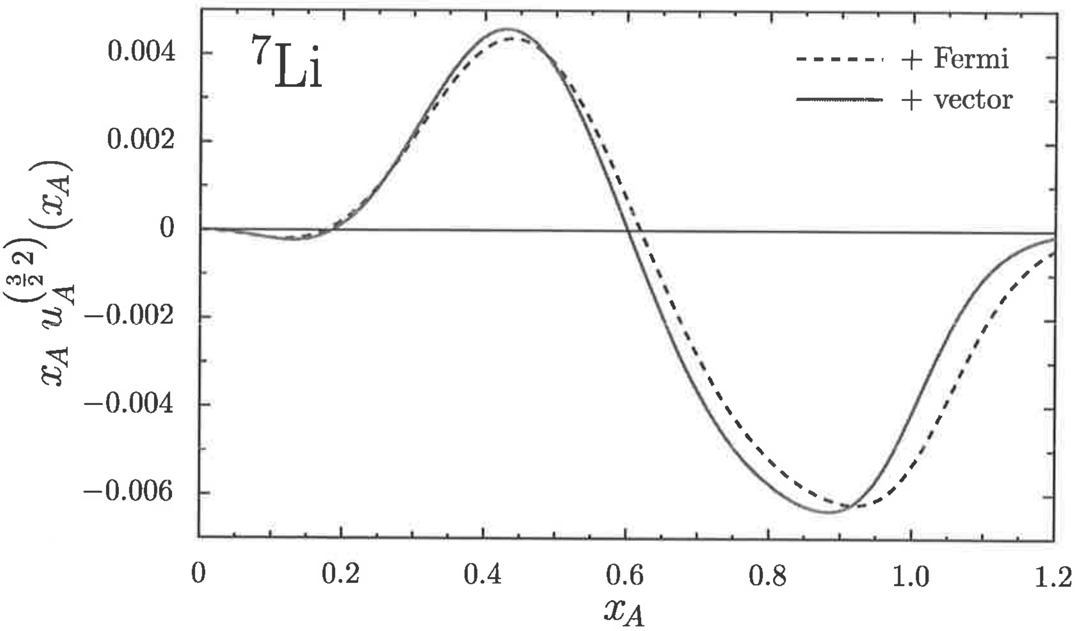

Figure I.3: Spin-independent 2$^{\text{nd}}$ ($K = 2$) multipole u-quark distributions in ^{7}Li.

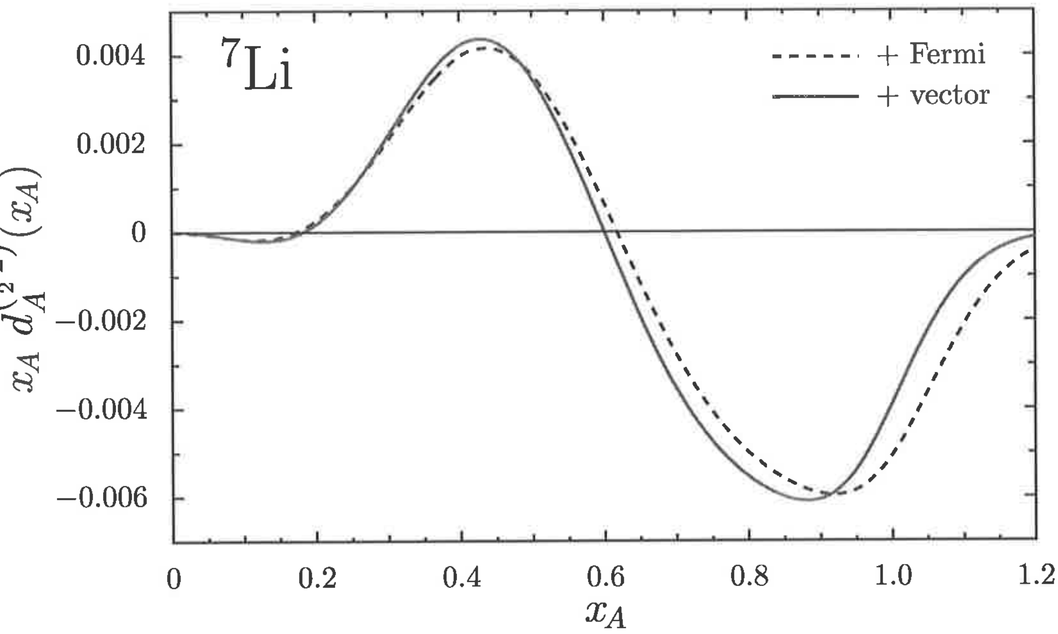

Figure I.4: Spin-independent 2[nd] ($K = 2$) multipole d-quark distributions in ^{7}Li.

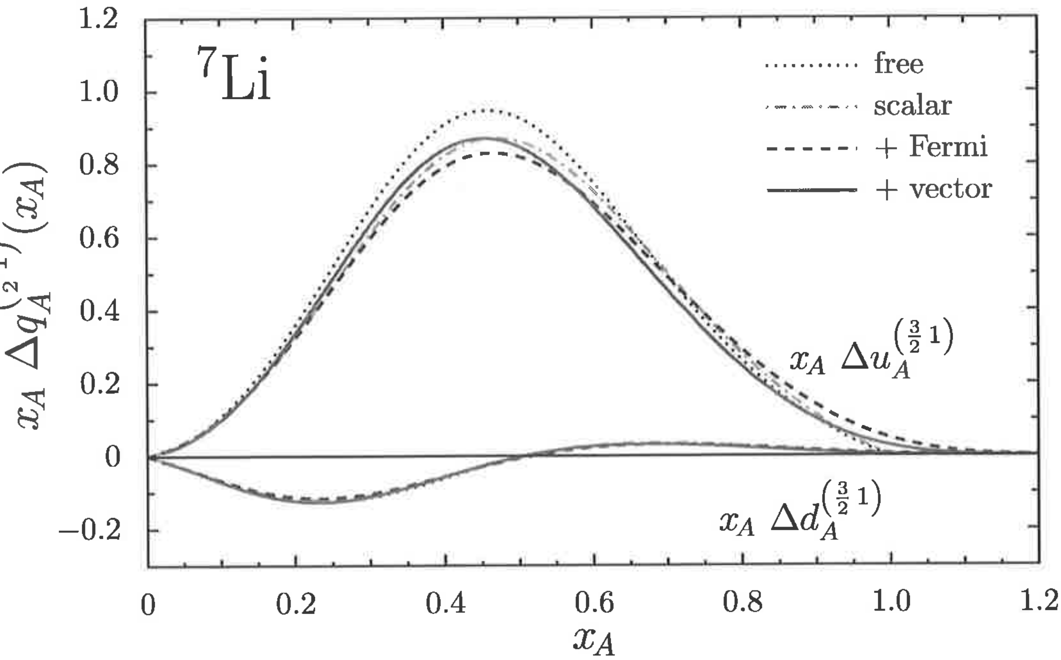

Figure I.5: Spin-dependent 1[st] ($K = 1$) multipole u- and d-quark distributions in ^{7}Li.

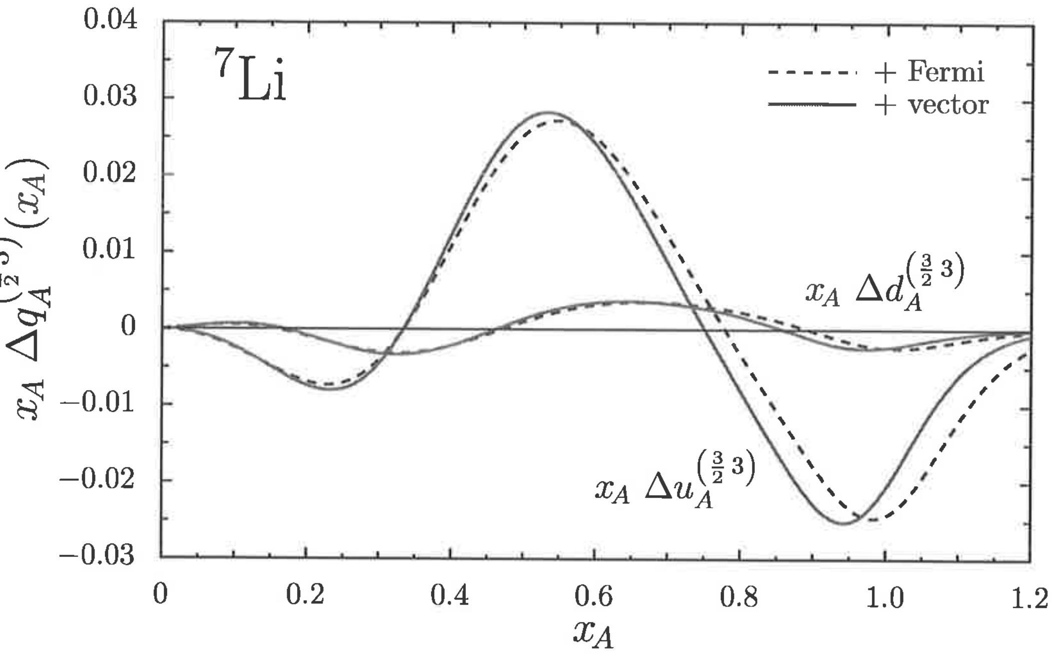

Figure I.6: Spin-dependent 2nd ($K = 3$) multipole u- and d-quark distributions in ^{7}Li.

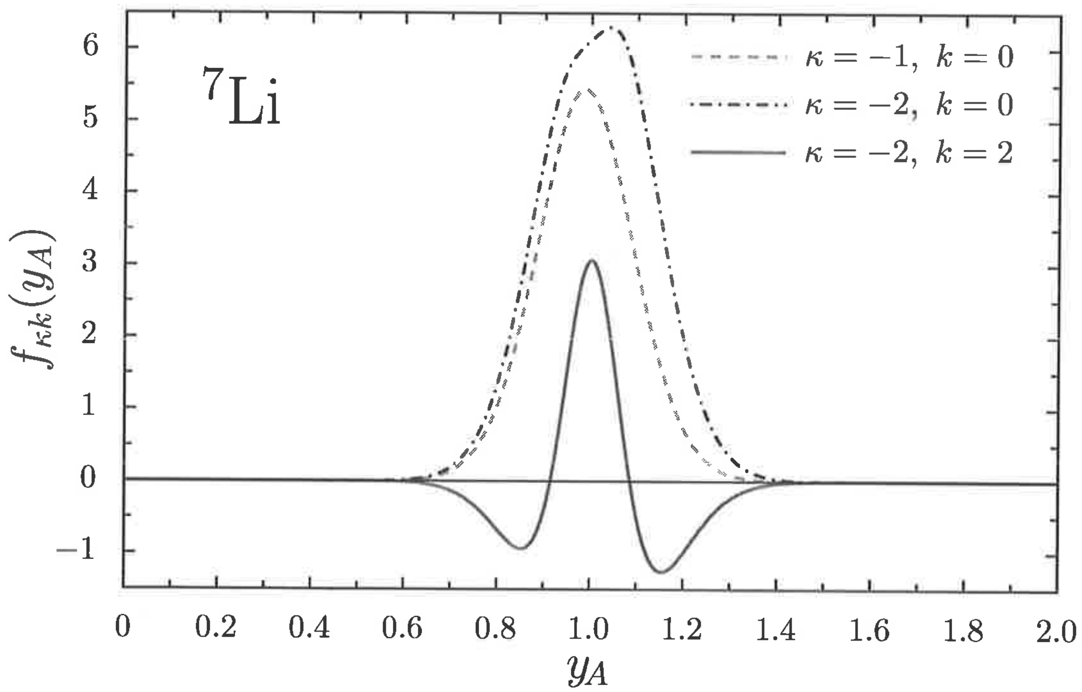

Figure I.7: All spin-independent nucleon multipole distributions, $f_{\kappa k}(y_A)$, in ^{7}Li.

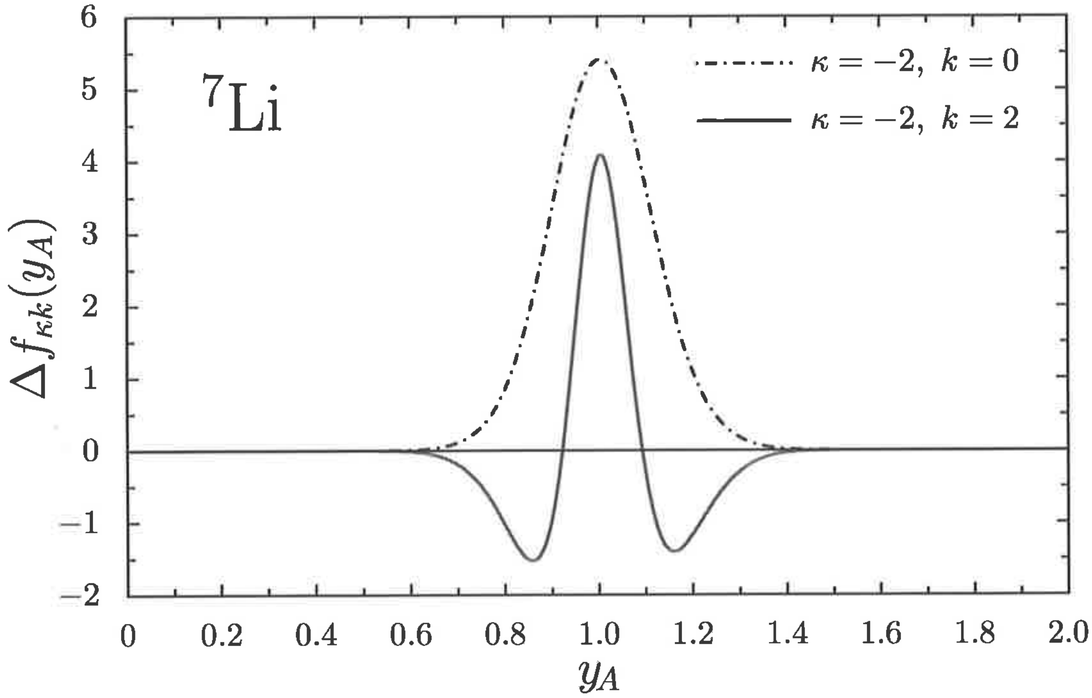

Figure I.8: All relevant spin-dependent nucleon multipole distributions, $\Delta f_{\kappa k}(y_A)$, in ^{7}Li.

I.2 ^{11}B

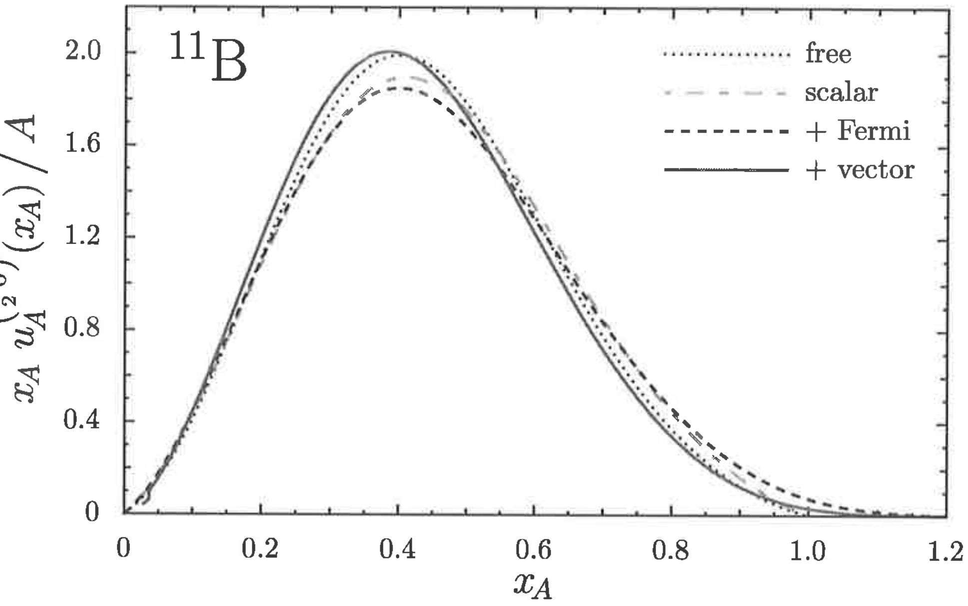

Figure I.9: Spin-independent 1st $(K = 0)$ multipole u-quark distributions in ^{11}B.

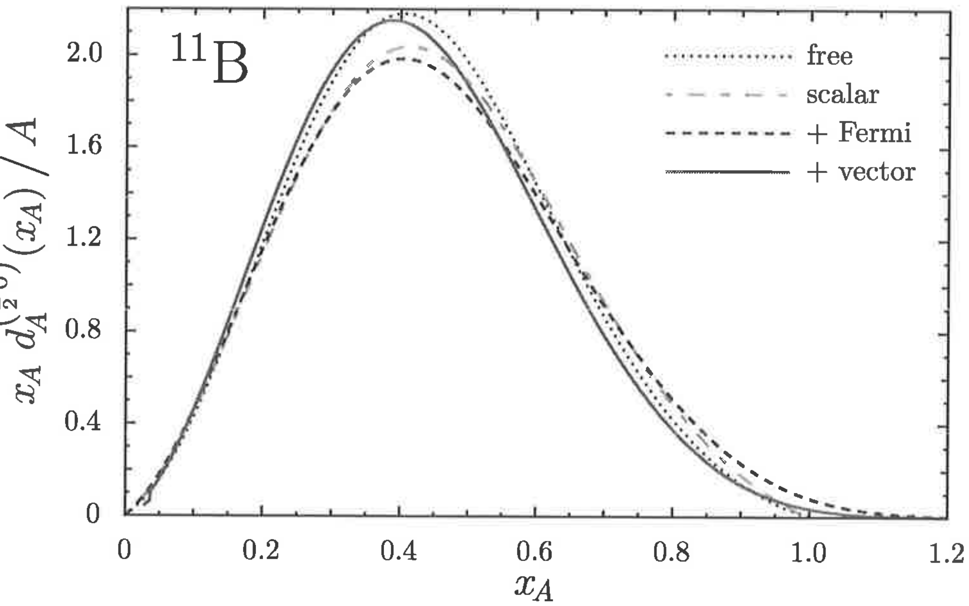

Figure I.10: Spin-independent 1st $(K = 0)$ multipole d-quark distributions in ^{11}B.

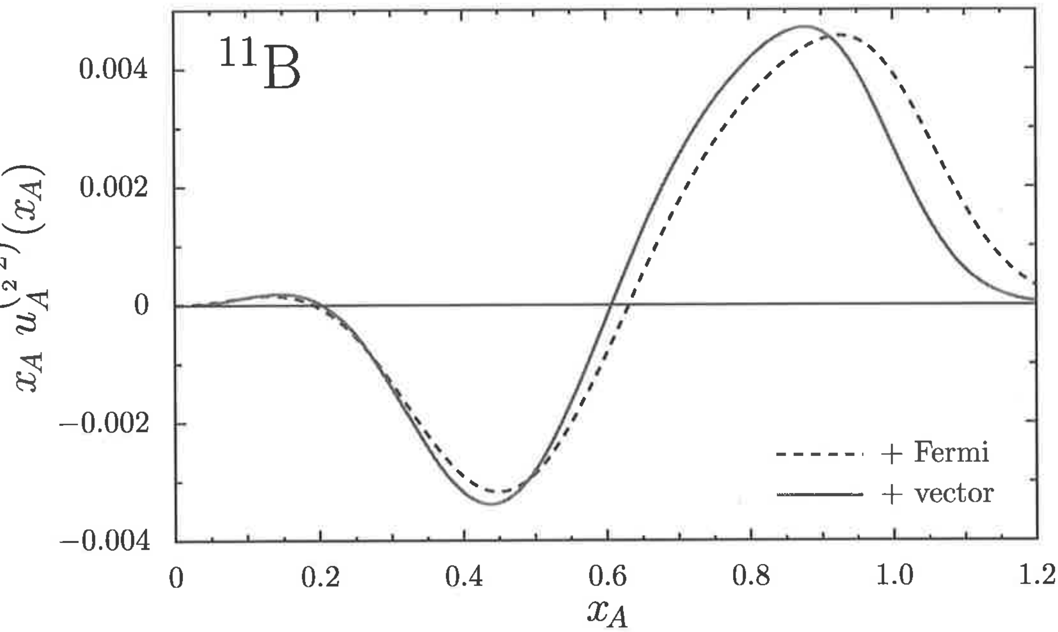

Figure I.11: Spin-independent 2nd ($K = 2$) multipole u-quark distributions in ^{11}B.

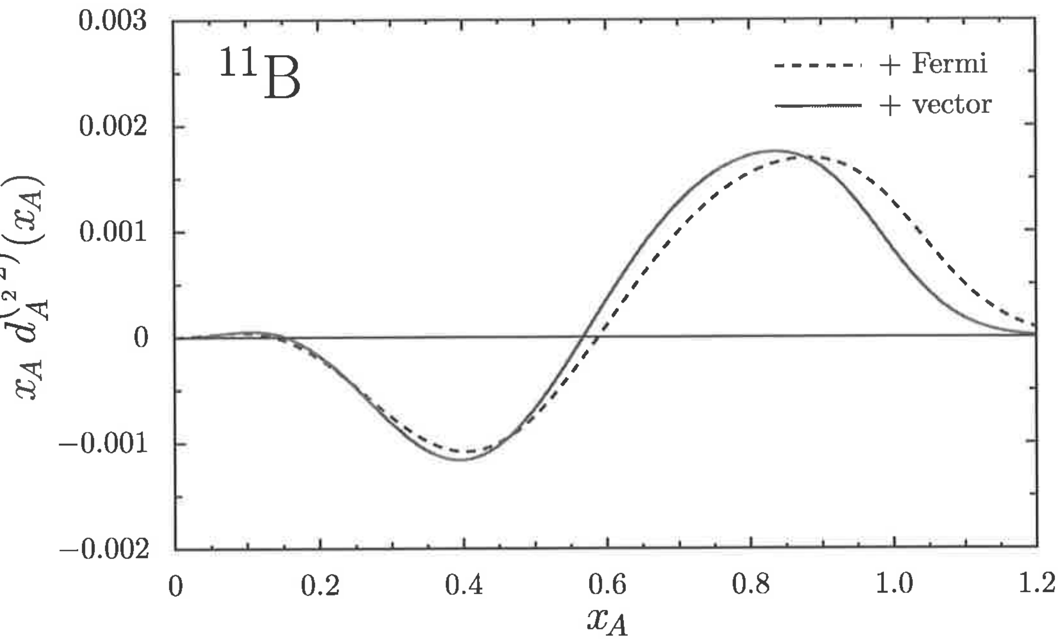

Figure I.12: Spin-independent 2nd ($K = 2$) multipole d-quark distributions in ^{11}B.

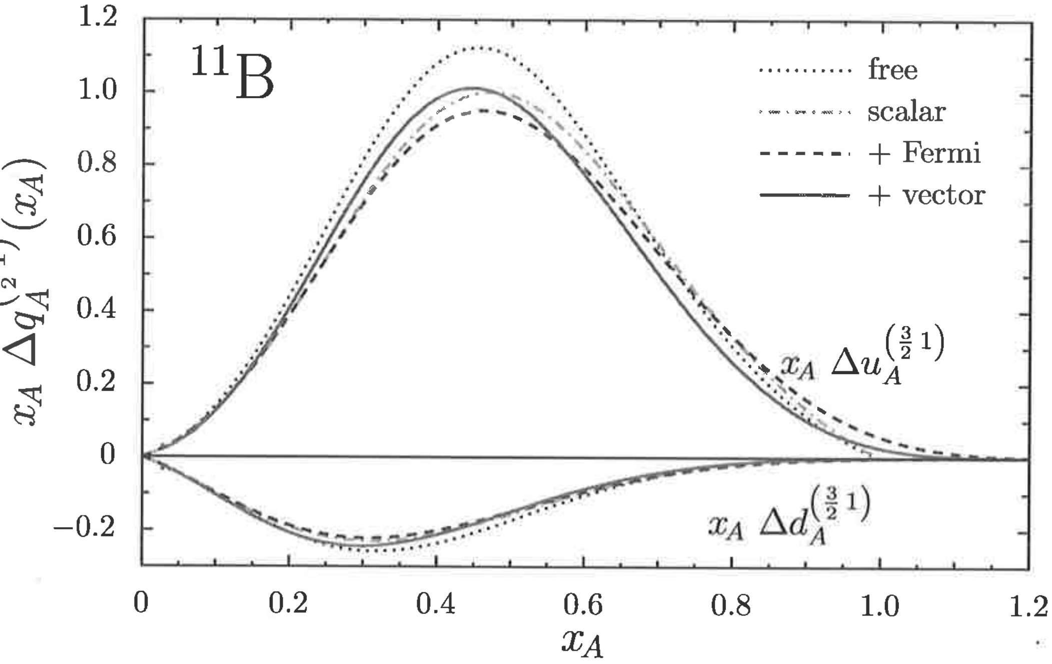

Figure I.13: Spin-dependent 1st ($K = 1$) multipole u- and d-quark distributions in ^{11}B.

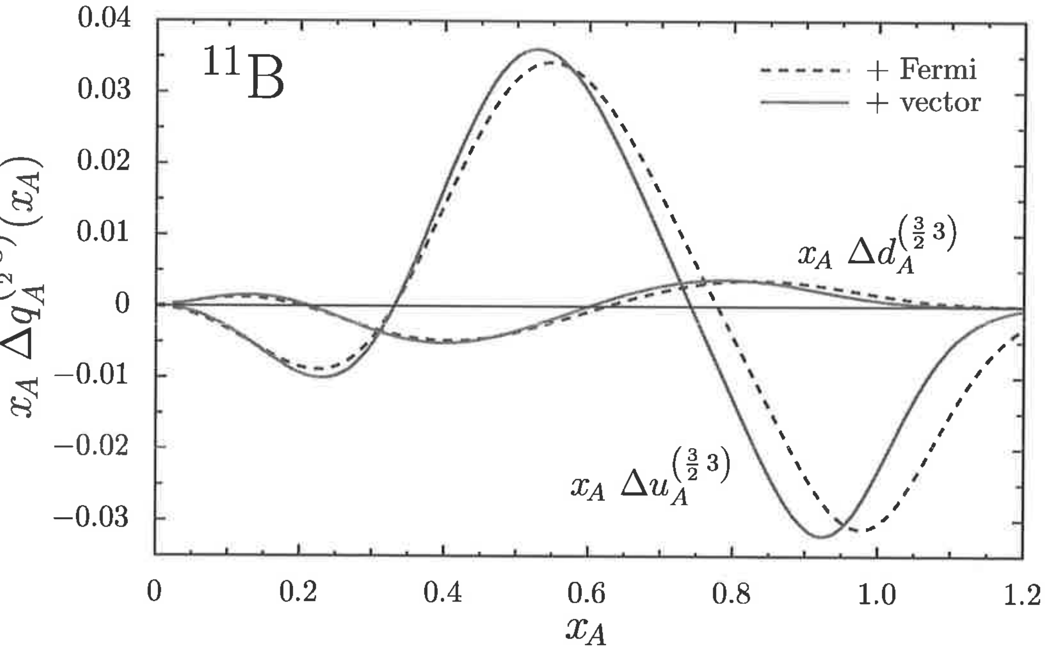

Figure I.14: Spin-dependent 2nd ($K = 3$) multipole u- and d-quark distributions in ^{11}B.

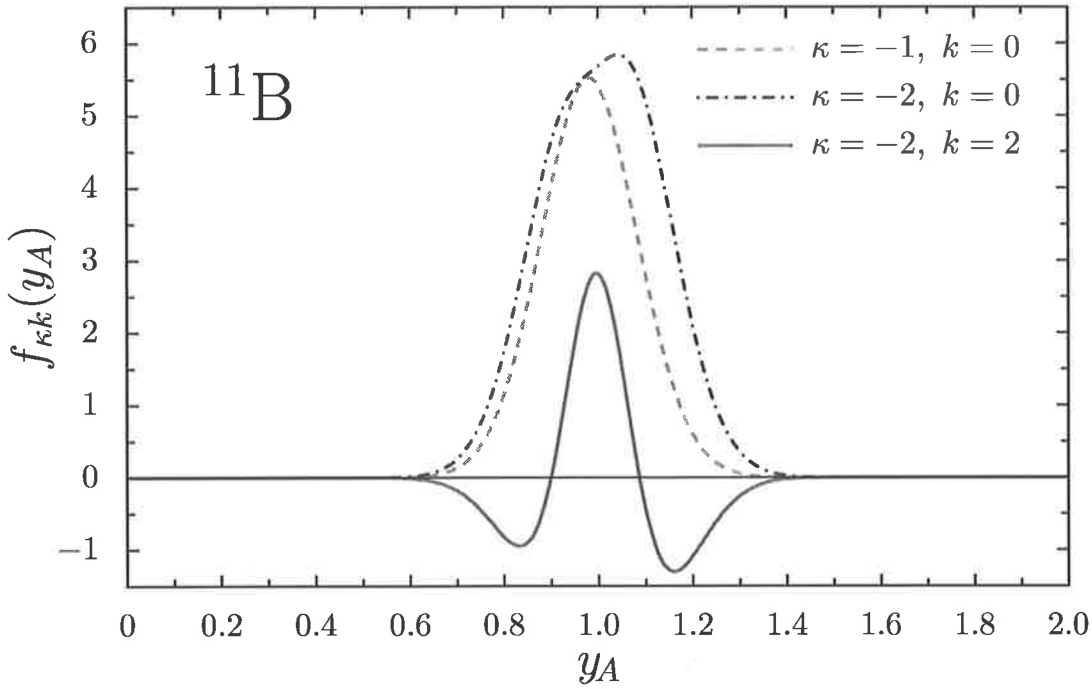

Figure I.15: All spin-independent nucleon multipole distributions, $f_{\kappa k}(y_A)$, in ^{11}B.

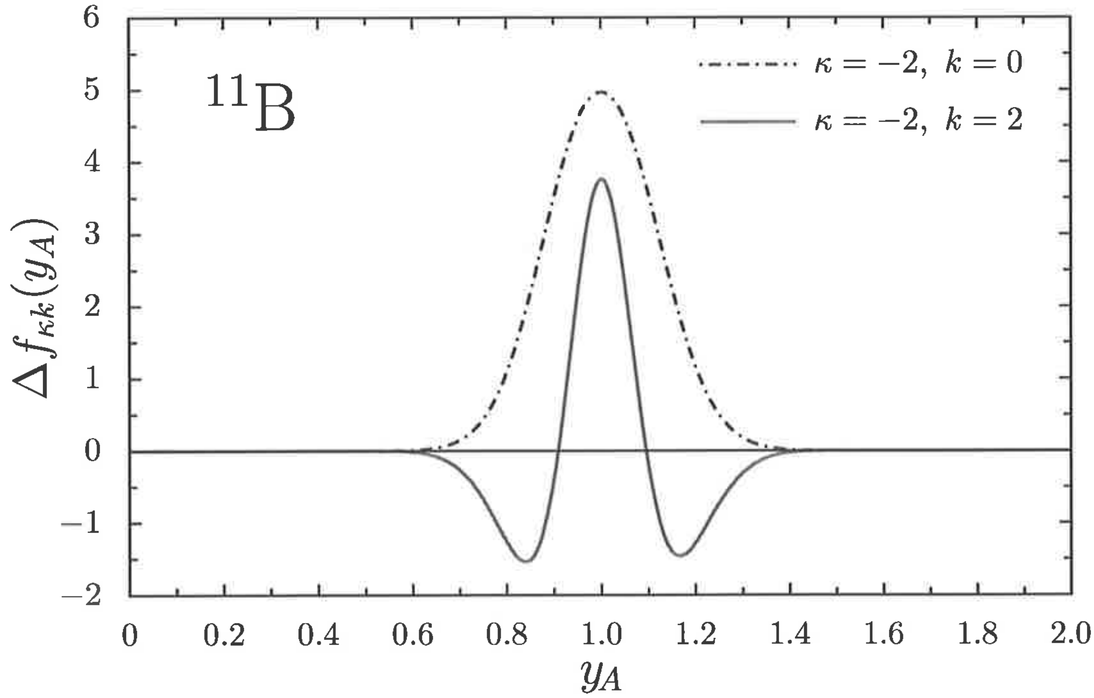

Figure I.16: All relevant spin-dependent nucleon multipole distributions, $\Delta f_{\kappa k}(y_A)$, in ^{11}B.

I.3 ^{12}C

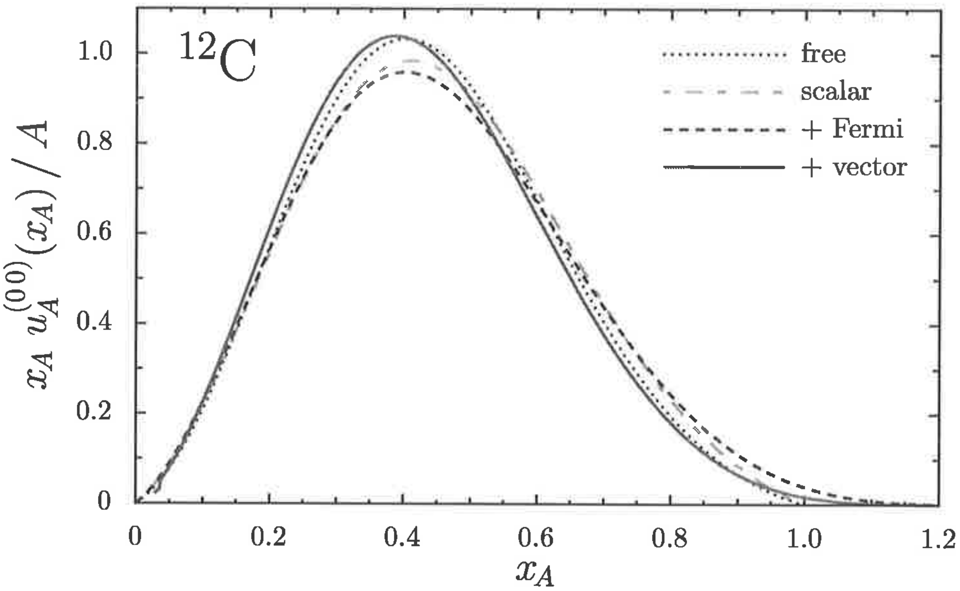

Figure I.17: Spin-independent 1st ($K = 0$) multipole quark distributions in ^{12}C. Note, in ^{12}C the up and down quark distributions are equal.

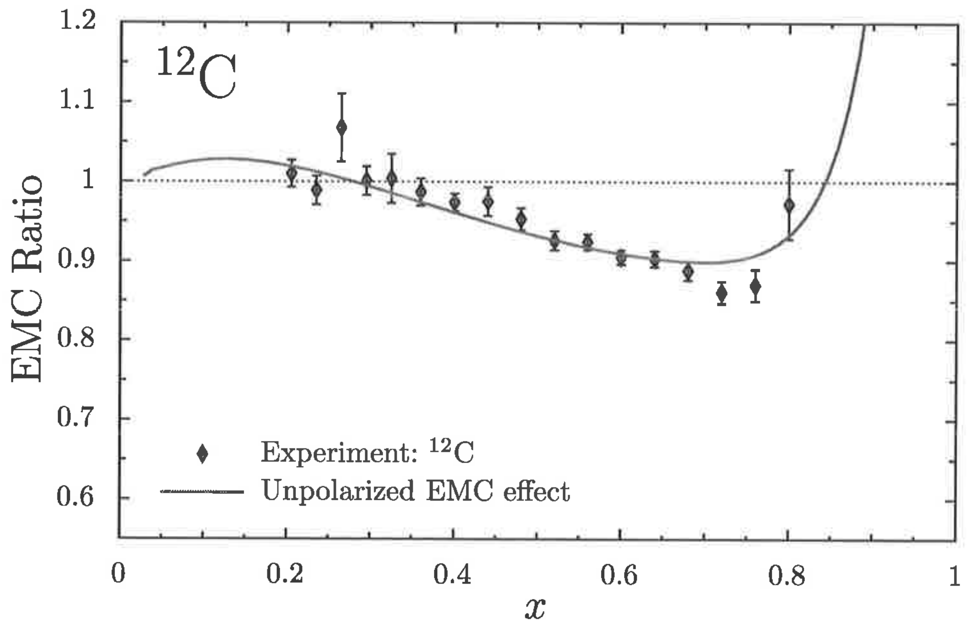

Figure I.18: The Unpolarized EMC ratio for ^{12}C. The experimental data is taken from Ref. [160].

I.4 ^{15}N

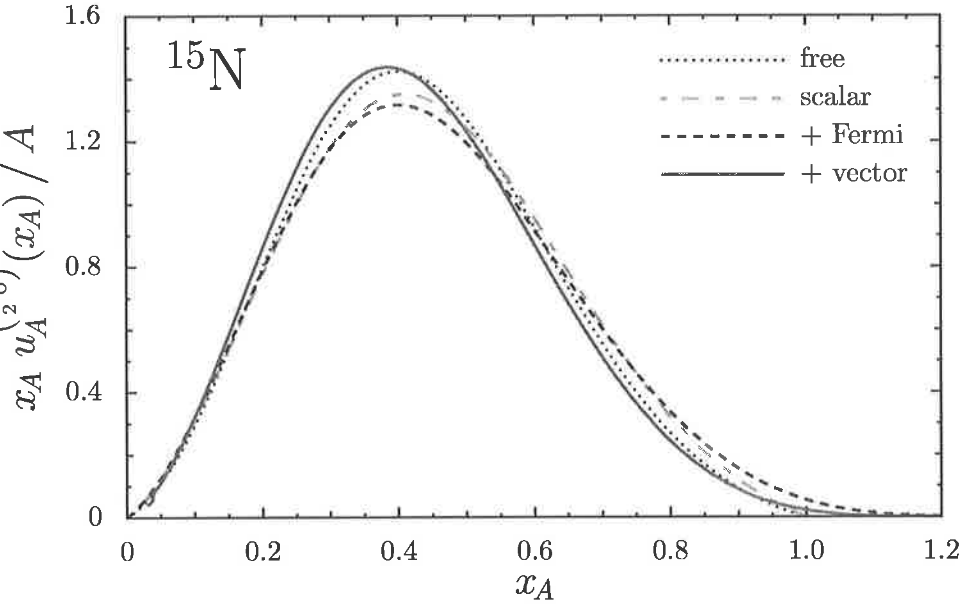

Figure I.19: Spin-independent 1st ($K = 0$) multipole u-quark distributions in ^{15}N.

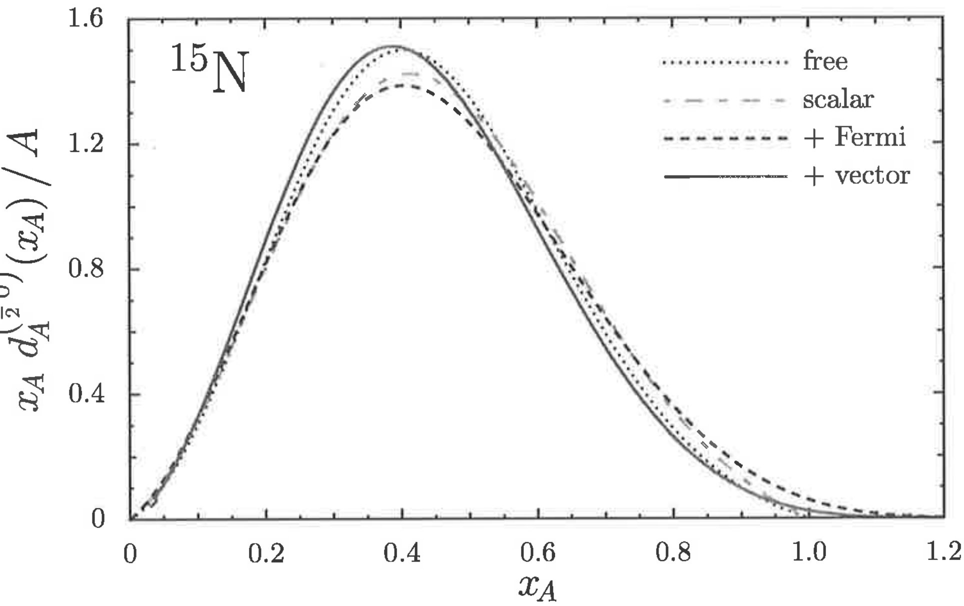

Figure I.20: Spin-independent 1st ($K = 0$) multipole d-quark distributions in ^{15}N.

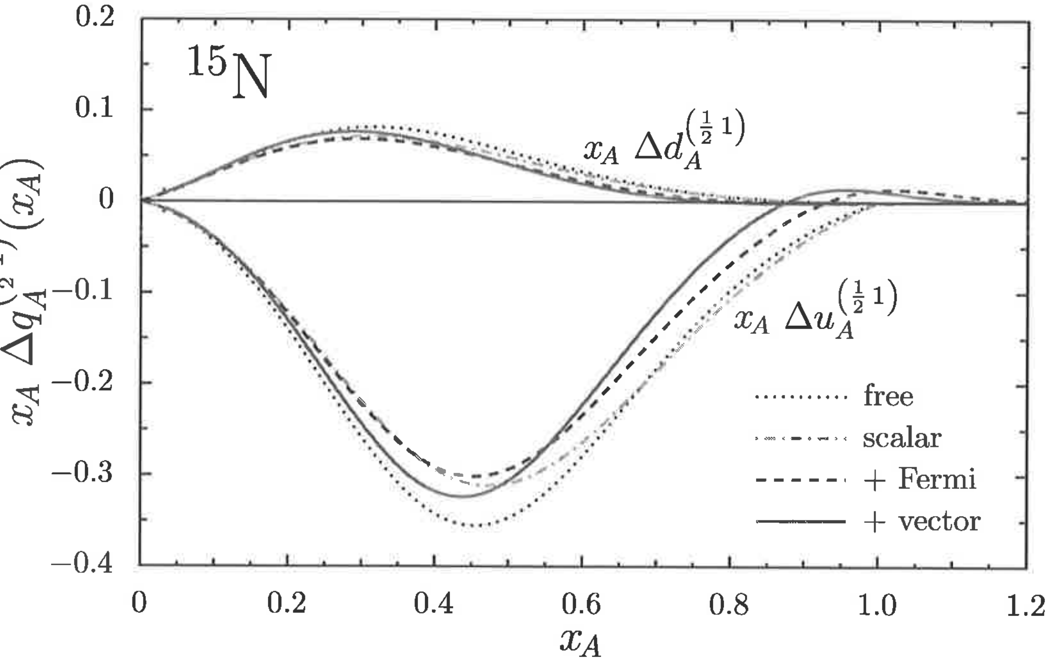

Figure I.21: Spin-dependent 1$^{\text{st}}$ ($K = 1$) multipole u- and d-quark distributions in ^{15}N.

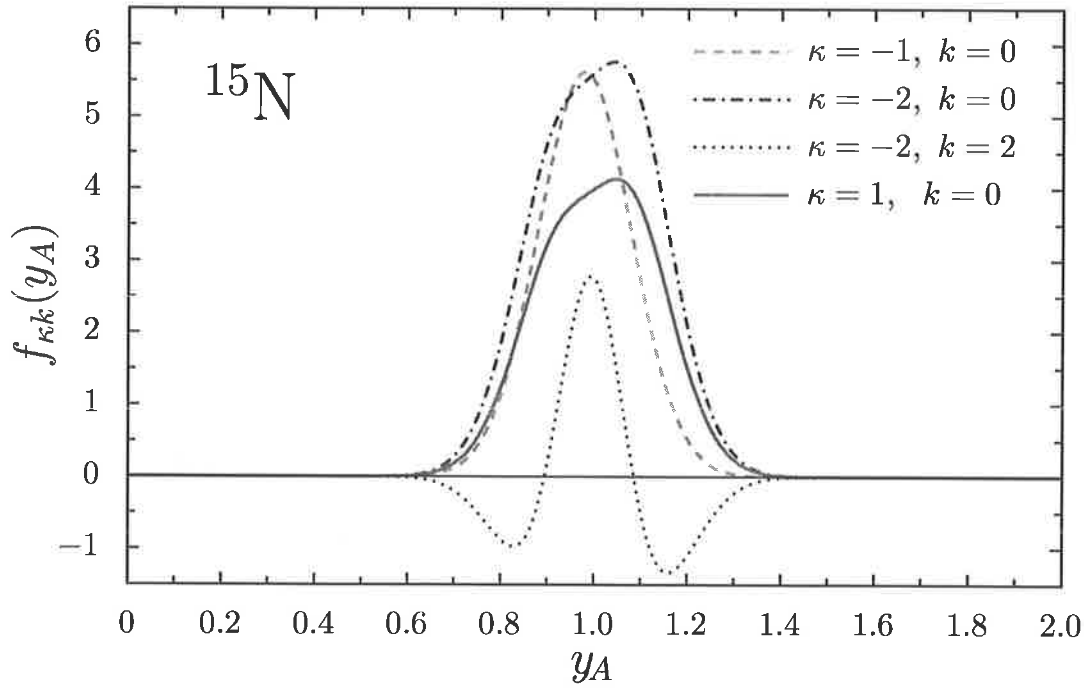

Figure I.22: All spin-independent nucleon multipole distributions, $f_{\kappa k}(y_A)$, in ^{15}N.

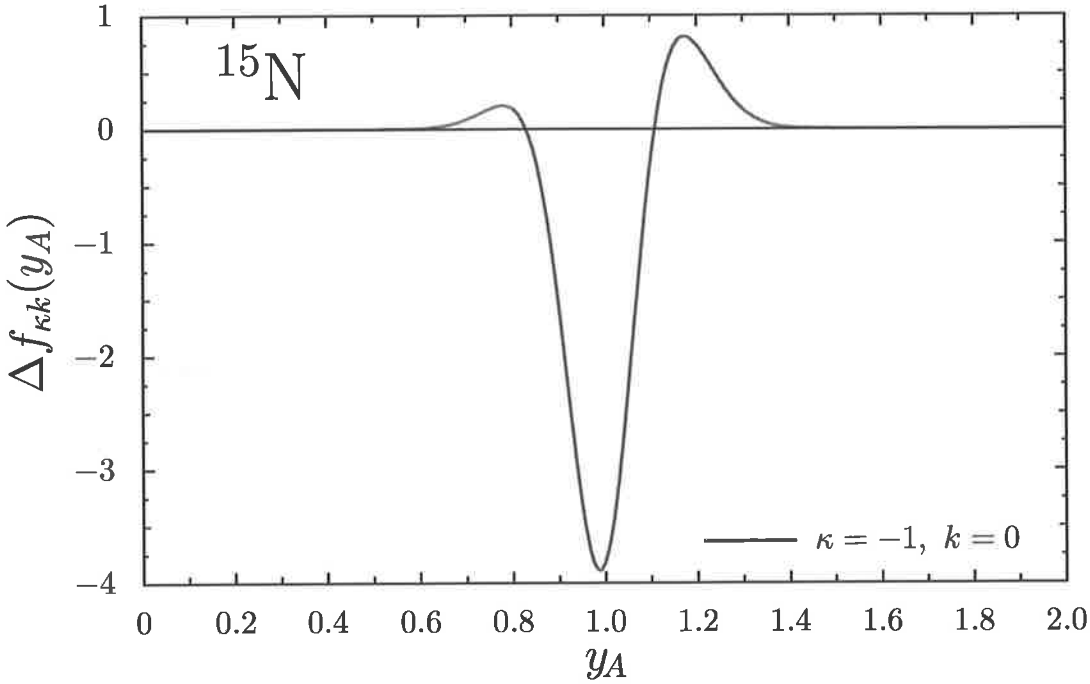

Figure I.23: All relevant spin-dependent nucleon multipole distributions, $\Delta f_{\kappa k}(y_A)$, in ^{15}N.

I.5 ^{16}O

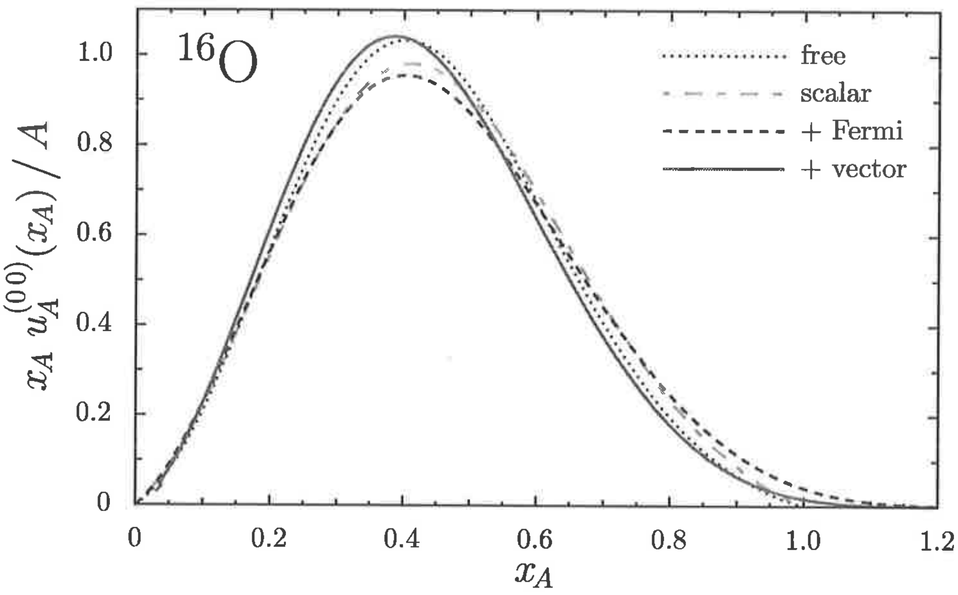

Figure I.24: Spin-independent 1st ($K = 0$) multipole quark distributions in ^{16}O. Note, in ^{16}O the up and down quark distributions are equal.

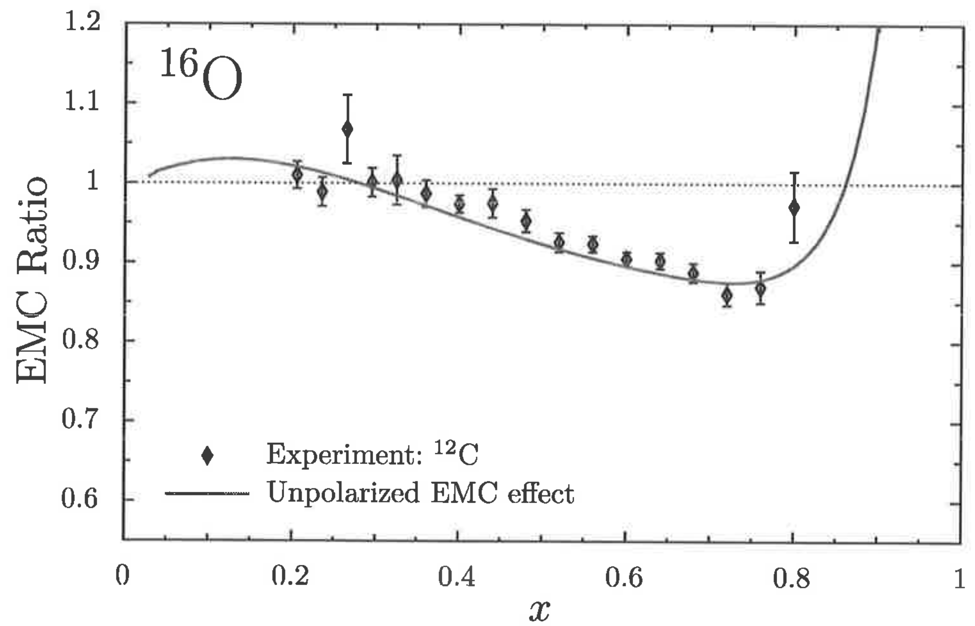

Figure I.25: The Unpolarized EMC ratio for ^{16}O. The experimental data is taken from Ref. [160].

I.6 ^{27}Al

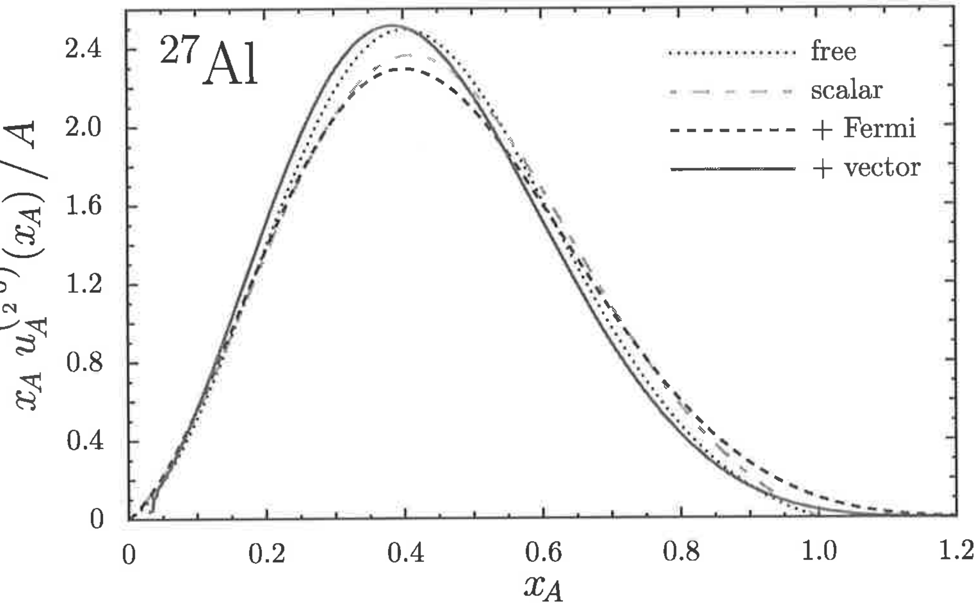

Figure I.26: Spin-independent 1st ($K = 0$) multipole u-quark distributions in ^{27}Al.

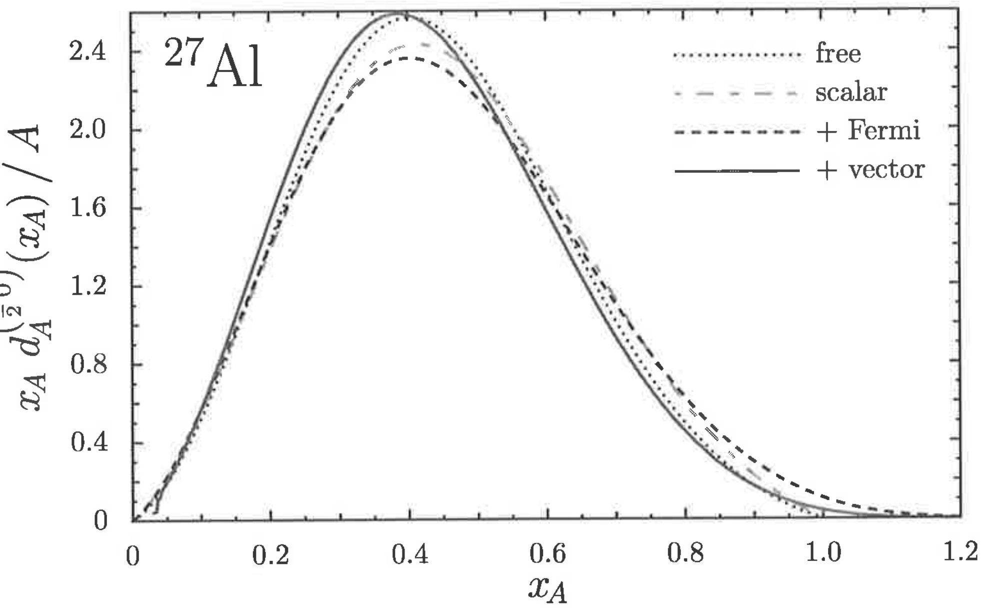

Figure I.27: Spin-independent 1st ($K = 0$) multipole d-quark distributions in ^{27}Al.

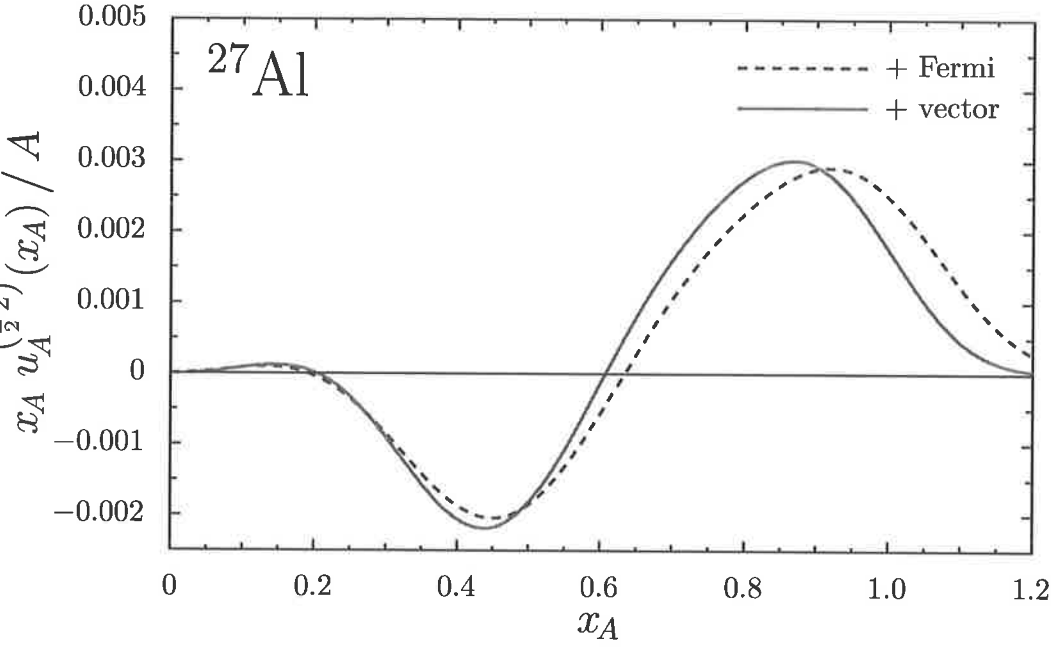

Figure I.28: Spin-independent 2$^{\text{nd}}$ ($K = 2$) multipole u-quark distributions in ^{27}Al.

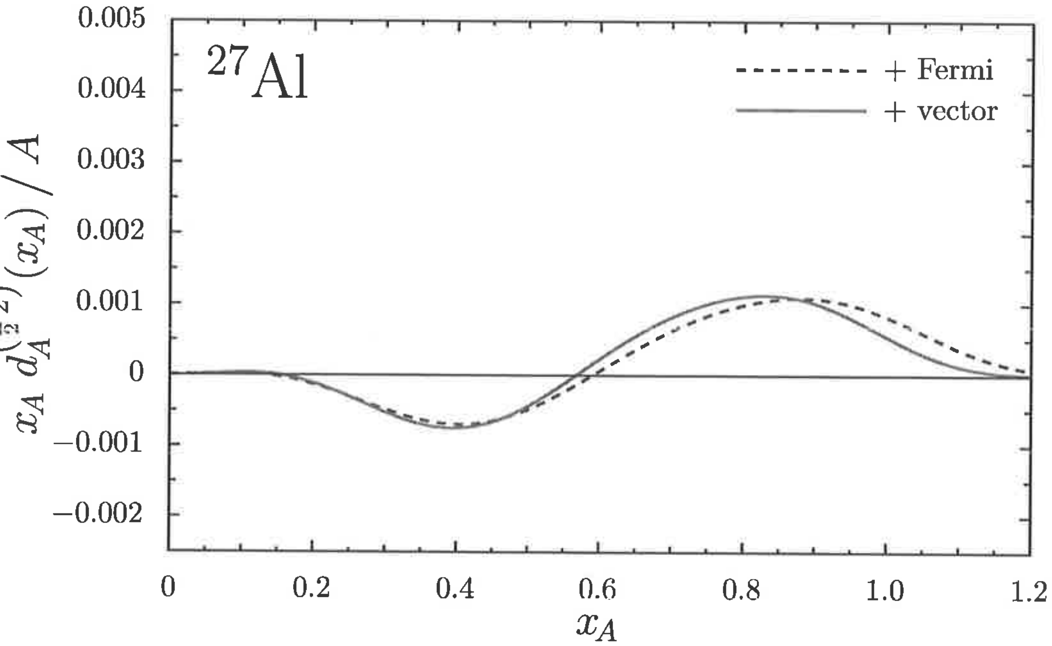

Figure I.29: Spin-independent 2$^{\text{nd}}$ ($K = 2$) multipole d-quark distributions in ^{27}Al.

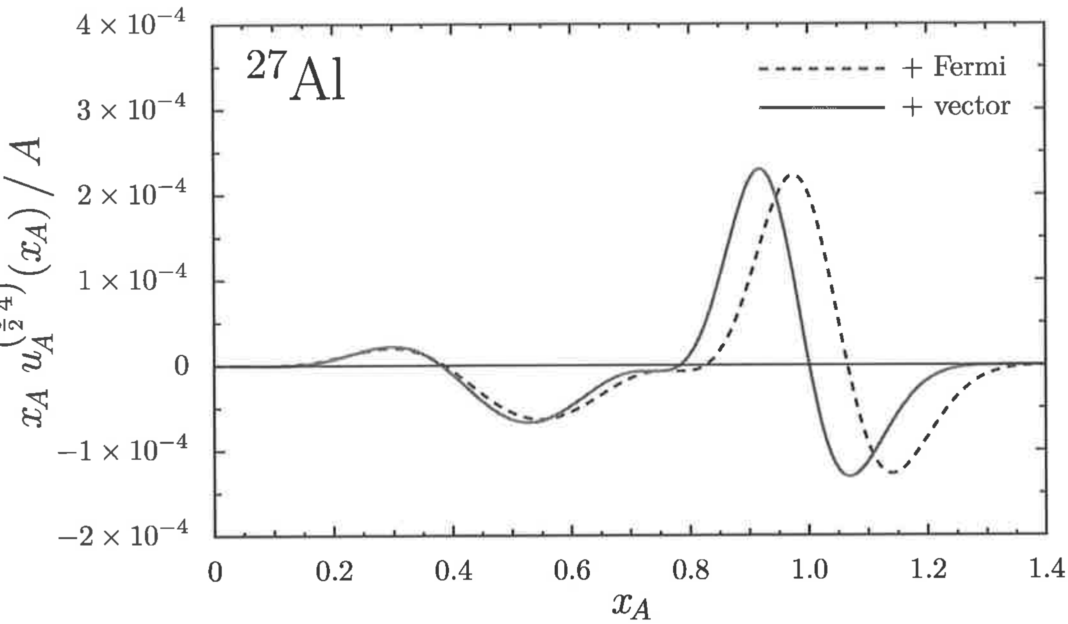

Figure I.30: Spin-independent 3rd ($K = 4$) multipole u-quark distributions in ^{27}Al.

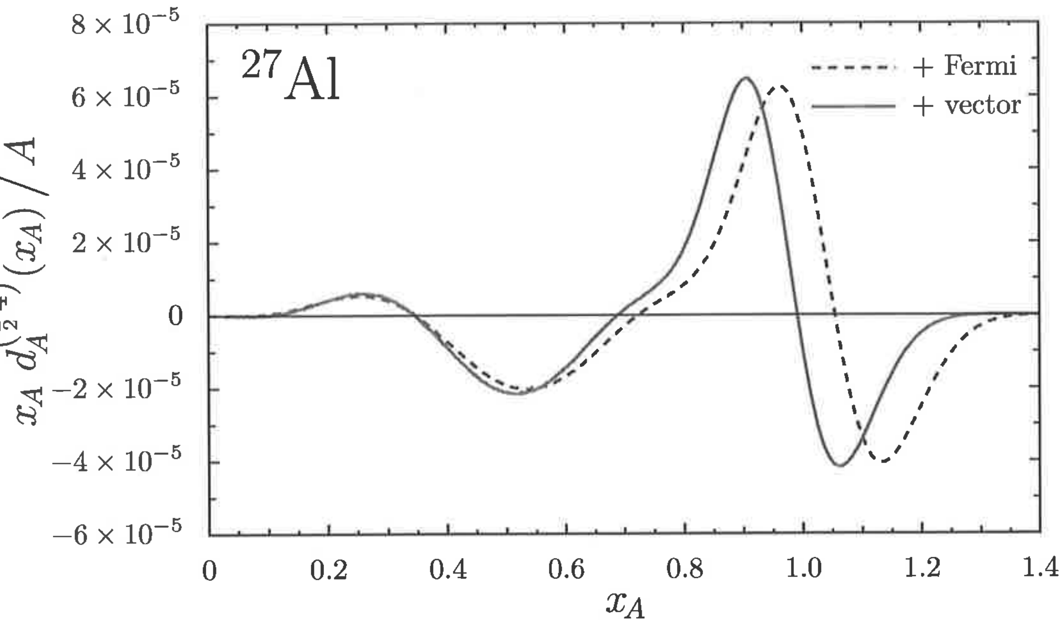

Figure I.31: Spin-independent 3rd ($K = 4$) multipole d-quark distributions in ^{27}Al.

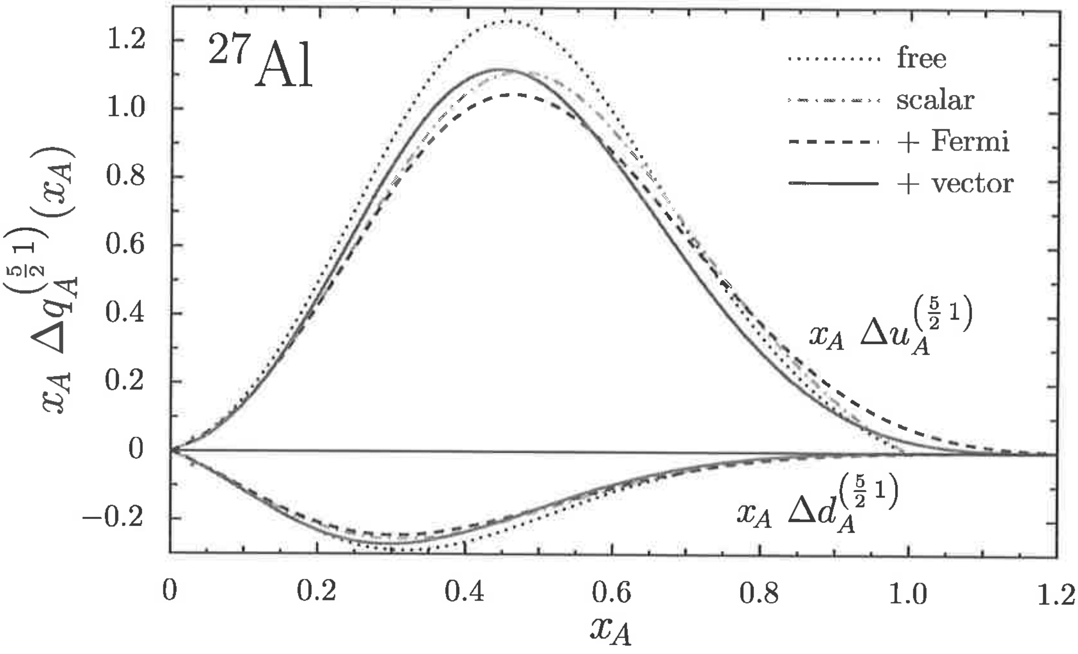

Figure I.32: Spin-dependent 1st ($K = 1$) multipole u- and d-quark distributions in ^{27}Al.

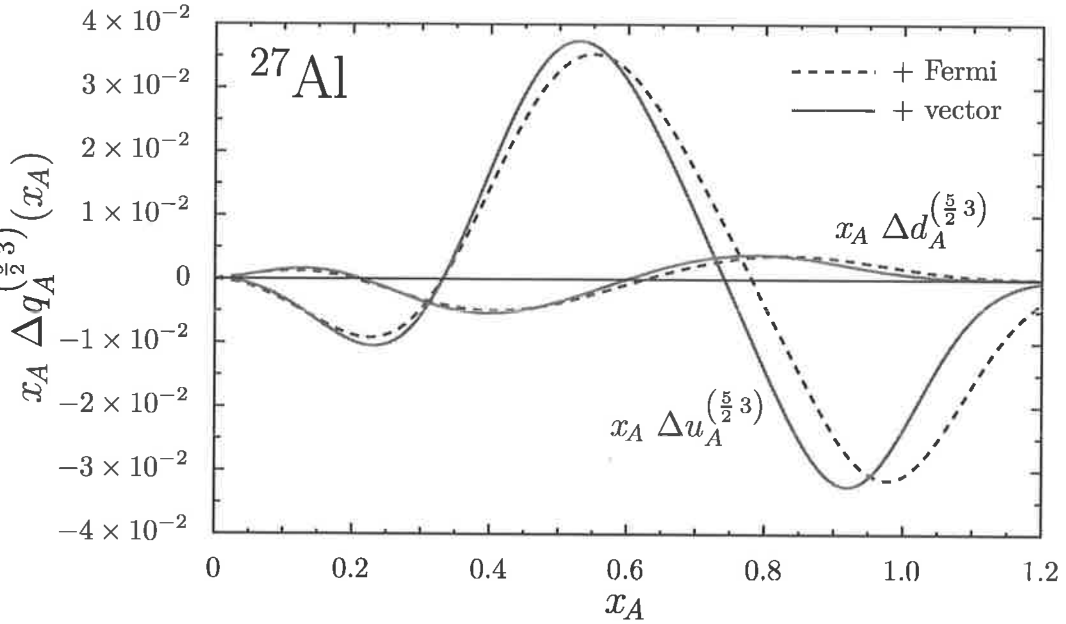

Figure I.33: Spin-dependent 2nd ($K = 3$) multipole u- and d-quark distributions in ^{27}Al.

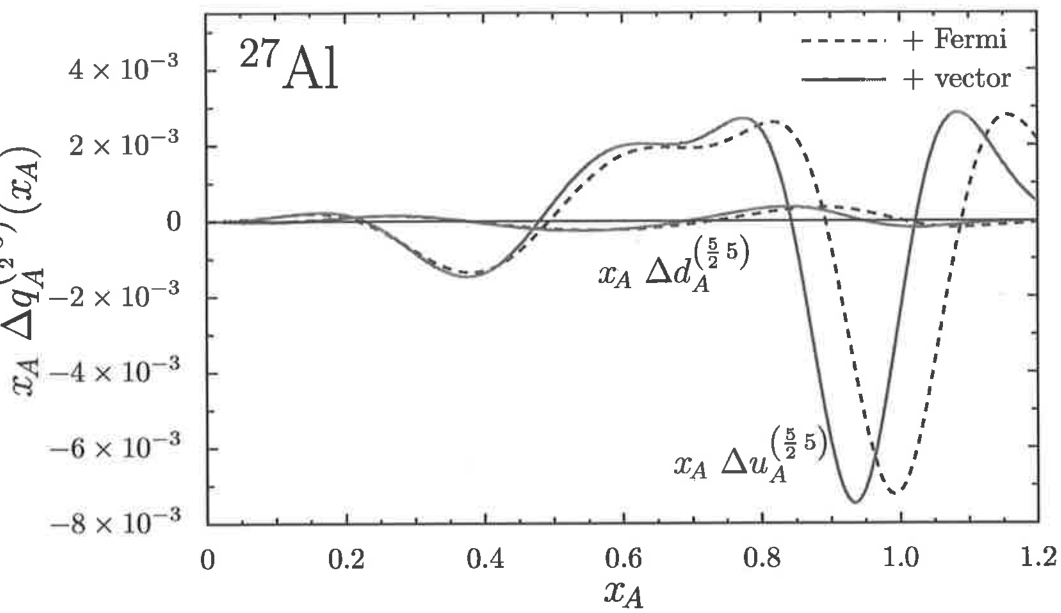

Figure I.34: Spin-dependent 3$^{\text{rd}}$ ($K = 5$) multipole u- and d-quark distributions in ^{27}Al.

I.7 ^{28}Si

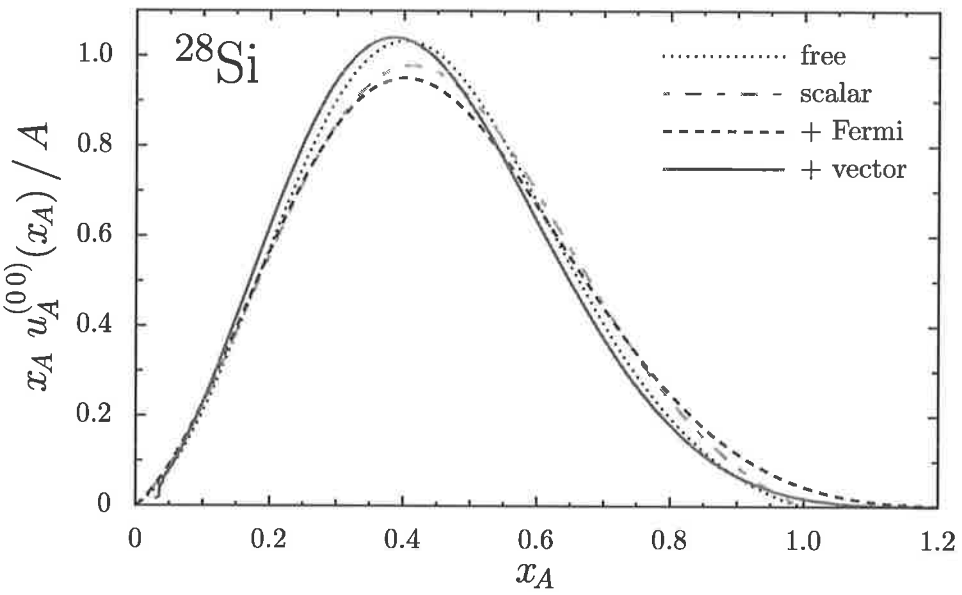

Figure I.35: Spin-independent 1[st] ($K = 0$) multipole quark distributions in ^{28}Si. Note, in ^{28}Si the up and down quark distributions are equal.

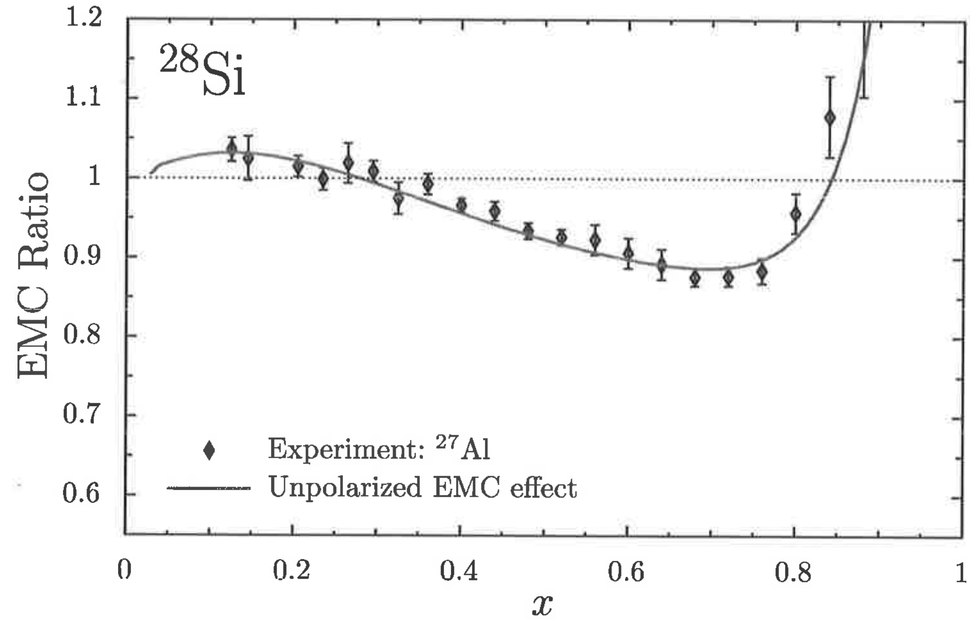

Figure I.36: The Unpolarized EMC ratio for ^{28}Si. The experimental data is taken from Ref. [160].

Bibliography

[1] J. D. Bjorken. Asymptotic sum rules at infinite momentum. *Phys. Rev.*, 179:1547–1553, 1969.

[2] J. Ashman et al. A measurement of the spin asymmetry and determination of the structure function g(1) in deep inelastic muon proton scattering. *Phys. Lett.*, B206:364, 1988.

[3] Stanley J. Brodsky, John R. Ellis, and Marek Karliner. Chiral symmetry and the spin of the proton. *Phys. Lett.*, B206:309, 1988.

[4] M. Hirai, S. Kumano, and N. Saito. Determination of polarized parton distribution functions and their uncertainties. *Phys. Rev.*, D69:054021, 2004.

[5] Guido Altarelli and Graham G. Ross. The anomalous gluon contribution to polarized leptoproduction. *Phys. Lett.*, B212:391, 1988.

[6] Guido Altarelli and G. Ridolfi. Understanding the proton spin structure: A status report. *Nucl. Phys. Proc. Suppl.*, 39BC:106–117, 1995.

[7] Hai-Yang Cheng. The proton spin puzzle: A status report. *Chin. J. Phys.*, 38:753, 2000.

[8] Steven D. Bass. The spin structure of the proton. *Rev. Mod. Phys.*, 77:1257–1302, 2005.

[9] J. H. Kim et al. A measurement of $\alpha_s(q^2)$ from the gross-llewellyn smith sum rule. *Phys. Rev. Lett.*, 81:3595–3598, 1998.

[10] A. D. Martin, R. G. Roberts, W. J. Stirling, and R. S. Thorne. Uncertainties of predictions from parton distributions. ii: Theoretical errors. *Eur. Phys. J.*, C35:325–348, 2004.

[11] J. J. Aubert et al. The ratio of the nucleon structure functions f2(n) for iron and deuterium. *Phys. Lett.*, B123:275, 1983.

[12] Vernon D. Barger and R. J. N. Phillips. *COLLIDER PHYSICS.* REDWOOD CITY, USA: ADDISON-WESLEY (1987) 592 P. (FRONTIERS IN PHYSICS, 71).

[13] C. Itzykson and J. B. Zuber. *QUANTUM FIELD THEORY.* Mcgraw-hill, New York, 1980. International Series In Pure and Applied Physics.

[14] Michael E. Peskin and D. V. Schroeder. *An Introduction to quantum field theory.* Westview, U.S.A., 1995.

[15] Robert L. Jaffe. Spin, twist and hadron structure in deep inelastic processes. 1996.

[16] M. Anselmino, A. Efremov, and E. Leader. The theory and phenomenology of polarized deep inelastic scattering. *Phys. Rept.*, 261:1–124, 1995.

[17] W. K. H. Panofsky. Electromagnetic interactions: Low q^2 electrodynamics: Elastic and inelastic electron (and muon) scattering. Presented at 14th Int. Conf. on High Energy Physics, Vienna, Aug 1968.

[18] Elliott D. Bloom et al. High-energy inelastic e p scattering at 6-degrees and 10- degrees. *Phys. Rev. Lett.*, 23:930–934, 1969.

[19] Martin Breidenbach et al. Observed behavior of highly inelastic electron - proton scattering. *Phys. Rev. Lett.*, 23:935–939, 1969.

[20] Richard P. Feynman. Very high-energy collisions of hadrons. *Phys. Rev. Lett.*, 23:1415–1417, 1969.

[21] R. P. Feynman. *Photon-hadron interactions.* 1972. Reading 1972, 282p.

[22] R. L. Jaffe. Deep inelastic scattering with application to nuclear targets. 1985. Lectures presented at the Los Alamos School on Quark Nuclear Physics, Los Alamos, N.Mex., Jun 10-14, 1985.

[23] W. M. Yao et al. Review of particle physics. *J. Phys.*, G33:1–1232, 2006.

[24] Jr. Callan, Curtis G. and David J. Gross. High-energy electroproduction and the constitution of the electric current. *Phys. Rev. Lett.*, 22:156–159, 1969.

[25] Raymond Brock et al. Handbook of perturbative qcd: Version 1.0. *Rev. Mod. Phys.*, 67:157–248, 1995.

[26] John C. Collins, Davison E. Soper, and George Sterman. Factorization of hard processes in qcd. *Adv. Ser. Direct. High Energy Phys.*, 5:1–91, 1988.

[27] R. Keith Ellis, Howard Georgi, Marie Machacek, H. David Politzer, and Graham G. Ross. Perturbation theory and the parton model in qcd. *Nucl. Phys.*, B152:285, 1979.

[28] F. M. Steffens and W. Melnitchouk. Target mass corrections revisited. *Phys. Rev.*, C73:055202, 2006.

[29] Vincenzo Barone, Alessandro Drago, and Philip G. Ratcliffe. Transverse polarisation of quarks in hadrons. *Phys. Rept.*, 359:1–168, 2002.

[30] R. L. Jaffe. Spin structure functions. 1992.

[31] John C. Collins and Davison E. Soper. Parton distribution and decay functions. *Nucl. Phys.*, B194:445, 1982.

[32] V. N. Gribov and L. N. Lipatov. Deep inelastic e p scattering in perturbation theory. *Sov. J. Nucl. Phys.*, 15:438–450, 1972.

[33] Guido Altarelli and G. Parisi. Asymptotic freedom in parton language. *Nucl. Phys.*, B126:298, 1977.

[34] John B. Kogut and Leonard Susskind. Scale invariant parton model. *Phys. Rev.*, D9:697–705, 1974.

[35] John B. Kogut and Leonard Susskind. Parton models and asymptotic freedom. *Phys. Rev.*, D9:3391–3399, 1974.

[36] Alessandro Cafarella and Claudio Coriano. Direct solution of renormalization group equations of qcd in x-space: Nlo implementations at leading twist. *Comput. Phys. Commun.*, 160:213–242, 2004.

[37] Alessandro Cafarella, Claudio Coriano', and Marco Guzzi. Nnlo logarithmic expansions and exact solutions of the dglap equations from x-space: New algorithms for precision studies at the lhc. *Nucl. Phys.*, B748:253–308, 2006.

[38] F. M. Steffens, W. Melnitchouk, and Anthony W. Thomas. Charm in the nucleon. *Eur. Phys. J.*, C11:673–683, 1999.

[39] A. Vogt. Efficient evolution of unpolarized and polarized parton distributions with qcd-pegasus. *Comput. Phys. Commun.*, 170:65–92, 2005.

[40] W. Furmanski and R. Petronzio. A method of analyzing the scaling violation of inclusive spectra in hard processes. *Nucl. Phys.*, B195:237, 1982.

[41] S. Kumano and J. T. Londergan. A fortran program for numerical solution of the altarelli- parisi equations by the laguerre method. *Comput. Phys. Commun.*, 69:373–396, 1992.

[42] Claudio Coriano and Cetin Savkli. QCD evolution equations: Numerical algorithms from the laguerre expansion. *Comput. Phys. Commun.*, 118:236–258, 1999.

[43] M. Miyama and S. Kumano. Numerical solution of q**2 evolution equations in a brute force method. *Comput. Phys. Commun.*, 94:185–215, 1996.

[44] M. Hirai, S. Kumano, and M. Miyama. Numerical solution of q**2 evolution equations for polarized structure functions. *Comput. Phys. Commun.*, 108:38, 1998.

[45] M. Hirai, S. Kumano, and M. Miyama. Numerical solution of q**2 evolution equation for the transversity distribution delta(t)(q). *Comput. Phys. Commun.*, 111:150–166, 1998.

[46] T. Muta. *Foundations of quantum chromodynamics. Second edition*, volume 57. 1998.

[47] M. Anselmino, V. Barone, A. Drago, and N. N. Nikolaev. Accessing transversity via j/psi production in polarized p(pol.) anti-p(pol.) interactions. *Phys. Lett.*, B594:97–104, 2004.

[48] A. V. Efremov, K. Goeke, and P. Schweitzer. Transversity distribution function in hard scattering of polarized protons and antiprotons in the pax experiment. *Eur. Phys. J.*, C35:207–210, 2004.

[49] Jacques Soffer. Positivity constraints for spin dependent parton distributions. *Phys. Rev. Lett.*, 74:1292–1294, 1995.

[50] Vincenzo Barone et al. Antiproton proton scattering experiments with polarization. 2005.

[51] E. Leader and E. Predazzi. *An Introduction to gauge theories and modern particle physics. Vol. 1: Electroweak interactions, the new particles and the parton model*, volume 3. 1996.

[52] E. Leader and E. Predazzi. *An Introduction to gauge theories and modern particle physics. Vol. 2: CP violation, QCD and hard processes*, volume 4. 1996.

[53] Anthony W. Thomas and Wolfram Weise. *The Structure of the Nucleon.* Wiley-VCH, Berlin, 2001.

[54] J Dudek and R.D. Young. personal communication.

[55] Yoichiro Nambu and G. Jona-Lasinio. Dynamical model of elementary particles based on an analogy with superconductivity. ii. *Phys. Rev.*, 124:246–254, 1961.

[56] Yoichiro Nambu and G. Jona-Lasinio. Dynamical model of elementary particles based on an analogy with superconductivity. i. *Phys. Rev.*, 122:345–358, 1961.

[57] Julian S. Schwinger. On gauge invariance and vacuum polarization. *Phys. Rev.*, 82:664–679, 1951.

[58] W. Bentz and Anthony W. Thomas. The stability of nuclear matter in the nambu-jona-lasinio model. *Nucl. Phys.*, A696:138–172, 2001.

[59] John Bardeen, L. N. Cooper, and J. R. Schrieffer. Microscopic theory of superconductivity. *Phys. Rev.*, 106:162, 1957.

[60] John Bardeen, L. N. Cooper, and J. R. Schrieffer. Theory of superconductivity. *Phys. Rev.*, 108:1175–1204, 1957.

[61] Michal Praszalowicz and Andrzej Rostworowski. Pion and vacuum properties in the nonlocal njl model. 2002.

[62] U. Vogl and W. Weise. The nambu and jona lasinio model: Its implications for hadrons and nuclei. *Prog. Part. Nucl. Phys.*, 27:195–272, 1991.

[63] S. Lawley, W. Bentz, and A. W. Thomas. The phases of isospin asymmetric matter in the two flavor njl model. *Phys. Lett.*, B632:495–500, 2006.

[64] S. Lawley, W. Bentz, and A. W. Thomas. Nucleons, nuclear matter and quark matter: A unified njl approach. *J. Phys.*, G32:667–680, 2006.

[65] Gerard 't Hooft. Computation of the quantum effects due to a four- dimensional pseudoparticle. *Phys. Rev.*, D14:3432–3450, 1976.

[66] Veronique Bernard, R. L. Jaffe, and Ulf G. Meissner. Strangeness mixing and quenching in the nambu-jona-lasinio model. *Nucl. Phys.*, B308:753, 1988.

[67] S. Klimt, M. Lutz, U. Vogl, and W. Weise. Generalized su(3) nambu-jona-lasinio model. part. 1. mesonic modes. *Nucl. Phys.*, A516:429–468, 1990.

[68] R. J. Crewther. Chirality selection rules and the u(1) problem. *Phys. Lett.*, B70:349, 1977.

[69] R. J. Crewther. Status of the u(1) problem. *Riv. Nuovo Cim.*, 2N8:63–117, 1979.

[70] R. J. Crewther. Effects of topological charge in gauge theories. *Acta Phys. Austriaca Suppl.*, 19:47–153, 1978.

[71] Alexander A. Osipov, Brigitte Hiller, and Joao da Providencia. Multi-quark interactions with a globally stable vacuum. *Phys. Lett.*, B634:48–54, 2006.

[72] Alexander A. Osipov, Brigitte Hiller, Alex H. Blin, and Joao da Providencia. Effects of eight-quark interactions on the hadronic vacuum and mass spectra of light mesons. 2006.

[73] K. Suzuki and H. Toki. Flavor su(4) baryon and meson masses in diquark quark model using the pauli-gursey symmetry. *Mod. Phys. Lett.*, A7:2867–2875, 1992.

[74] A. Buck, R. Alkofer, and H. Reinhardt. Baryons as bound states of diquarks and quarks in the nambu-jona-lasinio model. *Phys. Lett.*, B286:29–35, 1992.

[75] N. Ishii, W. Bentz, and K. Yazaki. Baryons in the njl model as solutions of the relativistic faddeev equation. *Nucl. Phys.*, A587:617–656, 1995.

[76] H. Mineo, Shin Nan Yang, Chi-Yee Cheung, and W. Bentz. Generalized parton distributions of the nucleon in the nambu-jona-lasinio model based on the faddeev approach. *Phys. Rev.*, C72:025202, 2005.

[77] S. P. Klevansky. The nambu-jona-lasinio model of quantum chromodynamics. *Rev. Mod. Phys.*, 64:649–708, 1992.

[78] E. E. Salpeter and H. A. Bethe. A relativistic equation for bound state problems. *Phys. Rev.*, 84:1232–1242, 1951.

[79] Murray Gell-Mann, R. J. Oakes, and B. Renner. Behavior of current divergences under su(3) x su(3). *Phys. Rev.*, 175:2195–2199, 1968.

[80] Gerard 't Hooft. A planar diagram theory for strong interactions. *Nucl. Phys.*, B72:461, 1974.

[81] Edward Witten. Baryons in the 1/n expansion. *Nucl. Phys.*, B160:57, 1979.

[82] Edward Witten. Global aspects of current algebra. *Nucl. Phys.*, B223:422–432, 1983.

[83] R. Alkofer, H. Reinhardt, and H. Weigel. Baryons as chiral solitons in the nambu-jona-lasinio model. *Phys. Rept.*, 265:139–252, 1996.

[84] R. T. Cahill, Craig D. Roberts, and J. Praschifka. Baryon structure and qcd. *Austral. J. Phys.*, 42:129–145, 1989.

[85] Su-zhou Huang and John Tjon. Nucleon solution of the faddeev equation in the nambu-jona- lasinio model. *Phys. Rev.*, C49:1702–1708, 1994.

[86] I. R. Afnan and Anthony W. Thomas. Fundamentals of three-body scattering theory. *Top. Curr. Phys.*, 2:1–47, 1977.

[87] L. D. Faddeev. *Mathematical problems of the quantum theory of scattering for a three-particle system.* Atomic Energy Research Establishment, 1964.

[88] W. Glockle. *The Quantum Mechanical Few-Body Problem.* Springer, Berlin, Germany, 1983.

[89] D. Iagolnitzer. *Scattering in Quantum Field Theories.* Princeton University Press, Princeton, New Jersey, 1993.

[90] H. Mineo, W. Bentz, N. Ishii, and K. Yazaki. Axial vector diquark correlations in the nucleon: Structure functions and static properties. *Nucl. Phys.*, A703:785–820, 2002.

[91] M. Kato, W. Bentz, K. Yazaki, and K. Tanaka. A modified nambu-jona-lasinio model for mesons and baryons. *Nucl. Phys.*, A551:541–579, 1993.

[92] T. Watabe and H. Toki. The chiral quark soliton model for the nucleon. *Prog. Theor. Phys.*, 87:651–661, 1992.

[93] Markus Diefenthaler. Transversity measurements at hermes. *AIP Conf. Proc.*, 792:933–936, 2005.

[94] Xiaodong Jiang. The program of transversity experiments at jefferson lab. Invited talk at Single-Spin Asymmetries, June 1-3, 2005, Brookhaven National Laboratory.

[95] H. Mineo, W. Bentz, N. Ishii, A. W. Thomas, and K. Yazaki. Quark distributions in nuclear matter and the emc effect. *Nucl. Phys.*, A735:482–514, 2004.

[96] M. Oettel, R. Alkofer, and L. von Smekal. Nucleon properties in the covariant quark diquark model. *Eur. Phys. J.*, A8:553–566, 2000.

[97] Pieter Maris and Craig D. Roberts. Dyson-schwinger equations: A tool for hadron physics. *Int. J. Mod. Phys.*, E12:297–365, 2003.

[98] I. C. Cloet, W. Bentz, and A. W. Thomas. Spin-dependent structure functions in nuclear matter and the polarized emc effect. *Phys. Rev. Lett.*, 95:052302, 2005.

[99] H. Mineo, W. Bentz, and K. Yazaki. Quark distributions in the nucleon based on a relativistic 3-body approach to the njl model. *Phys. Rev.*, C60:065201, 1999.

[100] Dietmar Ebert, Thorsten Feldmann, and Hugo Reinhardt. Extended njl model for light and heavy mesons without q anti-q thresholds. *Phys. Lett.*, B388:154–160, 1996.

[101] G. Hellstern, R. Alkofer, and H. Reinhardt. Diquark confinement in an extended njl model. *Nucl. Phys.*, A625:697–712, 1997.

[102] A. W. Schreiber, A. I. Signal, and Anthony W. Thomas. Structure functions in the bag model. *Phys. Rev.*, D44:2653–2662, 1991.

[103] Y. Goto et al. Polarized parton distribution functions in the nucleon. *Phys. Rev.*, D62:034017, 2000.

[104] J. Blumlein and H. Bottcher. Qcd analysis of polarized deep inelastic scattering data and parton distributions. *Nucl. Phys.*, B636:225–263, 2002.

[105] M. Gluck, E. Reya, M. Stratmann, and W. Vogelsang. Models for the polarized parton distributions of the nucleon. *Phys. Rev.*, D63:094005, 2001.

[106] A. W. Thomas and F. Myhrer. personal communication.

[107] A. V. Efremov and O. V. Teryaev. Spin structure of the nucleon and triangle anomaly. JINR-E2-88-287.

[108] R. L. Jaffe and Xiang-Dong Ji. Chiral odd parton distributions and drell-yan processes. *Nucl. Phys.*, B375:527–560, 1992.

[109] Hyun-Chul Kim, Maxim V. Polyakov, and Klaus Goeke. Nucleon "tensor charges" in the chiral quark–soliton model. *Phys. Rev.*, D53:4715–4718, 1996.

[110] M. Wakamatsu and T. Kubota. Chiral symmetry and the nucleon spin structure functions. *Phys. Rev.*, D60:034020, 1999.

[111] K. Suzuki and W. Weise. Chiral constituent quarks and their role in quark distribution functions of nucleon and pion. *Nucl. Phys.*, A634:141–165, 1998.

[112] S. Aoki, M. Doui, T. Hatsuda, and Y. Kuramashi. Tensor charge of the nucleon in lattice qcd. *Phys. Rev.*, D56:433–436, 1997.

[113] M. Fukugita, Y. Kuramashi, M. Okawa, and A. Ukawa. Proton spin structure from lattice qcd. *Phys. Rev. Lett.*, 75:2092–2095, 1995.

[114] A. D. Martin, R. G. Roberts, W. J. Stirling, and R. S. Thorne. Uncertainties of predictions from parton distributions. i: Experimental errors. ((t)). *Eur. Phys. J.*, C28:455–473, 2003.

[115] I. C. Cloet, W. Bentz, and A. W. Thomas. Spin-dependent parton distributions in the nucleon. *Nucl. Phys. Proc. Suppl.*, 141:225–232, 2005.

[116] W. Melnitchouk and Anthony W. Thomas. Neutron / proton structure function ratio at large x. *Phys. Lett.*, B377:11–17, 1996.

[117] X. Zheng et al. Precision measurement of the neutron spin asymmetries and spin-dependent structure functions in the valence quark region. *Phys. Rev.*, C70:065207, 2004.

[118] Glennys R. Farrar and Darrell R. Jackson. Pion and nucleon structure functions near x = 1. *Phys. Rev. Lett.*, 35:1416, 1975.

[119] M. Botje. A qcd analysis of hera and fixed target structure function data. *Eur. Phys. J.*, C14:285–297, 2000.

[120] F. E. Close. Nu w(2) at small omega' and resonance form-factors in a quark model with broken su(6). *Phys. Lett.*, B43:422–426, 1973.

[121] A. D. Martin, R. G. Roberts, W. J. Stirling, and R. S. Thorne. Nnlo global parton analysis. *Phys. Lett.*, B531:216–224, 2002.

[122] K. Ackerstaff et al. Flavor decomposition of the polarized quark distributions in the nucleon from inclusive and semi-inclusive deep- inelastic scattering. *Phys. Lett.*, B464:123–134, 1999.

[123] A. Airapetian et al. Measurement of the proton spin structure function g1(p) with a pure hydrogen target. *Phys. Lett.*, B442:484–492, 1998.

[124] X. Zheng et al. Precision measurement of the neutron spin asymmetry a(1)(n) and spin-flavor decomposition in the valence quark region. *Phys. Rev. Lett.*, 92:012004, 2004.

[125] B. Adeva et al. A next-to-leading order qcd analysis of the spin structure function g1. *Phys. Rev.*, D58:112002, 1998.

[126] K. Abe et al. Measurements of the proton and deuteron spin structure functions g1 and g2. *Phys. Rev.*, D58:112003, 1998.

[127] A. Bodek et al. A comparison of the deep inelastic structure functions of deuterium and aluminum nuclei. *Phys. Rev. Lett.*, 51:534, 1983.

[128] R. G. Arnold et al. Measurements of the a-dependence of deep inelastic electron scattering from nuclei. *Phys. Rev. Lett.*, 52:727, 1984.

[129] D. F. Geesaman, K. Saito, and Anthony W. Thomas. The nuclear emc effect. *Ann. Rev. Nucl. Part. Sci.*, 45:337–390, 1995.

[130] Jason R. Smith and Gerald A. Miller. Return of the emc effect: Finite nuclei. *Phys. Rev.*, C65:055206, 2002.

[131] C. J. Benesh, T. Goldman, and Jr. Stephenson, G. J. Valence quark distribution in a = 3 nuclei. *Phys. Rev.*, C68:045208, 2003.

[132] P. A. M. Guichon and A. W. Thomas. Quark structure and nuclear effective forces. *Phys. Rev. Lett.*, 93:132502, 2004.

[133] G. Chanfray and Magda Ericson. Nuclear matter saturation in a relativistic chiral theory and qcd susceptibilities. 2004.

[134] Brian D. Serot and John Dirk Walecka. The relativistic nuclear many body problem. *Adv. Nucl. Phys.*, 16:1–327, 1986.

[135] M. M. Sharma. Compressibility of nuclear matter from shell effects in nuclei. 1999.

[136] Brian D. Serot and John Dirk Walecka. Recent progress in quantum hadrodynamics. *Int. J. Mod. Phys.*, E6:515–631, 1997.

[137] I. Sick and D. Day. The emc effect of nuclear matter. *Phys. Lett.*, B274:16–20, 1992.

[138] Gerald A. Miller and Jason R. Smith. Return of the emc effect. *Phys. Rev.*, C65:015211, 2002.

[139] P. A. M. Guichon. A possible quark mechanism for the saturation of nuclear matter. *Phys. Lett.*, B200:235, 1988.

[140] K. Saito and Anthony W. Thomas. Composite nucleons in scalar and vector mean fields. *Phys. Rev.*, C52:2789–2791, 1995.

[141] Pierre A. M. Guichon, Koichi Saito, Evgenii N. Rodionov, and Anthony W. Thomas. The role of nucleon structure in finite nuclei. *Nucl. Phys.*, A601:349–379, 1996.

[142] P. A. M. Guichon, H. H. Matevosyan, N. Sandulescu, and A. W. Thomas. Physical origin of density dependent force of the skyrme type within the quark meson coupling model. *Nucl. Phys.*, A772:1–19, 2006.

[143] Michele Arneodo. Nuclear effects in structure functions. *Phys. Rept.*, 240:301–393, 1994.

[144] Gunther Piller and Wolfram Weise. Nuclear deep-inelastic lepton scattering and coherence phenomena. *Phys. Rept.*, 330:1–94, 2000.

[145] A. Arima, K. Shimizu, W. Bentz, and H. Hyuga. Nuclear magnetic properties and gamow-teller transitions. *Adv. Nucl. Phys.*, 18:1–106, 1987.

[146] J. Morgenstern and Z. E. Meziani. Is the coulomb sum rule violated in nuclei? *Phys. Lett.*, B515:269–275, 2001.

[147] Andreas Aste, Cyrill von Arx, and Dirk Trautmann. Coulomb distortion of relativistic electrons in the nuclear electrostatic field. *Eur. Phys. J.*, A26:167–178, 2005.

[148] S. Strauch et al. Polarization transfer in the he-4(e(pol.),e' p(pol.))h-3 reaction up to q**2 = 2.6-(gev/c)**2. *Phys. Rev. Lett.*, 91:052301, 2003.

[149] S. Dieterich et al. Polarization transfer in the he-4(e(pol.),e' p(pol.)h-3 reaction. *Phys. Lett.*, B500:47–52, 2001.

[150] J. M. Udias and Javier R. Vignote. Relativistic nuclear structure effects in (e,e' vecp). *Phys. Rev.*, C62:034302, 2000.

[151] Ding-Hui Lu, Anthony W. Thomas, K. Tsushima, Anthony G. Williams, and K. Saito. In-medium electron nucleon scattering. *Phys. Lett.*, B417:217–223, 1998.

[152] Pervez Hoodbhoy, R. L. Jaffe, and Aneesh Manohar. Novel effects in deep inelastic scattering from spin 1 hadrons. *Nucl. Phys.*, B312:571, 1989.

[153] R. L. Jaffe and Aneesh Manohar. Deep inelastic scattering from arbitrary spin targets. *Nucl. Phys.*, B321:343, 1989.

[154] I. C. Cloet, W. Bentz, and A. W. Thomas. Nucleon quark distributions in a covariant quark-diquark model. *Phys. Lett.*, B621:246–252, 2005.

[155] W. Detmold, G. A. Miller, and J. R. Smith. Role of the nuclear vector potential in deep inelastic scattering. *Phys. Rev.*, C73:015204, 2006.

[156] S. Cohen and D. Kurath. Effective interactions for the 1p shell. *Nucl. Phys.*, 73:1–24, 1965.

[157] B. S. Pudliner, V. R. Pandharipande, J. Carlson, Steven C. Pieper, and R. B. Wiringa. Quantum monte carlo calculations of nuclei with a ≤ 7. *Phys. Rev.*, C56:1720–1750, 1997.

[158] L. D. Landau and E. M. Lifshitz. *Quantum Mechanics, Non-relativistic Theory.* Pergamon, New York, 1977.

[159] V. Guzey and M. Strikman. Nuclear effects in g1(a)(x,q**2) at small x in deep inelastic scattering on li-7 and he-3. *Phys. Rev.*, C61:014002, 2000.

[160] J. Gomez et al. Measurement of the a-dependence of deep inelastic electron scattering. *Phys. Rev.*, D49:4348–4372, 1994.

[161] B. A. Brown and B. H. Wildental. Gamow-teller transitions and magnetic properties of nuclei and shell evolution. *Phys. Rev. C*, 28:2397, 1983.

[162] Toshio Suzuki, Rintaro Fujimoto, and Takaharu Otsuka. Gamow-teller transitions and magnetic properties of nuclei and shell evolution. *Phys. Rev.*, C67:044302, 2003.

[163] Jason R. Smith and Gerald A. Miller. Polarized quark distributions in nuclear matter. *Phys. Rev.*, C72:022203, 2005.

[164] F. M. Steffens, K. Tsushima, Anthony W. Thomas, and K. Saito. Spin dependent parton distributions in a bound nucleon. *Phys. Lett.*, B447:233–239, 1999.

[165] John B. Kogut and Davison E. Soper. Quantum electrodynamics in the infinite momentum frame. *Phys. Rev.*, D1:2901–2913, 1970.

[166] A. Messiah. *Quantum Mechanics.* Dover Publications, 2006.